NORTHWESTERN UNIVERSITY

Control of Mitochondrial Function and Cell Cycle Progression by PGC-1-Related Coactivator (PRC)

A DISSERTATION

SUBMITTED TO THE GRADUATE SCHOOL
IN PARTIAL FULFILLMENT OF THE REQUIREMENTS

for the degree

DOCTOR OF PHILOSOPHY

Field of Integrated Graduate Program in the Life Sciences

By

Kristel Vercauteren

EVANSTON, ILLINOIS

December 2008

ABSTRACT

Control of Mitochondrial Function and Cell Cycle Progression by
PGC-1-Related Coactivator (PRC)

Kristel Vercauteren

PRC is a PGC-1 coactivator family member responsive to serum growth factors and up regulated in proliferating cells. Unlike PGC-1α and PGC-1β, PRC has not been studied extensively and and its function or regulation remains largely unknown. Both PGC-1α and PGC-1β have been shown to be important regulators of mitochondrial biogenesis, in part through the nuclear respiratory factor-1, NRF-1. PRC has been found to directly interact with and co-activate NRF-1, but no direct link between PRC and mitochondrial proliferation has been reported. **We hypothesize that PRC controls mitochondrial function linked to cell proliferation.** In this dissertation project, we established that PRC can *trans*-activate the promoters of genes encoding mitochondrial transcription factors through NRF-1 and NRF-2, and we found a positive correlation between PRC up regulation by serum and increased expression of these factors. Furthermore, we demonstrated that PRC likely functions through NRF-2 *in vivo* by existing in a complex with another coactivator involved in cell proliferation and NRF-2. Another correlation between PRC and mitochondrial proliferation and cell growth was demonstrated by the inhibition of respiratory growth on galactose by a dominant negative fragment of PRC. Also, the induction of PRC by serum is mainly transcriptional and does not require *de novo* protein synthesis, and serum stimulation markedly increases occupancy of the cytochrome c promoter *in vivo* by PRC. The most important focus of this dissertation was to investigate whether PRC can

stimulate mitochondrial biogenesis directly by gain- and loss-of-function studies. The stable silencing of PRC expression with two different short hairpin RNAs resulted in cell cycle defects and a severe reduction in respiratory function in the context of proliferation of structurally abnormal mitochondria, **establishing that PRC is an important regulator of cell proliferation, respiratory gene expression and mitochondrial biogenesis**. Global gene profiling of PRC deficient cells also indicated more pleiotropic effects of PRC. Unfortunately, PRC gain-of-function studies remained inconclusive. Together, these studies help us gain more insight in the regulation of the nucleo-mitochondrial communication and may lead to a better understanding and possibly therapeutic interventions for human mitochondrial diseases.

ACKNOWLEDGMENTS

Thanks to my advisor Richard Scarpulla for giving me the opportunity to do research in his lab, teaching me critical thinking, and providing valuable scientific advice and insightful discussions.

Thanks to my committee members Warren Tourtellotte, Steve Adam, Navdeep Chandel and former member David Dean, who re-located during my PhD candidacy, for their suggestions and helpful comments regarding my work, and their precious time.

Thanks to former Scarpulla lab members Lei Huo and Ulf Andersson. They are both excellent scientists who got me started in the lab and taught me many experimental techniques. Thanks also to former lab members Vita-Maria Marino and Raymond Al Pasko. I enjoyed working with all of them.

Thanks to my best friends Alina Fridberg and Natalie Gleyzer. Alina was always willing to discuss experiments with me and to offer advice and good humor. I thank her for the numerous times she helped me out with babysitting so that I could get some work done. I really enjoyed collaborating with Natalie. She is an outstanding research technologist and a great asset to the Scarpulla lab. Over the years, she has turned from a colleague into a very close friend of mine. I am grateful to both of them for supporting me when times were tough, both inside and outside the lab, and for letting me share everything with them, whether it was science-related or not. I could not have finished this journey without them!

Thanks to my dear friend Jurgen Vanhauwe, without whom I probably would not have ended up in Chicago. I am grateful for his expert scientific advice, innovative ideas, encouragement, enthusiasm, infinite curiosity, and his support and friendship over the years.

Thanks to all my friends for their social and emotional support, and helping me keep things in perspective.

Thanks to my parents and family for being there for me while far away. A special thanks to my mom, who visited me for three weeks to help me take care of my daughter and chores, so that I had more time to work. Dankjewel mama en papa!

Thanks to my daughter Abby for making me smile and already teaching me many things a PhD never could!

PREFACE

This dissertation contains an Introduction (Chapter 1) and Background section (Chapter 2), followed by four chapters (Chapter 3-6) which each constitute a complete research article. Towards Chapter 3 (Gleyzer N, Vercauteren K, and Scarpulla RC, **Control of mitochondrial transcription specificity factors (TFB1M and TFB2M) by nuclear respiratory factors (NRF-1 and NRF-2) and PGC-1 family coactivators**, *Mol Cell Biol*, 2005), I contributed Figure 3.11 and the RNase protection assays (not shown) and collaborated in the isolation of the hTFB1M and hTFB2M promoters, Figures 3.9A and 3.10. In Chapter 4 (Vercauteren K, Pasko RA, Gleyzer N, Marino VM, and Scarpulla RC, **PGC-1-related coactivator: immediate early expression and characterization of a CREB/NRF-1 binding domain associated with cytochrome c promoter occupancy and respiratory growth**, *Mol Cell Biol*, 2006), I was responsible for Figure 4.2 and Table 4.1 and the experimental design of Figure 4.1. Chapter 5 is a research manuscript (Vercauteren K, Gleyzer N, and Scarpulla RC, **PGC-1-related coactivator complexes with HCF-1 and NRF-2beta in mediating NRF-2(GABP)-dependent respiratory gene expression**, *J Biol Chem*, 2008), towards which I contributed Figure 5.2B, Figure 5.8 and Table 5.1. I collaborated in the writing of the research article in Chapter 6 (Vercauteren K, Gleyzer N, and Scarpulla RC, **Short hairpin RNA-mediated silencing of PGC-1-related coactivator (PRC) results in a severe respiratory chain deficiency associated with the proliferation of aberrant mitochondria**, *J Biol Chem*, In press), and I contributed all Figures, except Figures 6.7 and 6.13, and all Tables. Chapter 7 and Future Directions contain unpublished results that I generated during my doctoral research. This is followed by a Summary and Conclusion, list of References and an Appendix.

LIST OF ABBREVIATIONS

ATF-2	activating transcription factor-2
BAT	brown adipose tissue
BWB	binding wash buffer
cAMP	cyclic AMP
CAR	coxsackie and adenoviral receptor
ChIP	chromatin immunoprecipitation
COX	cytochrome c oxidase
CREB	cyclic AMP response element-binding protein
Cyt b	cytochrome b
Cyt c	cytochrome c
δ-ALAS	δ-aminolevulinate synthase
bp	base pairs
DN	dominant-negative
ERR	estrogen-related receptor
FL	full length
FOXO	forkhead box O1
FXR	farnesoid X receptor
GABP	GA-binding protein
GFP	green fluorescent protein
HA	hemagglutinin
HCF-1	host cell factor-1

HMG high-mobility-group

hmtPAP human mitochondrial poly(A) polymerase

HMW high molecular weight

HNF-4α hepatocyte nuclear factor-4α

hPNPase human polynucleotide phosphorylase

Ig immunoglobulin

kb kilobase pairs

kDa kilodalton

mtDNA mitochondrial DNA

mTERF mitochondrial termination factor

ND6 NADH dehydrogenase 6

NRF nuclear respiratory factor

OD optical density

O_H heavy strand origin of replication

O_L light strand origin of replication

ORF open reading frame

OXPHOS oxidative phosphorylation

P-CREB phospho-CREB

PGC peroxisome proliferator-activated receptor gamma coactivator

P_H heavy-strand promoter

P_L light-strand promoter

POLRMT mitochondrial RNA polymerase

POLγ mitochondrial DNA polymerase γ

PPAR	peroxisome proliferator-activated receptor
PRC	PGC-1-related coactivator
RAR	retinoic acid receptor
SDH	succinate dehydrogenase
SDS-PAGE	sodium-dodecyl sulfate-polyacrylamide gel electrophoresis
shRNA	short hairpin RNA
TAD	*trans*-activation domain
Tfam	mitochondrial transcription factor A
TFB	mitochondrial transcription factor B
TR	Tet repressor
TR	thyroid receptor
tRNA	transfer RNA
Trx	thioredoxin
TWINKLE	mitochondrial TWINKLE helicase
UCP	uncoupling protein
UTR	untranslated region
WAT	white adipose tissue
wt	wild type

The important thing is not to stop questioning. Curiosity has its own reason for existing. One cannot help but be in awe when he contemplates the mysteries of eternity, of life, of the marvelous structure of reality. It is enough if one tries merely to comprehend a little of this mystery every day. Never lose a holy curiosity.

Albert Einstein

TABLE OF CONTENTS

LIST OF FIGURES

LIST OF TABLES

CHAPTER 1:

INTRODUCTION

Many essential metabolic pathways are compartmentalized in mitochondria, including fatty acid oxidation and the biosynthesis of pyrimidines, amino acids, nucleotides, phospholipids and heme. However, ATP synthesis through electron transfer and oxidative phosphorylation (OXPHOS), thereby providing most of the cellular energy, is likely the most important function of this organelle. Due to their origin as free-living bacteria, mitochondria contain their own genome. The human mitochondrial genome is a rather small, double-stranded closed circular molecule that contains 16569 base pairs (1) **(Figure 1.1)**. Mammalian cells contain thousands of mtDNA molecules that are packaged in several hundred nucleoids, which are thought to be fundamental for mtDNA inheritance and segregation (2). Human mitochondrial DNA (mtDNA) encodes 37 genes, 2 ribosomal RNAs (12S and 16S), 22 transfer RNAs, and 13 polypeptides, and lacks introns **(Figure 1.1)**. Interestingly, all encoded proteins are components of the respiratory complexes of the OXPHOS system. Because of the limited coding capacity of mtDNA, the nuclear genome must provide the other respiratory subunits and the majority of the proteins involved in maintenance, replication, and expression of the mitochondrial genome. Therefore, the correct function of the respiratory chain depends on an orchestrated cross-talk between the two genomes, nuclear and mitochondrial.

Figure 1.1. Map of human mtDNA.

Genomic organization and structural features of the human mitochondrial genome are depicted in a circular map showing heavy and light strand. Protein coding and rRNA genes are interspersed with 22 tRNA genes (black bars denoted by the single-letter amino acid code). Duplicate tRNA genes for leucine (L) and serine (S) are distinguished by their codon recognition (parentheses). The D-loop regulatory region contains the L- and H- strand promoters (P_L and P_H), with arrows showing the direction of transcription. The H-strand origin of replicaton (O_H) is located within the D-loop, whereas the origin of L-strand replication (O_L) is displaced by about two-thirds of the genome within a cluster of five tRNA genes. Protein coding genes include the following: cytochrome oxidase (COX) subunits 1, 2, and 3; NADH dehydrogenase (ND) subunits 1, 2, 3, 4, 4L, 5, and 6; ATP synthase (ATPS) subunits 6 and 8; cytochrome b (Cyt*b*). ND6 and the 8 tRNA genes transcribed from the L-strand as template are underlined, whereas the remaining protein coding and RNA genes transcribed from the H-strand as template are not.

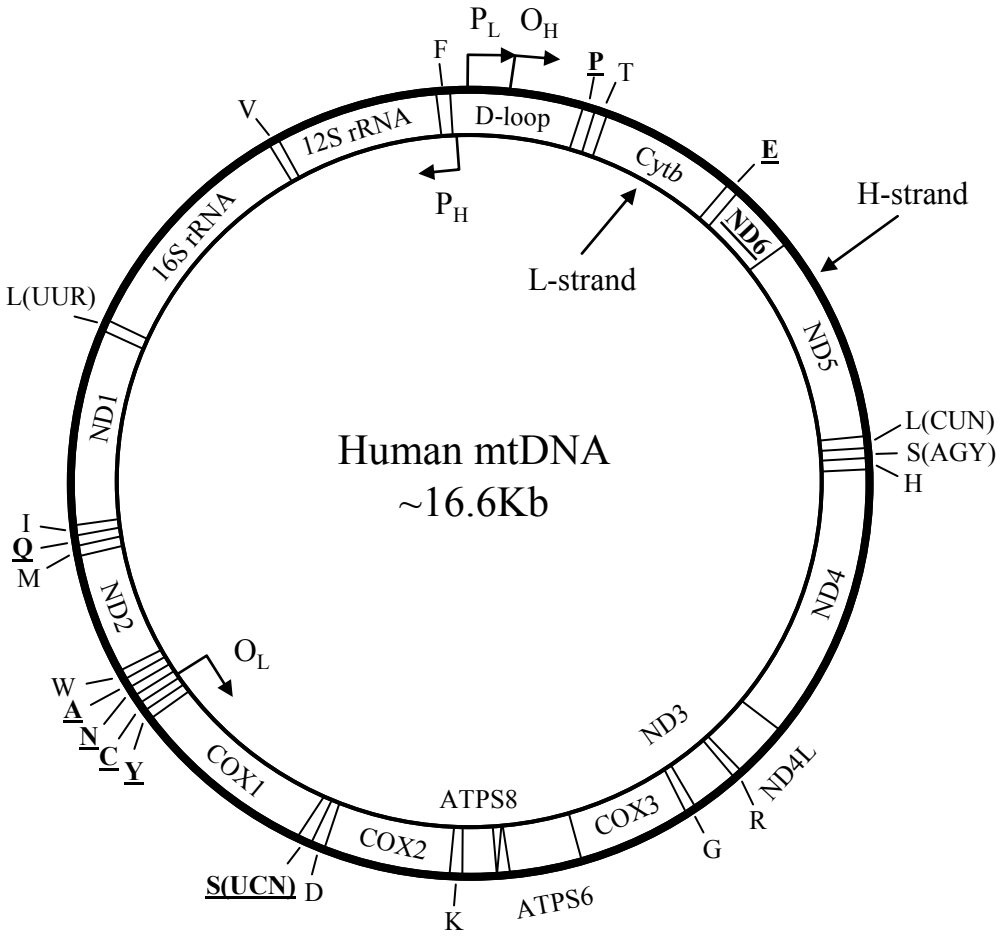
P_L O_H
F
P
T
V
12S rRNA
D-loop
Cytb
E
H-strand
P_H
L-strand
ND6
16S rRNA
L(UUR)
ND5
ND1
L(CUN)
S(AGY)
H
Human mtDNA
~16.6Kb
I
Q
M
ND4
ND2
O_L
W
A
N
C
Y
ND3
COX1
ATPS8
COX3
ND4L
R
G
COX2
S(UCN)
D
K
ATPS6

MtDNA replication

The *cis*-elements responsible for the regulation of mtDNA replication and transcription are mostly located within a small non-coding DNA fragment, the D-loop regulatory region (3). On the other hand, all the *trans*-acting factors involved in mtDNA replication and transcription are completely dependent on nuclear-encoded gene products. Many nuclear-encoded factors involved in mtDNA replication have been characterized in recent years. The DNA polymerase devoted to mtDNA synthesis is DNA polymerase γ. It has both 5' → 3' DNA polymerase and proofreading 3' → 5' exonuclease activities and is highly conserved from yeast to man (4). In humans, it forms a heterotrimer composed of 1 large catalytic subunit (POLγA; 140 kDa) and 2 small accessory subunits (POLγB; 55 kDa) (2). Another essential component of mtDNA replication is the RNase mitochondrial RNA processing (RNase MRP) (reviewed in (5)). This ribonucleoprotein contains a nucleus-encoded RNA (MRP RNA) necessary for catalytic activity. It is thought to generate the primers for the initiation of H-strand DNA replication by cleavage of the L-strand transcript, but robust evidence for this is lacking (reviewed in (2)). A mitochondrial single-stranded DNA-binding protein (mtSSB) that stabilizes unwound DNA is also an essential part of the replication machinery. A helicase, TWINKLE, has been identified that seems to be required for mtDNA copy number and maintenance as shown by both gain- and loss-of-function studies (6). Other factors, such as RNase H1 and a topoisomerase (TOP1mt), have also been associated with mtDNA replication, but are still poorly characterized (reviewed in (2,5)). It is very likely that additional factors, yet to be identified, are involved in mtDNA replication.

There is a lot of controversy concerning the mechanism of mtDNA replication. The majority of evidence points to an asynchronous and asymmetrical replication of the two strands of the mammalian mtDNA, named heavy (H) and light (L) strand on the basis of their buoyant

density in a cesium chloride gradient (3). This model has been studied extensively by the group of Clayton, and has been the established model for mtDNA replication for over 25 years. The D-loop region contains the origin of replication of the H-strand (O_H), as well as the promoters for the H- and L-strand (P_H and P_L). Since the D-loop region is the control site for both transcription and replication, it is not surprising that these processes are tightly coupled. DNA synthesis starts in O_H and proceeds unidirectionally until the L-strand origin of replication, located two-thirds away around the genome, is reached. Once the parental H-strand is displaced and the O_L is single-stranded, mtDNA replication starts in the opposite direction. Recently, the above model for mtDNA replication has been questioned by Holt and colleagues (7-9). A more traditional coupled leading- and lagging-strand mechanism, progressing bidirectionally from multiple replication forks, has been proposed based on the detection of various replication intermediates in two-dimensional agarose gel electrophoresis of mtDNA, suggesting that cells may use one or the other mechanism in different physiological conditions. Recently, attempts to reconcile the two mechanisms have been proposed (10,11). So far, no consensus has been reached and new experimental approaches must be used to clarify the issue.

MtDNA transcription, termination and RNA processing

MtDNA transcription in mammalian cells is initiated at the two promoters, P_H and $P_{L,}$ found in the D-loop. Mitochondrial transcripts are polycistronic with the tRNA genes acting as punctuation signals (reviewed in (5)). The resulting polycistronic transcripts are subsequently processed to form the mature mRNAs and rRNAs. The mitochondrial transcription machinery consists of a single RNA polymerase (POLRMT), first identified in yeast (12) and later in humans (13), that shares sequence similarities with bacteriophage T7 and T3 RNA polymerases.

POLRMT cannot bind DNA and initiate transcription on its own. Proper initiation of transcription from P_H and P_L requires the collaboration of POLRMT, mitochondrial transcription factor A (Tfam) and one of the two mitochondrial transcription factors B (TFB1M and TFB2M). Tfam (previously called mtTF1 and mtTFA) is the first identified and the most well characterized *trans*-acting transcription factor in vertebrate mitochondria. This protein binds specifically to sequences upstream of the transcription start sites in both P_H and P_L. In addition to its role in transcription, Tfam is essential for mtDNA maintenance in yeast (14), and most likely in mammals, since a Tfam knockout mouse displays embryonic lethality and a depletion of mtDNA (15). While budding yeast contains one well-characterized mitochondrial transcription factor B, termed mtTFB, humans contain two recently identified isoforms of mtTFB, denoted TFB1M and TFB2M (16,17). Both TFB1M and TFB2M are capable of binding POLRMT and Tfam (16,18). These factors associate with mtDNA in a non-sequence dependent manner, and promote mtDNA transcription from both P_H and P_L in the presence of POLRMT and Tfam *in vitro* (16). While both proteins also have rRNA methyltransferase activity, it seems that over time TFB1M has evolved to be the more potent rRNA methyltransferase (19,20), while TFB2M seems to have evolved as the more efficient transcription factor (16). More recently, an additional factor, the human mitochondrial ribosomal protein MRPL12, has been demonstrated to interact with RNA polymerase POLRMT and stimulate mtDNA transcription *in vitro* (21).

The transcriptional termination signal of the heavy strand in vertebrate mitochondria is located within the gene for leucyl-tRNA, at the end of the 16S rRNA gene, and functions bidirectionally (22,23). It binds a *trans*-acting factor called mitochondrial transcription termination factor (mTERF) (24,25). The binding of mTERF is now found to be sufficient to terminate transcription *in vitro* (26). However, the existence of 3 addditional mTERF vertebrate

homologues, mTERF2-4, suggests that regulation of transcriptional termination in mammals may be more complex than originally thought (27). The factor mTERF3 has been shown to be a negative regulator of mitochondrial DNA transcriptional initiation *in vivo* (28). Interestingly, mTERF1 has now also been implicated in transcriptional stimulation and in DNA replication (reviewed in (2,29).

The enzymatic activities responsible for mitochondrial RNA processing have been partially characterized. Most RNA processing takes place at the junctions between tRNAs and other transcripts. The 5'-end processing is believed to be catalyzed by an RNase P activity and the 3'-end by an unidentified endonuclease (30). Recently, the gene encoding human mitochondrial poly(A) polymerase (hmtPAP), responsible for polyadenylating mitochondrial mRNAs, has been identified (31,32). In addition, human polynucleotide phosphorylase (hPNPase) has been implicated in regulating mtRNA processing and polyadenylation (32,33). The existence of other putative factor involved in mtRNA processing has been proposed (31,33). Mitochondrial mRNAs have no 5'-untranslated regions (UTR) and lack the 7-methylguanylate cap structure typical of cytoplasmic mRNAs (3).

Mitochondrial translation

The mitochondrial protein synthesis machinery has been poorly characterized so far (5). The mitoribosomes are located in the mitochondrial matrix. The 2 rRNAs and 22 tRNAs of the mitochondrial translation system are of mtDNA origin. The protein components necessary for translation, including mitoribosomal proteins, tRNA synthetases, and the initiation and elongation factors, are all encoded by nuclear genes. Many mitoribosomal proteins remain unidentified. Initiation and elongation factors, including mtIF2, mtIF3, mtEFTu, mtEFTs and

mtEFG, have been isolated. Several aminoacyl tRNA synthetases are starting recently to being characterized (reviewed in (5,34).

Regulation of mitochondrial replication and transcription

Different lines of evidence have shown that the concentration of the catalytic subunit of DNA polymerase γ is constitutively expressed, but that the amount of Tfam and mtSSB correlates with mtDNA copy number (35). The generation of the Tfam knockout mouse, displaying a depletion of mtDNA (15), and the generation of transgenic mice expressing human Tfam, displaying increased mtDNA copy number (36), confirms this. Furthermore, Tfam levels correlate well with increased mtDNA in ragged-red muscle fibers and decreased mtDNA levels in mtDNA-depleted cells (reviewed in (37)). In contrast, other data indicate that a reduction in the physiological levels of Tfam does not produce significant changes in mitochondrial transcript levels (38). Therefore, the potential existence of additional transcription factors has been suggested and evidence for this came with the discovery of the two mtTFB isoforms, TFB1M and TFB2M (16). Over expression of TFB2M is correlated with increased mtDNA transcription and replication, along with increased translation of a fraction of mtDNA encoded proteins and increased expression of TFB1M. Over expression of TFB1M did not affect the above processes but instead caused an increase in mitochondrial biogenesis (39). To date, no key limiting factor whose expression controls mtDNA copy number has been identified.

Nucleo-mitochondrial communication

Mitochondrial biogenesis is a complex process that involves proliferation (increasing the number of mitochondria) and differentiation or maturation (increasing the activity of individual

mitochondria). Energy demands vary substantially between the different cells and tissues of the organism. Moreover, the same tissue may need different energy supplies depending on the physiological circumstances. In addition, energy requirements can be different in specific cellular sub domains (1). The cell must be able to adapt to all these situations and change the mass, structure, function, and location of mitochondria depending on the local energy demand. This necessitates the cross-talk between the nuclear and mitochondrial genome. It is a great challenge for the future to study the mechanism of intergenomic communication. One approach to do this is to identify and characterize nuclear regulatory proteins that contribute to the biogenesis and function of mitochondria in mammalian cells. This is our laboratory focus. Two classes of nuclear transcriptional regulators that are important for nucleo-mitochondrial interactions have emerged in recent years (see (40) for an excellent review). The first class consists of DNA binding transcription factors. The nuclear respiratory factors, NRF-1 and NRF-2 (also known as GABP), are important members of this class of transcriptional regulators. The second class of nuclear regulators important for nucleo-mitochondrial interactions consists of the PGC-1 family of transcriptional coactivators, and includes the PPARγ coactivator PGC-1α, the PPARγ coactivator PGC-1β, and the PGC-1-related coactivator PRC.

Nuclear transcription factors acting on respiratory gene expression

1. Nuclear respiratory factors

To identify transcription factors that regulate the expression of nuclear genes required for mitochondrial respiratory activity, our lab analyzed the cytochrome c (cyt c) promoter and cytochrome c oxidase subunit IV (COXIV) promoter. This led to the discovery of the nuclear respiratory factors, NRF-1 and NRF-2 (GABP) (41,42). NRF-1 is required for maximum cyt c

promoter activity, while NRF-2 is necessary for maximum COXIV promoter function. Subsequently, functional NRF-1 sites have been identified in the promoters of many genes encoding OXPHOS subunits (reviewed in (43)). Similarly, NRF-2 is now known to act on several nuclear respiratory genes, many of which also contain NRF-1 sites. In addition, NRF-1 has been associated with the expression of factors involved in mitochondrial transcription and replication, the expression of heme biosynthetic enzymes, and certain protein import factors. In particular, the expression of Tfam and MRP RNA, main factors involved in mtDNA replication and transcription, is regulated by NRF-1 (44). Tfam contains a NRF-2 site as well. Also, the involvement of NRF-1 in the regulation of the δ-aminolevulinate synthase gene (δ-ALAS), which is the rate-limiting enzyme in heme biosynthesis within the mitochondrial matrix, is of particular importance (45). As mentioned above, recently two novel transcription factors have been discovered, TFB1M and TFB2M, that cooperate with mitochondrial RNA polymerase and Tfam to carry out basal transcription of mammalian mtDNA (16). As found by our lab, both these genes are regulated by NRF-1 and NRF-2 *in vitro* and *in vivo* (46) **(Chapter 3)**. Our lab also established that targeted disruption of the NRF-1 gene in mice resulted in early embryonic lethality associated with a deficiency in mitochondrial DNA (47). The mtDNA deficiency in these mice most likely resulted from the loss of a NRF-1 dependent pathway of mtDNA maintenance. The phenotype of NRF-2α-deficient mice is rather similar, in that they also die during early embryogenesis prior to implantation (48), but the effects on mitochondrial maintenance in these mice has not been determined. Recently, shRNA-mediated inhibition of both NRF-1 and NRF-2 has been linked to the down regulation of all 10 nucleus-encoded cytochrome oxidase subunits, providing additional evidence for the importance of these factors in respiratory chain expression (49,50).

This makes the NRFs excellent candidates to play a key role in nucleo-mitochondrial communication. However, the actual picture is likely more complex. There are respiratory genes that lack NRF-1 sites in their promoters and many other genes not related to mitochondrial function that contain NRF-1 sites, a situation also found with NRF-2. For example, a genome-wide analysis of transcription factor occupancy identified NRF-1 binding sites in many E2F target genes (51). This indicates a broader role for NRF-1 in other cellular functions (43). Since several of these non-mitochondrial related genes encode proteins involved in cell proliferation, chromosome maintenance and cell cycle regulation, NRF-1 is likely to be a regulator of cell growth.

2. Other transcription factors

In addition to the nuclear respiratory factors, other transcription factors, including ERRα, Sp1, YY1, and c-myc, also play a role in the expression of nuclear respiratory genes. There are also several motifs that are present in the promoters of some genes involved in mitochondrial biogenesis, including the OXBOX/REBOX motif, the Mt motifs and the MEF-2 and E-box consensus elements (5). Furthermore, other mitochondrion-related genes are regulated by different factors that are not used by respiratory genes, such as expression of fatty acid oxidation enzymes by PPARα (peroxisome proliferator-activated receptor α) or PPARδ. This complex situation prompts the question of how all these genes involved in mitochondrial function are coordinately regulated, so that a cellular program leading to mitochondrial biogenesis can be properly initiated and executed.

Transcriptional coactivators and nuclear respiratory gene expression

Transcriptional coactivators cannot bind DNA but instead interact with transcription factors and other coactivators to regulate gene expression. They enhance transcription by modifying the chromatin structure of the target gene or by associating with the RNA polymerase machinery. While the control of gene expression by varying the quantity or activity of transcription factors has been widely recognized, it has now become increasingly clear that transcriptional coactivators also substantially control gene expression through regulation of coactivator expression (52). Examples of coactivator-controlled pathways include OCA-B control of B-cell development, and myocardin regulation of smooth muscle cell differentiation. New evidence suggesting that the biological pathway leading to mitochondrial biogenesis results from the interplay between nuclear transcription factors and the PGC-1 family of coactivators, emerged recently.

1. PGC-1α

PGC-1α was the first member of this family to be identified and is by far the most characterized. PGC-1α was originally identified in a yeast two-hybrid screen designed to identify interacting partners of the nuclear hormone receptor PPARγ, a master regulator of adipogenesis, in murine brown fat cells (53). PGC-1α represented a novel protein and was named for PPAR Gamma Coactivator-1. PGC-1α is a nuclear protein of about 90 kDa and is expressed in brown fat, skeletal muscle, heart, kidney, and brain, all tissues with high energy demands and rich in mitochondria. The N-terminus of PGC-1α contains a potent activation domain rich in acidic amino acids, which also contains a LXXLL motif, a motif responsible for ligand-dependent

interaction of other coactivators with nuclear hormone receptors **(Figure 1.2)**. The C-terminal domain contains RNA processing motifs, such as an RS domain and an RNA recognition motif.

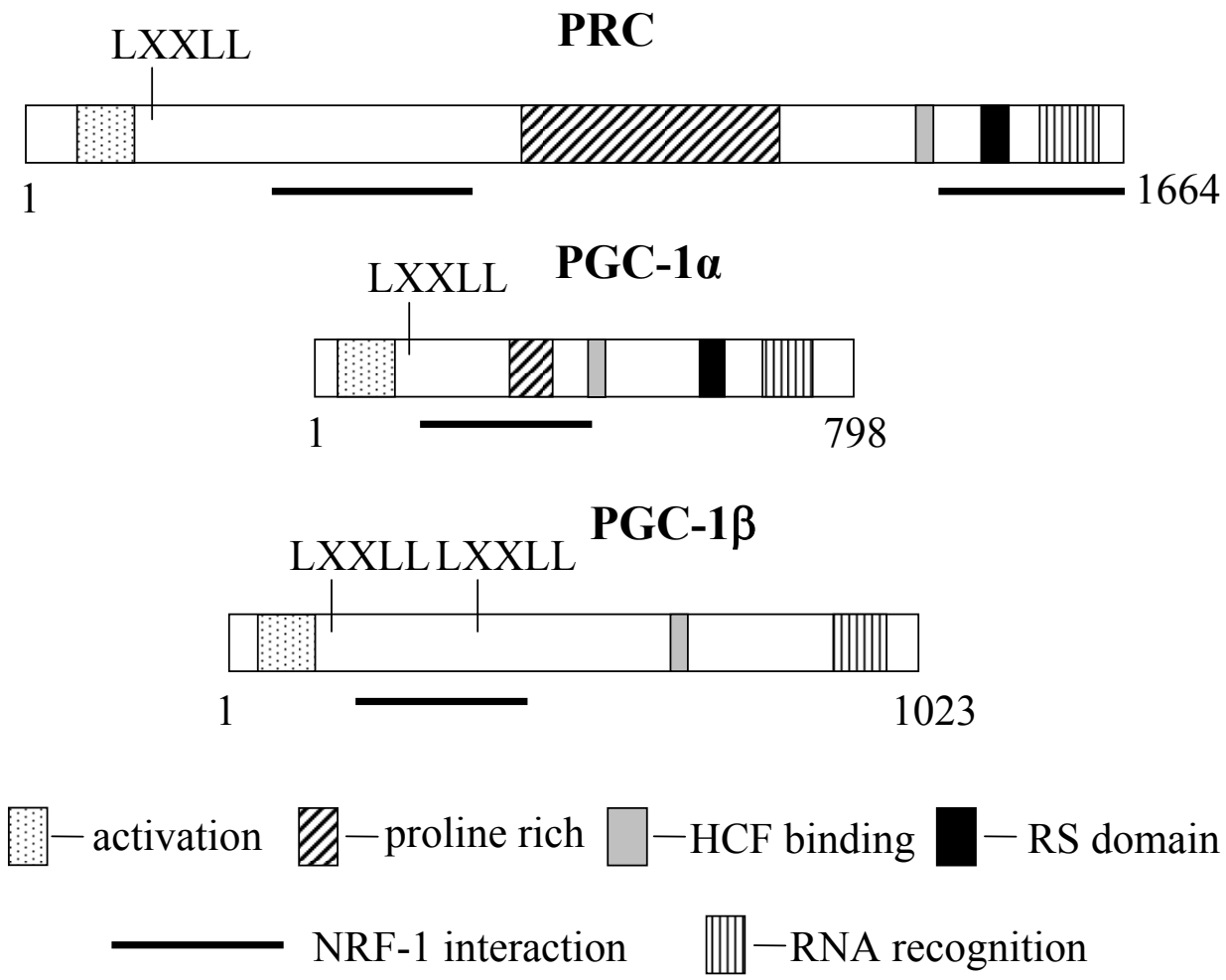

Figure 1.2. Diagram showing conserved domains between the PGC-1 coactivator family members PRC, PGC-1α, and PGC-1β.

Regions of similarity between the proteins are as follows: activation domain (stippled), proline-rich region (cross-hatched), HCF binding domain (solid grey), RS domain (solid black), and RNA recognition motif (vertically hatched). The NRF-1 interaction domain is underlined. Amino acid coordinates are indicated below each map.

Several gain-of-function studies demonstrate that PGC-1α is sufficient to stimulate mitochondrial biogenesis and expression of OXPHOS genes. First, ectopic expression of PGC-1α in cultured white fat cells induces an up regulation of uncoupling protein-1 (UCP-1) mRNA and several nuclear and mitochondrial genes of the OXPHOS pathway, including COXII and IV, and ATP synthetase (53). Second, ectopic expression of PGC-1α in cultured C2C12 myoblasts and myotubes activates expression of UCP-2, and of COXII and IV, ATP synthetase, and cytochrome c, associated with increased mtDNA content and mitochondrial proliferation (54). Third, PGC-1α also controls mitochondrial biogenesis and function in cultured cardiomyocytes and in the hearts of transgenic mice (55,56). Of particular interest is that cardiac-specific over expression of PGC-1α in transgenic mice resulted in excessive mitochondrial proliferation, leading to cardiac pathology. Lastly, over expression of PGC-1α in skeletal muscle of transgenic mice leads to mitochondrial biogenesis and the formation of mitochondrial-rich type I, oxidative ("slow-twitch") muscle fibers (57). These increases in oxidative metabolism and mitochondrial biogenesis indicate an important role for PGC-1α in these processes.

The question remained of how PGC-1α can regulate mitochondrial biogenesis and mitochondrial gene expression. Attention was drawn to the nuclear respiratory factors NRF-1 and NRF-2 since they have been shown to activate the transcription of a large number of genes involved in respiratory function (54). Several experiments now support a major role for NRF-1 in mediating the effects of PGC-1α on mitochondrial biogenesis. PGC-1 over expression in either myoblasts or myotubes results in increased expression of both NRF-1 and NRF-2 mRNA, and PGC-1α interacts physically with NRF-1 to *trans*-activate NRF-1 dependent promoters. Furthermore, expression of a dominant negative NRF-1 allele inhibits the mitochondrial biogenesis mediated by PGC-1α (54). PGC-1 can also stimulate expression of ERRα and co-

activate ERRα (58,59), thereby inducing expression of OXPHOS genes and mitochondrial biogenesis, in addition to the NRFs. These data are consistent with a broad role for PGC-1α as a key regulator of mitochondrial biogenesis.

Surprisingly, mice deficient in PGC-1α are viable and display a rather weak mitochondrial phenotype. Two groups independently created a PGC-1α null mouse, and both find that PGC-1α is not essential for normal embryologic development or mitochondrial biogenesis (60,61). Both groups report slightly decreased mitochondrial respiration and modestly reduced expression of mitochondrial genes in certain tissues. No changes in mitochondrial number or morphology were reported, with the exception of a modest reduction in mitochondrial biogenesis in skeletal muscle detected by Leone's group. Both PGC-1$\alpha^{-/-}$ mice display impaired thermogenic function during acute cold exposure, reduced muscle performance, heart abnormalities, and defects in the brain. There are also important differences found in both studies. Whereas Lin and colleagues found defects in gluconeogenesis in liver and increased postnatal mortality, no such defects were observed by Leone *et al*. The null animals created by the group of Lin are lean and resistant to diet-induced obesity, attributed to increased energy expenditure through hyperactivity. Instead, the mice from Leone's group are less active and have increased body mass, and also display heart abnormalities. The different phenotypes of both PGC-1α null mice likely result from a different genetic background of the two mouse strains and the use of different gene targeting strategies.

As mentioned before, most coactivators enhance transcription by remodeling chromatin structure or by associating with the RNA polymerase machinery. Most coactivators have been viewed as constitutively active components, using transcription factors mainly to localize their functions. In contrast, PGC-1α is shown to be in a relatively quiescent state when not bound to a

transcription factor. Docking of a transcription factor stimulates a conformational change in PGC-1α that permits binding of SRC-1 and CBP/P300, coactivators with histone acetyl transferase (HAT) activity, resulting in a large increase in transcriptional activity (62). PGC-1α can also stimulate gene expression by interacting with the thyroid receptor-associated protein (TRAP)/vitamin D receptor-interacting protein (DRIP)/Mediator complex that facilitates direct interaction with the transcription initiation machinery (63). Interestingly, there is also evidence that link PGC-1α-mediated transcription with mRNA processing through the association with splicing factors and RNA polymerase II (64).

Recent studies show that PGC-1α acts in a broader context that extends beyond mitochondrial respiration and biogenesis. PGC-1α regulates adaptive thermogenesis through the transcriptional co-activation of PPARγ and TR in the context of the UCP-1 promoter (53). It has also been implicated in the activation of genes of the mitochondrial fatty acid oxidation pathway in the heart through its ability to interact with and *trans*-activate through PPARα (65). PGC-1 is also involved in heme biosynthesis in the liver by co-activating the key rate limiting enzyme, δ-ALAS, through NRF-1 and FOXO1 (66). In muscle, PGC-1α can bind to and co-activate the muscle-specific transcription factor MEF-2, resulting in activation of the insulin-sensitive glucose transporter (Glut-4) gene expression and an increased glucose uptake (67). Both gain- and loss-of-function studies confirm a key role for PGC-1α in muscle fiber-type switching (57,68). Furthermore, PGC-1α is a potent regulator of gluconeogenesis. Over expression of PGC-1α in primary hepatocytes results in increased expression of the key enzymes of gluconeogenesis, phosphoenol pyruvate carboxykinase (PEPCK), fructose-1,6-bisphosphatase, and glucose-6-phosphatase, causing the hepatocytes to produce more glucose (69). PGC-1α *trans*-activates the PEPCK promoter through interaction with hepatocyte nuclear factor-4α

(HNF-4α) and the glucocorticoid receptor. The induction of liver lipoprotein expression is also mediated by the interaction PGC-1α with HNF-4α (70).

The involvement of PGC-1α in mitochondrial biogenesis and a variety of tissue-specific responses requires that its expression is tightly regulated, e.g. it is induced by cold in BAT, by exercise and decreased ATP levels in muscle, and fasting in liver. The expression of PGC-1α is regulated by a number of signaling pathways. A major regulator of PGC-1α transcription is cAMP signaling by cAMP response element binding protein (CREB) and activating transcription factor-2 (ATF-2) through binding to its promoter (71). In liver, CREB is activated by glucagon and cAMP, major positive factors inducing gluconeogenesis. In muscle, CREB is activated by calcium signaling (72). In BAT, ATF-2 is recruited to the PGC-1α promoter by β-adrenergic receptor activation (73). Interestingly, cGMP signaling has also been described to be involved in PGC-1α regulation by nitric oxide (74).

In conclusion, PGC-1α is involved in a whole array of different biological responses, but in all responses PGC-1α promotes gene expression patterns connected to energy metabolism.

2. PGC-1β

PGC-1β (also known as PERC or ERRL-1) is the second member of the new PGC-1 gene family, and is closely related to PGC-1α **(Figure 1.2)**. It shares the same tissue distribution, with highest expression levels in brown fat and heart (75-77). PGC-1β is also a potent regulator of the transcriptional activity of NRF-1 (75) and ectopic expression of PGC-1β in cultured hepatocytes or muscle cells promotes mitochondrial biogenesis as effectively as PGC-1α (78,79). However, in contrast to the cold-inducible expression of PGC-1α, the expression of PGC-1β is not increased in response to cold exposure. Instead, it is strongly induced during brown fat cell differentiation (75), indicating that PGC-1α and PGC-1β likely perform distinct roles in adipocyte differentiation and the regulation of other brown fat functions, such as adaptive thermogenesis. Similar to PGC-1α, PGC-1β plays a central role in hepatic lipid metabolism. It is highly induced in fasting liver and is involved in the β-oxidation of fatty acids by co-activating PPARα. However, it has no regulatory role in hepatic gluconeogenesis, presumably through its inability to interact with HNF-4α and FOXO1, and is not regulated by cAMP signaling (78). Hepatocyte-specific over expression of PGC1-β is shown to stimulate lipogenic gene expression and lipoprotein secretion in liver through regulation of the SREBP family of transcription factors and LXR and FOXA2 (80,81), which are not considered to be PGC-1α targets. Transgenic expression of PGC-1β in mice leads to hypermetabolism and resistance to obesity (82). PGC-1β also is important for muscle function. Skeletal muscle-specific over expression of PGC-1β causes induction of type IIx oxidative fast-twitching fibers by co-activation of MEF-2 (83).

Currently, 3 mouse lines are described with targeted disruption of PGC-1β. One mouse line expresses a hypomorphic mutant protein lacking an internal 110-amino acid stretch that retains a substantial activity toward ERRα, the host cell factor, and SREBP-1c in transient

transfection assays (84). Two groups have created knock-out mice with complete ablation of PGC-1β (85,86). All mice lines appear viable and healthy. The expression of mitochondrial genes (not necessarily reflected in protein levels) is reduced in all three lines, and decreased mitochondrial content is observed in heart and skeletal muscle, confirming that PGC-1β regulates mitochondrial function. However, no altered respiration was observed in isolated mitochondria. The knockout mice exhibit no overt metabolic failure under non-stressed conditions, in part due to compensatory mechanism as demonstrated by increased expression of PGC-1α in some (85) or all (86) tissues examined. This is in contrast to the PGC-1α null mice where PGC-1β mRNA levels were unchanged in skeletal muscle and brown fat, suggesting it cannot compensate for defects caused by the loss of PGC-1α (60). The studies agree that loss of PGC-1β affects hepatic lipid metabolism by causing accumulation of lipids in the liver under certain conditions, due to effects on SREBP. Both PGC-1$\beta^{-/-}$ mice show cardiac defects. The group of Sonoda also reported greatly decreased activity in the null animals during the dark cycle. Overall, there seems to be a functional overlap between PGC-1α and PGC-1β, but specific effects of PGC-1β exist that cannot be compensated for by PGC-1α.

A few studies have now addressed the effects of combined deficiency of PGC-1α and PGC-1β to further dissect the individual contributions of each coactivator. ShRNA-mediated silencing of PGC-1β in brown preadipocytes from mice lacking PGC-1α causes a total loss of mitochondrial biogenesis and mitochondrial respiration associated with brown fat differentiation (87). Very recently, it was demonstrated that mice doubly deficient in PGC-1α and PGC-1β die shortly after birth due to heart failure and display dramatic mitochondrial abnormalities in heart and brown adipose tissue, indicating that the actions of both coactivators are required for the

mitochondrial biogenesis that takes place in the developing murine heart and brown adipose tissue (88).

3. PRC

Since the expression of PGC-1α is limited to certain tissues and physiological conditions, our lab was interested to look for other regulated coactivators that function through NRF-1 and display distinct biological functions. Searching the HUGE database (Kazusa DNA research institute) for similarities to PGC-1α, the closest related sequence was hypothetical protein KIAA0595, a protein with no assigned function, nor was it submitted as a full-length coding sequence (89). Although the overall sequence similarity to PGC-1α is on the lower side, the spatial organization of specific regions is conserved and significant sequence similarity can be found within these regions **(Figure 1.2)**. The highest homology between PGC-1α and PRC occurs at the N-terminus and the C-terminus. Both proteins contain an N-terminal transcriptional activation domain, including an acidic region and the LXXLL motif. The C-terminal region contains an RNA-binding motif and an arginine-serine-rich (RS) domain. In addition, there is a proline-rich region in the middle of both proteins that is more extensive in PRC, and is consistent with an unstructured conformation. Like PGC-1α, PRC augments NRF-1 dependent transcription of several promoters, presumably through its direct interaction (*in vitro* and *in vivo*) with the DNA-binding domain of NRF-1. In contrast to PGC-1α, PRC is expressed ubiquitously in murine and human tissues and is not cold-inducible. However, PRC is rapidly up regulated when quiescent, starved fibroblasts are induced to reenter the cell cycle in response to serum. It is interesting to note that PGC-1α is not expressed in quiescent or proliferating mouse 3T3 fibroblasts. Thus, it is likely that PGC-1α and PRC provide complementary functions in

governing mitochondrial biogenesis. The control of mitochondrial biogenesis in response to adaptive thermogenesis seems to be mediated specifically by PGC-1α, while PRC seems to govern mitochondrial biogenesis specifically in response to proliferative signals. It is not yet clear whether the other biological functions described so far for PGC-1α, like its role in glucose metabolism for example, can also be carried out by PRC.

Mitochondrial dysfunction

The involvement of mitochondrial dysfunction in a variety of human diseases, including diabetes, Parkinson's disease, cancer, and age-related disorders is increasingly recognized (90). Pathogenic mutations affecting mitochondrial oxidative phosphorylation cause mitochondrial diseases with very complex and varied clinical phenotypes. It is estimated that 1 in 5000 live births is affected by mitochondrial disorders. Examples of OXPHOS-related disorders in humans are Leigh syndrome, Friedreich's ataxia, lactic acidosis, encephalomyopathies, and opthalmoplegia. Common symptoms include neurodegeneration, muscle defects, deafness, blindness, diabetes and cardiomyopathy. OXPHOS diseases are unique in that they can be caused by defects in mitochondrial or nuclear DNA. Deletions, duplications and point mutations in mtDNA have been recognized for a long time as causes of mitochondrial disorders. A pathogenic mutation can be present in all copies (homoplasmy) or only in a fraction of all copies (heteroplasmy) of mtDNA in a somatic mammalian cell. Patients with heteroplasmic mtDNA mutations often have widely varying levels of mutated mtDNA in different organs, and even in different cells of a single organ. Therefore, patients with the same phenotype can have different genetic mutations, and patiens with the same mutation often display different phenotypes. This makes diagnosis of mitochondrial diseases a challenging task. Only more recently, nuclear genes

responsible for OXPHOS-related disorders have been identified, despite the fact that nuclear genes encode hundreds of proteins involved in mitochondrial biogenesis and oxidative phosphorylation (91). Nuclear DNA effects can result in impaired integrity and function of the respiratory chain complexes, and in defects affecting mtDNA transcription, translation or replication. The number of nuclear OXPHOS-related genes proven to be associated with mitochondrial disorders is increasing rapidly. The development of several mouse models of mitochondrial disease contributed greatly to the identification of these genes. Also, the study of transcriptional regulators that control the expression of nuclear genes important for mitochondrial function certainly helped accelerate this process. Dissecting the function of these regulatory factors is therefore of fundamental biological interest, and may lead to therapeutic interventions for human diseases associated with mitochondrial dysfunction. In particular, PGC-1α's role in many metabolic processes suggests it might be useful as a therapeutic target for diabetes or obesity (92). PGC-1α has also been implicated in Huntington's disease, Alzheimer's disease and Parkinson's disease (93) and Duchenne muscular dystrophy (94). It is interesting to note that some human diseases have been mapped to the PRC locus (chromosome 10q24.3-24.3) or to the vicinity thereof: an autosomal dominant progressive external ophtalmoplegia, type I, has been assigned to chromosome 10q23.3-23.4 and 10q23.31-25.1; Thiel-Behnke corneal dystrophy has been linked to 10q23-24 (89). It is intriguing to speculate that mutations in the PRC locus reduce NRF-1 target gene expression, which in turn compromises mitochondrial respiratory function. PRC is also significantly up regulated in thyroid oncocytomas, tumors characterized by mitochondrial proliferation (95).

Hopefully, the study of these transcriptional regulators of nuclear mitochondrial genes will help us to identify and further characterize the genes involved in mitochondrial diseases and find new approaches to fight these diseases in humans.

CHAPTER 2:

BACKGROUND

Most of this dissertation research builds on a project initiated by Ulf Andersson with the identification of the PGC-1-related coactivator PRC. As mentioned in the **Introduction (Chapter 1)**, our lab discovered PRC while searching the HUGE database (Kazusa DNA research institute) for regulated coactivators that function through NRF-1, like PGC-1α, and that display distinct biological function. We found that PRC was a 177 kDa protein with no significant overall sequence similarity to PGC-1α, but the spatial organization of specific regions and the sequence within those regions was conserved **(Figure 1.2)**. Unlike PGC-1α, which is highly tissue-specific, PRC is ubiquitously expressed in murine and human tissues. Rabbit anti-PRC(95-533) serum was prepared and confocal immunofluorescence microscopy revealed that PRC predominantly localizes to the nucleus, as is expected for a transcriptional coactivator. In contrast to PGC-1α, PRC is not cold-inducible, suggesting that these proteins likely have distinct functions in adaptive thermogenesis. However, expression of PRC was found to be up regulated rapidly and robustly upon serum-stimulation of quiescent, starved Balb/3T3 fibroblasts. PRC expression was induced within 3 hours and was maintained for at least 12 hours. Notably, PGC-1α is not expressed in either quiescent or proliferating Balb/3T3 cells, again suggesting distinct roles for these two related coactivators. In analogy with PGC-1α, the ability of PRC to co-activate NRF-1-dependent promoters was tested. When co-transfected with NRF-1, PRC was able to activate a 4xNRF1/luc construct approximatly 3-fold. Testing different promoters, it was shown that the δ-ALAS promoter was the most responsive to PRC (5-fold activation of the basal activity). When either of the two NRF-1 sites in this promoter was mutated, PRC activation was

diminished two- to threefold; when both were mutated, PRC was not longer able to co-activate this promoter. The cyt c and Tfam promoter are also responsive to PRC, although to a lesser extent (~2-fold activation). Consistent with its co-activation of NRF-1 dependent promoters, PRC was found to interact directly with NRF-1 *in vitro* and *in vivo*. S-protein pull-down assays showed that two domains of PRC, encompassing PRC amino acids 95 to 533 and amino acids 1379 to 1664, interact with the DNA binding domain of NRF-1. In order to map the PRC activation domain, a series of fusion proteins between PRC and the GAL4 DNA binding domain were expressed in mouse fibroblasts and tested for their ability to activate the 5xGAL4 luciferase reporter plasmid in transient transfection assays. A potent activation domain was found in the PRC amino-terminal region, on either side of residue 133. Interestingly, this region shows significant sequence similarity with the amino-terminus of PGC-1α, and the PGC-1α activation domain has been mapped to this region. It was also confirmed that the PRC activation domain is required for its ability to co-activate NRF-1.

The ability of PRC to activate transcription from several NRF-1 dependent promoters through a direct interaction with the DNA-binding domain of NRF-1 is remarkably similar to its related family member(s), PGC-1α (and PGC-1β). PGC-1α is considered to be a master player in mitochondrial biogenesis, in part through this direct interaction with NRF-1. The structural and functional similarity between PGC-1α and PRC supports a regulatory role for PRC in mitochondrial biogenesis. Given that PRC is only modestly cold-induced but is rapidly induced upon serum-stimulation of starved fibroblasts, conditions where PGC-1α is not expressed, it seems likely that both coactivators provide complementary functions in mitochondrial biogenesis.

We hypothesize that PRC is an important regulator of mitochondrial function in response to proliferative signals.

Additional evidence is needed to demonstrate an *in vivo* role for PRC in mitochondrial biogenesis. We propose to design a combination of gain- and loss-of-function studies to test this hypothesis. We expect that PRC suppression and ectopic expression will help us to identify the downstream events for which PRC is important. We hypothesize that the signaling pathway leading to mitochondrial biogenesis will be seriously disturbed, by the resulting effects on NRF-1 and NRF-2 target gene expression.

To establish an *in vivo* role for PRC in mitochondrial biogenesis we wanted to suppress PRC function by RNA interference. It has been a long road to obtain successful silencing of PRC. In our first attempt, we used a chemically synthesized small interfering RNA (siRNA) obtained from Dharmacon. To select a sequence for siRNA duplex design, it was advised to start 75 bases downstream from the start codon and to locate the first AA dimer, and to record the next 19 nucleotides following the AA dimer. Upon transfection of mouse Balb/3T3 fibroblasts with a PRC siRNA or a control siRNA duplex that targets the luciferase mRNA using Oligofectamine (Invitrogen), down regulation of the luciferase message was seen but no suppression of PRC mRNA or protein was detected. Because of the high costs of chemically synthesized siRNAs we decided not to develop more siRNA duplexes and to discontinue this option.

Around the same time, Ambion introduced a new kit to construct siRNA oligonucleotides by *in vitro* transcription with T7 RNA polymerase. Hereby, two 29-mer DNA oligonucleotides, with 21 nucleotides encoding the siRNA and 8 nucleotides complementary to the T7 promoter primer, are synthesized and desalted. In separate reactions, the two siRNA oligonucleotide

templates are hybridized to a T7 promoter primer. The 3' ends of the hybridized oligonucleotides are extended with Klenow DNA polymerase to create double-stranded siRNA transcription templates. The sense and antisense siRNA templates are then transcribed separately by T7 RNA polymerase and the resulting RNA transcripts are hybridized to create double-stranded RNA. Following RNase digestion and clean-up, the end product is a double-stranded 21-mer siRNA with 3' terminal uridine dimers that can be transfected into mammalian cells to reduce the expression of the target mRNA. We generated a 3 siRNAs targeting PRC mRNA and a siRNA specific to the GAPDH gene (with the sense and antisense control DNA template supplied with the kit). Using a variety of transfection reagents (Lipofectamine 2000 (Invitrogen), Oligofectamine (Invitrogen) or siPORT Lipid (Ambion)) to introduce these double-stranded siRNAs into Balb/3T3 cells, we were able to detect some reduction of the control GAPDH mRNA, but no reduction of GAPDH protein, PRC target mRNA and protein was detected.

We think our inability to silence PRC in both of these systems resulted from rather low transfection efficiency and the use of older, more primitively designed RNA duplexes, causing them to be rather inefficient. Also, although we tested multiple siRNAs targeting PRC with the Ambion *in vitro* transcription kit, we only tested one chemically synthesized siRNA from Dharmacon, which is not a sufficient number to get good gene silencing for most genes. Not all shRNAs for a certain gene have the same (if any) silencing effect, and the current literature recommends synthesizing at least 4 duplexes for each gene (96). Another possibility we considered, is that PRC is a gene that cannot be silenced by RNA interference. It has been reported that low abundant genes and genes that are more tightly regulated are much harder to suppress by gene silencing (97).

The mammalian RNA interference field advanced rapidly while we were working on this project. It became possible to deliver short hairpin RNAs (shRNAs) into mammalian cells by a DNA plasmid vector or viral vector. Next, we chose to retrovirally deliver PRC shRNAs using a system based on the research article by Devroe and Silver (98) to facilitate entry of shRNAs into cells and to obtain stable knockdown cells. The authors combine two well-described and commercially available systems, pSilencer 1.0/U6 (Ambion) and pMSCVpuro (BD Biosciences). Our slightly different approach used the vector pMSCV-IRES-GFP (a gift from Dr. Neil Clipstone, Loyola University), which is identical to pMSCVpuro with the exception that the puromycin cassette has been replaced by the IRES-GFP cassette. We synthesized 4 different shRNAs targeting PRC to account for the fact that the duplexes will affect PRC silencing to a different degree. Each shRNA was synthesized, annealed, kinase-treated and ligated into pSilencer 1.0/U6. Next, the U6 promoter and the oligonucleotide region complementary to PRC was liberated from pSilencer 1.0/U6-PRC by restriction digest and inserted into pMSCV-IRES-GFP, generating pMSCV-IRES-GFP/U6-PRC. An additional plasmid containing an irrelevant hairpin was similarly constructed to serve as our negative control, thereby generating pMSCV-IRES-GFP/U6-control. The vectors pMSCV-IRES-GFP/U6-PRC#1-4 and pMSCV-IRES-GFP/U6-control were packaged in Phoenix Eco cells (provided by Dr. G. Nolan, Stanford University). Viral supernatant was collected 48 h post-transfection, pelleted for removal of non-adherent cells and cellular debris, and used to infect Balb/3T3 fibroblasts. Infection efficiency was assessed by following GFP expression with a fluorescent microscope. Selection with puromycin was not possible anymore since the puromycin cassette was replaced by IRES-GFP in our vector, but usually nearly all the cells were infected. Unfortunately, we were not able to detect any reduction in PRC mRNA or protein with each of the 4 different shRNAs tested.

Additionally, we purchased a commercially available vector from Open Biosystems expressing a PRC shRNA. For most genes multiple constructs were available, containing different duplexes, but there was only one construct for PRC. This construct was used to transiently transfect Balb/3T3 fibroblasts and was also integrated into a retrovirus to obtain stable expression in Balb/3T3 cells. Perhaps not very surprisingly, we were unsuccessful in obtaining good gene silencing.

Therefore, we used an alternative approach by constructing a dominant-negative form of PRC that only expresses the NRF-1/CREB interaction domain of PRC. We hypothesized this subfragment would suppress wild type PRC function by interacting with most or all NRF-1 and CREB molecules available in the cell, thus making it impossible for wt PRC to function properly. Expression of this PRC subfragment from a lentiviral vector inhibits respiratory growth on galactose in Balb/3T3 fibroblasts (99) **(Chapter 4, Figure 4.8)**, suggesting that PRC plays a role in respiratory chain expression *in vivo*. However, we were concerned that a dominant negative form of PRC interacts with many other molecules in the cell, and can therefore have many non-specific effects that are not directly mediated by PRC.

Our good experience with a lentiviral expression system and more advances in the RNA interference landscape triggered us to use a similar system to express newly designed PRC short hairpin RNAs to further dissect the *in vivo* role of PRC. This has been described in detail in **Chapter 6** (100).

Determining the *in vivo* actions of PRC on mitochondrial biogenesis and function by gain-of-function studies has also provided us with a few obstacles to overcome. Because this project was initiated by our lab with the discovery of PRC, many steps that were so crucial had to be optimized from scratch. For example, it required the development of three antibodies

against different epitopes of PRC and optimization of our Western blotting techniques to detect PRC protein.

Over expression of PRC, either by establishing a stable cell line or by retrovirus infection had previously not been successful (unpublished results – personal communication with Ulf Andersson). Although we were able to over express PRC mRNA to high levels, no induction of PRC protein was seen. Consequently, no induction of NRF-1 target genes was observed. We thought perhaps PRC is regulated post-transcriptionally or perhaps the protein is actively degraded to prevent its accumulation beyond physiological levels. However, as seen in **Chapter 4**, we later rejected both of these theories. The regulation of PRC induction occurs mostly at level of transcription **(Figure 4.1 and not shown)**. Furthermore, we were able to demonstrate expression of FL PRC protein above physiological levels upon transient transfection of HEK 293 cells with the mammalian expression vector FL PRC/pSV SPORT, constructed previously by Ulf Andersson in the lab **(Figure 4.2)**. However, no effects on gene expression were observed in HEK 293 cells producing large amounts of PRC protein (not shown). We contribute this to the fact that these cells are highly transformed, and are probably not a good system to study PRC, which is growth-regulated by serum. Because the other cell lines we work with exhibit low efficiency of transfection, we decided to use an adenoviral expression system. We had previously used an adenoviral vector from Dr. D.P. Kelly (Burnham institute for Medical Research, Orlando), constructed using the AdEasy system developed by the group of Vogelstein (101), to ectopically over express PGC-1α in cultured cells **(Chapter 3, Figure 3.10)**. Because of our success with PGC-1α, we decided to use the same system to over express PRC. All the necessary plasmids and cells were purchased from ATCC. This system involves a homologous recombination step in bacteria whereby the AdEasy-1 plasmid is recombined with pAdTrack-

CMV containing the gene of interest, thereby creating the recombinant adenviral plasmid. ATCC provided us with competent cells (AdEasier-1 cells) already containing the pAdEasy-1 plasmid. Initially, we had to screen far more bacterial recombinants than was described in order to obtain one that was correct. The adenoviral plasmids were transfected into the HEK 293 packaging cell line to start viral production. However, no cytopathic effect was observed. Increasing transfection efficiency or incubation time had no influence. We thought perhaps the full length PRC cDNA (~5kB) was too big to be packaged into adenovirus and decided this system was not suitable for over expressing PRC. More than two years later we received a letter from ATCC stating that the AdEasier-1 cells previously sent to us contain an AdEasy-1 plasmid that is missing a piece of DNA! Upon obtaining the right vector, we have since revisited this project as described in **Chapter 7**.

CHAPTER 3:

CONTROL OF MITOCHONDRIAL TRANSCRIPTION SPECIFICITY FACTORS (TFB1M AND TFB2M) BY NUCLEAR RESPIRATORY FACTORS (NRF-1 AND NRF-2) AND PGC-1 FAMILY COACTIVATORS

INTRODUCTION

The biogenesis of mitochondria requires the expression of a large number of genes encoded by both nuclear and mitochondrial genetic systems (5). However, because the protein coding capacity of mtDNA is limited to 13 respiratory subunits, nuclear genes must provide the vast majority of products required for mitochondrial oxidative functions and biosynthetic capacity. In addition, nuclear genes must play a predominant role in controlling mitochondrial transcription, translation and DNA replication.

Understanding the transcription and replication of mtDNA has been a major focus (4,102). The majority of evidence points to a mechanism of bi-directional replication where the replication origins for the two strands, termed heavy (H) and light (L) based on their buoyant densities, are displaced by about two-thirds of the genome. The D-loop regulatory region contains bi-directional promoters, (HSP) and (LSP), for transcribing H and L strands as well as the H-strand replication origin (O_H). The activities of both HSP and LSP require a 15 nucleotide conserved sequence motif that defines the core promoter. In addition, both promoters share an upstream enhancer that serves as the recognition site for Tfam (previously mtTF-1 and mtTFA) an HMG box protein that stimulates transcription through specific binding to the upstream enhancers.

In yeast, transcription is directed by a 145kD core polymerase and a 43kD specificity factor, also known as sc-mtTFB. The polymerase and specificity factor transiently interact and both are required for specific transcription initiation *in vitro* (103). A vertebrate polymerase and a specificity factor have been characterized biochemically in *Xenopus laevis* (104) and a cDNA that encodes human mitochondrial RNA polymerase has been isolated (13). Most recently, two isoforms of a human mitochondrial transcription specificity factor, termed TFB1M and TFB2M (also known as h-mtTFB), have also been identified (16,17). Although TFB1M has about one-tenth the transcriptional activity of TFB2M, both proteins work together with Tfam and mtRNA polymerase to direct proper initiation from HSP and LSP. Like sc-mtTFB, both TFBs are also related to rRNA methyltransferases and TFB1M can bind S-adenosylmethionine and methylate mitochondrial 12S rRNA (17,19). Interestingly, TFB1M can also contact the carboxy-terminal domain of Tfam (18). The region of contact between TFB1M and Tfam is essential for transcriptional activation and corresponds to a 29 amino acid domain that was previously identified as a Tfam activation domain.

A number of recent studies have contributed insights into the pathways regulating mitochondrial biogenesis in mammalian systems. The evidence supports a model whereby regulated coactivators communicate physiological signals to specific transcription factor targets. These events result in the activation of genes required for mitochondrial biogenesis and respiratory function (43,105). Two transcription factors, NRF-1 and NRF-2, act on the majority of nuclear genes encoding subunits of the respiratory complexes. They are also involved in the expression of mitochondrial transcription and replication factors (Tfam and MRP RNA), heme biosynthetic enzymes and other proteins required for respiratory function. Recently, consensus NRF-2 recognition sites have been observed in TFB1M and TFB2M promoters from both human

and mouse (16,17,106), suggesting that NRFs may be important regulators of these genes as well.

In addition to these transcription factors, a transcriptional coactivator, designated PGC-1α, can induce mitochondrial biogenesis by interacting with NRF-1 (54), PPARα (65) and possibly other nuclear factors. PGC-1α is markedly up-regulated in brown fat during adaptive thermogenesis and can induce mitochondrial biogenesis when expressed ectopically in cultured cells or in transgenic mice (54,55). A second coactivator, designated as PGC-1 related coactivator (PRC), has several structural features in common with PGC-1 including an activation domain, an LXXLL coactivator signature, and an RNA recognition motif (89). Unlike PGC-1α, PRC is not significantly induced during adaptive thermogenesis but is induced upon cell proliferation and down regulated when cells exit the cell cycle upon contact inhibition or withdrawal of serum. Both PGC-1α and PRC can *trans*-activate NRF-1 target genes that are necessary for the biogenesis of mitochondria and the expression of a functional respiratory chain (54,89). Both coactivators interact with NRF-1 *in vitro* and *in vivo* and a dominant negative allele of NRF-1 interferes with the mitochondrial proliferation by PGC-1α. Thus, the functional interplay between these factors appears to define a major regulatory pathway for the biogenesis of mitochondria.

It is of considerable interest to determine how the mtDNA transcriptional apparatus is controlled in the biogenesis of vertebrate mitochondria. The recent discovery of TFB1M and TFB2M raises the question of whether these factors are subject to regulatory pathways involving PGC-1 family coactivators and the nuclear respiratory factors. The coordinate control of the TFBs and Tfam would implicate a common set of nuclear factors in integrating the transcription

and replication of mtDNA with a program of mitochondrial biogenesis. The current study is directed at elucidating the involvement of this pathway in TFB expression.

RESULTS

Authentic recognition sites for nuclear respiratory factors 1 and 2 reside in the human TFB promoters. Nuclear respiratory factors (NRFs) have been implicated in the expression of both Tfam and MRP RNA, key constituents of the mitochondrial transcription and replication machinery. To explore whether TFB expression is also governed by NRFs, we cloned the human TFB promoters **(Figure 3.1)**. A search for transcription factor binding sites revealed relatively simple promoter structures consisting of recognition sites for NRF-1, NRF-2 and Sp1. In addition, the TFB1M promoter has a consensus AP-1 site. Both promoters have tandem NRF-2 sites and a NRF-1 site in close proximity to the transcription start site. In addition, the TFB1M promoter has two upstream Sp1 sites flanked by NRF-2 sites whereas the TFB2M promoter has a single upstream Sp1 site. A similar configuration of NRF and Sp1 sites has been observed in many well-characterized genes that are essential to the expression and function of the respiratory chain.

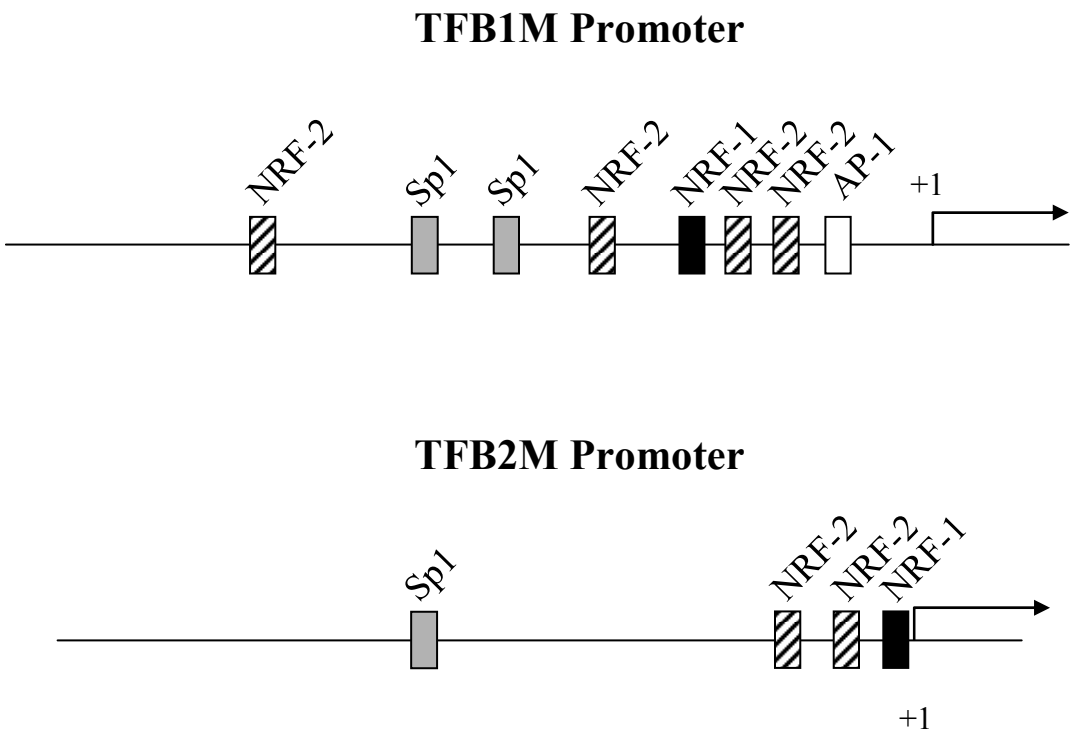

Figure 3.1. Schematic representation of hTFB1M and hTFB2M promoters.

The hTFB1M promoter was identified by aligning the CGI-75 cDNA (accession number NP_057104) corresponding to hTFB1M (17) with the human genomic sequence from chromosome 6 encoding this gene (accession number AL139101). The hTFB2M promoter was identified by aligning the human cDNA (accession number NM_022366) with the human genomic clone from chromosome 1 (accession number AL356583). The *cis*-acting elements, denoted by labeled rectangular boxes, were initially identified by the Match^{TM} internet search tool and by visual inspection of the sequence.

As shown in **Figure 3.2A**, the TFB1M and 2 NRF-1 sites are near perfect matches to the NRF-1 consensus and contain all of the essential nucleotides that are invariant in a large number of functional NRF-1 recognition sites (43). Similarly, the TFB NRF-2 sites contain the GGAA motifs that are characteristic of the binding sites for ETS family transcription factors, of which NRF-2 is a member **(Figure 3.2B)**. As originally observed in the COXIV promoter, these sites are often tandemly arranged in respiratory genes to promote cooperative high-affinity binding of NRF-2 (42,107). Like the COXIV promoter, both TFB promoters contain tandem NRF-2 sites that are separated by 16 nucleotides **(Figure 3.2B)**. This conservation of spacing suggests that cooperative binding of NRF-2 to these promoters may occur as well.

A

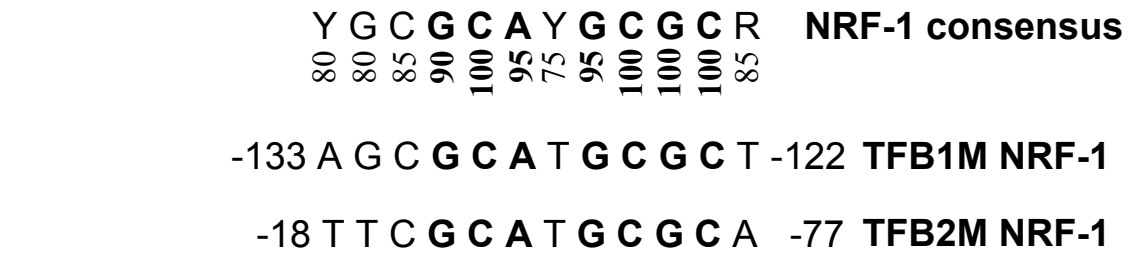

B

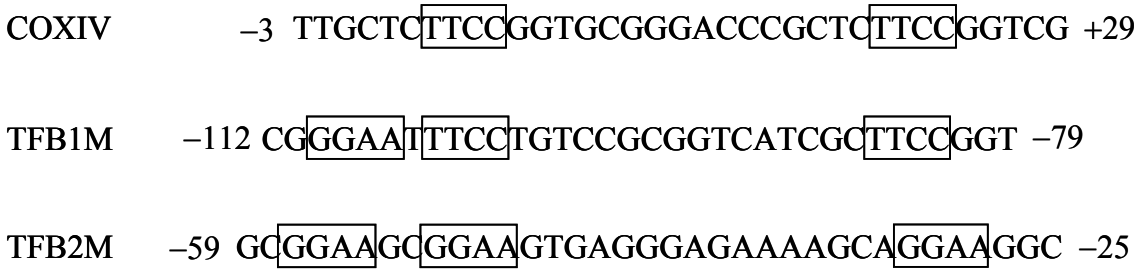

Figure 3.2. Comparison of hTFB NRF-1 and NRF-2 sites.

A. NRF-1 sites from hTFB1M and hTFB2M are compared to the consensus. Numbers below the consensus represent the percentage representation of the nucleotide at that position in over 20 functional NRF-1 sites. Highly invariant nucleotides are in boldface.

B. Comparison of tandemly arranged NRF-2 sites in the TFB promoters to those present in the COXIV promoter in which they were first identified. The GGAA core motifs are boxed. Numbers adjacent to the sequences denote the nucleotide positions relative to the mRNA 5' ends.

Both HeLa cell nuclear extract and purified recombinant NRF-1 were compared for their ability to form specific DNA-protein complexes with the TFB NRF-1 sites. As shown in **Figure 3.3**, DNA-protein complexes were formed using radiolabeled TFB1M and TFB2M NRF-1 oligomers. The complexes formed using crude nuclear extract or recombinant NRF-1 displayed identical electrophoretic migrations and were competed away by an excess of an unlabeled oligomer containing an authentic cytochrome *c* NRF-1 recognition sequence. The TFB-NRF-1 complexes were also "supershifted" upon inclusion of goat anti-NRF-1 serum in the binding reactions confirming that NRF-1 is present in the complex. Complexes formed with either TFB site were also competitively displaced by excess oligomers containing either site but not with those synthetic oligomers where essential guanine nucleotide contacts were mutated. No shifted complexes were observed in the absence of extract or recombinant protein (not shown). These results establish that the TFB NRF-1 sites are indistinguishable from those present in other respiratory gene promoters.

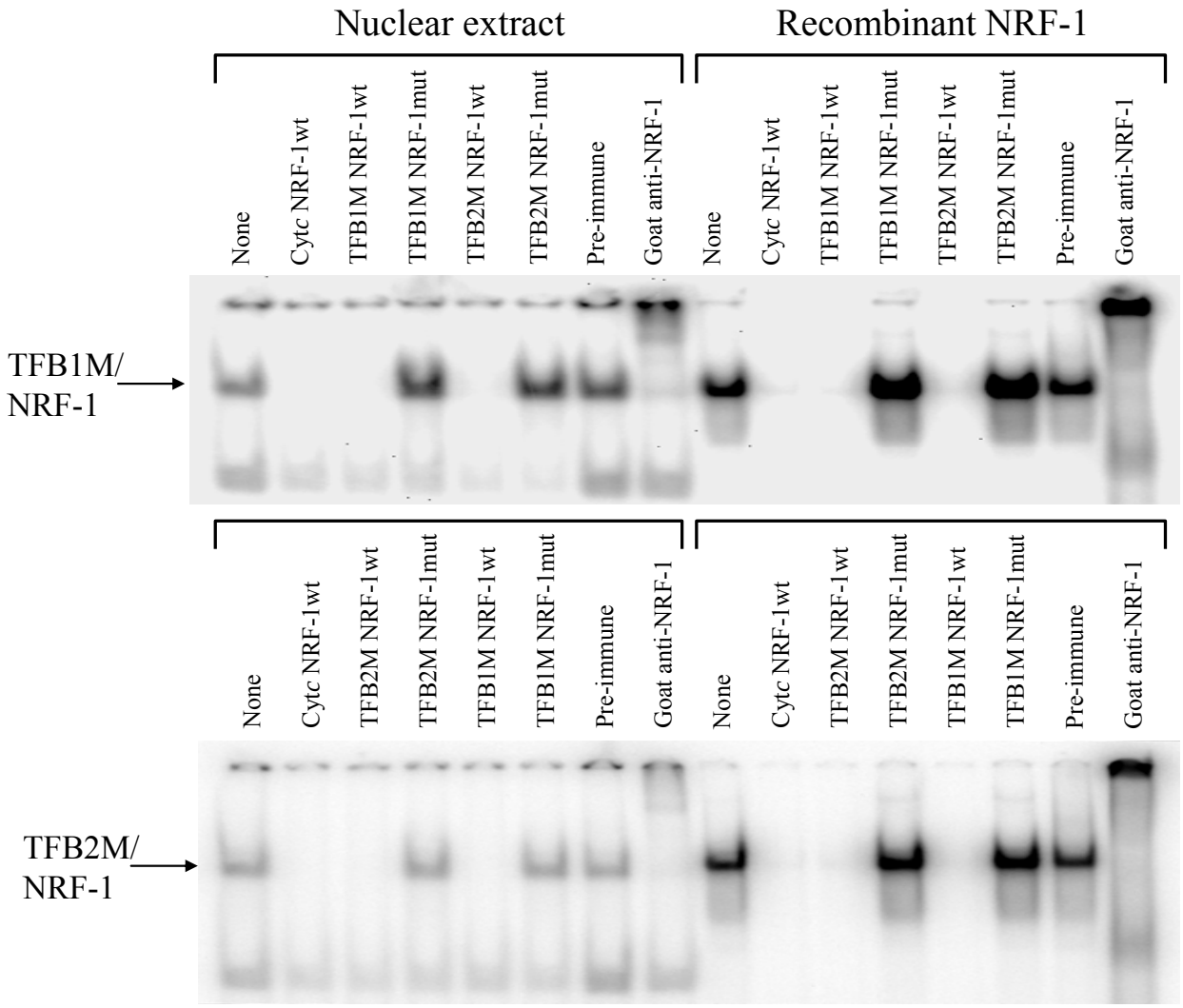

Figure 3.3. Specific binding of NRF-1 to recognition sites within the hTFB1M and hTFB2M promoters.

Radiolabeled synthetic oligonucleotides containing either the TFB1M or TFB2M NRF-1 sites were bound to either crude nuclear extracts or purified recombinant NRF-1 and the complexes (indicated by the arrow) separated by gel electrophoresis. The unlabeled competitor oligonucleotide or the supershifting antiserum added to the binding reaction are indicated above each lane.

Similar DNA binding experiments were conducted by comparing radiolabeled oligomers containing the tandem NFR-2 sites from the COXIV, TFB1M and TFB2M promoter regions. As shown in **Figure 3.4A**, identically migrating DNA-protein complexes were formed with all three synthetic NRF-2 oligomers using a crude heparin agarose chromatography fraction prepared from a HeLa cell nuclear extract. Fractionation of nuclear extracts on heparin agarose is necessary for detection of the NRF-2 DNA binding activity present in crude nuclear extracts (42). The complexes included a rapidly migrating complex containing the DNA-binding α subunit, a doublet of intermediate migration containing the α/γ and α/β heterodimers and a slowly migrating heterotetrameric α_2/β_2 complex **(Figure 3.4A)**. All of the complexes were competitively displaced by an excess of unlabeled COXIV oligomer containing authentic NRF-2 sites as well as by TFB1M and TFB2M NRF-2 oligomers. In addition, all of the complexes were "supershifted" by inclusion of rabbit anti-NRF-2α serum in binding reactions because they all contain the α-subunit. In contrast, only those complexes containing the β-subunit (α/β and α_2/β_2) were "supershifted" by inclusion of rabbit anti-NRF-$2\beta_1$ serum.

These results were confirmed using purified recombinant α and β_1 subunits. As shown in **Figure 3.4B**, the migration of DNA-protein complexes formed with recombinant subunits was identical for all 3 radiolabeled oligomers as was their ability to be "supershifted" by anti-NRF-2α and anti-NRF-$2\beta_1$ sera. Likewise, the complexes formed between a mixture of recombinant α and β_1 subunits and labeled COXIV, TFB1M or TFB2M NRF-2 oligomers were competed away by an excess of unlabeled oligomer containing each site but not by those where the GGAA binding motif had been mutated. No shifted complexes were observed in the absence of extract or recombinant protein (not shown). These results establish the authenticity of the TFB NRF-2 sites and their specificity of interaction with the transcription factor.

Figure 3.4. Specific binding of NRF-2 to recognition sites within the hTFB1M and hTFB2M promoters.

A. Radiolabeled synthetic oligonucleotides containing COXIV, hTFB1M or hTFB2M recognition sites were bound to an aliquot of partially purified nuclear extract that was eluted from heparin agarose at 0.25M NaCl. The indicated DNA/protein complexes were separated by gel electrophoresis. The unlabeled competitor oligonucleotide or the supershifting antiserum added to the binding reactions are indicated above each lane.

B. The same radiolabeled oligonucleotides as in panel *A* were bound to either recombinant NRF-2α (rec α) or a mixture of recombinant NRF-2α and NRF-2β_1 (rec α + β_1). The indicated DNA/protein complexes were separated by gel electrophoresis. The unlabeled competitor oligonucleotide or the supershifting antiserum added to the binding reactions are indicated above each lane.

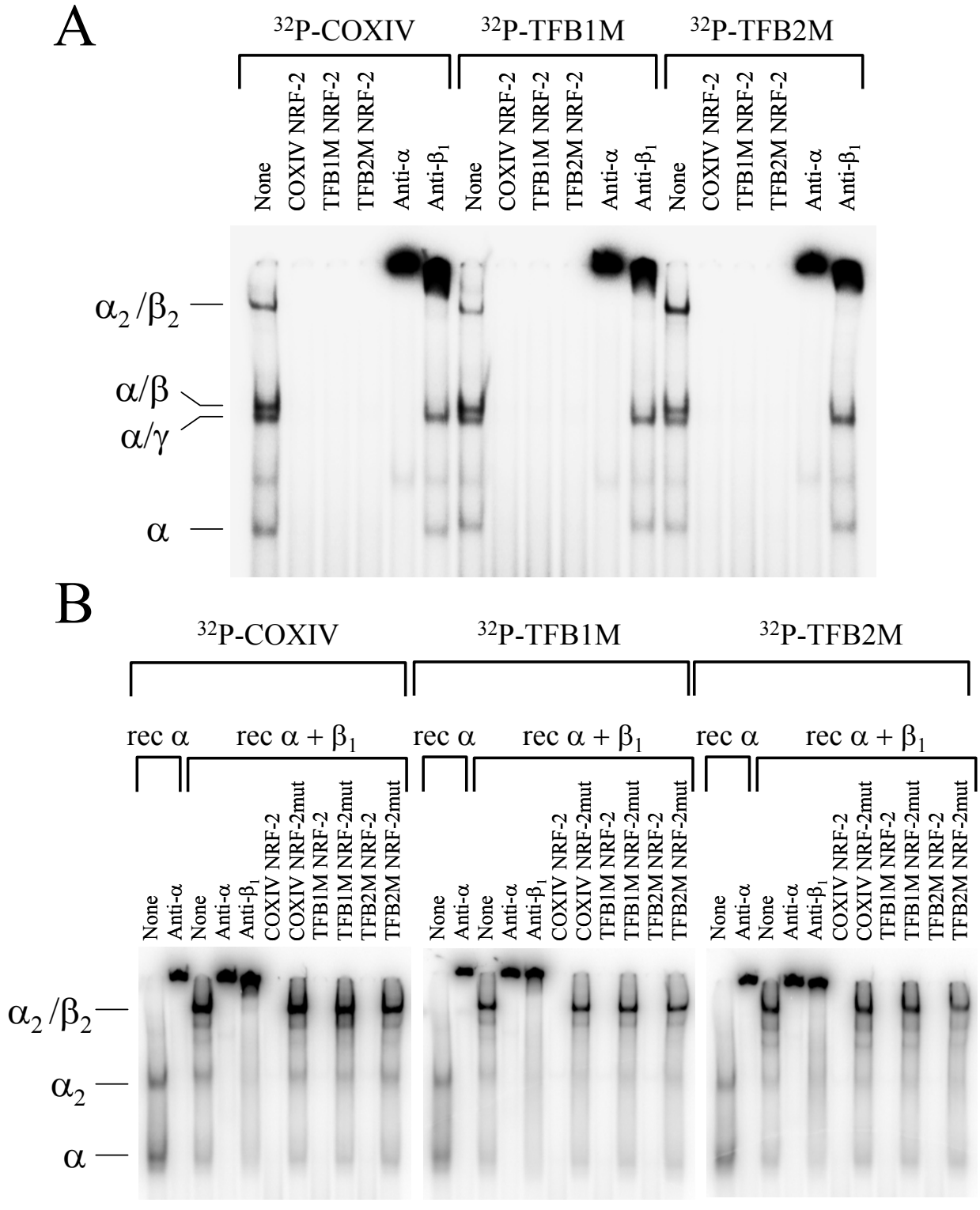
A
32P-COXIV
32P-TFB1M
32P-TFB2M
None
COXIV NRF-2
TFB1M NRF-2
TFB2M NRF-2
Anti-α
Anti-β1
α2/β2
α/β
α/γ
α
B
32P-COXIV
32P-TFB1M
32P-TFB2M
rec α
rec α + β1
None
Anti-α
Anti-β1
COXIV NRF-2
COXIV NRF-2mut
TFB1M NRF-2
TFB1M NRF-2mut
TFB2M NRF-2
TFB2M NRF-2mut
α2/β2
α2
α

Nuclear respiratory factors are major determinants of TFB promoter function. It was of interest to investigate the functional contribution of the NRF-1 and NRF-2 recognition sites within the context of the TFB1M and TFB2M promoters. To this end, a series of 5' deletions and point mutations were constructed in luciferase reporter plasmids and their effects on promoter function assayed by gene transfection. The 5' deletions were designed to progressively remove the sequences identified as transcription factor binding sites. As depicted in **Figure 3.5**, deletion of the TFB1M promoter to –316, removing the NRF-2 site most distal to the transcription start site, had little effect on activity whereas deletion to –201, removing the tandem Sp1 sites, increased activity several-fold. Competition mobility shift and supershifting assays demonstrated that these sites actually bind Sp1 (not shown). The results suggest that the Sp1 sites function as negative elements within the context of this promoter. Progressive removal of a second NRF-2 site by deletion to –143 reduced activity to 60 percent of wild-type but less than 20 percent of the –201 deletion indicating that this site exerts a strong positive effect on the truncated –201 promoter. Further deletion to –117, removing the NRF-1 site, resulted in an additional 9-fold reduction in activity to a level approximately 14-fold below wild-type. Removal of the tandem NRF-2 sites by deletion to –71 markedly reduced activity to minimally detectable levels with no significant further reduction observed by removal of the AP-1 site by deletion to –26. These results demonstrate that the NRF sites between –201 and –71 constitute major determinants of promoter function.

The results were confirmed by altering some of the key elements by the introduction of point mutations. In contrast to the Sp1 deletion, point mutations in the Sp1 sites increased activity by only 20 percent suggesting that upstream elements exert a compensatory positive effect upon removal of these sites. Again, competition mobility shift and supershifting assays

demonstrated that the wild-type but not the mutant sites bound Sp1 (not shown). Point mutations in the NRF-1 site exerted a large negative effect on promoter activity confirming its importance to promoter function. Interestingly, mutation of one of the tandem NRF-2 sites reduced activity several-fold whereas mutation of both reduced activity about 50-fold. This apparent cooperativity most likely results from the high affinity binding of the NRF-2 heterotetramer to these tandem sites.

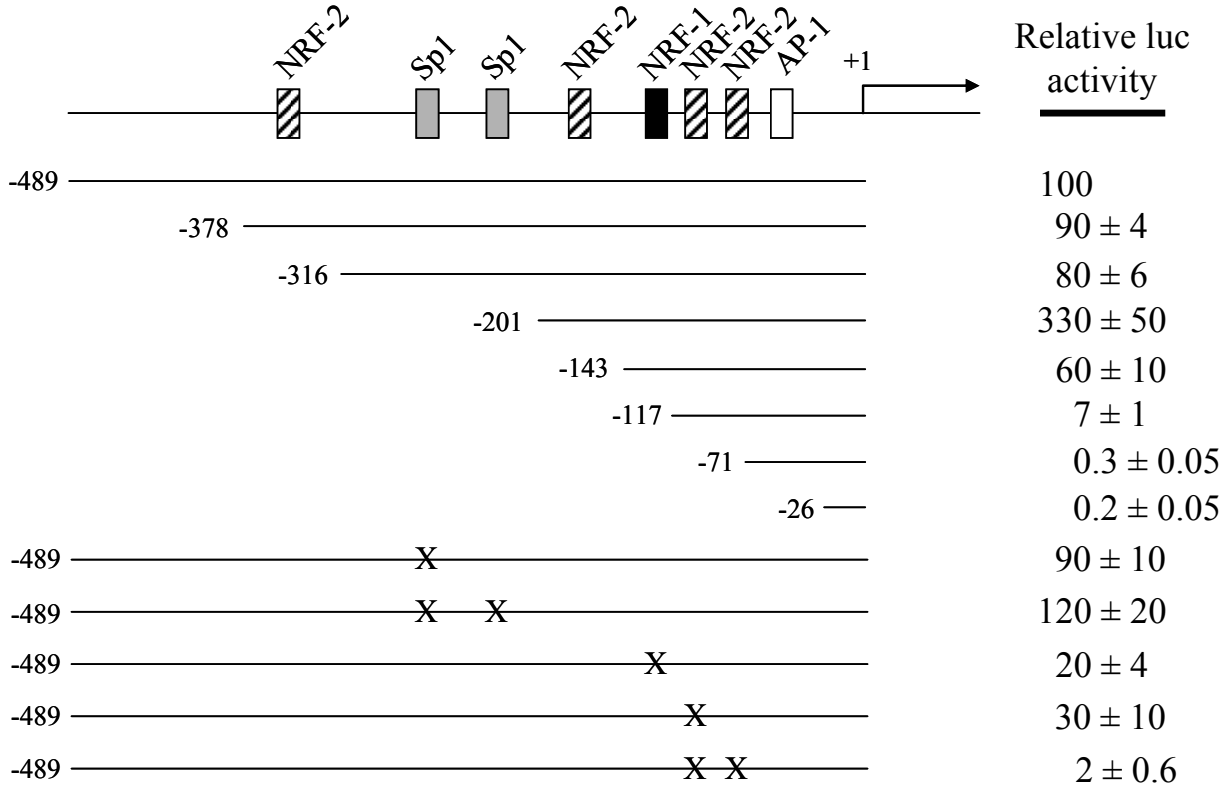

Figure 3.5. Mutational analysis of the hTFB1M promoter region.

A series of 5' deletions designed to progressively remove putative *cis*-acting elements was analyzed by gene transfection. The normalized luciferase activity obtained from the promoter fragment containing 489 nucleotides of 5' flanking DNA (-489) was designated as 100 percent. Point mutations represented by X were introduced into the –489 promoter as described under "Materials and Methods". The activities of all of the mutated promoters were expressed as a percentage of that obtained from the -489 promoter. Numbers represent the average ± standard error for three separate determinations.

A similar analysis was performed on the TFB2M promoter **(Figure 3.6)**. Deletion to –272 exerted a small positive effect on activity whereas deletion to –80, removing the single Sp1 site, modestly reduced activity to 60 percent of wild-type. As with the TFB1M promoter, the largest negative effects on activity occurred upon deletion of the NRF-1 and NRF-2 sites that are proximal to the transcription initiation site. Removal of the NRF-2 sites by deletion to –26 reduced activity to 1 percent of wild-type levels while further deletion of the NRF-1 site essentially eliminated any residual activity. Surprisingly, point mutations in the NRF-1 site alone had no effect on promoter activity, again suggesting that compensatory effects occur in the context of the full promoter. In addition, although mutation of the tandem NRF-2 sites reduced activity significantly, the synergism observed in the TFB1M promoter was not observed. However, combined mutation of all three NRF sites reduced activity over 30-fold to near background levels. These results are indicative of strong interactions between the NRF-1 and NRF-2 sites within the TFB2M promoter context.

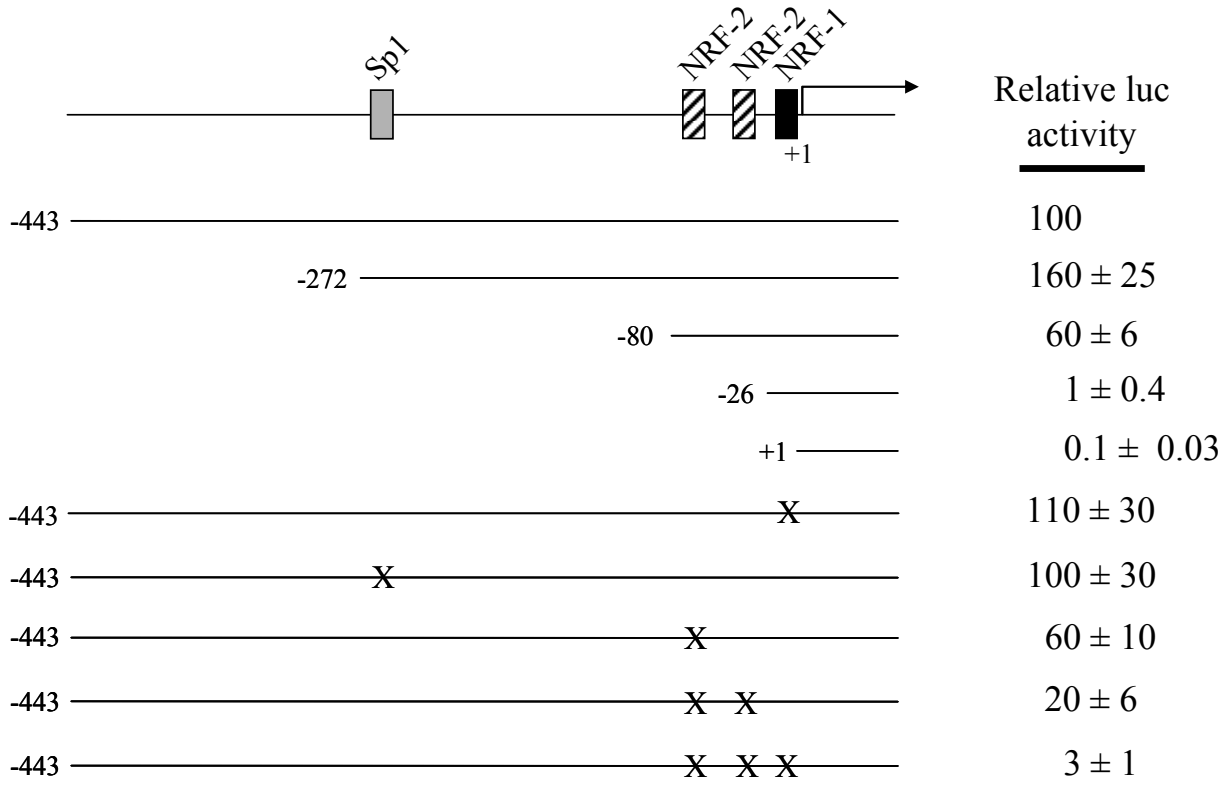

Figure 3.6. Mutational analysis of the hTFB2M promoter region.

A series of 5' deletions designed to progressively remove putative *cis*-acting elements was analyzed by gene transfection. The normalized luciferase activity obtained from the promoter fragment containing 443 nucleotides of 5' flanking DNA (-443) was designated as 100 percent. Point mutations represented by X were introduced into the –443 promoter as described under "Materials and Methods". The activities of all of the mutated promoters were expressed as a percentage of that obtained from the -443 promoter. Numbers represent the average ± standard error for three separate determinations.

NRF-1 and -2 binding sites in the TFB promoters are targets for *trans*-activation by the PGC-1 family coactivators. Regulation of mitochondrial biogenesis occurs through the induction of PGC-1α coactivator and its subsequent interaction with NRF-1 and other transcription factors (54). Both PGC-1α and PRC act through NRF-1 to induce NRF-1 target genes (89). *Trans*-activation experiments were performed in order to investigate the potential role of these coactivators in TFB gene expression. As shown in Figs. 3.7 and 3.8, both TFB promoters are *trans*-activated to an equivalent degree by PGC-1α and PRC. To identify the *cis*-elements that are required for the enhancement of promoter activity by the coactivators, each of the TFB promoter deletions was tested in the assay. It is clear that the full-length TFB1M promoter and the –201 deletion are similarly *trans*-activated by both PGC-1α and PRC **(Figure 3.7A)**. Further deletion beyond –201 removes the NRF sites that contribute most to promoter function and by deletion to –71, promoter activation is reduced to uninduced levels.

The requirement for the TFB1M NRF sites for promoter activation by the coactivators was confirmed by point mutation. As shown in **Figure 3.7B**, elimination of the Sp1 sites alone had no effect on promoter induction by either coactivator whereas mutation of the major NRF-1 and NRF-2 sites reduced or eliminated *trans*-activation by both coactivators. Similar experiments were conducted on the TFB2M promoter region. The results show that the -80 promoter, containing only the NRF sites, can support near maximal levels of *trans*-activation by PGC-1α or PRC **(Figure 3.8)**. Deletions removing these sites reduce or abolish promoter activation. The results support the conclusion that the NRF sites most proximal to the transcription start sites in both TFB promoters are the major targets for coactivator *trans*-activation.

Figure 3.7. *Trans*-activation of the hTFB1M promoter and its mutated derivatives by PGC-1α and PRC.

A. The hTFB1M promoter deletions shown in **Figure 3.5** were assayed for *trans*-activation by PGC-1α **(gray fill)** and PRC **(black fill)** by cotransfection with vectors expressing each coactivitor. Values are the average fold activation for three separate determinations ± standard error measured relative to the pSVsport negative control.

B. Same as panel *A* except that the indicated point mutations were assayed for *trans*-activation by the coactivators.

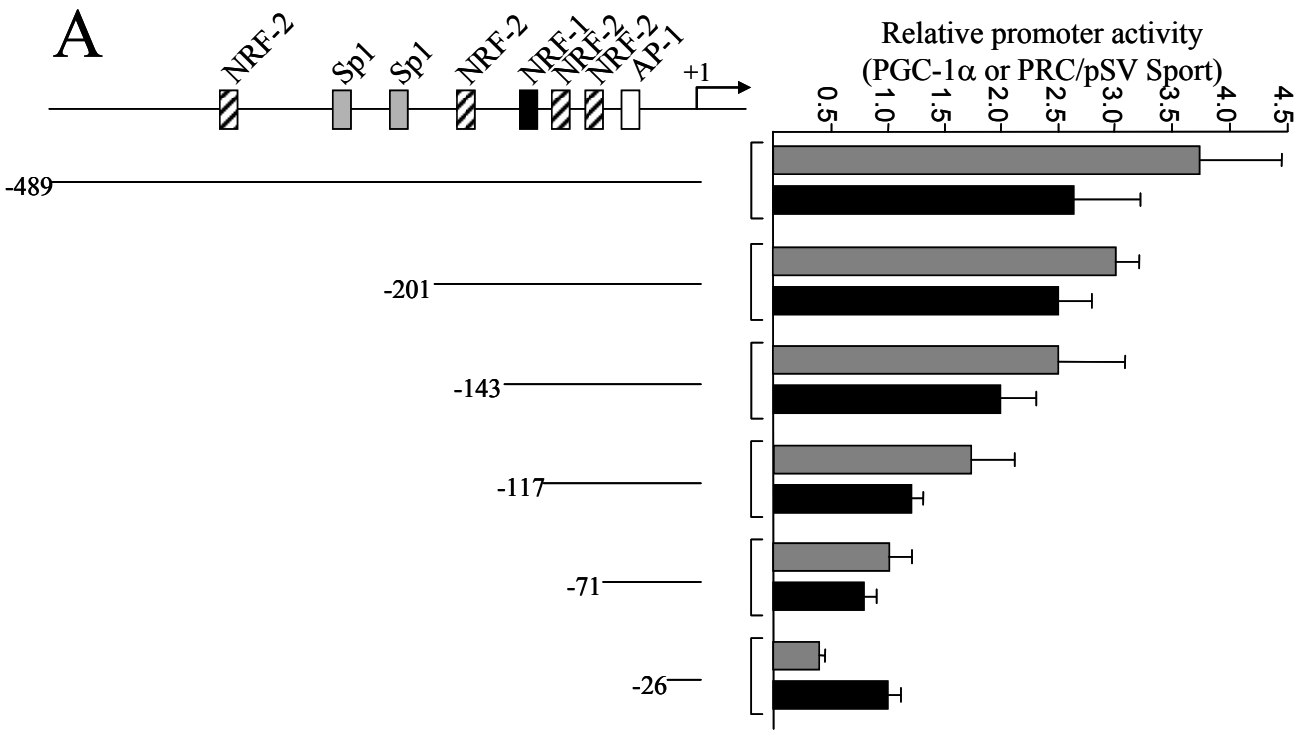
A
NRF-2
Sp1
Sp1
NRF-2
NRF-1
NRF-2
NRF-2
AP-1
+1
Relative promoter activity
(PGC-1α or PRC/pSV Sport)
0.5
1.0
1.5
2.0
2.5
3.0
3.5
4.0
4.5
-489
-201
-143
-117
-71
-26

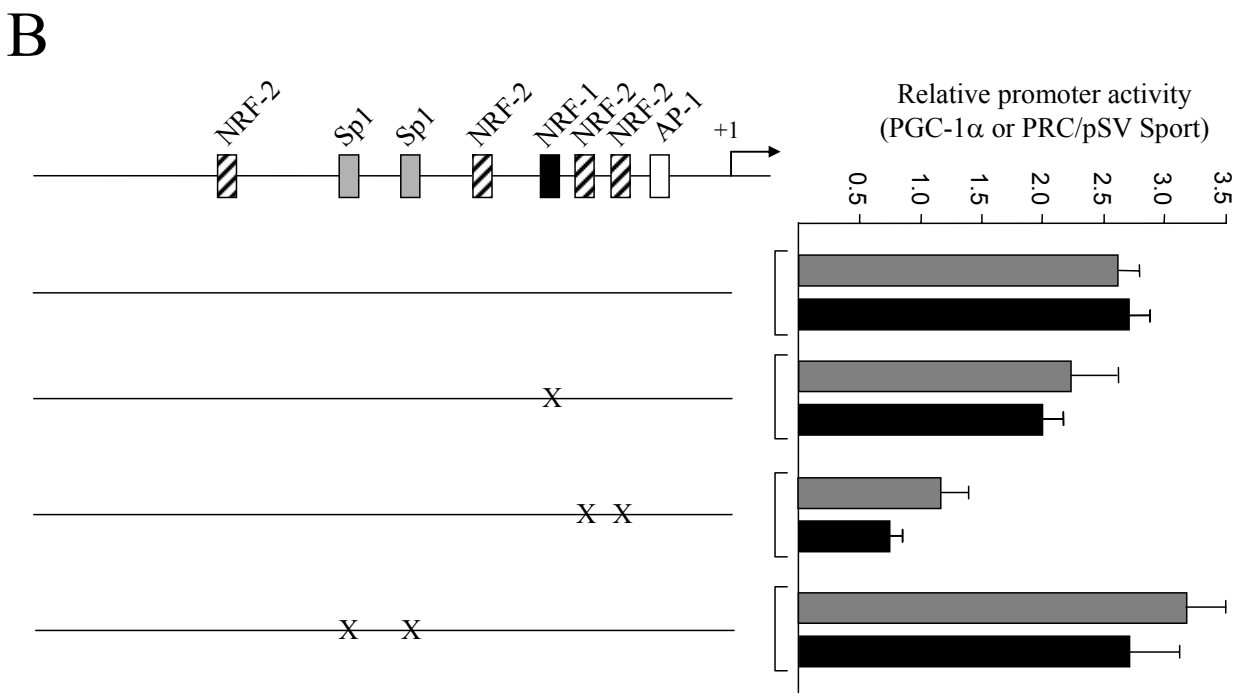
B
NRF-2
Sp1
Sp1
NRF-2
NRF-1
NRF-2
NRF-2
AP-1
+1
Relative promoter activity
(PGC-1α or PRC/pSV Sport)
0.5
1.0
1.5
2.0
2.5
3.0
3.5
X
X X
X X

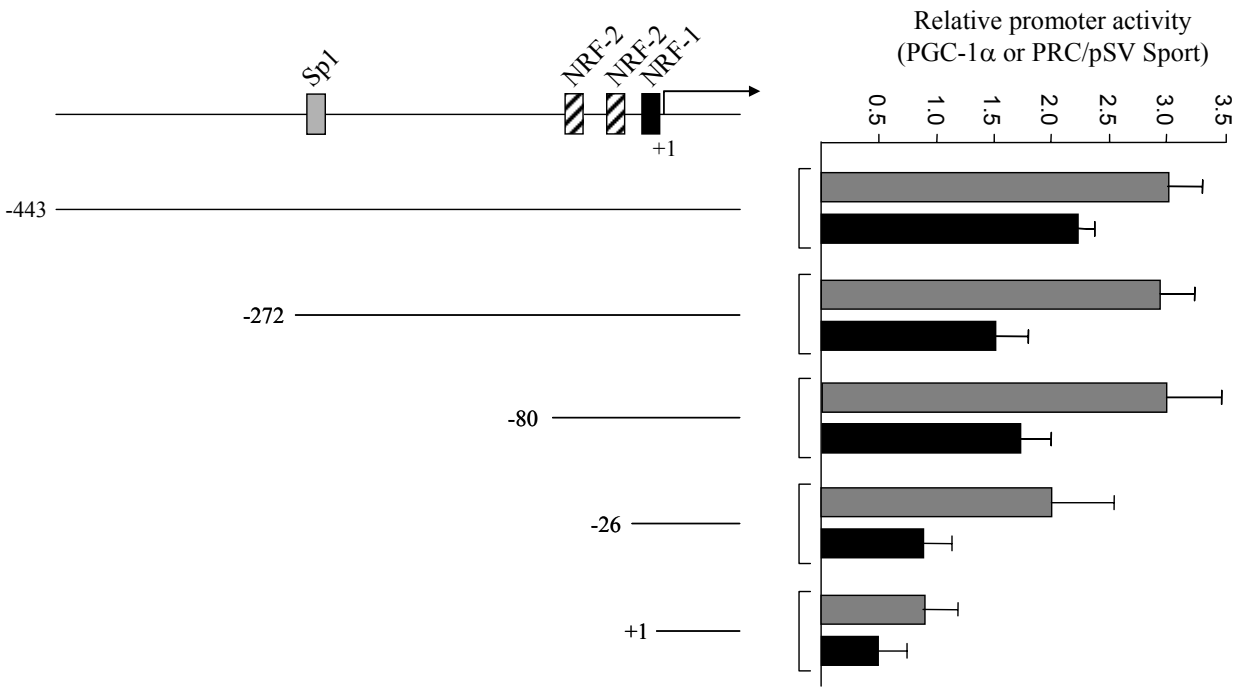

Figure 3.8. *Trans*-activation of the hTFB2M promoter and its mutated derivatives by PGC-1α and PRC.

The hTFB2M promoter deletions shown in **Figure 3.6** were assayed for *trans*-activation by PGC-1α **(gray fill)** and PRC **(black fill)** by cotransfection with vectors expressing each coactivitor. Values are the average fold activation for three separate determinations ± standard error measured relative to the pSVsport negative control.

TFB expression coincides with enhanced mitochondrial biogenesis. Nothing is known about whether the transcriptional control of TFB expression is associated with that of other genes implicated in the regulation of mitochondrial biogenesis and/or function. A series of real-time PCR assays was therefore developed to compare, quantitatively, the expression of a number of key genes involved in the process. The collection includes representatives from several classes of genes. The first consists of NRF target genes whose products function in the mitochondria, as represented by mitochondrial transcription factors (Tfam, TFB1M, and TFB2M) as well as respiratory proteins (cytochrome *c* and COXIV). A second class consists of the nuclear regulatory factors (NRF-1, PGC-1α and PRC) that regulate nuclear genes involved in mitochondrial respiratory function. A third class includes a mitochondrially-encoded respiratory subunit (COXII).

The expression of these genes was monitored in cellular systems where cytochrome *c*, a mitochondrial marker, is known to be up-regulated. In the first, quiescent fibroblasts were induced to proliferate in response to stimulation by serum growth factors. As shown previously (108) and in **Figure 3.9A**, this results in a rapid induction of both PRC and cytochrome *c* mRNAs. This induction is accompanied by increased mitochondrial respiratory activity. Notably, both TFB1M and TFB2M mRNAs are induced under these conditions suggesting that their up-regulation is an integral part of the program leading to cell growth. Interestingly, TFB1M mRNA is initially down regulated several fold before it is induced, a pattern that may be mediated by the negatively acting Sp1 sites that reside in the promoter. The induction of these factors is not part of a generalized transcriptional response because PGC-1α and COXIV are not induced beyond the level of the internal rRNA control. However, the mitochondrially-encoded COXII mRNA is induced in parallel with the factors (Tfam and the TFBs) required for its transcription. Thus, all

three NRF target genes encoding mitochondrial transcription factors are up-regulated in preparation for cell division.

In a second system, 3T3-L1 cells were allowed to differentiate into adipocytes, a process that is accompanied by enhanced mitochondrial biogenesis and a large induction of cytochrome *c* (109). As shown in **Figure 3.9B**, there is a striking increase in the expression of both nucleus (Cyt c and COXIV) and mitochondria encoded (COXII) respiratory subunit mRNAs upon differentiation. This is accompanied by the coordinate induction of Tfam, TFB1M and TFB2M. Again, the induction of these factors does not result from a generalized transcriptional response because the expression of PRC and NRF-1 remain unchanged. PGC-1α is induced upon differentiation whereas PRC is not, suggesting that PGC-1α is the coactivator that drives mitochondrial biogenesis during differentiation.

Figure 3.9. Expression of hTFB genes compared to that of a collection of regulatory and structural genes involved in mitochondrial biogenesis.

A. Gene expression was monitored during serum stimulation of quiescent BALB/3T3 fibroblasts by quantitative real-time PCR. The battery of genes examined represented nuclear regulatory factors (PRC, PGC-1α and NRF-1), mitochondrial transcription and replication factors (Tfam, TFB1M and TFB2M) and nucleus- (Cyt *c*, COXIV) and mitochondria- (COXII) encoded respiratory subunits. Relative steady-state mRNA levels were normalized to 18S ribosomal RNA as an internal control.

B. Relative mRNA expression was monitored during differentiation of fibroblasts to adipocytes for the same battery of genes as in *A*. Steady-state mRNA levels were normalized to ribosomal RNA and represent the average of at least three separate determinations with error bars denoting ± standard error.

A

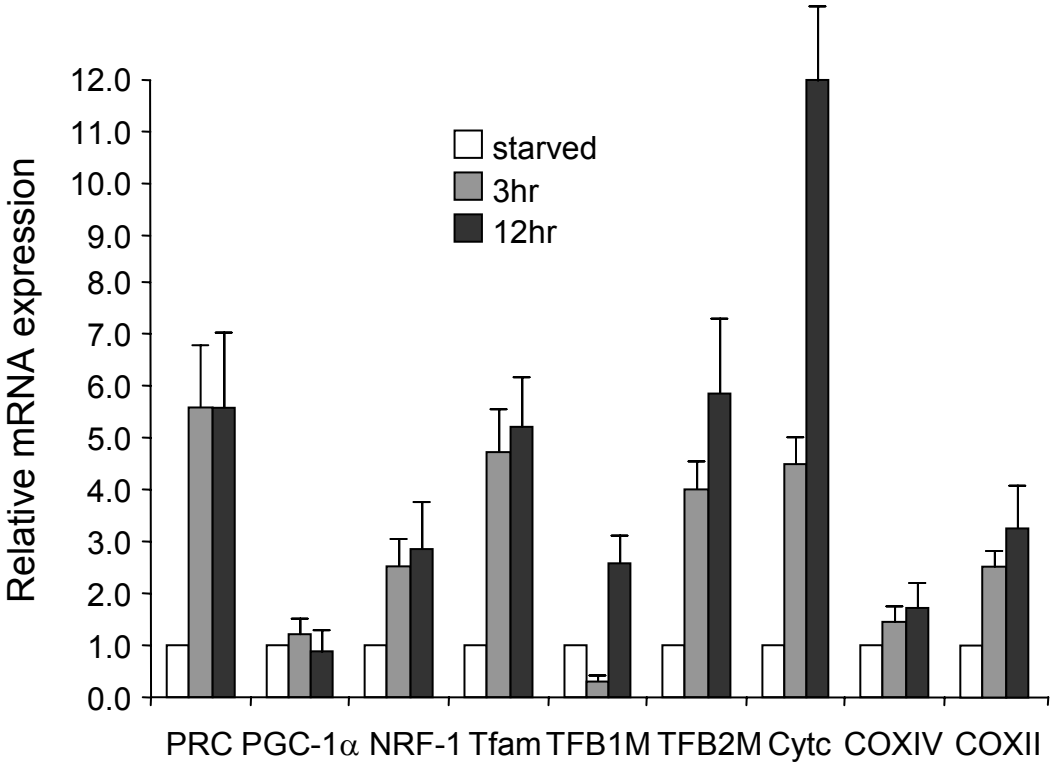
Relative mRNA expression
12.0
11.0
10.0
9.0
8.0
7.0
6.0
5.0
4.0
3.0
2.0
1.0
0.0
starved
3hr
12hr
PRC
PGC-1α
NRF-1
Tfam
TFB1M
TFB2M
Cytc
COXIV
COXII

B

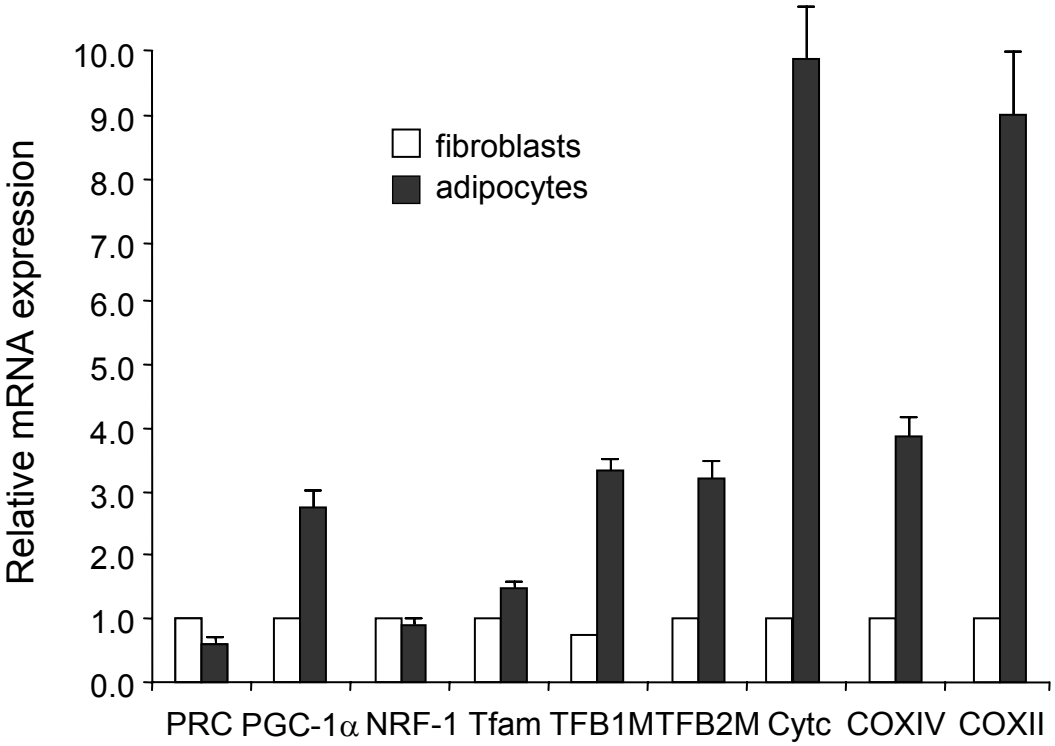
Relative mRNA expression
10.0
9.0
8.0
7.0
6.0
5.0
4.0
3.0
2.0
1.0
0.0
fibroblasts
adipocytes
PRC
PGC-1α
NRF-1
Tfam
TFB1M
TFB2M
Cytc
COXIV
COXII

Finally, to determine whether increasing the expression of a PGC-1 family coactivator is sufficient to induce TFB expression, C2C12 cells were infected with an adenovirus that drives the overproduction of PGC-1α. Expression of PGC-1α from this virus has been shown to up-regulate the expression of respiratory subunit mRNAs and mitochondrial biogenesis in cardiac myocytes (55). Although, C2C12 cells normally do not express PGC-1α, its expression is easily detected in infected cells **(Figure 3.10)**. Under these conditions, cytochrome *c* and both nuclear and mitochondrial COX subunit mRNAs are markedly induced relative to the GFP control. The induction of respiratory subunit mRNAs is accompanied by coordinate increases in transcripts encoding Tfam and the TFBs. The expression of β-actin is not induced and serves as a normalizing control. PRC and NRF-1 mRNAs are increased only modestly. These results are consistent with the notion that PGC-1α is limiting for expression of NRF target genes and that modulating its expression is sufficient to up-regulate endogenous genes encoding components of the mitochondrial transcriptional machinery.

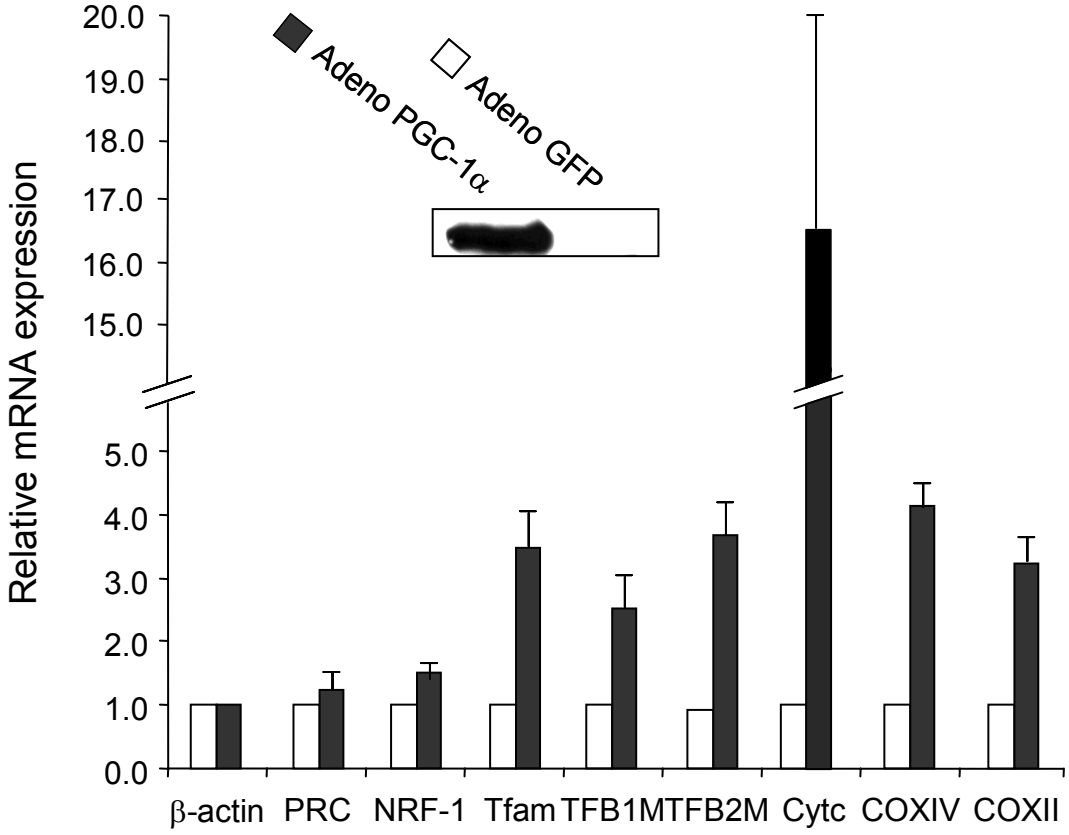

Figure 3.10. Expression of hTFB genes in response to ectopic expression of PGC-1α. Expression of mRNAs was measured in response to production of PGC-1α from an adenovirus vector in C2C12 myoblasts compared to a GFP-producing control. The inset panel shows the expression of PGC-1α protein by immunoblotting. Steady-state mRNA levels determined 72 h post infection were normalized to that of β-actin and represent the average of three separate determinations with error bars denoting ± standard error.

***In vivo* occupancy of TFB1M and TFB2M promoters by nuclear factors.** Chromatin immunoprecipitations (ChIP) were performed to determine whether the nuclear respiratory factors are actually bound to the TFB promoters *in vivo*. These experiments were carried out in human cells because the human promoters bind both factors *in vitro*. It is apparent from the results in **Figure 3.11**, that both NRF-1 and NRF-2α are bound specifically to both hTFB1M and hTFB2M promoters *in vivo* as well. The immunoprecipitated promoter fragments were not detected in the absence of antibody or when an unrelated anti-DLC antibody was used. In addition, no NRF-1- or NRF-2α-dependent product was obtained using primers specific for a region in the β-actin gene **(Figure 3.11)**, which lacks recognition sites for these factors, or when the analysis was performed using primers specific for the TFB 5'-flanking regions that are upstream from the NRF recognition sites (not shown). No difference in NRF occupancy of these promoters was observed in the presence of over expressed PGC-1α. This suggests that the mechanism for PGC-1α activation of these promoters does not involve a major increase in the recruitment of either NRF to the promoter. In preliminary experiments, we failed to detect PGC-1α at either promoter in cells over expressing the protein from an adenovirus vector compared to a GFP-expressing control (not shown).

Figure 3.11. NRF-1 and NRF-2*α* occupancy of TFB1M and TFB2M promoters *in vivo* detected by chromatin immunoprecipitation.

Hela cells infected with AdGFP- or AdPGC-1-expressing virus were subjected to chromatin immunoprecipitation (ChIP) assays as described in "**Materials and Methods**". Input lanes show the PCR product derived from chromatin prior to immunoprecipitation. Antibodies used for immunoprecipitation are indicated above each lane. Precipitated DNA was analyzed by semi-quantitative PCR using primer sets specific for the TFB1M or TFB2M promoter or the control β-actin fragment as indicated. Sizes of the DNA standards indicated at the left are, from top to bottom: 1207, 540, 400 (doublet), 275, and 166 bp.

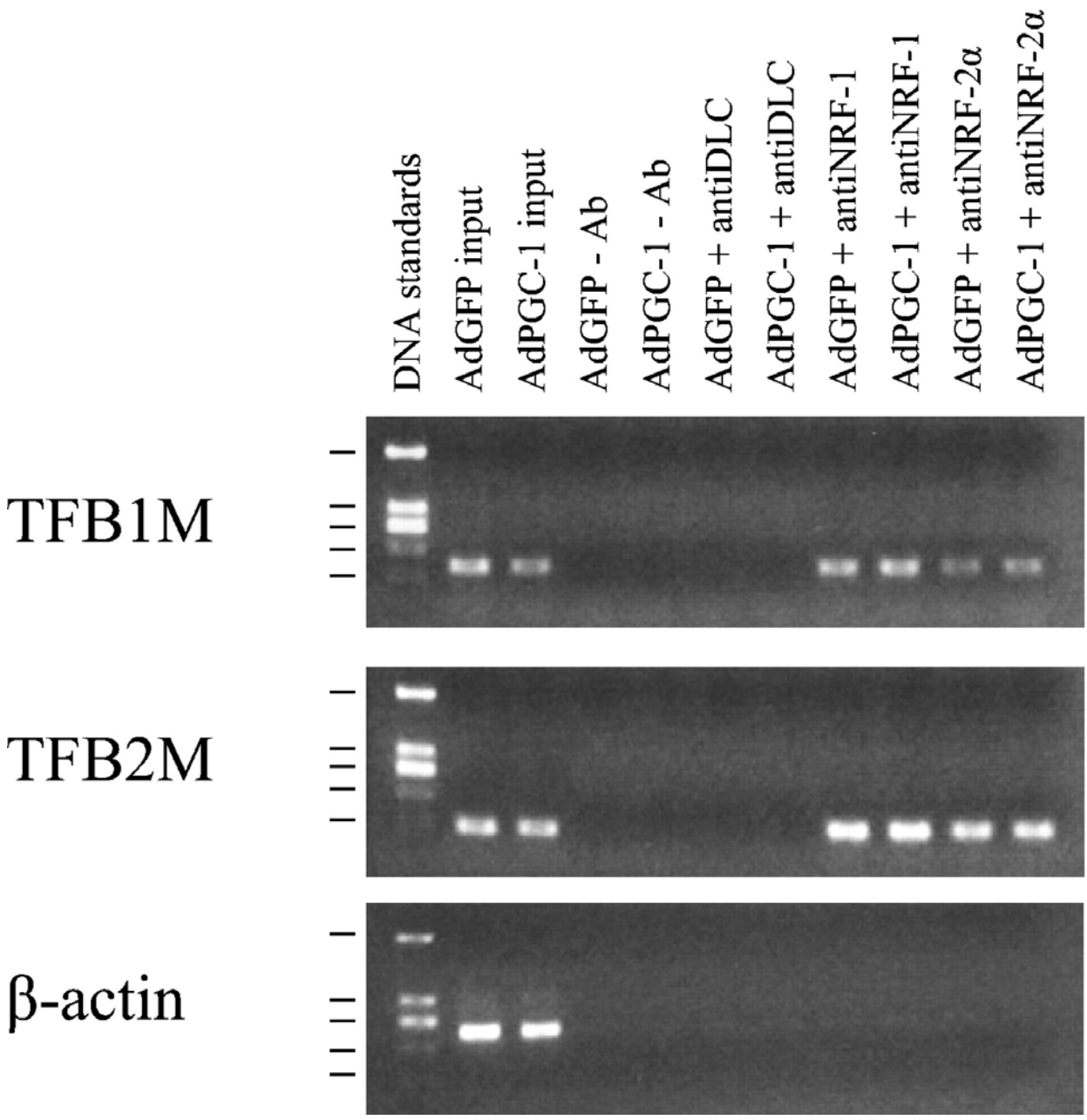
DNA standards
AdGFP input
AdPGC-1 input
AdGFP - Ab
AdPGC-1 - Ab
AdGFP + antiDLC
AdPGC-1 + antiDLC
AdGFP + antiNRF-1
AdPGC-1 + antiNRF-1
AdGFP + antiNRF-2α
AdPGC-1 + antiNRF-2α
TFB1M
TFB2M
β-actin

DISCUSSION

Major advances have been made in characterizing factors required for mitochondrial transcription. Early on, Tfam was identified as a vertebrate factor that binds a specific sequence motif within HSP and LSP and stimulates transcription in the presence of mt RNA polymerase. Tfam is related to yeast ABF2p and both proteins are required for mtDNA maintenance in their respective organisms (14,15). Although the existence of a vertebrate homologue of yeast sc-mtTFB was supported by studies in *Xenopus*, its molecular cloning was elusive (104,110). However, the recent cloning and characterization of the human and mouse TFB transcription specificity factors supports the idea that mitochondrial transcription, in organisms as divergent as yeast and humans, occurs through the concerted action of a small number of proteins. Both TFBs work through a single mitochondrial RNA polymerase to stimulate transcription in the presence of Tfam. Although the TFBs bind DNA in a sequence independent manner, neither DNA binding nor the RNA methyltransferase activities of these factors is required for transcriptional activation (18). TFB1M is thought to facilitate promoter-specific recognition by binding the carboxy-terminal transcriptional activation domain of Tfam. This represents a significant departure from the yeast system where ABF2p does not have an activation domain and does not stimulate transcription (111). Currently there is no explanation as to why there are two TFB isoforms or why TFB1M is markedly less active than TFB2M in transcriptional simulation.

Despite these advances, little is known about the regulatory pathways that govern mitochondrial transcriptional expression. Previous studies demonstrated that the human Tfam promoter is subject to regulation by NRFs suggesting that these factors might be involved in integrating the expression of respiratory subunits with components of the mitochondrial transcriptional machinery (44). Here, we establish that the human nuclear genes encoding

TFB1M and TFB2M are also subject to regulation by NRF-1 and NRF-2. This reinforces the idea that common transcriptional regulators link the expression of key mitochondrial transcription factors to that of respiratory chain subunits. The arrangement of the consensus NRF-1 and NRF-2 sites present in both of the human TFB promoters is similar to that found in many nuclear genes required for mitochondrial respiratory function (105). Of particular note is the conservation of spacing between tandem NRF-2 sites between the TFB and COXIV promoters. This is optimal for promoting high-affinity binding of the heterotetrameric NRF-2 complex (107). The TFB NRF sites can bind NRFs, either from crude extracts or as purified recombinant proteins, in a manner that is indistinguishable from previously authenticated sites present in the cytochrome *c* and COXIV genes. In addition, mutagenesis experiments establish that the TFB NRF sites are major determinants of promoter function. These *in vitro* results are corroborated by the chromatin immunoprecipitation assays, which clearly show occupancy of both TFB promoters by NRF-1 and NRF-2α *in vivo*.

It is notable that the NRF-1 sites do not appear to be conserved in the rodent Tfam or TFB promoters whereas the NRF-2 and Sp1 sites are present in both human and rodents (106,112). This is atypical in that NRF-1 sites in respiratory subunit promoters are usually conserved between mammalian species (113). NRF-1 is either not involved in expression of the rodent Tfam and TFB promoters or it participates in expression through protein-protein contacts rather than high affinity protein-DNA contacts. It is of interest in this context that NRF-1 can *trans*-activate the rat Tfam promoter and can bind a non-consensus GC-rich element near the transcription start site (112). The Sp1 consensus sites appear to be the only other *cis*-acting elements that affect promoter activity. Interestingly, the TFB1M Sp1 sites function as negative elements within the promoter context whereas the TFB2M Sp1 site exerts a positive effect on

transcription. Such differences in the action of Sp1 have been documented in respiratory gene promoters. In general, Sp1 exerts a positive effect on many COX promoters but is also known to act negatively in the ANT2 (114) and ATP synthase β-subunit (115) promoters. The physiological significance of these findings remains to be explored.

A current model for mitochondrial biogenesis involves the coordination of nuclear transcription factors through interactions with regulated coactivators of the PGC-1 family (37,43,105). The docking of NRFs and other transcription factors with PGC-1α and its relatives may induce a conformational change in these coactivators. This allows the assembly of additional cofactors containing histone modifying enzymatic activities that promote gene expression. These assemble by interaction with a transcriptional activation domain that is conserved among family members (62). An important characteristic of the PGC-1 family coactivators is that their expression is regulated physiologically (92). PGC-1α, the founding member of the group, is induced during adaptive thermogenesis through a cAMP-dependent pathway that is activated by β-adrenergic stimulation. PGC-1α is also up-regulated by cAMP during fasting where it promotes the expression of gluconeogenic enzymes. PGC-1β, a putative homologue of PGC-1α, is similarly up-regulated in fasted liver but not during thermogenesis in brown fat. Likewise, PRC is not regulated during thermogenesis but is induced by serum growth factors and down-regulated upon withdrawal of serum or contact inhibition (89). Despite these differences in their responses to regulatory signals, all three family members can bind NRF-1 and promote the *trans*-activation of NRF-1 target genes.

The data presented here place TFB1M and TFB2M among the growing list of genes that can be *trans*-activated by PGC-1 family coactivators. It is clear that the *trans*-activation of both TFB promoters by PGC-1α and PRC maps to their NRF-1 and NRF-2 recognition sites. As

previously observed for the cytochrome *c* and Tfam promoters, the Sp1 sites do not appear to be direct or indirect targets for these coactivators (54,89). We also observe no direct binding of Sp1 to either PRC or PGC-1α in *in vitro* binding assays (Pasko and Scarpulla, unpublished). Thus, as observed for respiratory chain components, it is likely that physiological control of TFB expression is exerted through NRF-1, NRF-2 and the PGC-1 family coactivators.

The mRNA expression results are consistent with the argument that many of the regulatory factors that have been implicated in mitochondrial biogenesis are coordinately regulated. Previous work established that cytochrome *c* mRNA is markedly induced upon serum stimulation of quiescent fibroblasts and that this induction is preceded by the rapid increase in PRC mRNA. This result is confirmed here using a real time PCR assay to measure these transcripts quantitatively. Under these conditions TFB1M and TFB2M mRNAs are also induced suggesting that these factors are up-regulated as part of the program of cell growth. The initial reduction of TFB1M mRNA expression at 3hrs of serum treatment was also verified by RNAse protections (not shown). Under certain conditions it may be desirable to reduce TFB1M expression relative to that of TFB2M because TFB2M is the more potent of the two in driving mitochondrial transcription. It is notable that the mitochondrial COXII transcript is also induced. Induction of mitochondrial transcripts is consistent with the model since their expression requires the action of Tfam and one or both TFBs.

Even more dramatic results were obtained using an adipocyte differentiation model. Previous work demonstrated that cytochrome *c* protein levels increase approximately 20-fold upon differentiation of 3T3-L1 fibroblasts to adipocytes (109). This was accompanied by increases in a number of other mitochondrial proteins and to elevated oxygen consumption suggesting that mitochondrial biogenesis itself is enhanced. Here, we show large increases in

nuclear (Cyt *c*, COXIV) and mitochonrially (COXII) encoded respiratory subunit mRNAs including a 10-fold induction of cytochrome *c*. Both TFBs along with Tfam mRNAs are also markedly induced upon differentiation indicating that coordinate increases in these mitochondrial transcriptional regulators are part of the program of mitochondrial biogenesis in this system. Of the nuclear regulatory factors examined, only PGC-1α is induced. This contrasts with serum growth response where PRC mRNA is induced and PGC-1α is not. On this basis it is tempting to speculate that PRC may function as a growth regulatory factor whereas PGC-1α is more involved in differentiation as observed here and in brown fat.

We have not yet been successful in over expressing PRC. However, the over expression of PGC-1α from an adenovirus vector increased the expression of respiratory subunit mRNAs along with those for Tfam and the TFBs. This demonstrates a causal relationship between increased PGC-1α expression and the induction of the TFBs as part of a program of mitochondrial biogenesis. This result is consistent with the results of others showing that elevated PGC-1α is sufficient to induce mitochondrial biogenesis (54). It remains to be determined whether modifications of the activators or coactivators play a role in controlling target gene expression. For example, the phosphorylation of NRF-1 that occurs in response to serum growth factors (108,116) may enhance its ability to utilize a particular coactivator. Nevertheless, the results show that varying the expression of a PGC-1 family coactivator is sufficient to coordinately induce all of the known factors required for the transcription of mtDNA. This contributes to the integration of mitochondrial transcription and replication with the expression of the respiratory apparatus. Questions remain concerning the mechanism by which the coactivators induce gene expression. One possibility is that the PGC-1 family coactivators induce the expression of nuclear respiratory factors. Over expression of PGC-1α in

mouse myoblasts and myotubules has been associated with a dramatic increase in NRF-1 and NRF-2α mRNA levels (54). Here, we observe a small but significant increase in NRF-1 transcript levels in response to serum stimulation but little or no increase upon adipocyte differentiation or upon PGC-1α over expression in mouse myoblasts. The reasons for the discrepancy with previous findings are unknown. However, the latter results are consistent with the ChIP experiments, which show no major increase in NRF-1 or NRF-2α promoter occupancy in response to PGC-1α over expression. An alternative but not mutually exclusive notion is that the coactivators work through direct interaction with their cognate transcription factors. Although we did not detect PGC-1α in a NRF complex at the TFB promoters by ChIP assay, there is good evidence that both PGC-1α and PRC form a functional complex with NRF-1 both *in vivo* and *in vitro* (54,89). By contrast, we detect no direct interaction between either PGC-1α or PRC with NRF-2α or NRF-2β (unpublished observation) suggesting that if such an interaction exists it may be mediated by a third party. The negative ChIP result does not allow us to rule out the possibility that PGC-1α is present in a promoter-associated complex. PGC-1α is known to interact with many transcriptional components including transcription factors, other coactivators and RNA splicing factors. Thus, it is possible that in the crosslinked complex, the epitopes recognized by the available antibody are inaccessible. Future studies should resolve these important mechanistic questions.

MATERIALS AND METHODS

Plasmids.

The hTFB1M promoter (accession number AL139101) was isolated by PCR amplification of HeLa DNA using sense

(5’AAAAAAGGTACCAGCATCTGCAGAGCGGCGGTTCT3’) and antisense (5’AAAAAAAAGCTTCCAACCCTACCTCACCCAGGACCT3’) primers that yield a PCR product containing *Acc*65I (5’end) and *Hind*III (3’end) restriction sites to facilitate cloning into luciferase reporter plasmid, pGL3Basic (Promega). After verifying the amplified product by sequencing, the *Acc*65I-*Hind*III fragment was cloned first into pGEM-T and then into pGL3 Basic to generate pGL3Basic/hTFB1Mwt. Similarly, the hTFB2M promoter (accession number AL356583) was isolated by PCR amplification of HeLa DNA using sense (5’AAAAAAGGTACCTGTTTCCAGCCCCACTCGGCGACAT3’) and antisense (5’AAAAAAAAGCTTTTCTGGCGTCCGGGCCAGGTCAAG 3’) primers with the incorporated *Acc*65I (5’end) and *Hind*III (3’end) restriction sites. After verifying the PCR product by sequencing, the hTFB2M promoter was cloned into the *Acc*65I-*Hind*III sites of pGL3Basic to generate pGL3Basic/hTFB2Mwt.

A series of 5’ deletions of the hTFB1M promoter was generated by PCR amplification of pGEM-T/hTFB1Mwt using a nested set of 5’ deletion primers containing the *Acc*65I restriction site and an antisense primer derived from the T7 promoter. The primers denoted by the deletion end-points with the *Acc*65I cloning site underlined are as follows:

-378 GACAGGTACCTAGAACGTTAAAG

-316 CGGTACCACCTCTCAGAGCAACT

-201 CGGTACCCCCCCGGCTCTCACA

-143 TCTCGCGGTACCACTTAGCGCAT

-117 CTCGGTACCCCGGGAATTTCCT

-71 AGGTACCACCAATGGGGCTGACT

-26 AGGTACCTCCCCTGCGCGTTTCT

A series of 5' deletions of the hTFB2M promoter was generated by PCR amplification of pGL3Basic/hTFB2M wt using a nested set of 5'end deletion primers containing the *Acc*65I restriction site and a reverse primer (5'CTTTATGTTTTTGGCGTCTTCC3') corresponding to GLprimer2 from Promega. All amplified 5' deletion fragments from hTFB1M and hTFB2M promoters were cloned into *Acc*65I-*Hind*III sites of pGL3Basic plasmid and verified by sequencing. The primers denoted by the deletion end-points with the *Acc*65I cloning site underlined are as follows:

-272 TGGAGGAGGTACCTCTCGCCTTT

-80 ACTCAGGTACCTCGGGCGGCTGA

-26 CAGGTACCCTCCGCTGTTCGCAT

+1 GGTACCAGTGTTTACTTCCGCTT

Site-directed mutagenesis of NRF-1, NRF-2, and Sp1 sites on both promoters was performed by PCR utilizing pGL3Basic/hTFB1M and two wild type plasmids as templates. Pairs of internal overlapping oligonucleotides with the desired mutations along with flanking pGL3Basic primers (sense: 5'ACTAGCAAAATAGGCTGTCC 3', anti-sense: 5'CTTTATGTTTTTGGCGTCTTCC 3') were used to generate mutations (117). After verifying all site-directed mutations by sequencing, the mutant promoters were subcloned as *Acc*65I-*Hind*III fragments into pGL3Basic. Sense (S) and antisense (AS) mutagenesis primers with mutated nucleotides underlined are as follows:

hTFB1M/NRF-1mut(S) GGACTTAGCGGAATTCCTCTCAGCAC

hTFB1M/NRF-1mut(AS) GTGCTGAGAGGAATTCCGCTAAGTCC

hTFB1M/NRF-2Amut(S) CAGCACGCCGAGATCTAGCTGTCCGCGG

hTFB1M/NRF-2Amut(AS) CCGCGGACAGCTAGATCTCGGCGTGCTG

hTFB1M/NRF-2Bmut(S) GCGGTCTTCGATATCGGTGGGATA

hTFB1M/NRF-2Bmut(AS) TATCCCACCGATATCGAAGACCGC

hTFB1M/Sp1Amut(S) TGTCCAGGCCTGCAGTCGTCCCGCC

hTFB1M/Sp1Amut(AS) GGCGGGACGACTGCAGGCCTGGACA

hTFB1M/Sp1Bmut(S) TCCCCGTAGCTCGAGCAGGAGAAGC

hTFB1M/Sp1Bmut(AS) GCTTCTCCTGCTCGAGCTACGGGGA

hTFB2M/NRF-1mut(S) CCGCTGTTCGACTGATCAGGCTCTAG

hTFB2M/NRF-1mut(AS) CTAGAGCCTGATCAGTCGAACAGCGG

hTFB2M/NRF-2Amut2(S) AGCCGAGGCTCAAGCCCAAGTGAGGGA

hTFB2M/NRF-2Amut2(AS) TCCCTCACTTGGGCTTGAGCCTCGGCT

hTFB2M/NRF-2Bmut2(S) GGGAGAAAAGCAACAAGGCTCCGCTG

hTFB2M/NRF-2Bmut2(AS) CAGCGGAGCCTTGTTGCTTTTCTCCC

hTFB2M/Sp1mut(S) CTCGCCTTTCGACAGCGTCTCCCTCTGC

hTFB2M/Sp1mut(AS) GCAGAGGGAGACGCTGTCGAAAGGCGAG

Other plasmids used in transfections were δ-ALAS(-479)wt/pGL3, δ-ALAS(-479)m1m2/pGL3), FL PRC/pSV Sport (89) and PGC-1/pSV Sport (54).

Electromobility shift assays.

Nuclear extracts from HeLa cells were prepared as described (118). The following oligonucleotides (mutated nucleotides underlined) were employed in binding assays:

TFB1M/NRF-1: GATCCGGACTTAGCGCATGCGCTCTCAGCA
GCCTGAATCGCGTACGCGAGAGTCGTTCGA

TFB1M/NRF-1mut: GATCCGGACTTAGCGGAATTCCTCTCAGCA
GCCTGAATCGCCTTAAGGAGAGTCGTTCGA

TFB2M/NRF-1: GATCCTCCGCTGTTCGCATGCGCAGGCTCTA
GAGGCGACAAGCGTACGCGTCCGAGATTCGA

TFB2M/NRF-1mut: GATCCTCCGCTGTTCGGAATTCCAGGCTCTA
GAGGCGACAAGCCTTAAGGTCCGAGATCGA

TFB1M/NRF-2: GATCCGCCGGGAATTTCCTGTCCGCGGTCATCGCTTCCGGTGGGA
GCGGCCCTTAAAGGACAGGCGCCAGTAGCGAAGGCCACCCTTCGA

TFB1M/NRF-2mut: GATCCGCCGTCTATTAGATGTCCGCGGTCATCGCTAGAGGTGGGA
GCGGCAGATAATCTACAGGCGCCAGTAGCGATCTCCACCCTTCGA

TFB2M/NRF-2: GATCCAGGCGGAAGCGGAAGTGAGGGAGAAAAGCAGGAAGGCTCA
GTCCGCCTTCGCCTTCACTCCCTCTTTTCGTCCTTCCGAGTTCGA

TFB2M/NRF-2mut: GATCCAGGCTCTAGCTCTAGTGAGGGAGAAAAGCATCTAGGCTCA
GTCCGAGATCGAGATCACTCCCTCTTTTCGTAGATCCGAGTTCGA

ratCO4/NRF-2: GATCCTTGCTCTTCCGGTGCGGGACCCGCTCTTCCGGTCGCGA
GAACGAGAAGGCCACGCCCAGGGCGAGAAGGCCAGCGCTTCGA

ratCO4/NRF-2mut: GATCCTTGCTCTAGAGGTGCGGGACCCGCTCTAGAGGTCGCGA
GAACGAGATCTCCACGCCCAGGGCGAGATCTCCAGCGCTTCGA

RC4(-172/-147): GATCCTGCTAGCCCGCATGCGCGCGCACCTTA
GACGATCGGGCGTACGCGCGCGTGGAATTCGA

Annealed oligonucleotides were 3'-end-labeled using Klenow enzyme and purified by QIAquick Nucleotide Removal kit (Qiagen). Binding reactions (20µl) contained either 5µg of

nuclear extract, 200pg of recombinant NRF-1 (113), or varying amounts of recombinant NRF-2α and NRF-2β_1 (107) in 25mM tris-HCl (pH 7.9), 6.25mM $MgCl_2$, 0.5mM EDTA, 10% (vol/vol) glycerol, 1mM dithiothreitol, 5μg of sonicated calf thymus DNA, ~0.15pmol of labeled oligonucleotides. Specific and nonspecific unlabeled competitor oligonucleotides were added to the binding reactions in 50-fold molar excess prior to the addition of labeled oligonucleotides. Reaction mixtures were incubated at room temperature for 15 min and DNA-protein complexes resolved by 5% polyacrylamide gel in Tris-borate-EDTA buffer at 300V. Supershifting was carried out by addition of 1μl of antiserum (either goat anti-NRF-1, rabbit anti-NRF-2α, rabbit anti-NRF-2β_1, or preimmune serum) to the binding reactions 10 min after the components were mixed, followed by an additional 5 min incubation before loading onto the gel. Gels were then dried and subjected to autoradiography.

Cell culture and transfections.

BALB/3T3 cells used in transfections were maintained in Dulbecco's modified Eagle's medium (DMEM) (Gibco) supplemented with 10% calf serum (HyClone) and 1% penicillin-streptomycin (Gibco). Nuclear extracts for EMSA were prepared from HeLa S3 cells (ATCC) grown in Ham's F12 media (CellGro). 3T3-L1 Fibroblasts (ATCC) were grown on 150-mm dishes in Dulbecco's modified Eagle's medium (Gibco) supplemented with 10% fetal bovine serum (HyClone) and 1% penicillin-streptomycin (Gibco). Fibroblasts were differentiated into adipocytes as described (109). Serum induction of quiescent BALB/3T3 cells was performed as described previously (108).

Transient transfections were performed by calcium phosphate precipitation as described (89). Cells were plated at a density of 2600-6200 cells per cm^2 in six-well plates, washed twice at

5 hrs post-transfection with Dulbecco's phosphate-buffered saline (PBS) (Gibco), and grown for additional 40 h in fresh media. Cell extracts were prepared and luciferase assays performed with PharMingen reagents. Values were normalized to β-galactosidase activity measured spectrophotometrically using the β-galactosidase enzyme assays system (Promega).

The recombinant adenoviral plasmids Ad-PGC-1 and Ad-GFP were a gift from D.P. Kelly (Washington University). The Ad-PGC-1 plasmid contains, in tandem, the GFP gene and the *myc* tagged PGC-1 cDNA, whereas the control Ad-GFP plasmid contains only the GFP gene (55).These plasmids were linearized and transfected into the packaging cell line 293 using Lipofectamine (Invitrogen, USA) and the resulting viral stock was amplified to high titer. C2C12 mouse myoblasts were infected and the infection efficiency was determined by GFP expression 24 h after infection. RNA was isolated with Trizol (Invitrogen, USA) at 72 h post infection and subjected to real time RT-PCR analysis.

Real-time Quantitative RT-PCR.

For real-time PCR expression analysis, cells were washed in PBS and total RNA was extracted using Trizol reagent (Gibco BRL). RNA samples were then DNase treated with a DNA-Free kit (Ambion) and analyzed for quality by Agilent 2100 Bioanalyzer. Treated RNA (500ng to 1μg) was reverse transcribed in 20 to 30μl reaction mixtures with random hexamer primers and the TaqMan Reverse Transcription Reagents kit (Applied Biosystems) according to the manufacturer's protocol. Target sequences were selected to span an exon/intron junction, except for COXII, which has no introns. Gene-specific primer/probe mixtures for each amplicon were manufactured by Applied Biosystems. Aliquots of the reverse-transcribed products were combined with TaqMan Universal PCR Master Mix (Applied Biosystems) and an appropriate

primer-probe mix in 20µl reactions. PCR amplifications were carried out in 384-well plates using the ABI Prism 7900HT Sequence Detection System and the results were analyzed with a Relative Quantification Study program using SDS 2.1 software (Applied Biosystems). Samples were analyzed in triplicate, and mRNA quantities were normalized against 18S RNA (primer-probe mix from Applied Biosystems). Reactions were carried out using the following conditions: an initial step of 2 min at 50˚C and 10 min at 95˚C, followed by 45 cycles of 15 s at 95˚C and 1 min at 60˚C. Relative gene expression levels were determined by comparative C_t method.

Chromatin immunoprecipitation.

Chromatin immunoprecipitations were performed using a modification of an established method (119). HeLa cells, infected for 48h with recombinant adenovirus-expressing GFP or PGC-1, were fixed with 1% formaldehyde for 10 min at 25ºC, lysed, and subjected to sonication. Soluble chromatin was first pre-cleared with a salmon sperm DNA/protein A agarose slurry for 3h at 4ºC and then immunoprecipitated at 4ºC overnight with rabbit anti-NRF-1 (116), anti-NRF-2α or anti-DLC (Dynein Light Chain) (120) antibodies or without the addition of antibodies. Immune complexes were collected by incubation with salmon sperm DNA/protein A agarose slurry for 1h at 4ºC, the beads washed extensively, and the chromatin immune complexes eluted. After de-crosslinking, DNA was purified using the QiaQuick PCR purification kit (Qiagen) and subjected to PCR using primer sets specific for the human TFB1M promoter (forward: 5'CCTAGTCCACCCGGCTCT 3', reverse: 5' GAGGAACCTGCGAGACCTAA 3'), TFB2M promoter (forward: 5' ACGGTCCACTCACAATCCTC 3', reverse: 5' CCCACGTGGAACATTTTCTG 3') and a control fragment from the human β-actin gene (forward: 5' GTCATCACCATTGGCAATGAG 3', reverse: 5' CGTCATACTCCTGCTTGCTG

3'). The regions of amplification included the NRF-1 and NRF-2α binding sites of both the TFB1M and the TFB2M promoters, whereas the region amplified in the β-actin gene does not bind the factors. Linearity of the PCR amplifications was established experimentally (TFB1M and TFB2M, 30 cycles; β-actin, 26 cycles) and PCR products were resolved on a 2% agarose gel and visualized by ethidium bromide staining.

ACKNOWLEDGMENTS

We thank Dr. Daniel P. Kelly of Washington University School of Medicine for the PGC-1α expressing adenovirus vector and antibodies.

This work was supported by United States Public Health Service grant GM32525-21.

CHAPTER 4:

PGC-1-RELATED COACTIVATOR (PRC): IMMEDIATE EARLY EXPRESSION AND CHARACTERIZATION OF A CREB/NRF-1 BINDING DOMAIN ASSOCIATED WITH CYTOCHROME *C* PROMOTER OCCUPANCY AND RESPIRATORY GROWTH

INTRODUCTION

Mitochondrial biogenesis relies upon the integrated expression of both the nucleo-cytosolic and mitochondrial genetic systems (5). Although mitochondria have their own DNA (mtDNA), in vertebrates a covalently closed circular molecule of approximately 16.5 kilobases, the protein coding capacity of this genome is limited to 13 polypeptide subunits of respiratory chain complexes I, III, IV and V. The only other products of mtDNA expression are the tRNAs and rRNAs of the mitochondrial translation system. This arrangement necessitates that nuclear genes encode the majority of respiratory chain subunits as well as all of the gene products required for the transcription and replication of mtDNA.

In recent years there have been significant inroads into understanding the transcriptional mechanisms that contribute to nucleo-mitochondrial interactions in mammalian systems (105). Key components of the mitochondrial transcriptional machinery have been characterized (121). These include a single mitochondrial RNA polymerase (POLRMT), a stimulatory factor (Tfam), which binds DNA and is required for maintenance of the mitochondrial genome, specificity factors (TFB1M and 2M) that interact with Tfam and the polymerase and a termination factor (mTERF), which may help regulate the rRNA/mRNA ratio. In addition, several nuclear transcription factors that act on nuclear genes required for mitochondrial function have been identified (122). These include the nuclear respiratory factors (NRF-1 and NRF-2), PPARα,

which functions in fatty acid oxidation, and most recently, ERRα, which is thought to act as a primary biogenesis factor. Many promoter studies over the years have pointed to the involvement of NRF-1 and 2 in the expression of the majority of respiratory chain subunits as well as in the expression of mitochondrial transcription factors (105). This work is supported by recent observations that NRF-1 occupies the promoters of many of these nuclear genes *in vivo* (51).

An important issue concerns the mechanisms governing the coordination of multiple transcription factors into a program of mitochondrial biogenesis. This has been resolved in part by the discovery of the PGC-1 family of regulated coactivators (123,124). The founding member of this family, PGC-1α, directs the expression of genes involved in energy metabolism in response to signaling pathways that mediate thermogenesis, gluconeogenesis, muscle fiber type switching and mitochondrial biogenesis. The control of mitochondrial biogenesis by PGC-1α occurs at least partly through its interaction with NRF-1, as evidenced by the finding that a dominant negative allele of NRF-1 can block mitochondrial biogenesis directed by ectopically expressed PGC-1α (54). A second family member, PGC-1-related coactivator (PRC), shares key structural motifs with PGC-1α including a potent activation domain, an LXXLL coactivator signature motif and both an R/S domain and RNA recognition motif (89). However, PRC mRNA is not induced during adaptive thermogenesis but is up regulated during the serum induced G_0 to G_1 transition from quiescence to proliferative growth in fibroblasts. Similarly, PRC mRNA is down regulated upon exit from the cell cycle, mediated either by serum withdrawal or by contact inhibition, suggesting that PRC is a growth-regulated coactivator. These differences in regulation between PRC and PGC-1α are intriguing in light of the fact that the two family members are indistinguishable in their ability to interact with NRF-1 and to *trans*-activate the promoters of NRF-1 target genes required for respiratory chain expression (46,89). The ability of PRC to work

through NRF-1, coupled with its induction in proliferating cells, suggests that it may be involved in coordinating cell growth with mitochondrial expression and function.

Cytochrome *c* has served as a model for understanding the genetic mechanisms regulating respiratory chain expression in both yeast and mammalian cells (125). Analysis of the rodent cytochrome *c* promoter led to the identification of NRF-1 as an activator of respiratory gene expression (41,126). In addition, the cAMP response element binding protein, CREB, activates the promoter through distinct recognition sites and mediates cytochrome *c* transcription in response to both cAMP (127) and serum (108). Serum-induced cytochrome *c* expression at both the mRNA and protein level in the G_0 to G_1 transition has been associated with a specific elevation of heme $c+c_1$ absorbance and enhanced mitochondrial respiration (108). Activation of both NRF-1 and CREB by phosphorylation was implicated in the transcriptional induction of the cytochrome *c* promoter. Moreover, NRF-1 and CREB recognition sites are required for maximal *trans*-activation of the cytochrome *c* promoter by PRC suggesting a potential relationship between growth-regulated cytochrome *c* expression and promoter activation by PRC (89). Here, we explore this possibility and find that PRC has the characteristics of an immediate early gene and can complex with CREB in a manner that is identical to its interactions with NRF-1. In addition, PRC occupies the cytochrome *c* promoter *in vivo* and promoter occupancy by the coactivator is enhanced upon serum-stimulation of quiescent cells. These results suggest that PRC can target key transcription factors as an early event in the genetic program of cell growth.

RESULTS

Immediate early expression of PRC. PRC mRNA is induced upon serum stimulation of quiescent BALB/3T3 fibroblasts and is down regulated upon serum withdrawal or contact

inhibition (89). The rapid induction of PRC under these conditions is reminiscent of the class of immediate early genes, which are defined by their induction in the absence of *de novo* protein synthesis (128). To test whether PRC belongs to this class, the serum induction of PRC was compared in the presence and absence of the cytosolic protein synthesis inhibitor, cycloheximide. As shown in **Figure 4.1A**, PRC transcripts are rapidly induced with similar kinetics in both the absence and presence of cycloheximide. This indicates that PRC mRNA synthesis and/or stabilization occurs through the use of preexisting proteins and does not require *de novo* protein synthesis. In addition, like other immediate early mRNAs, PRC transcripts are induced to a much higher level in the presence of cycloheximide (super induced) suggesting that PRC mRNA is stabilized in the absence of protein synthesis. This possibility was tested by measuring the half-life of PRC mRNA by treating cells with actinomycin D in both the absence and presence of cycloheximide. As shown in **Figure 4.1B**, PRC mRNA has a half-life of about 2 h and the PRC transcript is markedly stabilized in the presence of cycloheximide. It is possible that the regulated stabilization of PRC mRNA may account for its rapid induction in response to serum. This appears not to be the case because the half-life of PRC mRNA is similar in serum-starved, serum-stimulated and confluent cells **(Figure 4.1C)**. This indicates that PRC mRNA stabilization cannot account for PRC mRNA induction upon entry to the cell cycle and suggests that PRC up-regulation in proliferating cells occurs at the level of increased transcription initiation. This was confirmed by a nuclear run-on experiment showing increased levels of PRC nascent transcripts in response to serum stimulation (not shown).

Figure 4.1. Effect of cycloheximide on PRC mRNA induction and stabilization.

A. Serum-starved quiescent BALB/3T3 fibroblasts were serum stimulated for the indicated times in the absence or presence of 10 μg/ml cycloheximide. An asterisk denotes a *P* value of < 0.05 compared to corresponding values from untreated cells.

B. Quiescent BALB/3T3 cells were serum stimulated for 1 h in either the absence or presence of 10 μg/ml of cycloheximide, followed by treatment with 5 μg/ml actinomycin D. Asterisk denotes a *P* value of < 0.05 compared to values for cells treated with actinomycin D alone.

C. The PRC mRNA half-life was determined following treatment of starved cells, serum-stimulated cells or confluent cells with 5 μg/ml actinomycin D.

For all three panels total RNA was isolated at the indicated times and the relative amount of PRC mRNA was determined by quantitative real time PCR using 18S rRNA as an internal standard. Results are expressed as the mean ± standard errors of the means for three independent determinations.

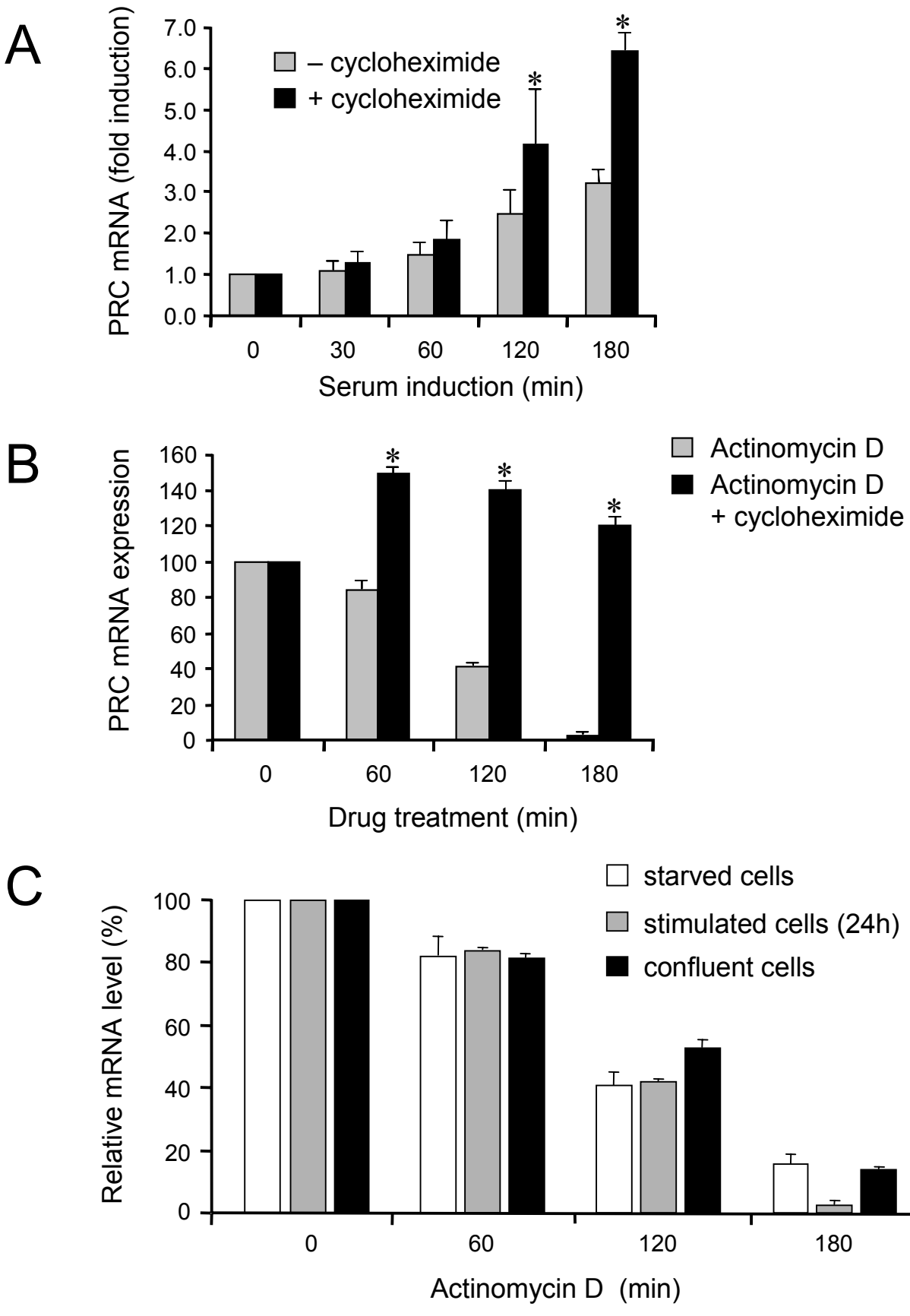
A
PRC mRNA (fold induction)
7.0
6.0
5.0
4.0
3.0
2.0
1.0
0.0
– cycloheximide
+ cycloheximide
*
*
0
30
60
120
180
Serum induction (min)
B
PRC mRNA expression
160
140
120
100
80
60
40
20
0
*
*
*
Actinomycin D
Actinomycin D
+ cycloheximide
0
60
120
180
Drug treatment (min)
C
Relative mRNA level (%)
100
80
60
40
20
0
starved cells
stimulated cells (24h)
confluent cells
0
60
120
180
Actinomycin D (min)

Antibodies to PRC were raised to measure PRC protein levels. These antibodies were initially tested in human 293FT cells because they were raised against human PRC subfragments. These cells also have a high transfection efficiency, which facilitates detection of protein expressed from transfected plasmids. The initial antibody, directed against a PRC subfragment encompassing amino acids 95 to 533, revealed multiple bands in extracts from cells transfected with empty control vector pSV-Sport. Only one of these bands corresponded to the 177kDa molecular mass predicted based on the PRC amino acid sequence **(Figure 4.2A, lane 1)**. However, this band was much diminished in an immunoblot using a second antibody raised against amino acids 1047 to 1379 **(lane 3)** and was absent using a third antibody directed against amino acids 400 to 467 **(lane 5).** A major band migrating at 250kDa was detected by all three antibodies suggesting that PRC migrates upon gel electrophoresis to a position greater than its predicted mass. To confirm that the 250kDa band was PRC, extracts were prepared from cells transfected with an expression vector (PRC/pSV-Sport) containing the entire PRC open reading frame. Immunoblots of these extracts using each of the three antibodies revealed enhanced expression of the 250kDa band **(Figure 4.2A, lanes 2, 4 and 6)** compared to extracts from the empty vector controls **(lanes 1, 3 and 5)**. These results unambiguously identify the 250kDa protein as PRC.

Mouse (BALB/3T3) and human (U2OS) serum responsive cell lines were used to determine whether the 250kDa PRC protein is induced in the transition between G_0 and G_1. Extracts were prepared from proliferating cells, serum starved cells and from starved cells that were serum-stimulated for 3 or 8 h. Immunoblots revealed that steady-state PRC protein levels were diminished upon serum starvation and induced upon serum stimulation of both mouse and human lines **(Figure 4.2B)**. In both cases, PRC was induced to levels equivalent to those found

in proliferating cells within 3 to 8 h of serum addition. This is consistent with the serum induction of PRC mRNA, which begins after 1h of serum addition **(Figure 4.1A)** and demonstrates that the up regulation of the PRC mRNA leads to increased steady-state levels of PRC protein.

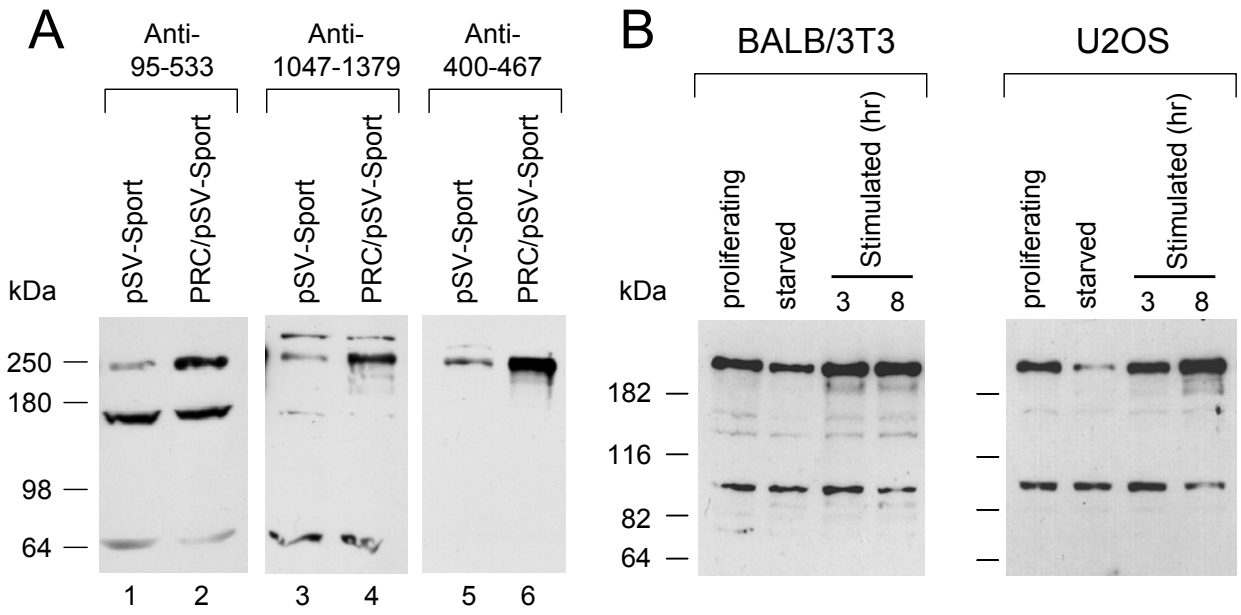

Figure 4.2. Identification and quantitation of PRC protein levels.

A. PRC protein was identified in 293FT cell extracts using antibodies raised to three different subregions (anti-PRC(95-533), anti-PRC(1047-1379) and anti-PRC(400-467)) of the molecule. Extracts were prepared from cells transfected with either empty vector (pSV-Sport) or vector expressing the full PRC open reading frame (PRC/pSV-Sport).

B. Total BALB/3T3 or U2OS cell extracts were prepared from proliferating cells, serum-starved cells or starved cells stimulated with serum for either 3 or 8h.

In both panels, proteins were detected following denaturing gel electrophoresis and immunoblotting with either the indicated antibodies (panel *A*) or anti- PRC(1047-1379) (panel *B*).

***In vitro* and *in vivo* interaction of PRC with CREB.** We demonstrated previously that cytochrome *c* is induced upon serum stimulation of quiescent BALB/3T3 cells and that the induced expression of this respiratory protein coincides with enhanced mitochondrial respiration (108). The cytochrome *c* promoter is a target for both NRF-1 and CREB transcription factors and promoter recognition sites for both of these factors were necessary for maximal serum-dependent promoter activation. Because PRC can *trans*-activate NRF-1 target genes through a specific interaction with the NRF-1 DNA binding domain (89), it was of interest to determine whether CREB is also a target for this coactivator. To this end, NRF-1 and CREB binding to PRC was compared using an S-tag pull-down assay (89) **(Figure 4.3)**. The results demonstrate that both NRF-1 and CREB bind to PRC subfragments B (amino acids 400-698) and D (amino acids 1379-1664) but not to LXXLL-containing subfragment A (amino acids 1-221) or to subfragment C (amino acids 1057-1379). As a control for binding specificity, host cell factor, which binds to a DHDY motif, binds only subfragment C containing this motif but not any of the other PRC subfragments including those binding both NRF-1 and CREB **(Figure 4.3)**. These results demonstrate that PRC can interact specifically with both NRF-1 and CREB suggesting it may be involved in cytochrome *c* promoter activation by both factors.

Figure 4.3. Comparison of the *in vitro* interaction between PRC and NRF-1, CREB or HCF.

A schematic representation of PRC is shown at top with the various functional domains indicated (*stippled*, activation domain; *cross hatched*, proline rich region; *gray*, consensus recognition site (DHDY) for host cell factor (HCF); *black*, R/S domain; *vertical hatched*, RNA recognition motif). Subfragments of PRC denoted as A, B, C or D with their amino acid coordinates shown in parentheses were used in S-tag pull down assays with ^{35}S-labeled transcription factors, NRF-1, CREB, or HCF. Binding of the various subfragments to each ^{35}S-radiolabeled transcription factor was compared to that of S-tagged thioredoxin as a negative control. Bound proteins were eluted from the S-protein agarose and visualized by autoradiography.

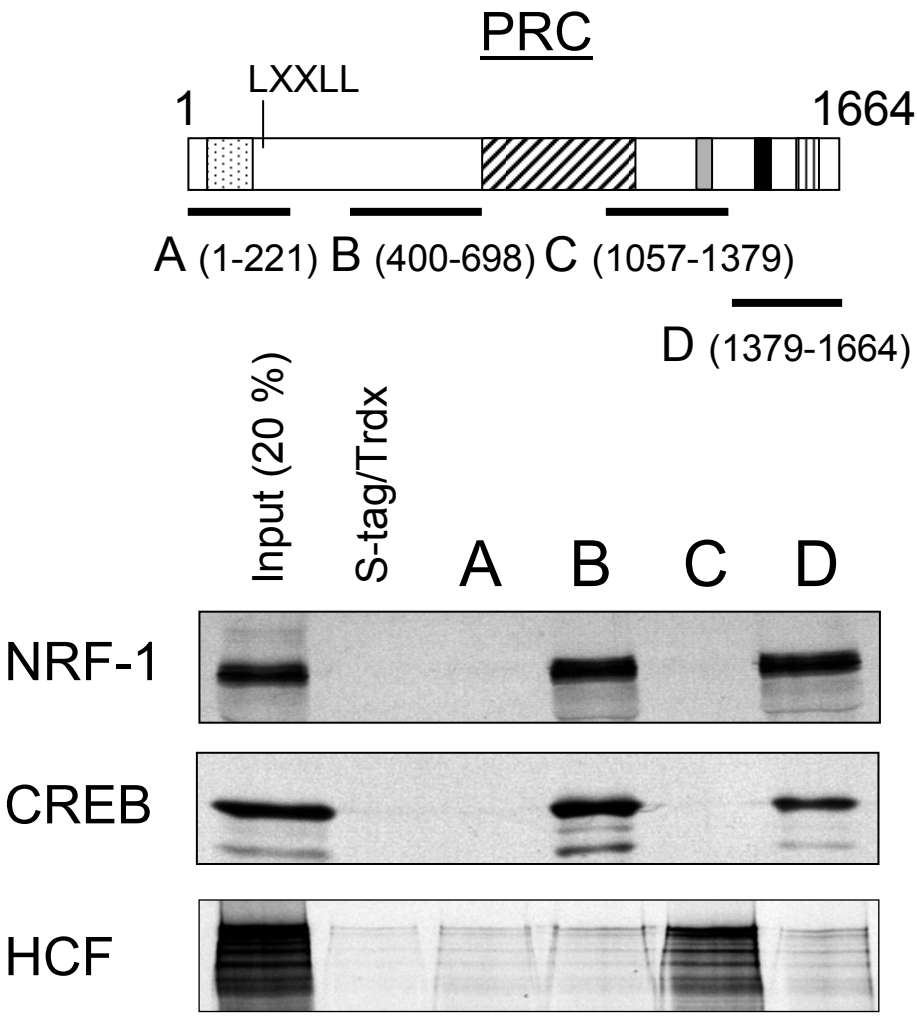
PRC
LXXLL
1
1664
A (1-221) B (400-698) C (1057-1379)
D (1379-1664)
Input (20 %)
S-tag/Trdx
A
B
C
D
NRF-1
CREB
HCF

If the interactions revealed by the *in vitro* binding assays are significant physiologically, it should be possible to detect a complex between PRC and CREB in cell extracts by co-immunoprecipitation. A vector designed to express hemagglutinin tagged CREB (CREB-HA) was introduced into 293FT cells by electroporation and cell extracts were immunoprecipitated either with control IgG or with purified anti-PRC(95-533) or anti-PRC(1047-1379). These cells were used for immunoprecipitation experiments because of their high transfection efficiency. Following gel electrophoresis, immunoblots were probed with mouse anti-HA monoclonal antibody. Both PRC antibodies at 2.5 μg resulted in the specific co-precipitation of a protein coinciding with the expected molecular mass of CREB **(Figure 4.4A, lanes 3 and 5)** and co-migrating with the CREB protein expressed in the cell extracts **(lane 7)**. Notably, increasing the concentration of anti-PRC 1047-1379 to 7.5 μg markedly enhanced the CREB signal **(lane 6)** whereas the same increase in anti-PRC 95-533 reduced the signal **(lane 4)**. This difference in the antibodies can be explained by the fact that a strong CREB interaction domain is localized to PRC amino acids 400-698 making it likely that the 95-533 antibody competes for CREB binding to PRC at the higher concentration. No such CREB interaction domain is localized to PRC amino acids 1047-1379 and thus the antibody directed against this region does not compete for CREB binding. No specific CREB band was detected in the IgG control at either concentration **(lanes 1 and 2)**. The results obtained for CREB were nearly identical to those obtained using goat anti-NRF-1 to probe an immunoblot following immunoprecipitation with anti-PRC 1047-1379 **(Figure 4.4B)**. NRF-1 was precipitated by anti-PRC 1047-1379 in a concentration-dependent manner confirming the specific interaction between PRC and NRF-1 observed previously (89) and demonstrating the validity of the assay for detecting PRC-transcription factor interactions.

These results confirm that CREB can enter into a complex with PRC in a manner that is indistinguishable from that observed for NRF-1.

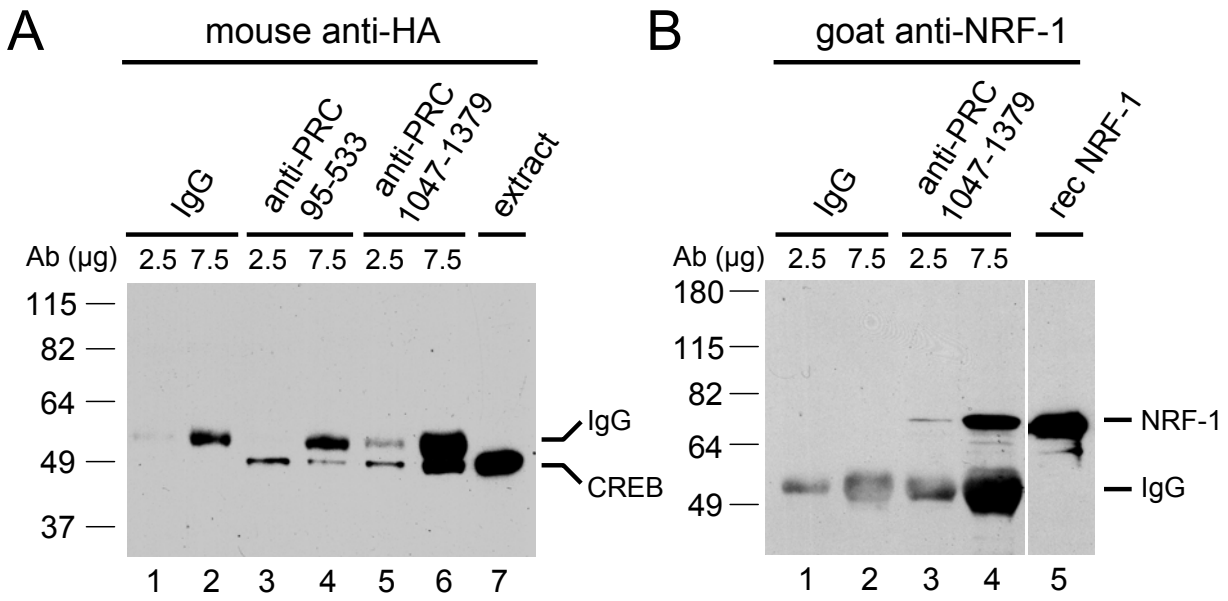

Figure 4.4. *In vivo* interaction between PRC and CREB.

A. HA-tagged CREB was expressed in 293FT cells following electroporation with pSG5/CREB-HA. Cell extracts were immunoprecipitated with either 2.5 or 7.5 µg respectively of rabbit IgG as a negative control **(lanes 1 and 2)**, anti-PRC(95-533) **(lanes 3 and 4)**, or anti-PRC(1047-1379) **(lanes 5 and 6)**. Immune complexes were brought down with protein A-agarose, washed, and run on an SDS-10% PAGE gel. For comparison, 20 µg of cell extract was run **(lane 7)**. After transfer, the immunoblot was probed with mouse anti-HA monoclonal antibody.

B. 293FT cell extracts were immunoprecipitated with either 2.5 or 7.5 µg rabbit IgG as a negative control **(lanes 1 and 2)** or anti-PRC(1047-1379) **(lanes 3 and 4)**. Immune complexes were precipitated and electroblotted as in *A*. For comparison, 2 ng of recombinant NRF-1 was run in **lane 5**. After transfer, the immunoblot was probed with goat anti-NRF-1. Molecular mass standards in kilodaltons are indicated at the left in each panel.

Molecular determinants of CREB binding to PRC. Both CREB and NRF-1 bind to PRC subfragments B and D, encompassing amino acids 400 to 698 and 1379 to 1664, respectively **(Figure 4.3)**. Deletion fine mapping within these regions was performed to assess whether the transcription factors bind to distinct sites within these PRC domains. A series of deletions within each domain was subjected to S-tag pull-down assays using *in vitro* translated NRF-1 and CREB. As shown in **Figure 4.5**, all of the fragments that bind CREB also bind NRF-1 and those that fail to bind CREB also fail to bind NRF-1. The 3' deletion breakpoint for the upstream domain was localized between amino acids 450 and 467 while the 5' deletion breakpoint was between amino acids 433 and 485. The smallest fragment binding both transcription factors was bounded by amino acids 433 to 467. Similarly the downstream domain was defined to amino acids 1379 to 1450, a region coinciding with the R/S domain. A comparison of the amino acid sequences of these binding sites does not reveal obvious sequence similarities although both contain clusters of basic amino acid residues. Thus, within the limits of resolution of this analysis, CREB and NRF-1 share the same binding sites within PRC.

Figure 4.5. Deletion fine mapping of the NRF-1/CREB interaction domains in PRC. Schematic representation of PRC is shown at top, with various functional domains indicated as described in the legend to **Figure 4.3**. A series of deletions of the PRC(400-698) and (1379-1664) subfragments, shown to bind NRF-1 and CREB, was constructed and their *in vitro* binding to the two ^{35}S-labeled transcription factors was compared using the S-tag pull down assay. Binding of the various subfragments was compared to that of S-tagged thioredoxin as a negative control. Bound proteins were eluted from the washed beads and visualized by autoradiography. A schematic of the relative length of each deletion, with numbers at the right indicating their amino acid coordinates, is shown. The ability to bind (+) or not bind (-) each transcription factor in the *in vitro* pull down assay is indicated at the right of each subfragment. The amino acid sequence of the smallest subfragment to display significant binding is shown at bottom.

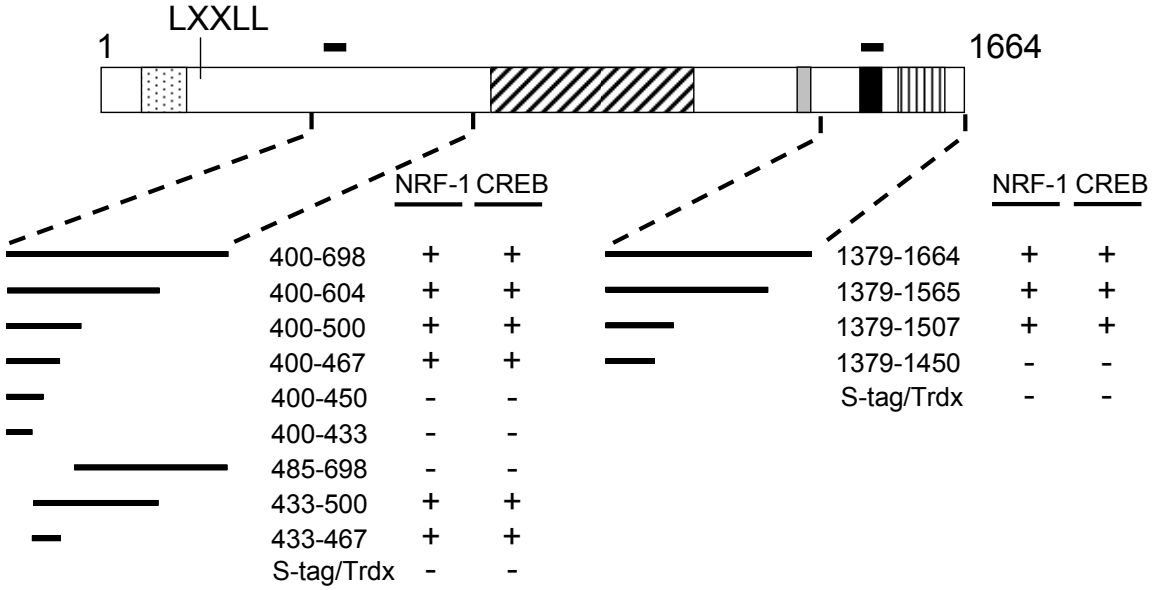

433-467

VVEPVVPKEPQNPPANAAPGSQRARKGRKKKSKEQ

1450-1507

SSRSRSRSLSPPHKRWRRSSCSSSGRSRRCSSSSSSSSSSSSSSSSSSSSRSRSRSPS

Previous domain mapping experiments demonstrated that PRC interacts with the NRF-1 DNA binding domain (89). A similar requirement for the CREB DNA binding domain was investigated by assaying a series of carboxy-terminal CREB deletions for their ability to bind both upstream and downstream CREB binding sites within PRC. Deletion of the CREB b-Zip DNA binding domain between amino acids 240 and 341 eliminated CREB binding to PRC sites encompassing amino acids 400 to 604 **(Figure 4.6, left panel)** and 1379 to 1664 **(Figure 4.6, right panel)**. Thus, the CREB DNA binding domain is required for the observed activator-coactivator interaction.

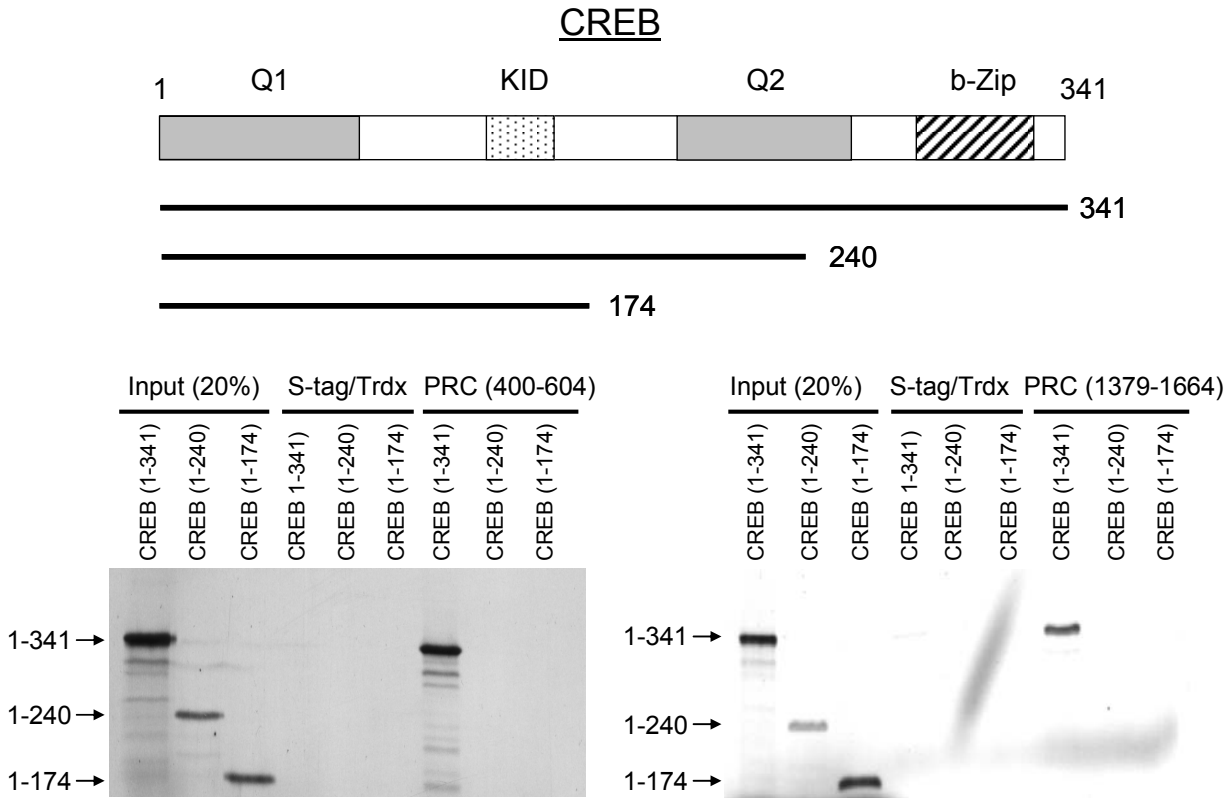

Figure 4.6. Deletion mapping the region of CREB required for binding PRC.

Schematic representation of CREB is shown at top, with various functional domains indicated. Full-length CREB and C-terminal deletions shown as solid lines below the diagram were ^{35}S-labeled and subjected to S-tag pull down assays using either the upstream CREB binding domain in PRC (amino acids 400 to 604) **(left panel)** or the downstream CREB binding domain (amino acids 1379 to 1664) **(right panel)**. Binding of the CREB subfragments to each PRC domain was compared to that of S-tagged thioredoxin as a negative control. Bound proteins were eluted from the washed S-protein agarose and visualized by autoradiography.

PRC *trans*-activation and dominant negative inhibition of respiratory growth. Both NRF-1 and CREB recognition sites are required for maximal *trans*-activation of the cytochrome *c* promoter by PRC (89). The finding of two distinct transcription factor interaction domains on PRC raises the question of whether they are functionally equivalent for promoter activation. Experiments with PGC-1α revealed that the carboxy-terminal R/S domain is dispensable for transcription initiation but serves as a protein-protein interaction interface that recruits splicing factors and promotes the coupling of transcription and RNA processing (64). As shown in **Figure 4.7**, the full-length PRC (PRC(1-1664)) activates the cytochrome *c* promoter several fold over the control in a transient co-transfection assay. However, most of this activity is eliminated by deleting the CREB/NRF-1 interaction domain localized to amino acids 433 to 467 within the context of the full-length PRC (PRCΔ433-467). To test further the importance of the CREB/NRF-1 binding domain within this region, a fragment containing this domain (PRC(400-604)) was expressed in *trans* in a PRC co-transfection assay. Under conditions of increasing PRC(400-604), PRC *trans*-activation of the promoter was inhibited to a level identical to that achieved upon deletion of amino acids 433 to 467. Introduction of same amounts of vector expressing an adjacent control fragment (PRC(1-221)), which lacks a CREB/NRF-1 binding site, showed little or no inhibition. These results are consistent with the conclusion that the transcription factor interactions within this region are important for the transcriptional activity of PRC. Since the carboxy-terminal CREB/NRF-1 interaction domain maps to the R/S domain of PRC, one might predict, based on the results with PGC-1α, that this domain would not be required for *trans*-activation of the cytochrome *c* promoter. Interestingly, deletion of the PRC carboxy terminus, containing both the R/S domain and the RNA recognition motif (PRC(1-1379)), did not significantly reduce PRC *trans*-activation of the promoter suggesting that the

CREB/NRF-1 recognition site within the R/S domain is not required for transcription initiation. The results obtained are unlikely to result from differences in expression because the full-length PRC (PRC(1-1664)) and PRC(Δ433-467) were expressed at similar levels whereas PRC(1-1379) was expressed several fold higher (not shown).

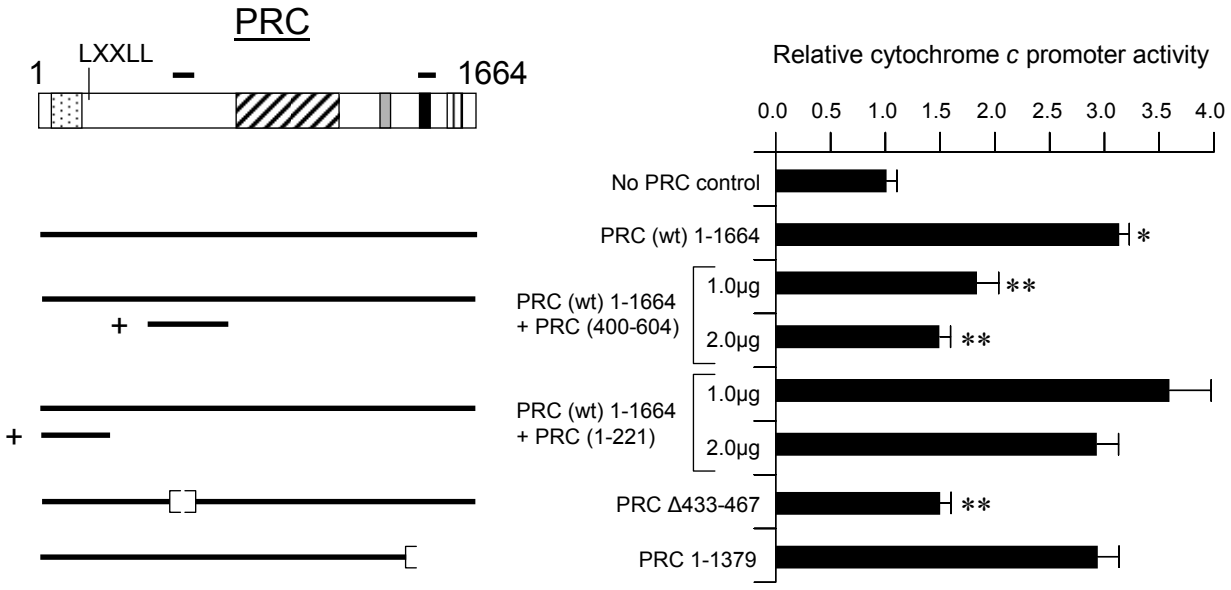

Figure 4.7. Determinants of PRC *trans*-activation of the cytochrome *c* promoter.

A cytochrome *c* promoter luciferase reporter construct was *trans*-activated by full-length PRC (PRC(1-1664)) or its mutated derivatives (PRC(Δ433-467) and PRC(1-1379)) in a transient co-transfection assay. Relative luciferase activity was measured in the absence of PRC subfragment or in the presence of 1 or 2 µg of plasmid expressing PRC(400-604) or PRC(1-221). Values were normalized for transfection efficiency using a *Renilla* luciferase control in a dual luciferase reporter system and represent the average ± S.E.M. for six separate determinations. A single asterisk indicates a *P* value of < 0.05 compared with values for the uninduced control. Double asterisks indicate *P* values of < 0.05 compared to values obtained from full-length PRC(1-1664) *trans*-activations. *wt*, wild type.

The dominant negative inhibitory effect of the PRC(400-604) subfragment in a transient transfection assay raised the question of whether this domain could inhibit biological function in growing cells. This possibility was tested by constructing a lentivirus vector designed to express this subfragment constitutively. Stable integrants were obtained following infection of BALB/3T3 cells with virus derived from the PRC(400-604) expressing construct and a control virus expressing bacterial tetracycline repressor (TR). TR was selected as the control because it is similar in size to the PRC subfragment and it has no known biological activity in mammalian cells. As shown in **Figure 4.8A**, these proteins were expressed in their respective cell lines but not in the wild-type controls. When plated on glucose growth medium, the PRC(400-604)-expressing cells displayed a small but reproducible growth lag relative to the TR control but showed no significant difference in growth rate **(Figure 4.8B)**. However, when plated on galactose growth medium, which requires mitochondrial respiration for the production of ATP, the PRC(400-604) expressing cells exhibited both a growth lag and a significant reduction in growth rate (approximately twofold) relative to the control **(Figure 4.8C)**. This result is consistent with the transfection data and supports an *in vivo* function for PRC in regulating respiratory growth.

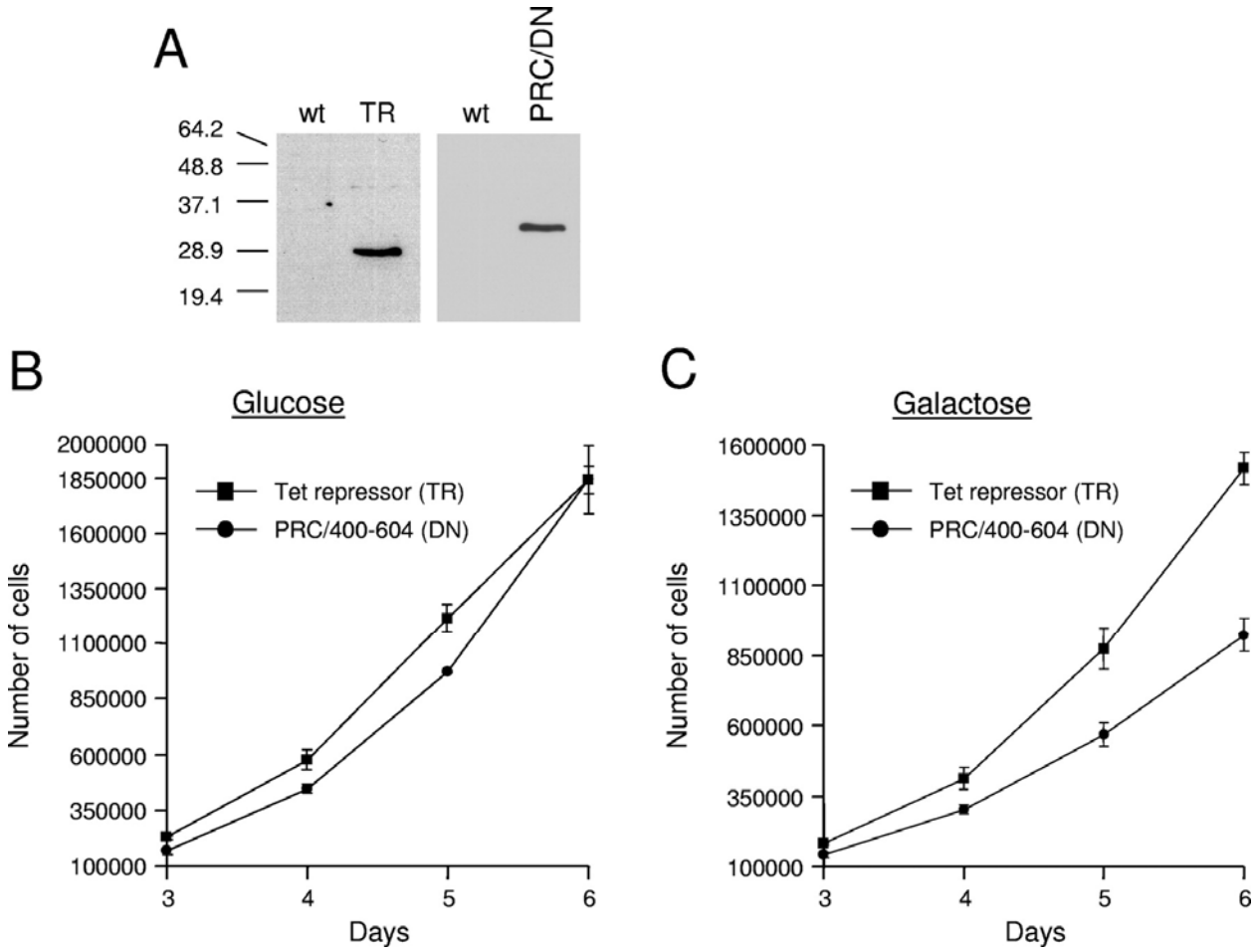

Figure 4.8. Growth comparison of PRC(400-604)-expressing cells to TR-expressing controls on media containing either glucose or galactose as the primary carbon source.

A. Immunoblotting of whole cell extracts from TR- or PRC/DN-expressing cells (DN, dominant negative) compared to that of wild type (wt). TR was detected using rabbit anti-TR antibody whereas PRC/DN was expressed from the lentivirus with a carboxy-terminal V5 tag and detected using anti-V5 antibody.

B. Growth of TR-and PRC/DN-expressing cells on glucose media.

C. Growth of TR- and PRC/DN-expressing cells on galactose media.

Growth curves in *B* and *C* represent the average ± S.E.M. for three separate determinations.

Serum induced promoter occupancy *in vivo*. If PRC targets the cytochrome *c* promoter through NRF-1 and CREB, one might expect that the up-regulation of PRC in the serum-induced transition from G_0 to G_1 would coincide with increased occupancy of the promoter by PRC *in vivo*. This was investigated by devising a quantitative chromatin immunoprecipitation (ChIP) assay using antibodies directed against NRF-1, CREB, phospho-CREB and PRC to assay the *in vivo* occupancy of the promoter by these factors in serum starved and serum stimulated cells. CREB and phospho-CREB serve as ideal internal controls because serum stimulation leads to the increased phosphorylation of CREB with little or no increase in CREB protein expression (108). The results of three independent experiments show significant occupancy of the cytochrome *c* promoter by PRC under conditions where the DNA bound transcription factors, NRF-1 and CREB, are also present **(Table 4.1)**. This supports the conclusion that all three factors associate with the promoter *in vivo* since they are all crosslinked to the same immunoprecipitated chromatin fragment. In addition, there is a significant increase in occupancy of the promoter by both PRC and NRF-1 at 8 h following serum stimulation of quiescent BALB/3T3 cells **(Table 4.1)**. This is the time frame where both PRC and cytochrome *c* expression are induced. CREB occupancy was increased only 1.4-fold whereas phospho-CREB was enhanced 3-fold to a level similar to that observed for PRC. These results provide *in vivo* evidence that PRC occupies the cytochrome *c* promoter and plays a regulatory role in transcriptional expression in the G_0 to G_1 transition.

Table 4.1. Chromatin immunoprecipitation (ChIP) analysis of cytochrome *c* promoter occupancy by PRC, NRF-1 and CREB upon serum stimulation of quiescent fibroblasts.

Precipitating antibody	Promoter occupancy[a]		Fold increase (stimulated/starved)[b]
	Starved (60 h)	Stimulated (8 h)	
Rabbit IgG	1.0	1.0	1.0
anti-NRF-1	38.9 ±17.1	98.5±9.1	2.5
anti-PRC (1047-1379)	3.8±1.1	11.9±1.5	3.1
anti-CREB	8.6±2.3	12.3±1.8	1.4
anti-phospho-CREB	15.3±3.3	45.7±3.4	3.0

[a]Values of relative promoter occupancy represent the average ± standard errors of the means for three separate determinations.

[b]Increases in levels of relative promoter occupancy for stimulated fibroblasts compared to corresponding levels for starved fibroblasts.

DISCUSSION

Investigations of the bi-genomic expression of the mitochondrial respiratory chain have contributed significant insights into understanding nucleo-mitochondrial interactions (105,122). The characterization of mammalian cytochrome *c* and cytochrome oxidase genes has led to the identification of nuclear respiratory factors, NRF-1 and NRF-2(GABP). In addition to their role in respiratory chain expression, these transcription factors have been associated with the expression of a variety of genes controlling diverse aspects of mitochondrial biogenesis including the transcription and replication of mtDNA. Important insights into the means by which transcription factors such as NRF-1 and 2 can be linked to extra cellular signals came with the discovery of the PGC-1 family of regulated coactivators (53). Although the three members of this family, PGC-1α, PGC-1β and PRC exhibit clear differences in regulation and transcription factor specificities, they all share the ability to bind NRF-1 and to *trans*-activate NRF-1 target genes (123). PGC-1α is the best-characterized family member and both gain and loss of function experiments have substantiated its role in mitochondrial biogenesis (54).

Here, we establish that PRC is a growth-regulated member of the PGC-1 coactivator family that has characteristics of an immediate early gene product. It is induced rapidly at both the mRNA and protein levels in response to serum stimulation of quiescent fibroblasts and its mRNA is super induced upon inhibition of protein synthesis by cycloheximide. The similarity of PRC mRNA half-life in serum starved, serum stimulated and confluent cells, coupled with the serum-induced increase in PRC nascent transcripts (not shown), indicate that transcriptional mechanisms regulate PRC expression. The rapid induction through preexisting factors coupled with a relatively short mRNA half-life is typical of immediate early gene products, which include chemokines, growth factors, protooncogenes, serine-threonine kinases and key enzymes

involved in nucleic acid metabolism among others (129). Although transcription factors are also well represented among immediate early gene products, to our knowledge serum-inducible transcriptional coactivators are not widely known. Coactivators that have been associated with immediate early gene expression, such as p62TCF and MKL1, are activated by phosphorylation and bind serum response factor (SRF), a potent activator of the growth factor response (130).

In addition to NRF-1, the cytochrome *c* promoter contains canonical CREB/ATF recognition sites and these sites have been linked to cytochrome *c* expression in response to both cAMP (127) and serum stimulation of quiescent fibroblasts (108). In the latter case, induction of cytochrome *c* mRNA was correlated with elevated levels of heme-containing holo-cytochrome *c* and enhanced mitochondrial respiration, presumably to help meet energy demands associated with cell division. It is of interest in this context that PRC utilizes the same NRF-1 and CREB/ATF recognition sites for maximal *trans*-activation of the cytochrome *c* promoter (89). The fact that PRC is rapidly induced upon serum stimulation, can bind NRF-1 and can *trans*-activate NRF-1 target genes suggested that it may function through a specific interaction with CREB as well. This possibility is intriguing in light of the fact that CREB, in addition to mediating a cAMP response to hormones, also plays a role in growth factor signaling. This mitogenic pathway involves phosphorylation of CREB by the $pp90^{rsk}$ family of protein kinases and the mitogen- and stress-activated kinases (MSKs) (131,132).

Here, we find that CREB and NRF-1 bind the same sites on PRC *in vitro* and that both factors exist in a complex with PRC *in vivo*. In addition, deletion of the CREB/NRF-1 binding site at amino acids 433 to 467 on PRC inhibits *trans*-activation of the cytochrome *c* promoter and a fragment containing this site (PRC(400-604)), when expressed in *trans*, can inhibit cytochrome *c* activation by full-length PRC. The same fragment specifically inhibits growth on galactose

when stably expressed from an integrated lentivirus. In contrast to glucose growth, where the bulk of the ATP produced is derived from glycolysis, growth on galactose requires mitochondrial respiration for ATP production because of the restricted metabolism of galactose through glucose 6-phosphate (133). Thus, specific dominant negative inhibition of respiratory growth on galactose by PRC(400-604) is consistent with a biological role for PRC in directing cell growth under conditions where energy is predominantly derived through oxidative phosphorylation. On this basis, one might predict that PRC deficiency would affect early postnatal development, when respiratory growth is enhanced, as well as tissues that rely heavily on oxidative energy. It will be of interest to determine both the stage of the cell cycle and the battery of genes affected by dominant negative inhibition of PRC. We note that prolonged growth on galactose abrogates the growth rate differential between the TR control cells and PRC(400-604)-expressing cells. This suggests that compensatory mechanisms may contribute to maintaining respiratory growth when PRC function is impaired.

These findings, together with the observation that both CREB and NRF-1 recognition sites are required for maximal PRC activation of the promoter (89), provide compelling evidence that PRC works through the interaction with both CREB and NRF-1. As previously observed for NRF-1 (89), CREB binding to PRC requires its DNA binding domain. NRF-1 has a unique DNA binding domain (113) while CREB binds DNA through a basic leucine zipper (bZip) domain (134,135). A similar requirement for the NRF-1 and PPARγ DNA binding domains, which are also structurally diverse, was found for the interaction of these transcription factors with PGC-1α (54). It remains an open question as to how the same regions on these coactivators recognize disparate DNA binding motifs in their cognate transcription factors. A second CREB/NRF-1 binding site within the PRC R/S domain appears not to function in transcription initiation. The

PGC-1α R/S domain is also dispensable for transcription initiation but is required for coupling transcription to RNA processing (64). A requirement for splicing would not be detected in the assay system reported here because the cytochrome *c* promoter construct is devoid of introns and thus expression of the luciferase reporter is independent of RNA splicing.

As shown here by quantitative ChIP assay, PRC occupies the cytochrome *c* promoter *in vivo*, and PRC occupancy of this promoter is enhanced upon serum stimulation of quiescent cells. We also observe PRC occupancy of the human cytochrome *c* promoter in 293FT cells (not shown). The fold-increase in PRC at the promoter in serum stimulated BALB/3T3 cells parallels the fold-increase in phosho-CREB detected using anti-phospho-CREB antibody in keeping with the fact that CREB phosphorylation occurs under these conditions. Anti-CREB antibody is an ideal negative control because steady state levels of CREB protein show little or no change upon serum stimulation (108) and likewise the fold occupancy of the promoter by CREB is only modestly elevated. Several members of the CREB/ATF family of factors recognize the canonical CREB binding site. The ChIP results using both anti-CREB and anti-phospho-CREB antibodies provide strong evidence that CREB is actually present at the cytochrome *c* promoter *in vivo*. The methodology does not allow absolute comparisons between antibodies because of differences in antibody affinity, accessibility of the various factors and efficiency of crosslinking. Nevertheless, the results support the conclusion that PRC induction and association with growth-regulated promoters represents a novel pathway for mediating the cellular response to proliferative signals.

The results in this work provide an alternative to the current model of CREB activation. It is well established that phosphorylation of CREB on Ser 133 promotes CREB binding to two structurally related coactivators, CBP and p300 (136). Binding these coactivators occurs through the CREB P-box, which contains Ser 133 (137). In contrast to PRC and other PGC-1 family

members, both CBP and p300 have intrinsic histone acetyltransferase activity, which facilitates transcriptional activation by promoting the remodeling of chromatin (138). PRC has a potent amino-terminal transcriptional activation domain that is highly similar to that found in PGC-1α (89). In PGC-1α, this domain associates with several coactivators that have intrinsic histone remodeling activities including CBP/p300 and SRC-1 (62). It is likely that targeting of CREB and NRF-1 by PRC would allow recruitment of these same coactivators to the transcription complex via the conserved PRC activation domain. It is possible that phosphorylation of either or both transcription factors stabilizes their interaction with PRC. Thus, PRC induction and interaction with promoter bound CREB and NRF-1 may represent an alternative mechanism to promote chromatin remodeling in response to mitogenic stimulation.

MATERIALS AND METHODS

Plasmids.

The plasmids FL-PRC/pBSII, FL-PRC/pSV-Sport, pET32b/PRC(1-221), pET32c/PRC(1047-1379) and pET32c/PRC(1379-1664) have been described (89). pET32a/PRC(400-698) was constructed using template FL-PRC/pBSII and primers PRC/*Bam*HI400S (AAAAAAGGATCCGCTGCTGTGCCCAAGGTA) and PRC/*Xho*I698AS (AAAAAACTCGAGCACTGCACCACGTCTGGG) to amplify a 900bp fragment that was inserted into *Bam*HI/*Xho*I digested pET32a. Similarly, pET32a/PRC(400-450), pET32a/PRC(400-467), pET32a/PRC(400-604), pET32a/PRC(433-467), pET32a/PRC(433-500), pET32a/PRC(450-500), pET32a/PRC(467-500), pET32a/PRC(485-698), pET32a/PRC(1379-1450), pET32a/PRC(1379-1507), and pET32a/PRC(1379-1565) were prepared by cloning PCR products into *Bam*HI/*Xho*I digested pET32a.

PRC (1-1379)/pSV-Sport was constructed by combining a 4kb *Xho*I/*Stu*I fragment from FL-PRC/pBSII with the *Sal*I/*Sna*BI fragment of pSV-Sport. The internal deletion in PRC(433/467)/pSV-Sport was introduced by PCR. A PCR product containing the PRC internal *Hin*dIII site at the 5' end and the deletion at the 3' end was amplified from FL-PRC/pBSII as template using primers PRC/*Hin*dIIIS (AAAAAAAAAAAGCTTCCTAGCTGGAGACCC) and PRC/Del 433-467AS (ACAGGCTGCTGGCTCCCTGGGCTTCAATAAGC). Similarly, a product with the deletion at the 5' end and the PRC internal *Eco*RI site at the 3' end was amplified from the same template with primers PRC/Del 433-467S (AAGCCCAGGGAGCCAGCAGCCTGTGTGGAAGG) and PRC/*Eco*RIAS (AAAAAAAAAGAATTCTCCAAGGCAGCTGCC). Equal amounts of the two products were mixed and amplified using primers PRC/*Hin*dIIIS and PRC/*Eco*RIAS and the resulting 850bp fragment was digested with *Hin*dIII/*Eco*RI and subcloned into *Hin*dIII/*Eco*RI digested FL-PRC/pBSII. PRC(Δ433-467)/pSV-Sport was generated by cloning the 5.2kb *Xho*I/*Not*I fragment from PRC(433-467)/pBSII into (*Sal*I/*Not*I) digested pSV-Sport.

pSG5/NRF-1 (139), pSG5/CREB (108) and pNCITE/HCF (140) have been described. Vectors for the expression of CREB deletions pSG5/CREB(1-174) and pSG5/CREB(1-280) were generated by PCR using pSG5/CREB as a template. The 520bp *Eco*RI/*Bam*HI CREB fragment generated by using PCR primers pSG5MCS (GGGCAACGTGCTGGTTATTGTGCTGTCTCA) and CREB/*Bam*HI174AS (TGGGATCCTGCTAAATTGGAGTTGGCACCG) was cloned into *Eco*RI/*Bam*HI digested pSG5 to create pSG5/CREB(1-174). pSG5/CREB(1-280) was constructed by substituting primer CREB/*Bam*HI280AS (AAAAAAGGATCCTTATTCAGCAGGCTGTGTAGG) for CREB/*Bam*HI174AS.

pSG5/CREB-HA was made by cloning the *Bgl*II/*Bam*HI PCR product generated using CREB/*Bgl*IIS (CTGATGGACAGCAGATCTTAGTGCCCAGCA) and CREB/*Bam*HI Stop HAAS (AAAGGATCCTTAAGCGTAATCGGGGACATCGTAAGGGTAATCTGATTTGTGGCAGTAAAG) into *Bgl*II digested pSG5/CREB. pSG5/PRC(400-604)-HA was made using template FL-PRC/pBSII and primers PRC/*Bam*HI/Sta400(S) (AAAAAAGGATCCCACCATGGCTGCTGTG) and PRC/*Bam*HI/StpHA604(AS) (AAAAAAGGATCCTCAAGCGTAATCGGGGACATCGTAAGGGTAAGGGCCAGC) to generate a 650bp fragment that was cloned into the *Bam*HI site of pSG5. pSG5/PRC(1-221)-HA was prepared with the same template and the primer pair PRC/*Bam*HI1(S) (AAAAAAGGATCCATGGCGGCGCGCCGG) and PRC/*Bam*HI/StpHA221(AS) (AAAAAAGGATCCTCAAGCGTAATCGGGGACATCGTAAGGGTACTTGGGGGAAGAGGTCTC). The PCR product was digested *Bam*HI and cloned into pSG5.

Plasmid constructs for the production of glutathione fusion proteins used for antibody purification were made by cloning subfragments of PRC into pGEX-3X. A PCR product for the construction of pGEX-3X/PRC(400-467) was generated using primers PRC/BamHIxx400S (AAAAGGATCCCCGCTGCTGTGCCCAAGGTA) and PRC/EcoRI467AS (ACAGGCGAATTCCTGCTCCTTGCTCTTCTT) with FL-PRC/pBSII as template. The amplification product was digested with *Bam*HI/*Eco*RI and cloned into *Bam*HI/*Eco*RI digested pGEX-3X. pGEX-3X/PRC(1047-1379) was generated in a similar fashion. Sequence verification of all constructs was performed by the Northwestern Biotech Core Facility.

Cell culture and transfections.

293FT cells were maintained in Dulbecco's modified Eagle's medium (DMEM, Invitrogen) with 10% fetal bovine serum (FBS, Hyclone), 1% penicillin/streptomycin (Invitrogen) and 0.1 mM non-essential amino acids (NEAA, Invitrogen). For transfection, proliferating cells were trypsinized, collected in PBS, and counted with a hemocytometer. The cells were resuspended in Opti-MEM (Invitrogen) (2.3×10^6 cells per 400 µl) and mixed with plasmid DNA. Transfections were completed by electroporating the mixture with the Bio-RAD Gene Pulser Xcell in a 2 mm cuvette according to the manufacturer's setting for 293 cells. Following electroporation, the cells were diluted in 10 ml fresh medium and plated on 10 cm tissue culture dishes.

For serum starvation experiments, BALB/3T3 fibroblasts were plated at a density of 875,000 per 150 mm dish in DMEM containing 10% calf serum, 100 units/ml penicillin and 100 µg/ml streptomycin, and allowed to grow for 48 h. The cells were then washed twice with PBS and serum-starved in DMEM containing 0.5% fetal bovine serum for 48-60 h. Following starvation, the cells were stimulated in DMEM containing 20% fetal bovine serum for the indicated times. The medium was changed 48 h after stimulation, and confluent cells were harvested 24 h later. U2OS cells were grown in McCoy's 5a medium with 1.5 mM L-glutamine (Invitrogen) supplemented with 10% fetal bovine serum (HyClone) and 1% penicillin/streptomycin (Invitrogen). Cells were starved in McCoy's 5a medium containing 0.1% fetal bovine serum for 18 h followed by stimulation in medium containing 20% fetal bovine serum for the indicated times.

Transient transfection of BALB/3T3 cells was performed by calcium phosphate precipitation as described previously (89). BALB/3T3 cells used in transfections were

maintained in Dulbecco's modified Eagle's medium (DMEM) (Invitrogen) supplemented with 10% calf serum (HyClone) and 1% penicillin-streptomycin (Invitrogen). Cells were plated at a density of 3000 cells per cm^2 in six-well plates and transfected with 100 ng of pGL3RC4/-326 reporter (108) and 4 ng of pRL-TK control vector (Promega). For *trans*-activation, 2 μg each of full-length PRC (PRC/pSV-Sport) or mutated derivatives (PRC (Δ433-467)/pSV-Sport or PRC (1-1379)/pSV-Sport) were co-transfected. For *trans*-inhibition, 2 μg of full-length PRC (PRC/pSV-Sport) was co-transfected with either 1 or 2 μg of pSG5/PRC (400-604)-HA or pSG5/PRC (1-221)-HA. After 5 h cells were washed twice with Dulbecco's phosphate-buffered saline (Invitrogen) and grown for an additional 40 h in fresh media. Cell extracts were prepared and luciferase assays were performed using the Dual Luciferase Reporter Assay System (Promega). Firefly luciferase activity from the cytochrome *c* promoter-luciferase reporter construct pGL3RC4/-326 (108) was normalized to *Renilla* luciferase luminescence from the cotransfected pRL-TK control vector.

RNA methods.

The requirement for protein synthesis on PRC mRNA induction was tested by subjecting BALB/3T3 fibroblasts to serum starvation as described above. The cells were stimulated with serum in the absence or presence of cycloheximide (10 μg/ml) and RNA was harvested at various times with Trizol (Invitrogen). PRC mRNA levels relative to the 18S rRNA control were determined by real-time RT-PCR as described (46). Results are expressed as the fold induction of PRC mRNA in stimulated versus starved cells.

The half-life of PRC mRNA in serum stimulated BALB/3T3 fibroblasts was determined by adding actinomycin D (5 μg/ml) to the medium at 8 h after serum stimulation. The PRC

mRNA half-life in starved BALB/3T3 fibroblasts was determined by adding actinomycin D (5 μg/ml) together with the starvation medium (DMEM + 0.5% FBS). The half-life of PRC mRNA in confluent BALB/3T3 fibroblasts was determined by adding actinomycin D (5 μg/ml) to confluent cultures. The effect of protein synthesis on PRC mRNA stability was determined by subjecting BALB/3T3 fibroblasts to serum starvation as described above. The cells were stimulated with serum for 1 h in the presence or absence of cycloheximide (10 μg/ml). After 1h the cells were washed twice with PBS and further stimulated for various times in the presence of 5 μg/ml actinomycin D. In each case total RNA was harvested with Trizol (Invitrogen) at various times following the addition of actinomycin D and PRC mRNA levels relative to the 18S rRNA control were determined by real-time RT-PCR as described (46).

Antibodies.

The preparation of affinity-purified anti-PRC(95-533) has been described (89). Thioredoxin fusion proteins used for immunization were prepared from BL21 CodonPlus(DE3)-RIL cells (Stratagene) transformed with either pET32a/PRC(400-467) or pET32c/PRC(1047-1379). Transformants were grown to 'log' phase (OD_{600} approximately 0.5) at 37^{o}C in LB with 0.1 mg/ml ampicillin and 34 μg/ml chloramphenicol. Induction was carried out at room temperature in the same media supplemented with IPTG to 1mM and grown 2.5 h. The cells were resuspended in 1/20 culture volume of binding wash buffer (BWB) (20 mM Tris-HCl, pH 7.5, 150 mM NaCl, 0.1%Triton X-100, 0.1 mM PMSF), lysed on ice for 30 min with lysozyme at 1mg/ml and frozen overnight at –80^{o}C. The lysate was thawed on ice, sonicated briefly in 10 s bursts and centrifuged at 20,000 x *g* for 20 min. The thioredoxin-fusion proteins trdx-PRC(400-467) and trdx-PRC(1047-1379) were purified from the soluble fraction of the lysates with 1ml

Ni-NTA Superflow (Qiagen) resin per 10 ml lysate. The slurry was mixed on rocking table 1 h at 4^{o}C. The resin was washed with 50 resin volumes 300 mM NaCl, 50 mM NaH_2PO_4, pH 7.5, 20 mM imidazole. The thioredoxin-fusion proteins were eluted with 300 mM NaCl, 50 mM NaH_2PO_4, pH 7.5, 250 mM imidazole and dialyzed overnight in PBS at 4^{o}C. Rabbit anti-PRC(400-467) and anti-PRC(1047-1379) sera were prepared commercially using the purified thioredoxin-fusion proteins as antigens (Harlan Bioproducts for Science). Antibodies were affinity purified on columns prepared by coupling glutathione S-transferase fusion proteins GST-PRC(400-467) and GST-PRC(1047-1379) produced from pGEX-3X/PRC(400-467) and pGEX-3X/PRC(1047-1379), respectively, to CNBr-activated sepharose 4B (Amersham) according to the manufacturer's instructions. The GST-fusion proteins were purified from soluble bacterial lysate by adding 1ml Glutathione Sepharose 4B (Amersham) resin per 10 ml lysate and rocking the slurry 1 h at 4^{o}C. The resin was washed with 50 resin volumes of 10 mM Tris-HCl, pH 8, 500 mM NaCl. The fusion proteins were eluted with 100 mM glycine, pH 2, collected in 0.1 elution volumes of 2.5 M Tris-HCl, pH 8. The eluted GST-fusion proteins were dialyzed in coupling buffer (0.1 M $NaHCO_3$, pH 8.5, 0.5 M NaCl) prior to coupling. The binding and elution of the antibodies from the affinity columns has been described (89). The affinity-purified antibodies were concentrated by ammonium sulfate precipitation and dialyzed against PBS.

Preparation and affinity-purification of goat anti-NRF-1 serum has been described previously (89,113). Mouse anti-HA monoclonal antibody was purchased from Covance Research Products (MMS-101R). The antibodies were used in coimmunoprecipitation experiments to detect NRF-1 and hemagglutinin-tagged CREB (CREB-HA), respectively. Rabbit anti-TR antibody and mouse anti-V5 antibody were obtained from Imgenex and Invitrogen, respectively.

S-Tag pulldown assay.

Pulldown assays were performed by a minor modification of a previous method (89). The expression of thioredoxin-fusion proteins and preparation of a soluble bacterial lysates was carried out as described above for the production of fusion proteins for antibody production. The thioredoxin-fusion proteins were purified with S-Protein Agarose resin (Novagen) by adding 100 µl of 50% S-Protein Agarose slurry to 1 ml bacterial lysate. The slurry was rocked at 4^{o}C for 1 h and the resin bound protein was removed by centrifugation for 1 min at 270 x *g*. Following aspiration of the supernatant, the resin was washed five times with 1 ml BWB and suspended in 150 µl BWB. The amount of a given fusion protein bound to the resin was estimated by SDS-PAGE electrophoresis of an aliquot followed by Coomassie Blue staining.

NRF-1, CREB (and its deletions) and HCF were ^{35}S-labelled by *in vitro* translation (TNT Reticulocyte Lysate System; Promega) according to the manufacturer. A 5 µl aliquot of translation reaction was mixed with approximately 1 µg thioredoxin fusion protein (in S-Protein slurry) in 500 µl binding buffer (65) and rocked at 4^{o}C for 1 h. The resin was washed five times with 500 µl binding buffer at 4^{o}C, suspended in 20 µl sample buffer (with β-mercaptoethanol) and boiled 5 min. The samples were separated by SDS-PAGE and visualized by autoradiography.

Coimmunoprecipitation and immunoblotting.

Approximately 13.5 x 10^{6} 293FT cells were transfected by electroporation with pSG5/CREB-HA and plated on three 15 cm tissue culture dishes as described above. An additional 13.5 x 10^{6} non-transfected 293FT cells were plated on three 15 cm tissue culture dishes. The cells were maintained at 37^{o}C for approximately 48 h and then lysed in NP-40 lysis

buffer (50 mM Tris-HCl [pH 8.0], 150 mM NaCl, 1% NP-40, 2.5 mM Na_2VO_4, 5 mM NaF, 0.1 mM PMSF, 0.1 mM EDTA and mini-Complete Protease Inhibitor Cocktail (Roche)) as described previously (89). The protein concentration of each whole cell extract was determined by Bradford assay (BioRad) using known concentrations of BSA as standards. Purified rabbit immunoglobulin G (IgG; Sigma) control, affinity-purified anti-PRC(95-533) or affinity-purified anti-PRC(1047-1379) (2.5or 7.5 μg of each) was added to 500 μg whole cell extract (pSG5/CREB-HA-transfected or non-transfected) in a total volume of 250 μl NP-40 lysis buffer. After 1 h incubation on ice, 15 μl Protein A-agarose (Roche) was added, and the incubation continued an additional 1 h on a rocking table at 4^{o}C. The immunoprecipitate was centrifuged for 1 min at 270 x *g* and washed four times with 500 μl NP40 lysis buffer. The rabbit IgG control and anti-PRC immunoprecipitates were resuspended in 20 μl sample buffer containing β-mercaptoethanol, subjected to 10% SDS-PAGE and transferred to a nitrocellulose membrane (Schleicher and Schuell) using a Trans Blot SD Semi-Dry Electrophoretic Transfer Cell (BioRad) with Towbin transfer buffer (141). Immunoblots from pSG5/CREB-HA transfected cells were probed with mouse monoclonal anti-HA antibody (Covance) whereas those from non-transfected cells were probed with affinity-purified goat anti-NRF-1 antibody.

For detection of PRC protein, whole cell extracts were prepared as described above and subjected to 7.5% SDS-PAGE and transferred to nitrocellulose membranes (Schleicher & Schuell) with HMW transfer buffer (50mM Tris, 380mM Glycine, 0.1% SDS, and 20% methanol) using a Mini Trans-Blot Cell tank transfer system (Bio-Rad). Immunoblots were probed with anti-PRC(95-533) (89), anti-PRC(400-467) or anti-PRC(1047-1379). Proteins were visualized using SuperSignal West Pico Chemiluminescent substrate (Pierce Biotechnology).

Chromatin immunoprecipitation.

Starved and 8 h serum-stimulated BALB/3T3 fibroblasts were fixed in 1% formaldehyde for 10 min at 25ºC. Chromatin immunoprecipitations (ChIP) were performed as described previously (46,119) with control IgG antibodies (Sigma), anti-NRF-1 (116), anti-PRC(1047-1379) (this work), anti-CREB and anti-phospho-CREB antibodies (Santa Cruz Biotechnology). Salmon sperm DNA/protein G Agarose (Roche Diagnostics) was used instead of salmon sperm DNA/protein A Agarose (Roche Diagnostics) for the precipitation with goat anti-phosho-CREB because protein A cannot efficiently bind goat IgG. Immunoprecipitated promoter fragments were quantitated by real-time PCR on the ABI PRISM 7900HT sequence detection system with the SYBR Green PCR Mastermix (Applied Biosystems). The primers used for real-time PCR were specific for the mouse cytochrome *c* promoter (forward: GTTACCTGAGCCGAGCCACAC, reverse: TGACGTAACCGCACCTCATTGG) and were used to amplify a promoter fragment that includes the NRF-1 (-156/-145 relative to the transcription initiation site) and CREB (-262/-255 and -110/-103) recognition sites. The $\Delta\Delta C_T$ method (142) was used to calculate the relative quantity of immunoprecipitated cytochrome *c* promoter DNA from serum-starved or -stimulated cells. The ΔC_T value was calculated by subtracting the average cycle threshold (C_T) value of the input DNA from the average C_T value of the immunoprecipitated DNA. $\Delta\Delta C_T$ was then calculated by subtracting the ΔC_T value of the ChIP with control IgG from the ΔC_T value of the ChIP with specific antibody. The results were expressed as the relative levels of promoter occupancy by the various factors compared with levels for control IgG for quiescent and serum-stimulated cells.

Lentivirus methods and cell growth determinations.

Stable BALB/3T3 cell lines constitutively expressing PRC(400-604) or the *tetR* gene encoding the Tet repressor (TR) (as a control) were generated using a ViraPower T-REx Lentiviral Expression System according to the manufacturer's protocol (Invitrogen). Briefly, lentivirus was produced by transfecting the 293FT producer cell line with the expression constructs pLenti4/TO/V5-DEST-PRC(400-604) or pLenti6/TR. BALB/3T3 cells were infected with the viral supernatants and stably transduced cells were selected using the appropriate antibiotic. Growth rates for both cell lines were determined by growing freshly thawed cells to sub confluence and then plating 20,000 cells in 6-cm dishes containing DMEM supplemented with 10% calf serum, 1% penicillin-streptomycin, 1mM sodium pyruvate, and either 5mM glucose or 5mM galactose. Cells were fed daily and counted from days 3 through 6 using a hemocytometer.

Statistical analysis.

Statistical comparisons of the data were made by *t*-test. The level of significance was set at P values of < 0.05 in all cases.

ACKNOWLEDGMENTS

We thank Winship Herr of Cold Spring Harbor Laboratories for the gift of pNCITE/HCF. This work was supported by United States Public Health Service grant GM32525-23.

CHAPTER 5:

PGC-1-RELATED COACTIVATOR (PRC) COMPLEXES WITH HCF-1 AND NRF-2β IN MEDIATING NRF-2(GABP)-DEPENDENT RESPIRATORY GENE EXPRESSION

INTRODUCTION

Mitochondria produce the bulk of cellular energy through their oxidation of pyruvate and fatty acids. Chemical bond energy is converted to reducing equivalents that are used by the electron transport chain of the inner mitochondrial membrane to establish an electrochemical proton gradient. Dissipation of this gradient drives the synthesis of ATP and the generation of heat (143,144). Mitochondria are semiautonomous in that they contain their own genetic system based on a multicopy mitochondrial DNA (mtDNA) genome. In vertebrates, a covalently closed circular mtDNA of approximately 16.5 kb encodes 13 essential protein subunits of respiratory complexes I, III, IV and V along with the 22 tRNAs and 2 rRNAs required for their translation within the mitochondrial matrix (90,145,146). This limited coding capacity necessitates that nuclear genes specify most of the numerous gene products required for the molecular architecture and biochemical functions of the organelle (105,122). These include the majority of respiratory chain subunits, all of the protein constituents of the mitochondrial translation system and all of the gene products required for the transcription and replication of mtDNA.

At the transcriptional level, nucleo-mitochondrial interactions rely upon nucleus-encoded transcription factors and transcriptional coactivators. Certain of these factors direct the transcription of mtDNA while others act on nuclear genes required for the biogenesis and function of the organelle (122,146). Among the latter are the nuclear respiratory factors, NRF-1 and NRF-2(GABP). These proteins were identified as activators of cytochrome *c* (41,126) and

cytochrome oxidase (139) genes and have subsequently been associated with the expression of many genes whose products contribute essential mitochondrial functions, particularly those related to the respiratory apparatus (105,122). In addition, both factors have also been implicated in functions related to cell proliferation (51,147), results consistent with the early embryonic lethality associated with targeted disruptions of NRF-1 (47) or NRF-2(GABP) (48) in mice.

In addition to these transcription factors, members of the PGC-1 family of inducible coactivators act as intermediaries between the environment and the transcriptional machinery specifying a number of important pathways related to cellular energetics (123,148). PGC-1α, the founding member of the family, was originally identified for its role in adaptive thermogenesis in brown fat (53). The coactivator is induced robustly in brown fat in response to cold exposure and participates in the induction of uncoupling protein 1. In addition, PGC-1α orchestrates a program of mitochondrial biogenesis in part by serving as a *trans*-activator of NRF-1 and NRF-2 target genes (54). The coactivator binds NRF-1 in a manner similar to that observed for PPARγ and directs expression of respiratory subunits as well as mtDNA transcription and replication factors (46,54). PGC-1β, a close relative of PGC-1α, also functions as a NRF-1 coactivator (75) but differs from PGC-1α in mediating biological responses in liver and muscle (78,83).

A third PGC-1 family member was designated as PRC (PGC-1-related coactivator) (89). Although divergent from PGC-1α in overall sequence, PRC has a number of structural features that are spatially conserved including a potent amino-terminal activation domain, a central proline-rich region, an arginine/serine rich domain (R/S domain) and an RNA recognition motif (RRM). However, PRC differs from PGC-1α in that it is not induced significantly during adaptive thermogenesis but rather exhibits the properties of a cell growth regulator (89). PRC mRNA and protein are markedly down regulated when cultured cells exit the cell cycle as a

result of serum starvation or contact inhibition. The mRNA and protein are also rapidly induced upon serum stimulation of quiescent cells in the G_0 to G_1 transition. This induction is insensitive to cycloheximide and thus occurs in the absence of *de novo* protein synthesis (99). Moreover, cycloheximide treatment leads to super induction and stabilization of PRC mRNA. These properties are characteristic of the class of immediate early genes whose rapid responses to growth factors represent the earliest events in the genetic program leading to cell proliferation (129).

Like PGC-1α, PRC binds NRF-1 both *in vitro* and *in vivo* and directs the expression of NRF-1 target genes related to respiratory chain expression (46,89). In addition, both PRC and PGC-1α are known to utilize NRF-2 binding sites to *trans*-activate NRF-2-dependent promoters in transfected cells (46). However, neither coactivator has been shown to interact directly with NRF-2. This suggests that PRC or PGC-1α coactivation through NRF-2 may require a third party that binds both the transcription factor and the coactivators. An ideal candidate for such a role is HCF-1 (host cell factor-1). HCF-1 is an abundant, chromatin-associated protein that was first identified through its participation in the VP16 activation of the herpes simplex virus immediate-early genes (149). A large 2035-amino acid HCF-1 precursor is cleaved autocatalytically to generate multiple amino- and carboxy-terminal fragments that remain associated noncovalently (150,151). HCF-1 is expressed ubiquitously and is required for cell cycle progression. A temperature-sensitive mutation in the β-propeller domain of HCF-1 results in G_0/G_1 arrest at the nonpermissive temperature (152). The cell cycle arrest is reversed at the permissive temperature and the cells reenter the proliferative cycle. Moreover, specific HCF-1 subunits promote exit from mitosis and progression through G_1 (153).

In addition to its interaction with VP16, HCF-1 binds NRF-2(GABP) through the transcriptional activation domain on the NRF-2β(GABPβ) subunit (154). Mutations that interfere with NRF-2(GABP) *trans*-activation also block binding to HCF-1 suggesting that HCF-1 functions as a NRF-2(GABP) coactivator. Here, we establish that PRC exists in a complex with HCF-1 and NRF-2β. The sequence requirements for interactions between PRC and HCF-1 and between HCF-1 and NRF-2β are the same as those required for PRC *trans*-activation of NRF-2-dependent transcription. Finally, chromatin immunoprecipitations coupled with loss of function experiments demonstrate that the PRC-containing complex associated with the promoter of a key mitochondrial transcription factor contributes to the expression of mitochondrial transcripts and respiratory enzyme activity. The results establish that HCF-1 is a functional intermediary in the PRC *trans*-activation of at least a subset of NRF-2 target genes required for mitochondrial respiratory function.

RESULTS

Similarities and differences in transcription factor recognition by PRC and PGC-1α. PRC is similar to PGC-1α in both its structure and in its ability to *trans*-activate NRF target genes. Here, we compare the two coactivators for their ability to interact with relevant transcription factors using a thioredoxin pull-down assay. As shown in **Figure 5.1**, PRC differs from PGC-1α in its interaction with several nuclear hormone receptors. PRC shows little if any specific interaction with PPARγ under conditions where specific binding of PPARγ to PGC-1α subfragments A, B and D is evident. The results also confirm that the interaction between PGC-1α and PPARγ is ligand independent since MCC-555, a thiazolidinedione ligand for PPARγ, fails to enhance the signal. In contrast to PRC, PGC-1α engages in ligand-dependent binding to both

TRβ and RAR through a domain containing the LXXLL coactivator signature motifs (53). This result is confirmed in **Figure 5.1**, which shows ligand-dependent binding of PGC-1α subfragments A and B to both TRβ and RAR. Under similar conditions only weak ligand-independent binding is observed to PRC subfragments B and D, neither of which contain the LXXLL motif. A PRC fragment bounded by amino acids 1-700 spanning fragments A and B also exhibited a weak ligand-independent interaction with both nuclear hormone receptors (not shown). These results are suggestive of functional differences between the two coactivators in their interactions with nuclear hormone receptors.

Figure 5.1. Comparison of nuclear hormone receptor binding to PRC and PGC-1α.

The *in vitro* binding of PRC and PGC-1α subfragments to the nuclear hormone receptors PPARγ, TRβ and RAR was determined by S-tag pull-down assay as described under "Materials and Methods". *Trdx*, thioredoxin. Schematic representation of PRC and PGC-1α is shown above with the various functional domains indicated (*stippled*, activation domain; *cross hatched*, proline rich region; *gray shaded*, consensus recognition site (DHDY) for host cell factor (HCF); *solid*, R/S domain; *vertical hatched*, RNA recognition motif). Subfragments of each coactivator denoted as A, B, C or D with their amino acid coordinates shown in parentheses were used in S-tag pull down assays with ^{35}S-labeled nuclear hormone receptor. Binding of the various subfragments to each ^{35}S-radiolabeled receptor was compared to that of S-tagged thioredoxin as a negative control. Ligand dependent binding was determined by inclusion of the indicated receptor ligand in the binding reaction as described under "Materials and Methods". Bound proteins were eluted from the S-protein agarose and visualized by autoradiography.

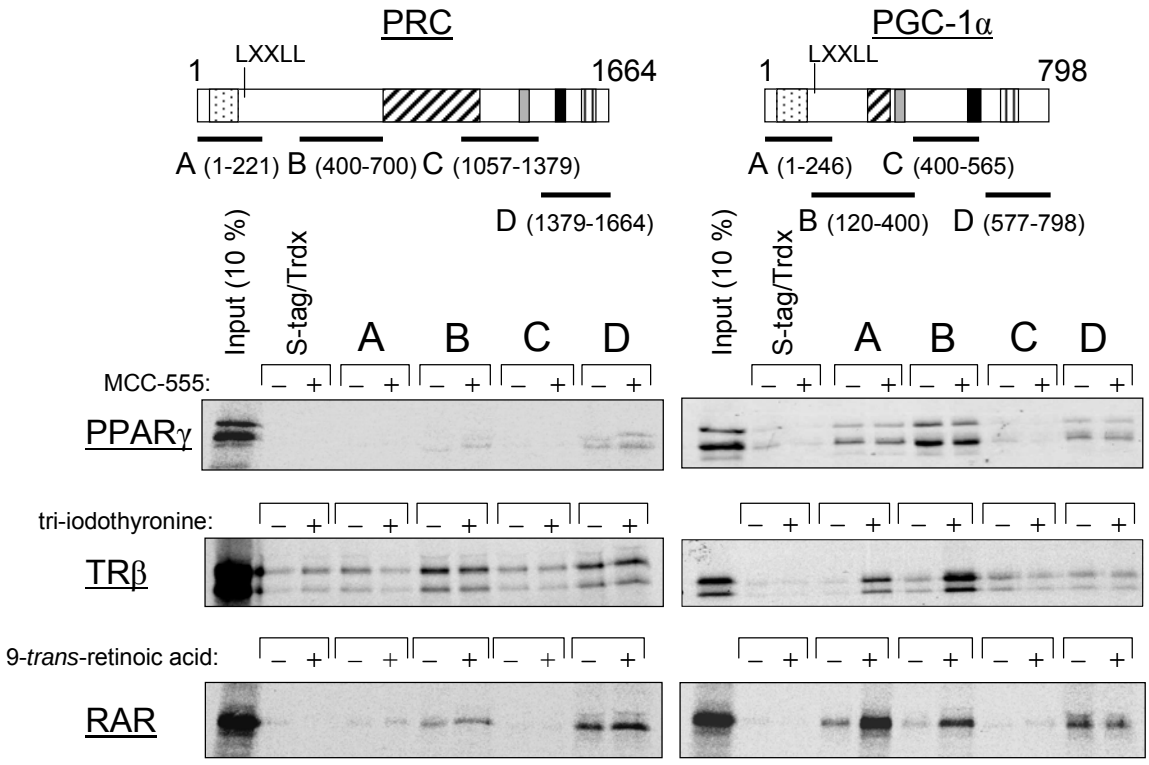
PRC
1
LXXXLL
1664
A (1-221)
B (400-700)
C (1057-1379)
D (1379-1664)
PGC-1α
1
LXXXLL
798
A (1-246)
C (400-565)
B (120-400)
D (577-798)
Input (10 %)
S-tag/Trdx
A
B
C
D
MCC-555:
PPARγ
tri-iodothyronine:
TRβ
9-trans-retinoic acid:
RAR

PRC and PGC-1α were also compared for their ability to bind transcription factors implicated in the expression of the mitochondrial respiratory chain. As shown in **Figure 5.2A**, both PRC and PGC-1α bind NRF-1, CREB and ERRα specifically through their respective subfragments B and D (99). The binding specificity is demonstrated by the fact that neither the thioredoxin control nor other subfragments (A or C) of either coactivator bind any of these transcription factors. CREB has been associated with the *trans*-activation of cytochrome *c* expression by PRC and is known to bind the same sites as NRF-1 within PRC subfragments B and D (99). The orphan nuclear hormone receptor ERRα is a target for PGC-1α- directed mitochondrial biogenesis (155). Notably, both PRC and PGC-1α bind ERRα through the same subfragments used for their interactions with NRF-1 and CREB **(Figure 5.2A)**.

Surprisingly, neither coactivator binds either the α or β subunit of NRF-2 **(Figure 5.2A)** despite the fact that the expressed NRF-2 subunits have been shown to interact with each other to produce a functional heterotetrameric complex (46). This is confirmed here by a mobility shift experiment showing that the *in vitro* translated NRF-2α and β subunits used in the pull down assay are capable of forming the expected heteromeric complexes. As shown in **Figure 5.2B**, *in vitro* translated NRF-2α binds a radiolabeled cytochrome oxidase subunit IV promoter fragment containing tandem NRF-2 recognition sites. Addition of the *in vitro* translated NRF-2β subunit results in the appearance of a slower migrating complex consistent with the formation of the NRF-$2\alpha_2/\beta_2$ heterotetramer (46). Both complexes are supershifted using anti-NRF-2α serum demonstrating that α is present in both. However, only the heteromeric complex containing NRF-2β is supershifted with anti-NRF-2β serum. This confirms the identity of these complexes and demonstrates that the *in vitro* translated subunits can interact. Thus, the failure of these subunits to bind PRC or PGC-1α is unlikely explained by their inability to engage in biologically relevant

interactions. The results demonstrate that the *trans*-activation of NRF-2 target genes by PGC-1α and PRC occurs in the absence of a direct interaction with this transcription factor.

Figure 5.2. Comparison of transcription factor binding to PRC and PGC-1α.

A. The *in vitro* binding of PRC and PGC-1α subfragments to transcription factors linked to respiratory chain expression (NRF-1, CREB, ERRα, NRF-2α and NRF-2β) and HCF-1 was determined by S-tag pull-down assay as described under "Materials and Methods". Schematic representation of PRC and PGC-1α is as shown in **Figure 5.1**. Subfragments of each coactivator denoted as A, B, C or D with their amino acid coordinates shown in parentheses were used in S-tag pull down assays with ^{35}S-labeled transcription factor. Binding of the various subfragments to each ^{35}S-radiolabeled factor was compared to that of S-tagged thioredoxin (*Trdx*) as a negative control. Bound proteins were eluted from the S-protein agarose and visualized by autoradiography.

B. NRF-2α and β subunits were translated *in vitro* as done for the pulldown assay except radiolabeled methionine was omitted from the reaction mixtures. NRF-2α or a mixture of NRF-2α and β subunits was subjected to mobility shift assay using a radiolabeled cytochrome oxidase subunit IV promoter fragment containing tandem NRF-2 recognition sites. Either 1 μl of preimmune serum as a negative control or 1 μl of rabbit anti-NRF-2α or anti-NRF-2β serum was added to binding reactions as indicated.

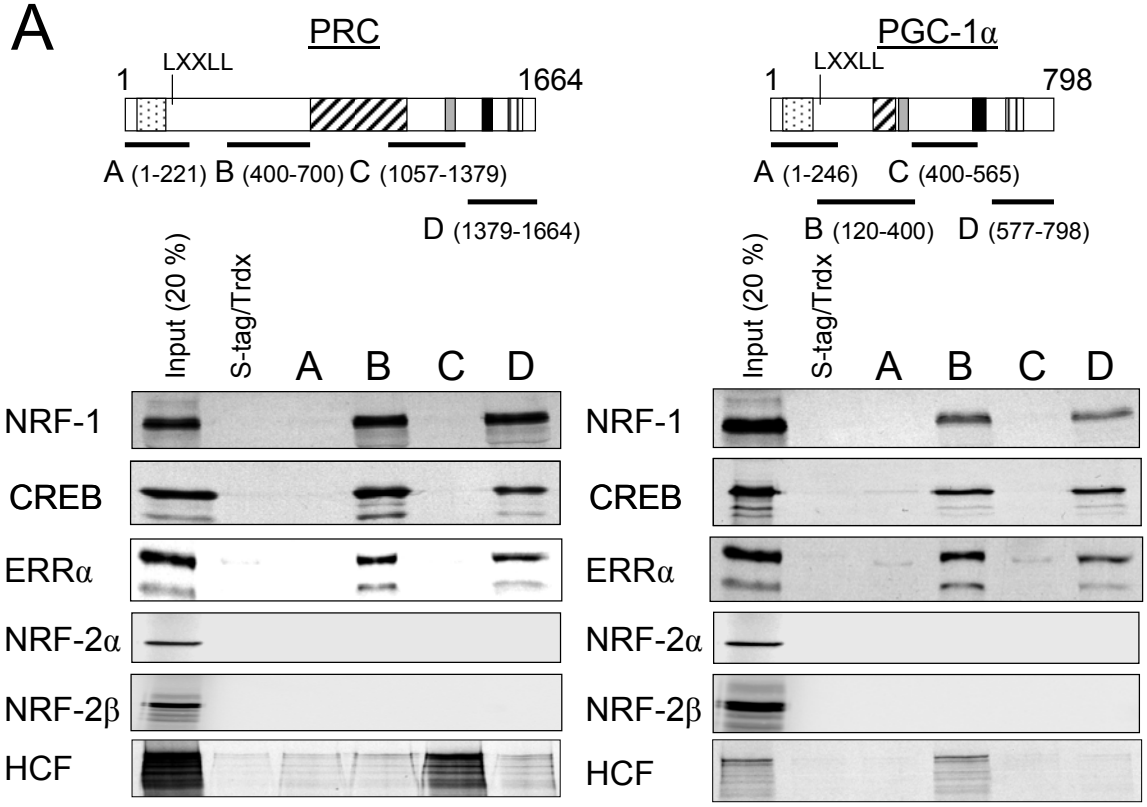
A
PRC
1
LXXLL
1664
A (1-221) B (400-700) C (1057-1379)
D (1379-1664)
PGC-1α
1
LXXLL
798
A (1-246) C (400-565)
B (120-400) D (577-798)
Input (20 %)
S-tag/Trdx
A B C D
NRF-1
CREB
ERRα
NRF-2α
NRF-2β
HCF

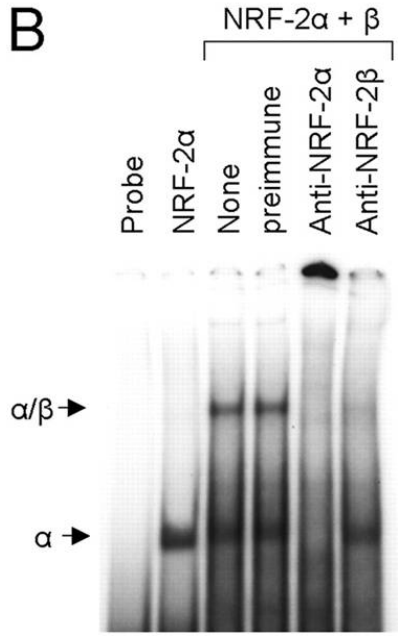
B
NRF-2α + β
Probe
NRF-2α
None
preimmune
Anti-NRF-2α
Anti-NRF-2β
α/β
α

Specific in vitro and in vivo binding of HCF-1 to PRC and NRF-2β. Although neither PGC-1 coactivator engages in a direct interaction with NRF-2, they may exist in a complex with NRF-2 through interaction with a third party that binds both the coactivator and the transcription factor. HCF-1 is an ideal candidate for such a function. HCF-1 acts as a NRF-2(GABP) coactivator (154) and also binds PGC-1α and β through a protein-protein interaction motif defined by the amino acid sequence DHDY (75). The data in **Figure 5.1** confirm the *in vitro* interaction of HCF-1 with PGC-1α subfragment B and also demonstrates specific HCF-1 binding to PRC subfragment C. In each case, the subfragment that binds HCF-1 is the only one containing the DHDY HCF-1 binding motif.

The focus of our work is on PRC as it relates to the regulation of mitochondrial biogenesis and cell growth. Because of the proposed role of PRC and HCF-1 as cell growth regulators, it was of interest to determine whether PRC and HCF-1 exist in a complex *in vivo*. To this end, PRC was immunoprecipitated from whole cell extracts using anti-PRC serum. The immunoprecipitates were electrophoresed on denaturing gels and co-precipitation of HCF-1 was assayed by immunoblotting using anti-HCF-1 serum. As shown in **Figure 5.3A**, copious amounts of anti-HCF-1 reactive material was detected in the anti-PRC immunoprecipitates under conditions where the preimmune control showed only a weak signal. The observed HCF-1 heterogeneity is expected because the full-length 2035-amino acid HCF-1 precursor is cleaved autocatalytically into several amino- and carboxy-terminal fragments that remain associated *in vivo* (150,151). The identity of the precipitated protein as HCF-1 was further verified by expressing hemagglutinin (HA) tagged HCF-1 from a transfected vector and then assaying for HA-tagged HCF-1 in anti-PRC immunoprecipitates with anti-HA antibody. As shown in **Figure 5.3B**, the immunoprecipitates contained a major anti-HA reactive protein corresponding to the

full-length HCF-1 expressed in cell extracts. In addition, several minor species likely representing autocatalytic products were also observed. Although the relative abundance of each species differed substantially between the immunoprecipitated endogenous **(Figure 5.3A)** and transfected **(Figure 5.3B)** HCF-1, there was generally good correspondence between the masses of the protein species represented. The exception was a major species migrating below the 116 kDa standard that was present in immunoprecipitates of endogenous but not transfected protein. This is almost certainly a carboxy-terminal cleavage product that would not be detected in the transfected extracts because the HA tag is expressed on the amino-terminus of HCF-1. These results support the conclusion that PRC and HCF-1 exist in a complex *in vivo*.

Figure 5.3. *In vivo* interaction between PRC and HCF-1.

A. Cell extracts from human 293FT cells were immunoprecipitated with either rabbit preimmune serum as a negative control or rabbit anti-PRC(1047-1379). Immune complexes were brought down with protein A-agarose, washed, and run on an SDS-10% PAGE gel. For comparison, cell extract was run in the indicated lane. After transfer, the immunoblot was probed with rabbit anti-HCF-1 antibody. A lighter exposure of the anti-PRC(1047-1379) lane is shown in the adjacent panel.

B. HA-tagged HCF-1 was expressed in 293FT cells following electroporation with pCGN HCF(2-2035)9E10. 293FT cell extracts were immunoprecipitated with either rabbit preimmune serum as a negative control or anti-PRC(1047-1379). Immune complexes were precipitated and electroblotted as in *A*. For comparison, total cell extract was run in the indicated lane. After transfer, the immunoblot was probed with mouse anti-HA monoclonal antibody.

Molecular mass standards in kilodaltons are indicated at the left in each panel.

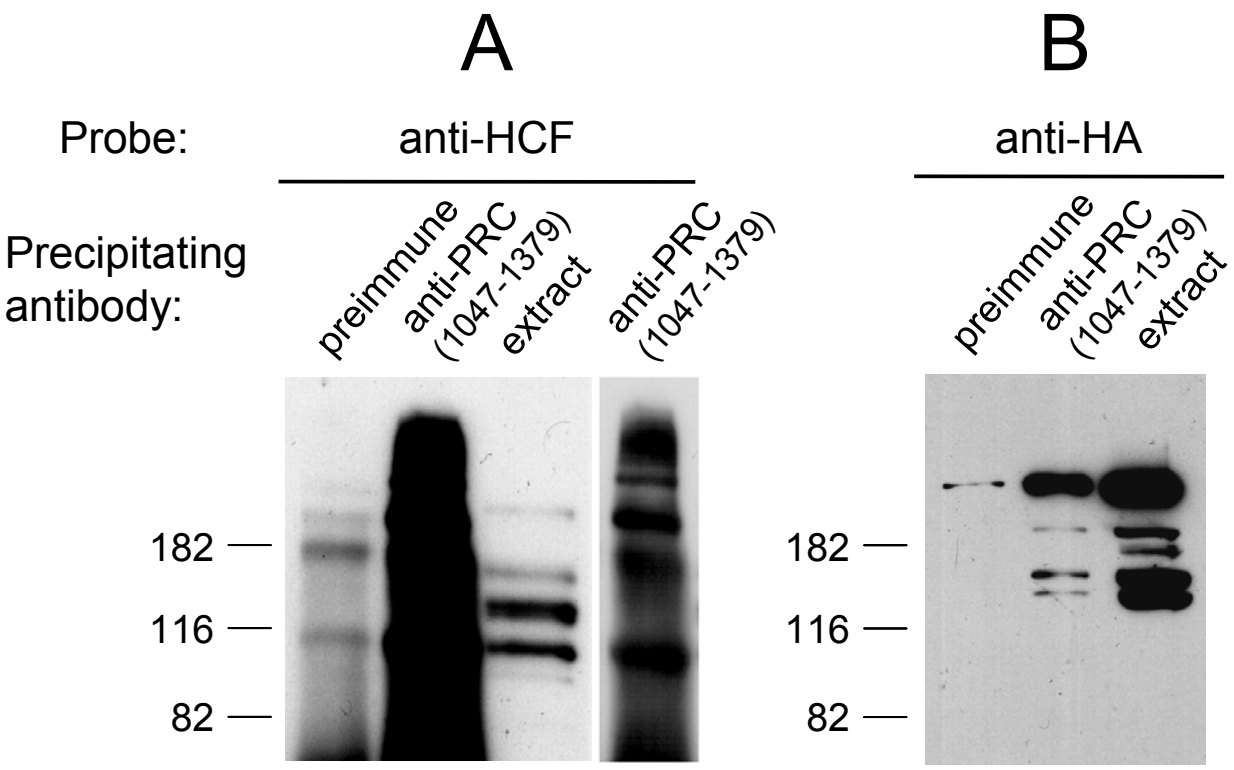
A
B
Probe:
anti-HCF
anti-HA
Precipitating antibody:
preimmune
anti-PRC (1047-1379)
extract
anti-PRC (1047-1379)
preimmune
anti-PRC (1047-1379)
extract
182
116
82
182
116
82

If NRF-2 exists in a ternary complex with PRC and HCF-1, one would expect that NRF-2 would be immunoprecipitated with antibodies directed against either PRC or HCF-1. This was investigated by expressing an HA tagged derivative of the NRF-2β subunit and immunoprecipitating the cell extracts with anti-PRC or anti-HCF-1 antibodies. In this experiment, CREB serves as a positive control because its *in vitro* and *in vivo* interaction with PRC has already been demonstrated (99). The results in **Figure 5.4A** confirm the immunoprecipitation of CREB with anti-PRC serum. Interestingly, ERRα serves as negative control because, despite the fact that it interacts specifically with PRC in the *in vitro* assay **(Figure 5.2A)**, antibodies to PRC failed to immunoprecipitate the expressed protein from cell extracts **(Figure 5.4B)**. Under these conditions, a robust and specific immunoprecipitation of NRF-2β is detected using anti-PRC serum **(Figure 5.4C)**. The slightly increased migration observed following immunoprecipitation is likely the result of a spurious gel artifact rather than a specific modification because it affects both CREB and NRF-2β similarly.

The PRC-NRF-2 interaction was further established using untransfected cells by immunoprecipitating cell extracts with anti-NRF-2α or anti-NRF-2β sera and probing immunoblots with anti-PRC(1047-1379). As shown in **Figure 5.4E**, antibodies directed against either the NRF-2α or β subunits can immunoprecipitate PRC from cell extracts under conditions where the IgG or preimmune serum controls do not. The formation of a complex between endogenously expressed proteins demonstrates that the interaction is not dependent on the expression of NRF-2 as a tagged protein from a transfected vector. Thus, although NRF-2 fails to bind PRC *in vitro*, it exists in a complex with PRC in cell extracts. In addition, NRF-2β is also immunoprecipitated with anti-HCF-1 antibody **(Figure 5.4D)** confirming the previous findings of others that GABPβ, the mouse homologue of human NRF-2β, interacts directly with HCF-1

(154). Since PRC and HCF-1 exist in a complex **(Figure 5.3)** and NRF-2 does not bind PRC directly **(Figure 5.2A)** these data are consistent with the interpretation that NRF-2β enters into a complex with PRC through its interaction with HCF-1.

Figure 5.4. *In vivo* binding of NRF-2 to PRC and HCF-1.

A. As a positive control, HA-tagged CREB was expressed in 293FT cells following electroporation with pSG5/CREB-HA. Cell extracts were immunoprecipitated with rabbit preimmune serum as a negative control or anti-PRC(1047-1379).

B. As a negative control, HA-tagged ERRα was expressed in 293FT cells following electroporation with pSG5/ERRα-HA. Cell extracts were immunoprecipitated as in panel *A*.

C. HA-tagged NRF-2β was expressed in 293FT cells following electroporation with pSG5/NRF-2β-HA. Cell extracts were immunoprecipitated as in panels *A* and *B*.

D. HA-tagged NRF-2β was expressed in 293FT cells following electroporation with pSG5/NRF-2β-HA. Cell extracts were immunoprecipitated with rabbit preimmune serum as a negative control or with rabbit anti-HCF-1 antibody.

For panels *A*-*D*, the immunoblot was probed with mouse anti-HA monoclonal antibody.

E. Cell extract from untransfected cells was subject to immunoprecipitation with anti-NRF-2α, anti-NRF-2β or the controls rabbit IgG or preimmune serum. The immunoblot was probed with rabbit anti-PRC(1047-1379).

For each panel, cell extract was run in the indicated lane with molecular mass standards in kilodaltons indicated at the left.

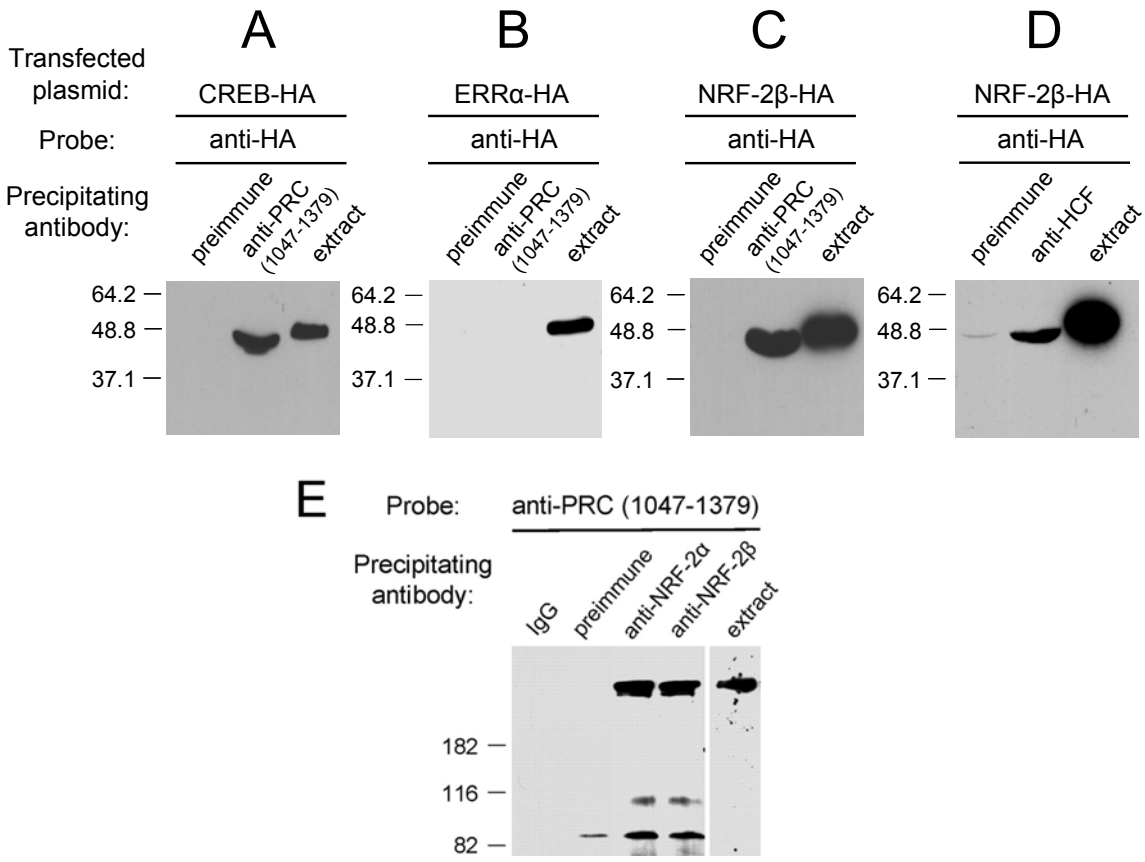
A
B
C
D
Transfected plasmid:
CREB-HA
ERRα-HA
NRF-2β-HA
NRF-2β-HA
Probe:
anti-HA
anti-HA
anti-HA
anti-HA
Precipitating antibody:
preimmune
anti-PRC (1047-1379)
extract
preimmune
anti-PRC (1047-1379)
extract
preimmune
anti-PRC (1047-1379)
extract
preimmune
anti-HCF
extract
64.2
48.8
37.1
64.2
48.8
37.1
64.2
48.8
37.1
64.2
48.8
37.1
E
Probe:
anti-PRC (1047-1379)
Precipitating antibody:
IgG
preimmune
anti-NRF-2α
anti-NRF-2β
extract
182
116
82

PRC trans-activation through NRF-2 requires both the HCF-1 binding site on PRC and essential hydrophobic residues within the NRF-2 activation domain. If the *in vivo* interactions among PRC, HCF-1 and NRF-2 observed by co-immunoprecipitation are functionally significant, the sequence motifs required for these interactions should play a role in the PRC mediated *trans*-activation through NRF-2. As demonstrated (**Figure 5.2A)**, PRC binds HCF-1 through a subfragment containing the DHDY HCF-1 binding site. In addition, it has been established that HCF-1 binding to GABPβ(NRF-2β) requires the same amino acid residues within the NRF-2β activation domain that are also required for transcriptional activation by NRF-2 (154,156). The requirement for these motifs was tested by measuring the PRC-dependent *trans*-activation of a Gal4-luciferase reporter in the presence of a Gal4-NRF-2β fusion protein. In this system, PRC *trans*-activates the reporter to a level approximately 6-7-fold above that achieved with the Gal4-NRF-2β fusion protein alone **(Figure 5.5)**. Site-directed deletion of the HCF-1 binding site on PRC (ΔDHDY) inhibits this activity significantly. The inhibition does not result from differences in expression from the transfected vectors because PRC (ΔDHDY) and PRC are expressed at similar steady-state levels **(Figure 5.5)**. The observed partial inhibition may reflect a requirement for more than a single contact. For example, PRC may be bound to the complex via DHDY but also through its interactions with other coactivators via its activation domain. Deletion of the NRF-2β activation domain (ΔTAD) completely abolishes *trans*-activation of the reporter by PRC in both the presence and absence of the DHDY motif **(Figure 5.5)**. These results establish that the HCF-1 interaction domains on both the coactivator (PRC) and the transcription factor (NRF-2β) are essential for maximal *trans*-activation by PRC.

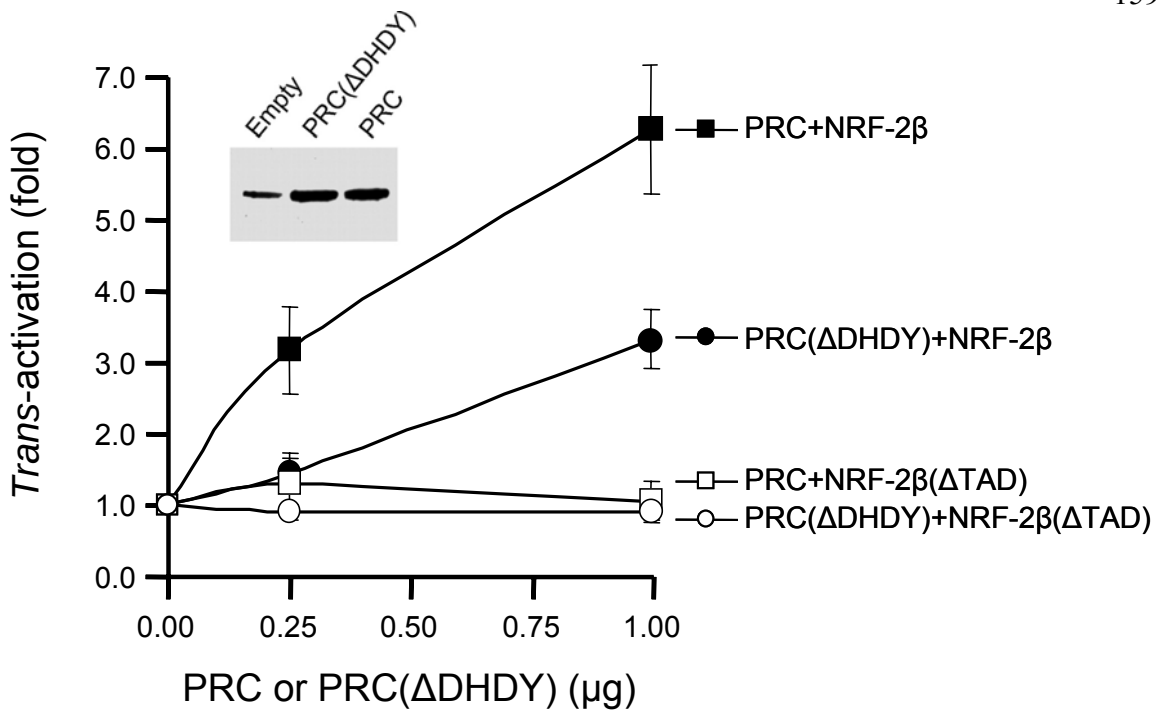

Figure 5.5. Molecular determinants of PRC *trans*-activation through promoter bound NRF-2β.

PRC *trans*-activations were carried out using a Gal4/luc reporter plasmid. Nearly full-length NRF-2β_1 wild type or the same protein containing a deletion in the activation domain (ΔTAD) was directed to the luc promoter through their expression as fusions to Gal4(1-147) as described under "Materials and Methods". The fold *trans*-activation by either PRC **(filled and open squares)** or a mutated derivative lacking the DHDY HCF-1 consensus-binding site (ΔDHDY) **(filled and open circles)** was determined by measuring luciferase activity following cotransfection with either 0.25 or 1.0 μg of plasmid expressing each construct. Values were normalized to *Renilla* luciferase to correct for differences in transfection efficiency. Inserted panel shows the steady-state PRC expression in cells transfected with pSV Sport (empty vector), pSV Sport/N-myc PRC(ΔDHDY) or pSV Sport/N-myc PRC.

To investigate whether the NRF-2 activation domain is sufficient for *trans*-activation by PRC, a Gal4 fusion containing only the essential region of the NRF-2β activation domain bounded by amino acids 258-327 (156) was constructed. This construct was *trans*-activated by PRC to a degree similar (7-8 fold) to that achieved using the full-length Gal4-NRF-2β fusion **(Figure 5.6)**. Gal4 alone gave no activity while *trans*-activation by PRC(ΔDHDY) was significantly reduced. Thus, the NRF-2β activation domain alone is sufficient for PRC-dependent *trans*-activation of the reporter.

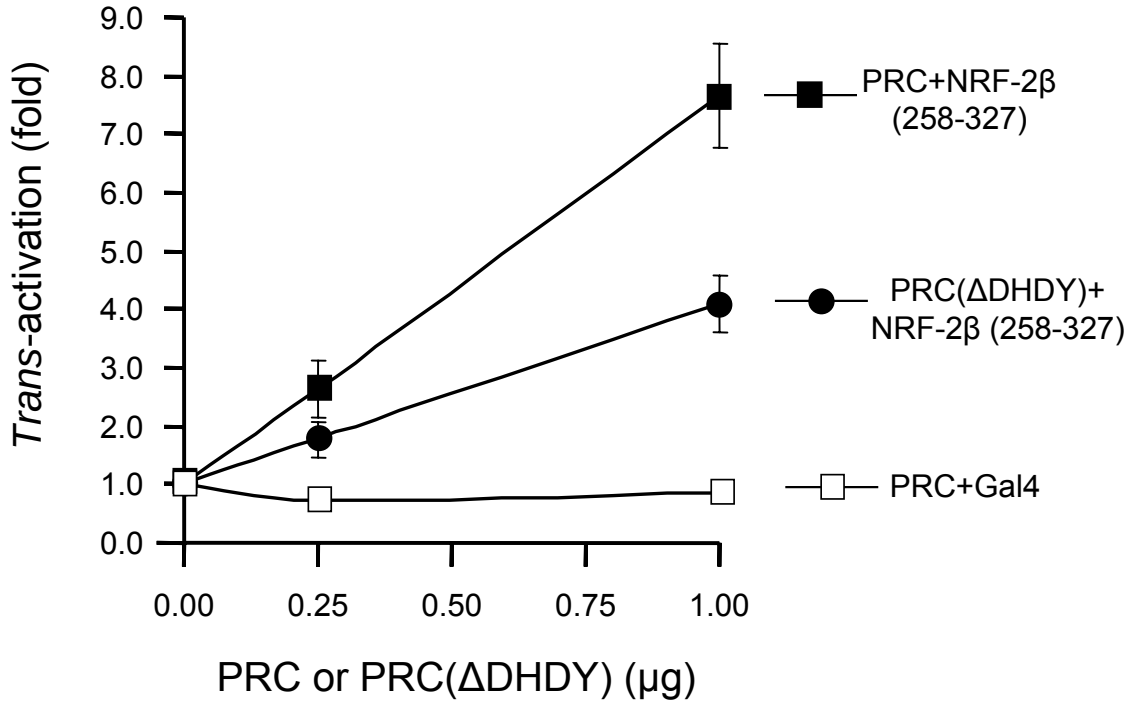

Figure 5.6. The NRF-2β activation domain is sufficient for *trans*-activation by PRC.

PRC *trans*-activations were carried out using a Gal4/luc reporter plasmid as in **Figure 5.5**. In this case, a fragment containing only the NRF-2β_1 activation domain (NRF-2β_1/258-327) was directed to the luc promoter through its expression as a fusion to Gal4(1-147) as described under "Materials and Methods". The fold *trans*-activation by either PRC **(filled squares)** or a mutated derivative lacking the DHDY HCF-1 consensus-binding site (ΔDHDY) **(filled circles)** was determined as in **Figure 5.5** and compared to that derived from PRC and Gal4(1-147) as a negative control **(open squares)**.

Clusters of hydrophobic amino acid residues within NRF-2β activation domain are essential for NRF-2 transcriptional activity (156). These same residues are also required for interaction between GABPβ(NRF-2β) and HCF-1 (154). In fact, those residues that contribute most to transcriptional activation are also the major contributors to HCF-1 binding to NRF-2β. Thus, if PRC *trans*-activation occurs through a complex containing PRC, HCF-1 and NRF-2, one would expect that *trans*-activation by PRC would require the same residues necessary for the NRF-2β-HCF-1 interaction and for NRF-2β-mediated transcription. This was tested using a series of NRF-2β activation domain mutants where clusters of amino acid residues containing either glutamines or hydrophobic residues were converted to alanines by site directed mutagenesis (156). As shown in **Figure 5.7**, conversion of glutamines within clusters 2 (Q270 and Q271) and 3 (Q295) of the NRF-2β activation domain reduced transcriptional activity by about 34 percent and had a similar effect on the fold *trans*-activation by PRC. By contrast, conversion of hydrophobic residues within clusters 2 (I274 and I276) or 3 (I297, I298 and V299) to alanines had much larger effect on NRF-2β transcription and a proportionately larger effect on *trans*-activation by PRC. Combined mutations in clusters 2 and 3 reduced NRF-2β transcription by over 90 percent and completely abolished *trans*-activation by PRC. These results establish that key amino acids required for both transcription by NRF-2β and for NRF-2β interaction with HCF-1 are also required for PRC-dependent *trans*-activation through NRF-2.

Gal4/NRF-2β$_1$ (261 1 — 270 2 — 295 3 — 305 4)		Relative activity	Fold PRC activation
258-327	⊢IQQVV—QQVITIV—QPIIV—QQVLTV⊣	100	8.1 ± 1.6
Mut 2Q, 3Q	⊢IQQVV—AAVITIV—APIIV—QQVLTV⊣	66.3 ± 10.6	5.5 ± 1.2
Mut 2Hy	⊢IQQVV—QQVATAV—QPIIV—QQVLTV⊣	19.1 ± 5.2	2.8 ± 0.5
Mut 3Hy	⊢IQQVV—QQVITIV—QPAAA—QQVLTV⊣	13.0 ± 3.5	1.5 ± 0.2
Mut 2Hy, 3Hy	⊢IQQVV—QQVATAV—QPAAA—QQVLTV⊣	7.4 ± 3.1	1.1 ± 0.3

Figure 5.7. The same NRF-2β activation domain hydrophobic residues are required for interaction with HCF-1 and for *trans*-activation by PRC.

Either glutamines or hydrophobic amino acids within glutamine-containing hydrophobic clusters 2 and 3 of the NRF-2β activation domain were converted to alanines **(underlined)**. Gal4 fusion constructs containing the wild type activation domain (NRF-2β$_1$/258-327) or the alanine substitution mutants were assayed for their activation of the Gal4/luc reporter (*Relative activity*) and for their ability to support the *trans*-activation of the same reporter by PRC (*Fold PRC activation*). Values were normalized to *Renilla* luciferase to correct for differences in transfection efficiency and represent the average ± S.E.M. for five separate determinations.

In vivo occupancy of NRF-2-dependent promoters by NRF-2β, PRC and HCF. If a complex containing NRF-2, PRC and HCF-1 is physiologically significant, one might expect that all three components occupy NRF-2-dependent promoters *in vivo*. In a previous study, we established that the promoters from both isoforms of mtTFB (mitochondrial transcription factor B) designated as TFB1M and TFB2M (16,17) were dependent on functional NRF-2 recognition sites for both their basal activity and for their *trans*-activation by PRC (46). In addition, chromatin immunoprecipitations revealed that NRF-2α was bound to both promoters *in vivo*. Based on these results, it was of interest to determine whether NRF-2β, PRC and HCF-1 were also localized to the TFB promoters *in vivo*. To this end chromatin immunoprecipitations (ChIP) were carried out using antibodies specific for each of these factors. As shown in **Table 5.1**, significant occupancy of both TFB promoters by NRF-2β, PRC and HCF-1 was detected. The signal is less robust for PRC compared to the other two factors possibly because of the low level of PRC expression or because of masking of the 1047-1379 epitope by protein-protein interactions within the chromatin-bound complex. Nevertheless, the results are consistent with the *in vitro* experiments showing a functional association among NRF-2β, PRC and HCF-1 and support the conclusion that all three factors can associate with NRF-2-dependent promoters *in vivo.*

Table 5.1. Chromatin immunoprecipitation (ChIP) analysis of mtTFB promoter occupancy by NRF-2β, PRC and HCF.

Precipitating antibody	Promoter occupancy[a]	
	TFB1M	TFB2M
Rabbit IgG	1.0	1.0
anti-NRF-2β	31.6 ± 7.9	59.8 ± 19.2
anti-PRC (1047-1379)	4.5 ± 0.5	4.4 ± 0.8
anti-HCF-1	44.2 ± 4.7	96.2 ± 12.1

[a]Values of relative promoter occupancy represent the average ± S.E.M. for three separate determinations.

Effects of shRNA-mediated PRC knockdown on TFB and cytochrome oxidase (COX) expression. The results presented are consistent with a pathway whereby PRC activates the expression of the TFBs and possibly other NRF-2 target genes through its interaction with an NRF-2/HCF-1 complex. One prediction of this model is that reduced PRC expression might lead to diminished mitochondrial transcript levels and the consequent reduction in respiratory enzyme activities. This was examined by constructing a lentivirus transductant of U2OS cells that expresses a small hairpin RNA designed to knock down the expression of PRC. The U2OS cell line was chosen because it is a contact inhibited human line that displays regulated cell-cycle expression of PRC (99). As shown in **Figure 5.8A**, one of the transductants tested (PRC shRNA#1) showed specific shRNA-mediated reduction in PRC protein expression. This transductant showed the largest reduction in PRC protein levels among 20 individual isolates tested. The inhibition was specific to the PRC shRNA because a transductant expressing a hairpin with a negative control sequence showed no reduction in PRC. Moreover, a lentivirus transductant expressing a lamin-specifc control hairpin displayed markedly reduced lamin expression and no change in the steady-state level of PRC. The knockdown of PRC protein in these cells was accompanied by reduced PRC mRNA expression as measured by quantitative real time RT-PCR **(Figure 5.8B)**. This coincided with diminished levels of TFB2M mRNA and two different mitochondrial transcripts encoding COXII and cytochrome *b*. Thus, reduced PRC expression is associated with the down regulation of transcripts encoding a key mitochondrial transcription factor (TFB2M) and mitochondrial respiratory chain subunits. Surprisingly, TFB1M mRNA was not diminished significantly in the PRC shRNA transductant and was expressed at levels equivalent to the β-actin negative control. This suggests that the effects of PRC likely depend on promoter context or unknown compensatory interactions. The downstream

effect of these changes in gene expression on respiratory activity was assessed by staining cells for cytochrome oxidase activity. As shown in **Figure 5.8C**, the PRC shRNA transductant displayed diminished COX staining compared to the robust staining observed in wild-type U2OS and transductants expressing the negative control hairpin. The results are consistent with a pathway whereby the PRC-dependent expression of NRF-2 target genes can mediate changes in the expression of a respiratory enzyme complex.

Figure 5.8. Down regulation of TFB2M, mitochondrial transcripts and cytochrome oxidase activity associated with stable shRNA-mediated knock down of PRC expression.

A. Lentivirus transductants of U2OS cells expressing shRNAs directed against a lamin shRNA control, PRC shRNA#1 or a negative control oligonucleotide. Cell extracts of each were subjected to immunoblotting with antibodies directed against lamin and PRC.

B. Total RNA was isolated from transductants expressing either the control sequence or PRC shRNA#1. Quantitative real time RT PCR was carried out with primers specific for PRC, β-actin, TFB1M, TFB2M, COXII and cytochrome *b* and the transcript levels for each in the PRC shRNA#1 transductant are expressed relative to those of the negative control.

C. Cytochrome oxidase activity staining was performed as described under "Material and Methods" on U2OS wild type cells and on transductants expressing the negative control oligonucleotide and PRC shRNA#1.

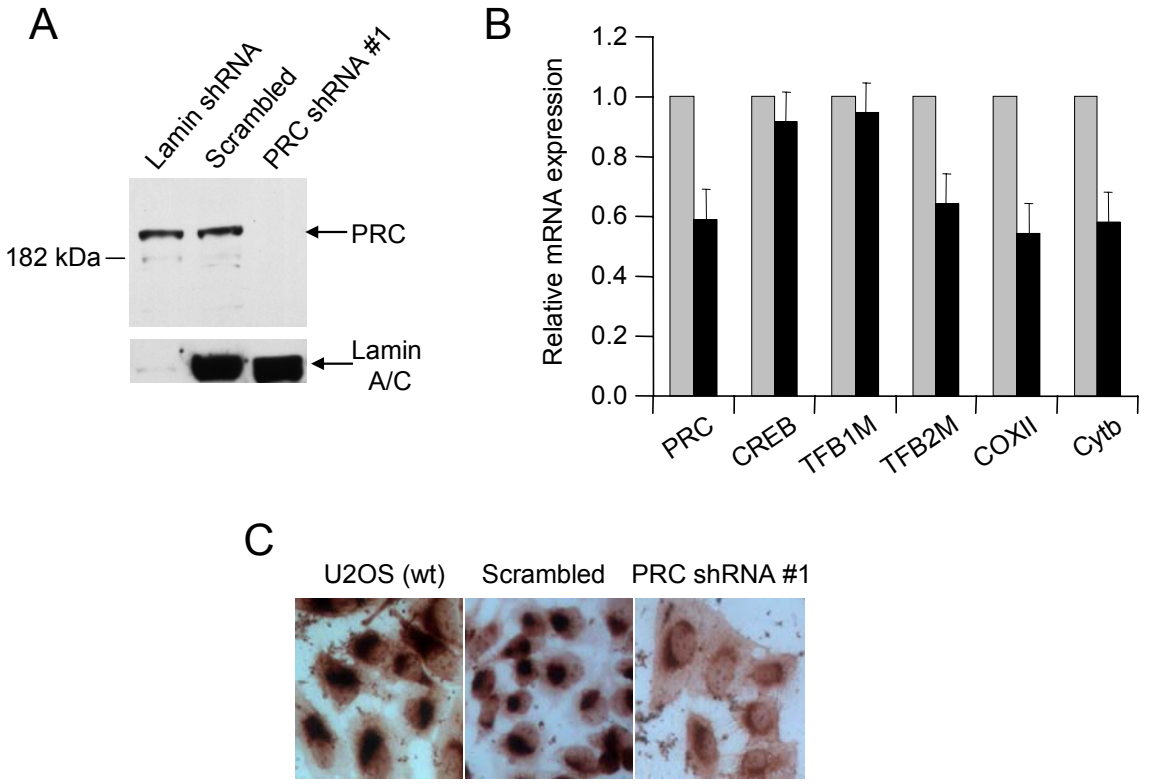
A
Lamin shRNA
Scrambled
PRC shRNA #1
182 kDa
PRC
Lamin
A/C
B
Relative mRNA expression
1.2
1.0
0.8
0.6
0.4
0.2
0.0
PRC
CREB
TFB1M
TFB2M
COXII
Cytb
C
U2OS (wt)
Scrambled
PRC shRNA #1

DISCUSSION

The PGC-1 family of regulated coactivators functions in the relay of environmental cues to the transcriptional machinery (122,148,157). This is accomplished partly through interactions with transcription factor targets that act on an array of genes governing programs of cellular energetics and differentiation. PGC-1α exhibits a broad range of transcription factor interactions that include a host of nuclear hormone receptors as well as transcription factors implicated in mitochondrial biogenesis, muscle fiber type switching and many other biological processes (105,148,157). The induction of PGC-1α by cAMP-dependent transcription and its post-translational modification are important means of its regulation by extracellular signaling events (71,158). PRC is defined as a member of the PGC-1 family by conservation of structural domains and by its ability to interact with NRF-1 in the activation of NRF-1 target genes involved in the expression of the respiratory chain (46,89). However, PRC expression differs from that of PGC-1α in that it is not induced during thermogenesis but rather responds to signals regulating cell proliferation (89,99). Here, we show that PRC also differs from PGC-1α in its interaction with nuclear hormone receptors. It shows only a weak interaction with PPARγ as well as ligand independent binding to TRβ and RAR. These results, along with its inability to respond to thermogenic signals, likely reflect significant divergence between PRC and PGC-1α in signaling *via* nuclear hormone receptor pathways.

In contrast to these differences in nuclear hormone receptor interactions, PRC and PGC-1α are virtually identical in their binding to an array of transcription factors that have been implicated in the expression of the respiratory chain. In particular, strong interactions by both coactivators with NRF-1 and ERRα are consistent with significant similarities between the two factors in their ability to *trans*-activate the promoters of target genes that specify respiratory

chain subunits and mitochondrial transcription factors. Surprisingly, neither coactivator engages in a direct interaction with NRF-2(GABP), despite the fact that both have been associated with NRF-2-dependent gene expression (46,54). Here, we demonstrate that HCF-1 serves as an important intermediary between PRC and NRF-2 target genes by binding both PRC and the NRF-2β subunit. Significant inhibition of PRC *trans*-activation function can be achieved by mutation of the DHDY HCF-1 consensus-binding site on PRC. This agrees with both the *in vitro* pull-down assays showing direct binding of HCF-1 to the DHDY-containing PRC subfragment and with immunoprecipitations showing that HCF-1 is precipitated from cell extracts using antibodies directed against PRC. The data also show that the NRF-2β transcriptional activation domain is both absolutely required and sufficient for PRC-directed transcriptional activation. This function is associated with key hydrophobic amino acid residues in the NRF-2β activation domain. This result is consistent with previous findings showing that the same hydrophobic residues are essential for binding of HCF-1 to NRF-2β(GABPβ) thus implicating HCF-1 as a coactivator of this transcription factor (154). The finding that all three proteins occupy NRF-2-dependent TFB promoters as demonstrated by chromatin immunoprecipitations reinforces the physiological significance of these interactions.

In addition to its structural and functional similarities with PGC-1α (46,54,89), a role for PRC in the expression of the respiratory chain is supported by the finding that a dominant negative PRC allele consisting of the NRF-1/CREB binding site inhibits respiratory growth on galactose when expressed in *trans* (99). Here, we show that PRC loss of function through shRNA-mediated knock down is associated with the down regulation of the TFB2M mRNA encoding a key mitochondrial transcription factor. This coincides with reductions in mitochondrial transcripts for respiratory subunits, one of which encodes COXII, an essential

subunit of the cytochrome oxidase complex. The down regulation of COXII mRNA in the PRC shRNA transductant is accompanied by reduced COX enzyme activity demonstrating the physiological consequences of these changes in gene expression. However, the normal level of TFB1M expression in the transductant indicates that PRC is not limiting for all NRF-2-dependent genes. This might be explained by unknown differences in promoter context or by promoter-specific compensatory interactions. It remains to be determined to what extent PRC selectively mediates the coordinate expression of the family of NRF target genes.

It is notable that the TFB1M and TFB2M isoforms have distinct biological functions. The TFB1M isoform is transiently down regulated relative to that of the TFB2M isoform in serum stimulated quiescent fibroblasts, suggesting that the latter is favored in the transition to proliferative growth (46). RNAi knockdown of the *Drosophila* B2 isoform results in reduced mtDNA transcription and copy number (159). This contrasts with RNAi knockdown of the B1 isoform, which has no effect on mtDNA transcription or replication but does result in reduced mitochondrial translation (160). This is consistent with the finding that over expression of *Drosophila* TFB2M but not TFB1M increases mtDNA copy number. These results match those obtained in human cells where over expression of human TFB2M but not TFB1M enhances mitochondrial transcription and transcription-primed replication (39). Thus, it is not surprising that we observe a decrease in mitochondrial transcript levels in the PRC shRNA transductant where only the TFB2M mRNA is down regulated. This appears sufficient to mediate changes in the mitochondrial transcriptional machinery in both *Drosophila* and human systems.

Our previous work has implicated PRC as a potential regulator of cell proliferation (89,99). It of interest in this context that PRC exists in a complex with HCF-1 and NRF-2 and that the molecular determinants of these interactions are required for maximal *trans*-activation by

PRC. HCF-1 and GABP(NRF-2) were both originally described as cellular factors required for the expression of Herpes simplex virus immediate early genes (150,161,162). Subsequently, HCF-1 was found to interact with a number of transcription factors, including VP16 and GABPβ(NRF-2β), as well as chromatin-remodeling cofactors (150,154). HCF-1 is an important component of a molecular switch that triggers immediate early gene expression by interacting with the VP16/Oct1 transcription factor complex (149). Moreover, genetic evidence supports an essential role for HCF-1 in progression beyond G_1 of the cell cycle, suggesting that it may serve as transcriptional coactivator for cell cycle regulated genes (152). This is especially interesting in light of the recent finding that GABP(NRF-2) can direct a D-cyclin-independent pathway of entry to the cell cycle (147). The association between HCF-1 and NRF-2(GABP) may serve to integrate the cell proliferative cycle with components of the mitochondrial biogenesis program related to the expression of the respiratory chain. PRC appears to be a regulated moiety of this complex that functions to enhance the basal expression of essential genes in preparation for cell division. Although antibodies directed against PRC can immunoprecipitate both HCF-1 and NRF-2β, its association with chromatin bound complexes may be transient. A transient association might facilitate a regulatory function and is consistent with the immediate early expression of PRC, its relatively rapid turnover and its low abundance (89,99). With the current results, it is now clear that HCF-1 binds all three members of the PGC-1 coactivator family. It interacts with both PGC-1α and β and enhances their transcriptional activities *in vitro* (75). Moreover, phosphorylation of both PGC-1α and GABPβ (NRF-2β) augments their ability to enter into a complex with HCF-1 in the regulation of neuromuscular gene expression (94). Although the three family members are differentially regulated, their association with HCF-1

appears to be fundamental to their ability to activate transcription through NRF-2 and possibly other transcription factors.

MATERIALS AND METHODS

Plasmids.

A PRC expression vector was constructed from pBSII/N-myc FL PRC, a modified derivative of the original pBSII/FL-PRC (89), by inserting a *Xho*I/*Not*I restriction fragment containing the full-length PRC coding region into *Sal*I/*Not*I digested pSV Sport. This vector, pSV Sport/N-myc FL PRC, was used as a template to delete the HCF-1 binding site (ΔDHDY: GACCATGACTAT) by PCR using a previously described strategy (99). The resulting *Dra*III/*Not*I PRC fragment containing the internal deletion of the codons specifying the DHDY HCF-1 binding site was then subcloned into *Dra*III/*Not*I digested pSV Sport/N-myc FL PRC to generate pSV Sport/ N-myc PRC (ΔDHDY). The Gal4-NRF-2β fusion constructs including the full-length NRF-2β as well as those containing only the activation domain and its variants with alanine substitution mutations have been described (107,156).

Plasmids pSG5/CREB-HA (99) and pCGN HCF(2-2035)9E10 (150) were constructed as described. The ERRα coding region used for the construction of the ERRα expression vector pSG5/ERRα-HA was generated by PCR using HeLa cDNA as template. The resulting PCR product was digested with *Bam*HI/*Bgl*II and cloned into *Bam*HI/*Bgl*II-digested pSG5. The NRF-2β expression vector, pSG5/NRF-2β-HA, was constructed by incorporating the HA-tag into the coding region from the original NRF-2β cDNA clone (107) by PCR. An activation domain deletion (ΔTAD) was introduced into the NRF-2β coding region by cutting the plasmid pSG5/NRF-2β-HA with *Pst*I and re-ligating to generate pSG5/NRF-2β-HA(ΔTAD). This

resulted in an in-frame 88-codon deletion encompassing NRF-2β amino acids 255 through 342. This deletion removed the entire NRF-2β transcriptional activation domain (ΔTAD) which was mapped previously to amino acids 258-327 (107,156).

Coimmunoprecipitation and immunoblotting.

Immunoprecipitations were carried out using either untransfected 293FT cells or cells transfected with hemagglutinin-tagged proteins. This human cell line was used for immunological methods because our antibodies were developed against the human factors, the cells exhibit abundant constitutive expression of PRC and they have a high transfection efficiency. Untransfected 293FT cells were grown to approximately ~70 % confluence and harvested for the preparation of cell extract. Hemagglutinin-tagged proteins were expressed by electroporating approximately $4.8x10^6$ 293FT cells with pCGN HCF(2-2035)9E10 (60 μg), pSG5/CREB-HA (20 μg), pSG5/ERRα-HA (50 μg) or pSG5/NRF-2β-HA (40 μg). Cells were plated in 15 cm tissue culture dishes and maintained at 37ºC for ~48 h. Extracts from untransfected and transfected cells were prepared by suspending cells in NP-40 lysis buffer (50 mM Tris-HCl, pH 8.0, 150 mM NaCl, 1% NP-40) containing mini-complete protease inhibitor cocktail (Roche) as described (89,99). Protein concentrations were measured by the Bradford assay (Bio-Rad). Immunoprecipitations were performed by adding 15 μl of rabbit pre-immune serum control, 15 μl of rabbit anti-PRC(1047-1379) serum (99), 2 μl of rabbit anti-HCF-1 serum (a generous gift from Winship Herr, University of Lausanne), 10 μl rabbit anti-NRF-2α or 15 μl rabbit anti-NRF-2β serum to 400-800 μg whole-cell extract in a total volume of 250 μl NP-40 lysis buffer. Reactions were incubated at 4ºC overnight on a rocking table followed by addition of 20 μl of protein A-agarose (Roche). After additional 3 h incubation at 4ºC,

immunoprecipitates were centrifuged at 12,000 x *g* for 20 sec at 4ºC, washed 4 times with 500 µl NP-40 lysis buffer and resuspended in 25 µl 2x sample buffer containing β-mercaptoethanol. For detection of PRC and HCF by immunoblotting, samples were subjected to electrophoresis on 8.5% denaturing acrylamide gels and transferred to nitrocellulose membranes (Schleicher & Schuell) with high-molecular-weight buffer as described (99). For detection of CREB, ERRα and NRF-2β, precipitates were subjected to electrophoresis on 12% denaturing acrylamide gels and transferred to nitrocellulose membranes using a Trans-Blot SD semidry electrophoretic transfer cell (Bio-Rad) with Towbin transfer buffer (89). Immunoblots were probed with either rat monoclonal high affinity (3F10) anti-HA-peroxidase antibody (Roche), rabbit anti-HCF antibody or rabbit anti-PRC(1047-1379) serum. Proteins were visualized using SuperSignal West Pico Chemiluminescent substrate (Pierce Biotechnology).

Transfections.

Transient transfections of BALB/3T3 cells were performed by calcium phosphate precipitation as described (89). This cell line was utilized for transfections because conditions for PRC *trans*-activations were originally developed using these cells (46,89,99). BALB/3T3 cells were maintained in Dulbecco's modified Eagle's medium (DMEM; Invitrogen) containing 10% calf serum (HyClone) and 1% penicillin-streptomycin (Invitrogen). Cells were plated at a density of 2,600 cells per cm^2 in six-well plates and transfected with 0.6 µg 5xGal4/Luc reporter and 45 ng of pRL-null control vector (Promega) together with different Gal4-NRF-2β fusion constructs. PRC *trans*-activations were performed by including either pSV Sport/N-myc FL PRC or pSV Sport/N-myc PRC (ΔDHDY) lacking the HCF-1 binding site (ΔDHDY). After 5-6 h, cells were washed twice with Dulbecco's phosphate-buffered saline (Invitrogen) and grown for an

additional 40 h in fresh media. Cell extracts were prepared, and luciferase assays were performed using the dual luciferase reporter assay system (Promega). Firefly luciferase activity from the 5xGal4/Luc reporter construct was normalized to *Renilla* luciferase luminescence from the pRL-null control vector.

S-tag pulldown assay.

Pulldown assays were performed as described (89,99). Binding of PRC and PGC-1α to the nuclear hormone receptors PPARγ, TRβ and RAR was determined in the presence and absence of 1 μM of the receptor ligands MCC-555, tri-iodothyronine and 9-*trans*-retinoic acid, respectively.

Mobility Shift Assays.

NRF-2α and β subunits were translated *in vitro* as performed for the S-tag pulldowns except for the omission of radiolabeled methionine. Subunits were subjected to mobility shift assay using a ^{32}P-labeled cytochrome oxidase subunit IV promoter oligonucleotide containing tandem NRF-2 recognition sites as described previously (46).

Chromatin immunoprecipitation.

Chromatin immunoprecipitations (ChIP) were performed on 293FT cells as described (99) using rabbit anti-NRF-2β, rabbit anti-PRC(1047-1379) (99), and rabbit anti-HCF-1 antibodies (a generous gift from Winship Herr, University of Lausanne) along with rabbit IgG as a control (Sigma). Immunoprecipitated promoter fragments were quantitated by real-time PCR on the ABI PRISM 7900HT Sequence detection system with the SYBR Green PCR Mastermix

(Applied Biosystems). The primers used for real-time PCR were specific for the human TFB1M and TFB2M promoter (46). Amplifications were performed in triplicate in each ChIP experiment, the results quantitated using the $\Delta\Delta C_T$ method (142) and expressed as the average of three independent experiments ± standard errors of the means.

Histochemistry.

For histochemical staining of cytochrome *c* oxidase activity (163), cells grown on glass coverslips were air-dried for 1 h at room temperature and then preincubated with 1 mM $CoCl_2$ in 50 mM Tris-HCl, pH 7.6, containing 10% sucrose for 15 min at room temperature. After rinsing with 0.1M sodium phosphate, pH 7.6, containing 10% sucrose, the cells were incubated for 6 h at 37 °C in incubation medium (10mg cytochrome c, 10mg DAB hydrochloride, 2mg catalase, 10% sucrose in 0.1 M sodium phosphate, pH 7.6). The coverslips were rinsed in 0.1 M sodium phosphate, pH 7.6, containing 10% sucrose and mounted in VectaMount AQ (Vector Laboratories). Images were captured on an upright Leica microscope (Leica Microsystems) under a total magnification of 200x.

Real-time quantitative RTPCR.

Transcript levels were quantitated by real-time RTPCR by extracting total RNA using Trizol (Invitrogen) from U2OS cells washed in phosphate-buffered saline. RNA samples were then DNase treated with the Turbo DNA-free kit (Ambion) and reverse transcribed with random hexamer primers and the TaqMan reverse transcription reagents kit (Applied Biosystems) according to the manufacturer's instructions. The reverse-transcribed RNA was then amplified by real-time PCR using the ABI PRISM 7900HT Sequence detection system with the Power SYBR

Green PCR Mastermix (Applied Biosystems). The primers used for real-time were specific for the following genes: PRC (hPRC sybr S: AGTGGTTGGGGAAGTCGAAG; hPRC sybr AS: CCTGCCGAGAGAGACTGAC), TFB1M (hTFB1 sybr S: CCTCCGTTGCCCACGATTC; hTFB1 sybr AS: GCCCACTTCGTAAACATAAGCAT), TFB2M (hTFB2 sybr S: CGCCAAGGAAGGCGTCTAAG; hTFB2 sybr AS: CTTTCGAGCGCAACCACTTTG), COXII (hCOXII sybr S: ACAGATGCAATTCCCGGACGTCTA; hCOXII sybr AS: GGCATGAAACTGTGGTTTGCTCCA), hcytochrome *b* (hcyt*b* sybr S: AATTCTCCGATCCGTCCCTA; hcyt*b* sybr AS: GGAGGATGGGGATTATTGCT) and β-actin (hβ-actin S: CATGTACGTTGCTATCCAGGC; hβ-actin AS: CTCCTTAATGTCACGCACGAT). Reactions were carried out using the following conditions: an initial step of 2 min at 50 °C and 10 min at 95 °C, followed by 45 cycles of 15 s at 95 °C and 1 min at 60°C. The results were analyzed using the Relative Quantification Study program with SDS 2.1 software (Applied Biosystems). Samples were analyzed in triplicate and mRNA quantities were normalized to 18S RNA. Relative gene expression levels were determined by the comparative C_t method and expressed as the average of at least three separate determinations ± s.e.m.

Generation of Lentivirus transductants expressing shRNA.

Double-stranded oligonucleotides targeting the PRC gene (PRCsh#1S: CACCGCCATCAGGACATCACCATCACGAATGATGGTGATGTCCTGATGGC; PRCsh#1AS: AAAAGCCATCAGGACATCACCATCATTCGTGATGGTGATGTCCTGATGGC) and a negative control sequence derived from the MISSION nontarget shRNA control vector (Sigma)

(control shS:

CACCCAACAAGATGAAGAGCACCAACTCGAGTTGGTGCTCTTCATCTTGTTG; control shAS: AAAACAACAAGATGAAGAGCACCAACTCGAGTTGGTGCTCTTCATCTTGTTG) were ligated into the pENTR/U6 vector using the BLOCK-iT U6 RNAi Entry Vector Kit (Invitrogen). The control hairpin contains four base pair mismatches to any known human or mouse gene (164). The resulting entry vectors were designated pENTR/PRCshRNA#1 and pENTR/control. The lentiviral expression vectors pLenti/PRCshRNA#1 and pLenti/control and pLenti-GW/U6-Lamin^{shRNA} were generated by transferring the U6-PRC and U6-control and U6-Lamin RNAi cassettes into the pLenti6/BLOCK-iT DEST vector using the LR recombination reaction. Lentiviral particles of these constructs were generated in 293FT cells using the BLOCK-iT Lentiviral RNAi Expression system according to the manufacturer's protocol (Invitrogen). U2OS cells were transduced with each lentiviral construct at a multiplicity of infection of 10 and stable shRNA-expressing clones were selected with blasticidin. U2OS cells were used because they are a human cell line that exhibits regulated expression of PRC (99). Clones were cultured and cell lysates prepared and analyzed by immunoblotting using an anti-Lamin A/C antibody (a generous gift from Robert Goldman, Northwestern University) and rabbit anti-PRC(1047-1379) (99).

ACKNOWLEDGMENTS

We are grateful to Dr. Robert Goldman (Northwestern University) and Dr. Winship Herr (University of Lausanne) for the gift of antibodies. We thank Raymond A. Pasko for expert technical assistance.

This work was supported by United States Public Health Service Grant GM32525-25 form the National Institutes of Health.

CHAPTER 6:

SHORT HAIRPIN RNA-MEDIATED SILENCING OF PGC-1-RELATED COACTIVATOR (PRC) RESULTS IN A SEVERE RESPIRATORY CHAIN DEFICIENCY ASSOCIATED WITH THE PROLIFERATION OF ABERRANT MITOCHONDRIA

INTRODUCTION

Mitochondria are semiautonomous organelles that function as important sites of biological oxidations and ATP production. Central to this function is the electron transport chain and oxidative phosphorylation system, which is comprised predominantly of five multisubunit protein complexes embedded in the mitochondrial inner membrane (143,165). Mitochondria contain their own genetic system directed by a covalently closed circular DNA genome whose entire protein coding capacity is devoted to the production of 13 protein subunits of respiratory complexes I, III, IV and V. Although essential, these subunits account for only a fraction of the protein composition with the majority of the respiratory subunits of nuclear origin (40,90). Its bi-genomic expression makes the respiratory apparatus unique among mitochondrial oxidative functions and poses an important biological problem in understanding the coordination of nuclear and mitochondrial gene expression.

A number of nucleus-encoded regulatory factors have been associated with the transcriptional control of both nuclear and mitochondrial genes that specify the respiratory apparatus in mammalian systems. Initial work identified nuclear respiratory factors, NRF-1 and NRF-2(GABP), as activators of nuclear cytochrome c and cytochrome oxidase genes. These factors have subsequently been associated with the expression of the majority of nuclear genes

specifying mitochondrial respiratory function. These include genes encoding the respiratory subunits themselves but also those specifying protein import and assembly factors, heme biosynthetic enzymes, ribosomal proteins and tRNA synthetases of the mitochondrial translation system and components of the mtDNA transcription and replication machinery (40,105). The latter include the nucleus-encoded mitochondrial transcription factors Tfam and the mtTFB isoforms, TFB1M and TFB2M, which act in conjunction with the mitochondrial RNA polymerase to maximize transcription from divergent heavy and light strand promoters (121,146). Mice with a targeted disruption of Tfam (15) or NRF-1 (47) have an embryonic lethal phenotype with loss of mtDNA, although lethality of the NRF-1 embryos occurs at an earlier stage suggesting that functions other than mitochondrial respiration are also disrupted (51). Recently, shRNA-mediated inhibition of both NRF-1 and NRF-2 has been linked to the down regulation of all 10 nucleus-encoded cytochrome oxidase subunits providing additional *in vivo* evidence for the importance of these factors in respiratory chain expression (49,50).

Insight into how diverse transcription factors might be coordinated into a program of mitochondrial biogenesis came with the discovery of the PGC-1 family of inducible coactivators. PGC-1α, the founding member of the family, displays a broad range of transcription factor interactions and biological functions (92,157). It is induced during adaptive thermogenesis in brown fat and can interact directly with NRF-1 in enhancing mitochondrial respiration and biogenesis (53,54). Ectopic over expression of PGC-1α in both cultured cells and in mice results in dramatic increases in mitochondrial content and the expression of a number of genes important for mitochondrial respiratory function (54,55). These properties are shared by PGC-1β, a close homologue of PGC-1α, that also acts as a potent activator of NRF target genes (123). However, targeted disruption of either PGC-1 coactivator in mice does not result in a dramatic

mitochondrial biogenesis defect (60,61,85). In both cases, the homozygous knockouts were viable and fertile with no gross abnormalities in mitochondrial number or morphology. This may be explained by compensatory interactions among the PGC-1 family members or other adaptive changes in the transcriptional machinery. Recently, it was demonstrated that mice doubly deficient in PGC-1α and PGC-1β die shortly after birth due to heart failure and display dramatic mitochondrial abnormalities in heart and brown adipose tissue (88) indicating that the actions of both coactivators are required for the mitochondrial biogenesis that takes place in the developing murine heart and brown adipose tissue .

A third PGC-1 family coactivator, designated PRC (PGC-1-related coactivator), has limited overall sequence similarity with PGC-1α or PGC-1β but shares key structural features that define the family. These include a conserved amino-terminal transcriptional activation domain, a central proline-rich region, a functional binding site for host cell factor and a carboxy-terminal R/S domain and RNA recognition motif (89). PRC binds NRF-1 and activates NRF-1 target genes but does not appear to be regulated significantly during adaptive thermogenesis. Rather, its expression is serum-induced in the absence of *de novo* protein synthesis and correlates with the cell proliferative cycle (99). Like the other PGC-1 coactivators, PRC binds HCF, an abundant chromatin component that is required for cell cycle progression (166). HCF is a NRF-2(GABP) coactivator (154) and exists in an *in vivo* complex with both PRC and NRF-2 (166). These *in vivo* interactions likely account for the *trans*-activation of NRF-2 target genes by PRC despite the absence of a direct interaction between PRC and NRF-2 subunits *in vitro*.

Expression of a PRC subfragment that binds NRF-1 and CREB inhibits respiratory growth (99), suggesting that PRC plays a role in respiratory chain expression *in vivo*. However, we were concerned that a dominant negative form of PRC interacts with many other molecules

in the cell, and can therefore have many non-specific effects that are not directly mediated by PRC**.** To further dissect the *in vivo* role of PRC, we wanted to suppress PRC function by RNA interference.

As explained in the **Background (Chapter 2)**, previous attempts to knockdown PRC failed. Since the start of this project, the knowledge of RNA interference in mammalian cells has been expanded tremendously, and new information has become available to improve the design of efficient shRNAs. Our experience with a lentiviral system to express a dominant negative form of PRC triggered us to use this system to express newly designed short hairpin RNAs targeting PRC.

Here, the effects of shRNA-mediated PRC knockdown on respiratory function and mitochondrial biogenesis are investigated in stable lentiviral transductants of human U2OS cells. Loss of PRC results in a severe reduction in respiratory energy production associated with the reduced expression and assembly of respiratory complexes. Surprisingly, this respiratory defect is associated with the proliferation of structurally defective mitochondria. In addition to the respiratory defect, PRC silencing was also implicated in the inhibition of cell cycle progression. Global changes in gene expression were consistent with both mitochondrial and growth phenotypes. The results implicate PRC as a regulatory link between respiratory chain expression and organelle biogenesis.

RESULTS

The *in vivo* function of PRC was investigated by constructing lentiviruses designed to express two different shRNAs, shRNA#1 and shRNA#4, targeting different regions of the PRC mRNA. Originally, we synthesized 4 different shRNAs to target PRC because not all shRNAs

for a certain gene have the same (if any) silencing effect (96). We selected two regions in PRC mRNA that were identical between human and mouse PRC (hairpin#1 and #4), providing us with flexibity in the choice of cell line used for lentiviral expression. In addition, we selected two hairpins specific for mouse PRC (shRNA#2 and #3). The algorithm used to select the short hairpin sequences was the RNAi Designer web tool from Invitrogen (see "Materials and Methods"). The annealed double-stranded oligos were first cloned into an entry vector, designated pENTR. An initial screening of the hairpins was performed before making viral constructs by transiently transfecting the pENTR constructs targeting human PRC into 293FT cells and monitoring the degree of PRC silencing. A pENTR construct containing shRNA#2, targeting mouse PRC, and a negative control shRNA that lacks identity with any known mouse or human sequence were also transfected into 293FT cells. As seen in **Figure 6.1A**, shRNA#1 caused the most robust silencing of endogenous PRC protein, while shRNA#4 caused partial PRC silencing, compared to the negative control shRNA. ShRNA#2 was able to also partially silence human PRC, thus invalidating its use as a negative control in human cells. When we co-transfected the PRC/pSV SPORT expression plasmid with shRNA#1 and #4, both hairpin constructs were able to dramatically reduce expression of PRC from this vector compared to a control shRNA **(Figure 6.1B)**. Based on these promising results, we decided to generate lentiviral expression constructs containing shRNA#1 and #4.

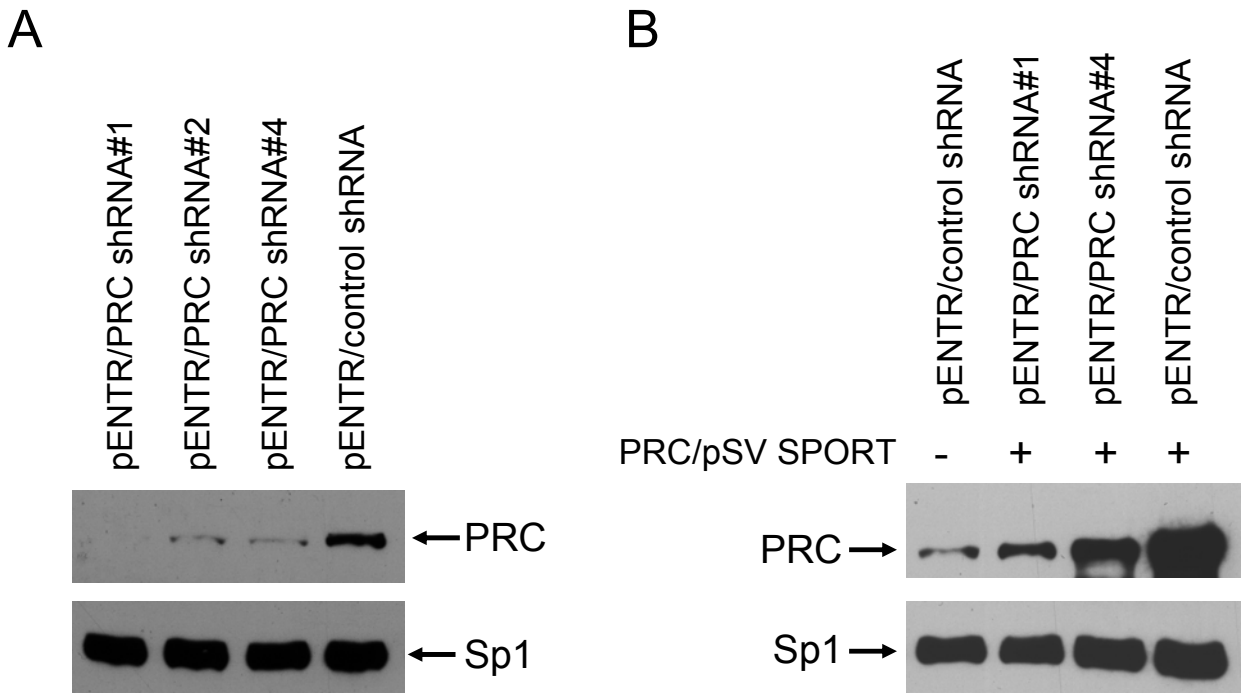

Figure 6.1. Transient expression of several short hairpins causes different degrees of PRC silencing.

A. Whole cell extracts were prepared from 293FT cells transiently transfected with the entry vector pENTR containing either a control shRNA, PRC shRNA#1, #2 or #4.

B. Whole cell extracts were prepared from 293FT cells transiently transfected with pENTR/control shRNA alone or pENTR/control shRNA, pENTR/PRC shRNA#1 and pENTR/PRC shRNA#4 plus PRC/pSV SPORT.

In both panels *A* and *B*, PRC and Sp1 proteins were detected by immunoblotting following denaturing gel electrophoresis using rabbit anti-PRC(1047-1379) and rabbit anti-Sp1 antibodies, respectively. Arrows indicate the position of PRC and Sp1.

Human U2OS cells were infected with these viruses and a number of stable transductants were selected in the presence of blasticidin. U2OS cells were chosen because they exhibit proper serum-regulated expression of PRC mRNA and protein, which are both down regulated in serum starved cells and rapidly up regulated upon serum stimulation of quiescent cells (99). Approximately 20 individual shRNA#1 and shRNA#4 transductants were screened for PRC protein levels by immunoblotting. Two of these were chosen for further study. As shown in **Figure 6.2A (lane 4)**, one of the shRNA#1 transductants had complete or nearly complete knockdown of PRC protein. Although none of the shRNA#4 transductants showed complete PRC knockdown, one expressed approximately 15 percent of control levels **(Figure 6.2A, lane 5)** as estimated by densitometry. The inhibition of PRC expression was specific in that lamin A/C protein levels were not altered in either transductant **(lanes 4 and 5)**. In addition, the negative control shRNA, lacking identity with any known mouse or human sequence, failed to affect the expression of PRC or the lamin A/C control **(lane 2)** and a lentiviral transductant expressing a shRNA specific to lamin exhibited complete knockdown of lamin expression without affecting PRC **(lane 3)**. In addition, as shown in **Figure 6.2B**, PGC-1α is undetectable by immunoblotting in wild type U2OS cells **(lane 3)** and in the lentiviral transductants **(lanes 4-6)** under conditions where PGC-1α protein expressed from Ad-PGC-1α is easily detected **(lane 2)**. Note the intense antibody reactive band below PGC-1α is likely a non-specific cross-reacting species because it is expressed in the Ad-GFP control **(lane 1).** Thus, the effects of PRC in these cells can be studied in the absence of detectable PGC-1α protein expression.

Figure 6.2. Silencing of PRC expression in U2OS cells by lentivirally delivered short hairpin RNAs.

A. Total cell extracts were prepared from wild type U2OS cells (wt), and from stable lentiviral transductants expressing the control shRNA, lamin shRNA, PRC shRNA#1 or PRC shRNA#4. PRC and lamin A/C proteins were detected by immunoblotting following denaturing gel electrophoresis using rabbit anti-PRC(1047-1379) and rabbit anti-lamin A/C antibodies, respectively, following division of the membrane at the indicated position (dashed line). Molecular mass standards in kilodaltons are indicated at the left.

B. Total cell extract was prepared from wild type U2OS cells (wt), adenovirus infected U2OS cells expressing either GFP (Ad-GFP) or PGC-1α (Ad-PGC-1α), and U2OS cell lentiviral transductants expressing control shRNA, PRC shRNA#1 or PRC shRNA#4. PGC-1α protein was detected by immunoblotting following denaturing gel electrophoresis using rabbit anti-PGC-1α serum.

Arrows indicate the positions of PRC, PGC-1α and lamin A/C.

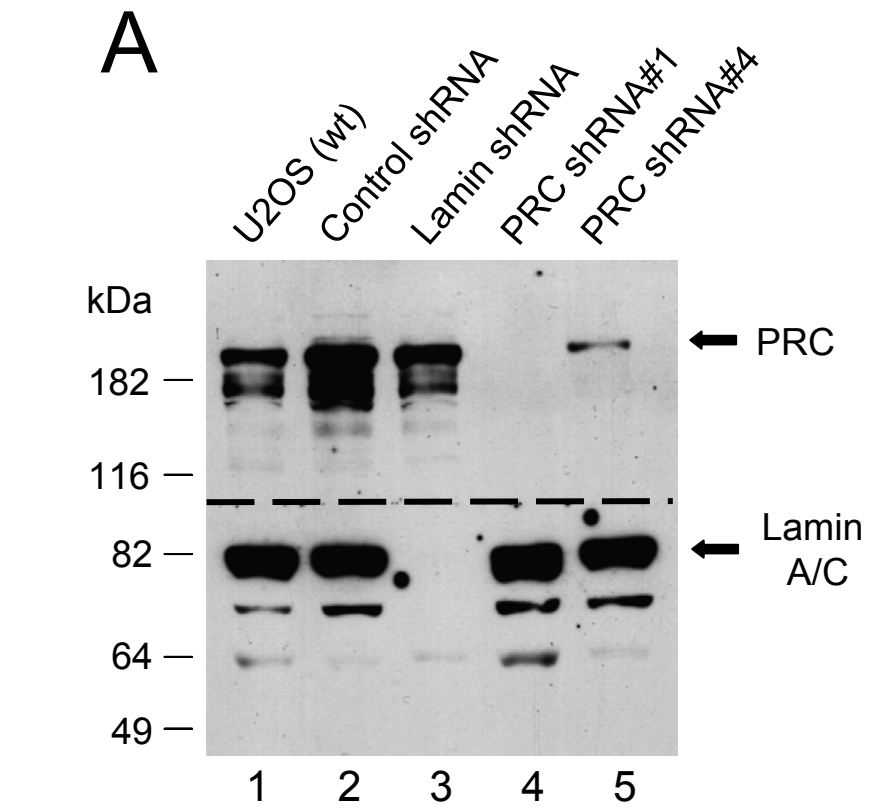
A
U2OS (wt)
Control shRNA
Lamin shRNA
PRC shRNA#1
PRC shRNA#4
kDa
182
116
82
64
49
PRC
Lamin
A/C
1
2
3
4
5

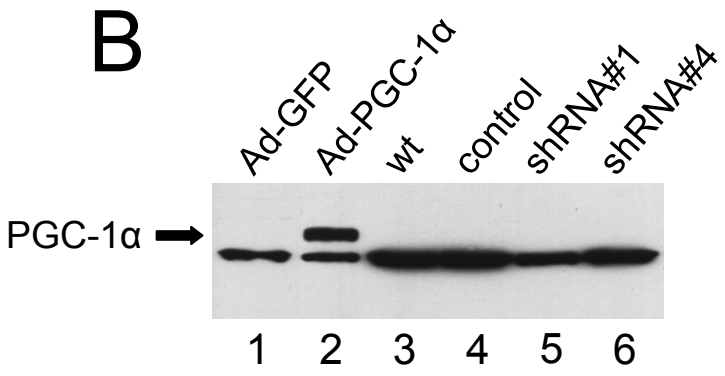
B
Ad-GFP
Ad-PGC-1α
wt
control
shRNA#1
shRNA#4
PGC-1α
1
2
3
4
5
6

Additional confirmation that the shRNAs specifically target PRC expression was obtained from Ad-NmycPRC infected cells. As shown in **Figure 6.3A**, PRC is abundantly over expressed in Ad-NmycPRC-infected control transductants **(lane 2)** compared to those infected with Ad-GFP **(lane 1)**. By contrast, PRC protein is undetectable in shRNA#1 transductants infected with Ad-NmycPRC **(lane 4)** or the Ad-GFP control **(lane 3)**. This result is not explained by a general defect in adenovirus expression in the shRNA#1 transductant because PGC-1α can be over expressed specifically from Ad-PGC-1α in the PRC shRNA#1 transductant **(lanes 5-6)**. Finally, a side-by-side comparison of Ad-NmycPRC infected transductants in **Figure 6.3B** shows over expression of PRC in the control **(lane 1)**, complete silencing of PRC in the shRNA#1 transductant **(lane 2)** and partial silencing of PRC expression in the shRNA#4 transductant **(lane 3)**. This parallels the relative level of PRC silencing observed in the uninfected transductant lines **(Figure 6.2A)**. The results establish that the PRC shRNAs can silence PRC protein levels specifically even when PRC is over expressed from a potent non-chromosomal transcriptional unit.

Figure 6.3. PRC expressed from an adenoviral vector is silenced in shRNA cells.

A. Immunoblots of total cell extracts from the control shRNA and PRC shRNA#1 transductants infected with either adenovirus Ad-NmycPRC, Ad-PGC-1α or the control Ad-GFP. PGC-1α protein was detected using rabbit anti-PGC-1α serum.

B. Comparison of PRC expression in Ad-NmycPRC infected control, shRNA#1 and shRNA#4 transductants.

In both panels PRC protein was detected using rabbit anti-PRC(1047-1379) serum.

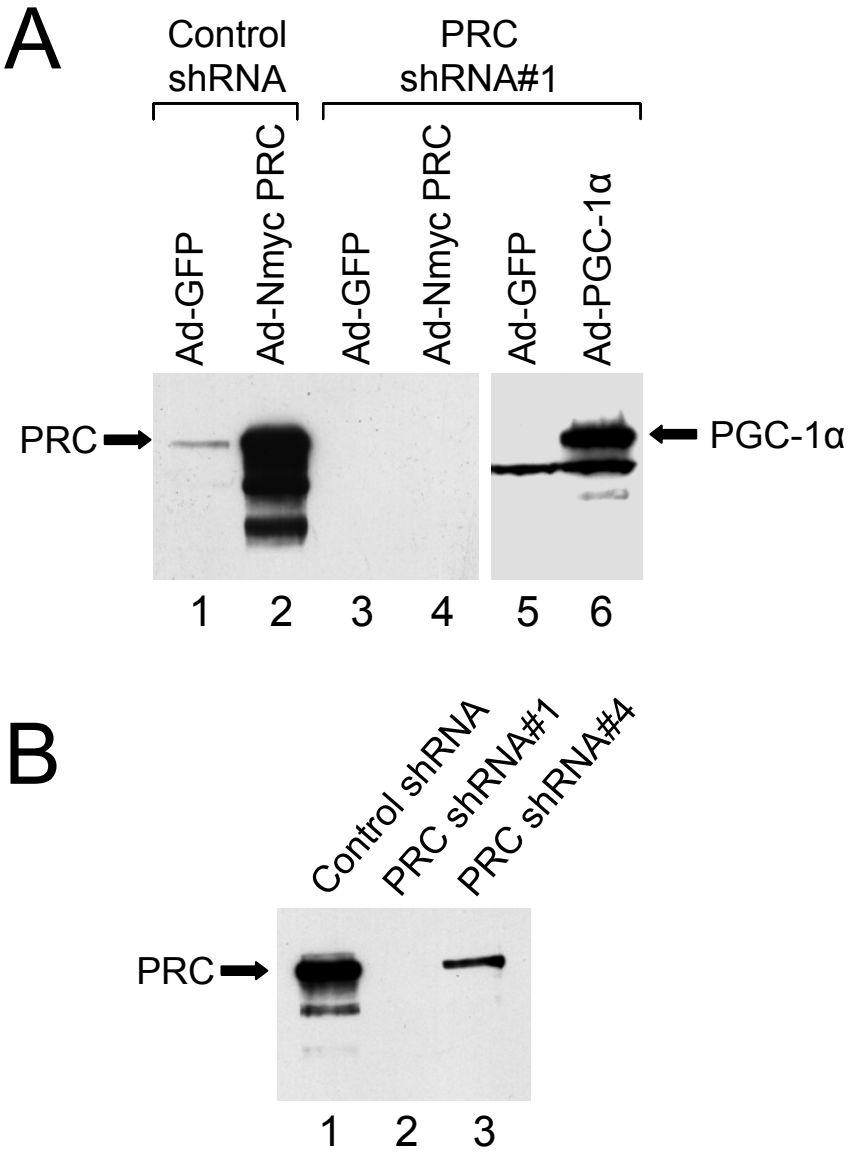
A
Control shRNA
PRC shRNA#1
Ad-GFP
Ad-Nmyc PRC
Ad-GFP
Ad-Nmyc PRC
Ad-GFP
Ad-PGC-1α
PRC
PGC-1α
1 2 3 4 5 6
B
Control shRNA
PRC shRNA#1
PRC shRNA#4
PRC
1 2 3

Both the shRNA#1 and #4 transductants showed a markedly reduced growth rate on glucose as a carbon source compared to that of wild type cells or the control transductant **(Figure 6.4A)**. Glucose growth does not require mitochondrial respiratory function and the growth inhibition by even partial loss of PRC suggests that PRC may affect cell growth by mechanisms that are independent of its effects on mitochondrial respiration. In contrast, the shRNA#1 and #4 transductants are markedly different in their rate of respiratory growth on galactose, which mainly depends on mitochondrial ATP production (133). The growth rate of the shRNA#4 transductant on galactose relative to the controls is diminished significantly **(Figure 6.4B)**. However, the shRNA#1 transductant displays a much more severe respiratory growth inhibition on galactose **(Figure 6.4B)**, suggesting that complete PRC silencing results in a severe defect in mitochondrial respiratory function. Interestingly, an independent shRNA#1 isolate (PRC shRNA#1b) had a PRC expression level equivalent to that in shRNA#4 and displayed similar growth retardation on glucose and galactose **(Figure 6.4A and B)**. The negative control transductant had a growth rate similar to wild type on both glucose and galactose, demonstrating that the growth defects are unrelated to lentiviral transduction or to the selection. The apparent PRC dose-dependent galactose growth inhibition displayed by shRNA#4 and two separate shRNA#1 transductants supports the conclusion that PRC is responsible for the inhibition of respiratory growth in these cell lines.

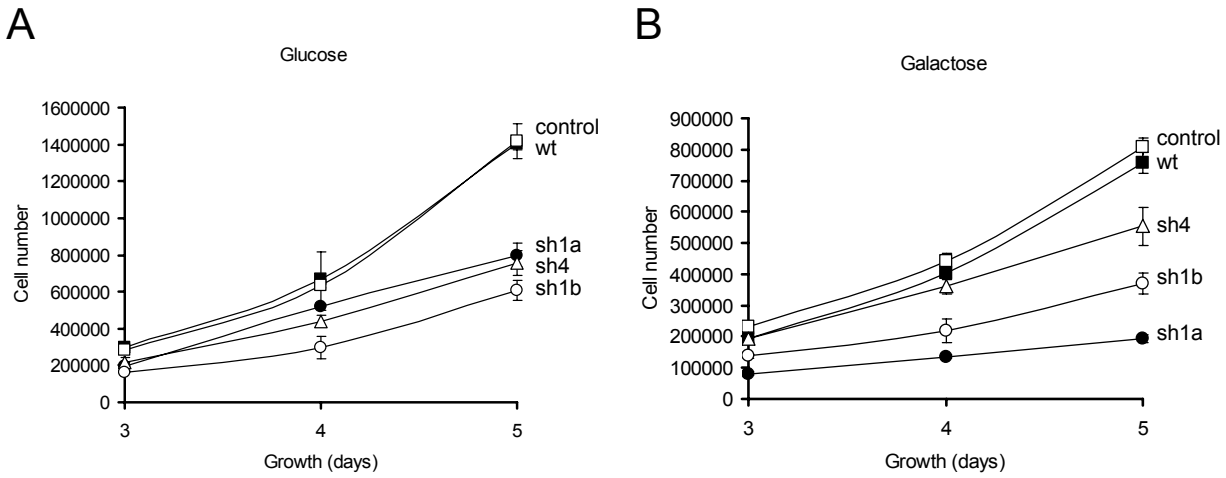

Figure 6.4. Growth of PRC shRNA transductants and controls on either glucose or galactose as the primary carbon source.

A. Growth of U2OS wild type (wt; closed squares), and lentiviral transductants expressing the control shRNA (control; open squares), PRC shRNA#1 (sh1a; closed circles), PRC shRNA#1b (sh1b; open circles) or PRC shRNA#4 (sh4; open triangles) on glucose media.

B. Growth of U2OS wild type (wt; closed squares), and lentiviral transductants expressing the control shRNA (control; open squares), PRC shRNA#1 (sh1a; closed circles), PRC shRNA#1b (sh1b; open circles) or PRC shRNA#4 (sh4; open triangles) on galactose media.

Growth curves in panels *A* and *B* represent the averages ± standard errors of the means for three separate determinations.

To further investigate the diminished growth on glucose in the shRNA#1 and #4 cells, we examined the cell cycle distribution of control shRNA, PRC shRNA#1 and shRNA#4 transductants after propidium iodide staining by flow cytometry. As seen in **Figure 6.5**, silencing of PRC significantly decreased the population of cells in S phase and increased the G_0/G_1 population compared to control shRNA cells. There was no significant effect on the percentage of cells in G_2/M phase. This indicates a cell cycle arrest with cells blocked in G_0/G_1 and inhibited entry into S phase. The cell cycle distribution of the control shRNA cells is not different from wild type U2OS cells (not shown). Interestingly, the percentage of shRNA#4 cells in G_0/G_1 and S phase was intermediate between control shRNA cells and PRC shRNA#1 cells, confirming that this is a dose-dependent response to reduced levels of PRC. Notably, no sub-G_1 population of apoptotic cells is present in any of the histograms. Hence, the decrease in cell proliferation in cells where PRC is silenced cannot be explained by induction of apoptosis. Furthermore, there was no indication of DNA polyploidy in the cell populations investigated.

This provides further evidence that PRC affects cell growth by influencing cell cycle distribution, independently of its effects on mitochondrial respiration.

Figure 6.5. Flow cytometric DNA content analysis of control shRNA, PRC shRNA#1 and PRC shRNA#4 cells stained with propidium iodide.

Flow cytometric DNA content analysis of control shRNA, PRC shRNA#1 and PRC shRNA#4 U2OS cells stained with propidium iodide. Representative DNA histograms are shown. Quantitative assessment of the cell cycle distributions are shown next to each histogram. The numbers indicate mean ± standard deviation for three independent determinations.

Control shRNA

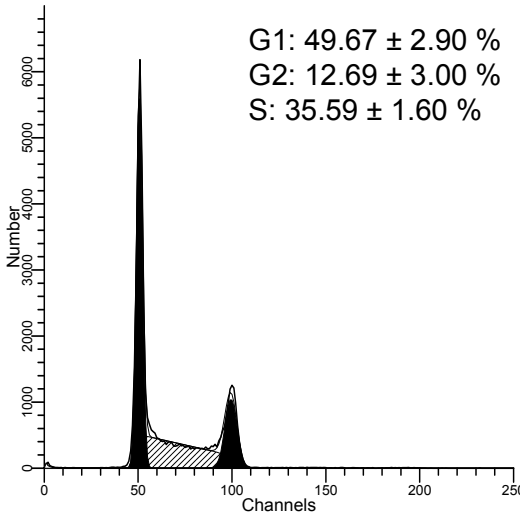

PRC shRNA#1

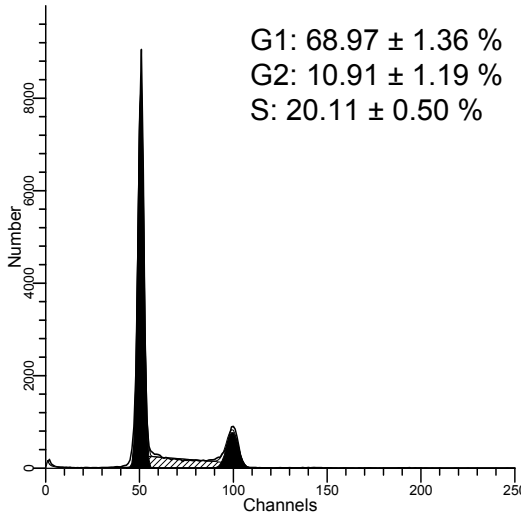

PRC shRNA#4

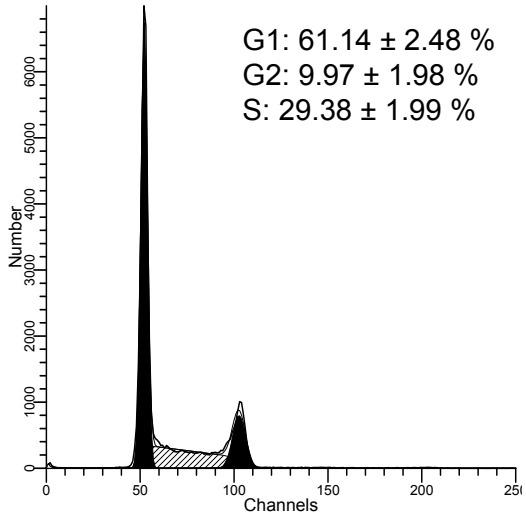

PRC is a transcriptional coactivator that operates, at least in part, through the nuclear respiratory factors, NRF-1 and NRF-2, to activate the expression of NRF target genes. Therefore, it is likely that the respiratory growth defect in the shRNA#1 transductant is associated with reduced expression of mRNAs encoding NRF target genes required for mitochondrial respiratory function. As shown in **Figure 6.6A**, silencing of PRC protein expression in the shRNA#1 and shRNA#4 transductants is accompanied by only a partial reduction of PRC mRNA suggesting that the two hairpins reduce PRC protein expression through both transcriptional and translational inhibition. The shRNA#4 transductant displays no or very small changes in mitochondrial gene expression, consistent with its much milder respiratory growth phenotype. Interestingly, both NRF-1 and NRF-2β mRNAs are diminished in the PRC shRNA#1 transductant, whereas those for NRF-2α and CREB are unchanged. The reduced expression of the nuclear transcription factor mRNAs is associated with a reduction of the mRNAs encoding the mitochondrial transcription factors (Tfam, TFB1M and TFB2M). The biggest decrease is in TFB2M, whose expression has recently been correlated with the transcription and replication of mtDNA in both human (39) and *Drosophila* (167) cells. Here, we observe the down regulation of 3 mitochondrial transcripts in the PRC shRNA#1 transductant **(Figure 6.6A)** (COXII, ND6 and Cyt*b*) but no significant change in mtDNA copy number normalized to 18S rDNA **(Figure 6.6B)**. The maintenance of mtDNA levels despite reductions in TFB2M and mitochondrial transcripts is surprising in light of the coupling of mtDNA transcription and replication (146). Nevertheless, the results suggest that PRC control over respiratory gene expression contributes to the respiratory growth defect.

Figure 6.6. Steady-state mRNA expression of regulatory and structural genes involved in mitochondrial respiratory function and estimation of mtDNA content.

A. Gene expression was monitored by quantitative real-time PCR using total RNA prepared from control shRNA, PRC shRNA#1, and PRC shRNA#4 transductants. The battery of genes examined represent nuclear regulatory factors (PRC, PGC-1α, NRF-1, NRF-2α, NRF-2β, CREB and SP-1), mitochondrial transcription factors (Tfam, TFB1M and TFB2M), and nucleus (Cyt *c*, COXIV, SDHB, UQCRC2 and ATP5A1)- and mitochondrion (COXII, ND6 and Cyt *b*)-encoded respiratory subunits. As a negative control we tested expression of β-actin. Relative steady-state mRNA levels were normalized to 18S rRNA as an internal control and values expressed relative to the shRNA control, which was assigned a value of 1. Values for PRC shRNA#1 (grey bars) and PRC shRNA#4 (black bars) are the averages ± standard deviation for at least three separate determinations.

B. Content of mtDNA was estimated by quantitative real-time PCR using total DNA prepared from control shRNA and PRC shRNA#1 transductants. Relative mtDNA content was determined using probes specific for the mitochondrial D-loop or the COXI transcriptional unit. Values (gray bars) were normalized to 18S rDNA as an internal control and expressed relative to those obtained from the shRNA control, which was assigned a value of 1, as the averages ± standard error of the mean for at least three separate determinations. Values were also normalized to the MitoTracker Green FM fluorescence per cell (black bars) derived from the numbers in **Table 6.1**.

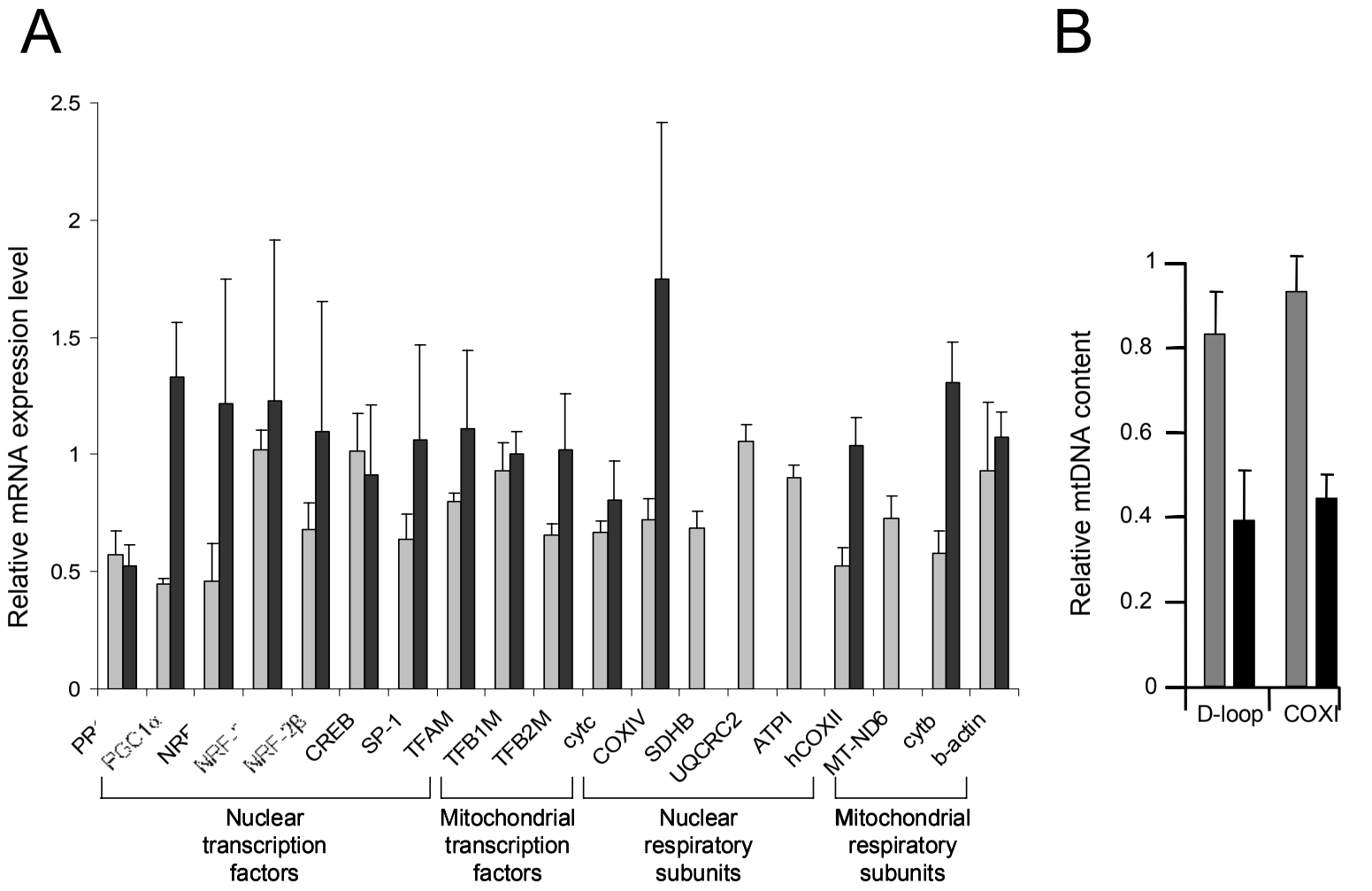
A
B
Relative mRNA expression level
2.5
2
1.5
1
0.5
0
PGC1α
NRF-2β
CREB
SP-1
TFAM
TFB1M
TFB2M
cytc
COXIV
SDHB
UQCRC2
ATPI
hCOXII
MT-ND6
cytb
b-actin
Nuclear transcription factors
Mitochondrial transcription factors
Nuclear respiratory subunits
Mitochondrial respiratory subunits
Relative mtDNA content
1
0.8
0.6
0.4
0.2
0
D-loop
COXI

Given the respiratory growth defect, one might expect a deficiency in the expression, assembly or function of the respiratory chain in the PRC shRNA#1 transductant. This was investigated by immunoblotting using a battery of antibodies directed against key subunits of all five respiratory complexes. The subunits were chosen because they are labile unless they are assembled into their respective complexes and thus their steady-state levels are thought to reflect those of the complexes in which they function. As shown in **Figure 6.7**, similar levels of the five subunits are detected in cell extracts from the wild-type U2OS cells, control shRNA and PRC shRNA#4 transductants. This suggests that there are no major differences in the expression or assembly of the five respiratory complexes in these cells. However, the PRC shRNA#1 transductant exhibits markedly diminished expression of several subunits. These include major reductions in COXII of complex IV, ND6 of complex I, and core protein 2 of complex III as well as a less pronounced but reproducible reduction in SDHB of complex II **(Figure 6.7)**. These changes do not result from a generalized reduction in respiratory gene expression because the α-subunit of F1-ATPase (ATP5A1) of complex V is expressed normally. It is interesting to note that both nuclear (SDHB, core 2) and mitochondrial (COXII, ND6) gene products exhibit diminished steady-state levels, suggesting that PRC affects the expression and/or the assembly of the products of both genomes. The reduced levels of COXII and ND6 correlate with reduced transcripts levels **(Figure 6.6A)** although the changes in protein expression appear quantitatively larger. Surprisingly, core protein 2 **(Figure 6.7)** but not its mRNA **(Figure 6.6A)** is dramatically down regulated whereas both SDHB protein **(Figure 6.7)** and mRNA **(Figure 6.6A)** are reduced in the shRNA#1 transductant. The reasons for the discrepancy between mRNA and protein for these respiratory subunits are unclear but may reflect gene-specific differences in transcriptional and post-transcriptional controls. PRC may control steady-state expression of respiratory

subunits through multiple means. For example, it may affect the expression of import or assembly factors or the mitochondrial or cytosolic translation machinery.

Figure 6.7. Mitochondrial respiratory subunit expression in lentiviral transductants and controls.

Total cell extract was prepared from wild type U2OS cells (wt) and lentiviral transductants expressing a control shRNA, PRC shRNA#1 or PRC shRNA#4. The indicated subunits from each of the five respiratory complexes were detected by immunoblotting following denaturing gel electrophoresis using a mixture of mouse monoclonal antibodies directed against each subunit. Heart mitochondrial extract was run as a control. Subunit designations for the respective complexes (I-V) are indicated at the left and gene names along with their nuclear (n) or mitochondrial (m) assignment are indicated at the right. The lower panel shows an immunoblot from an extended run of an electrophoresis gel used to resolve V-F1α and III-core2.

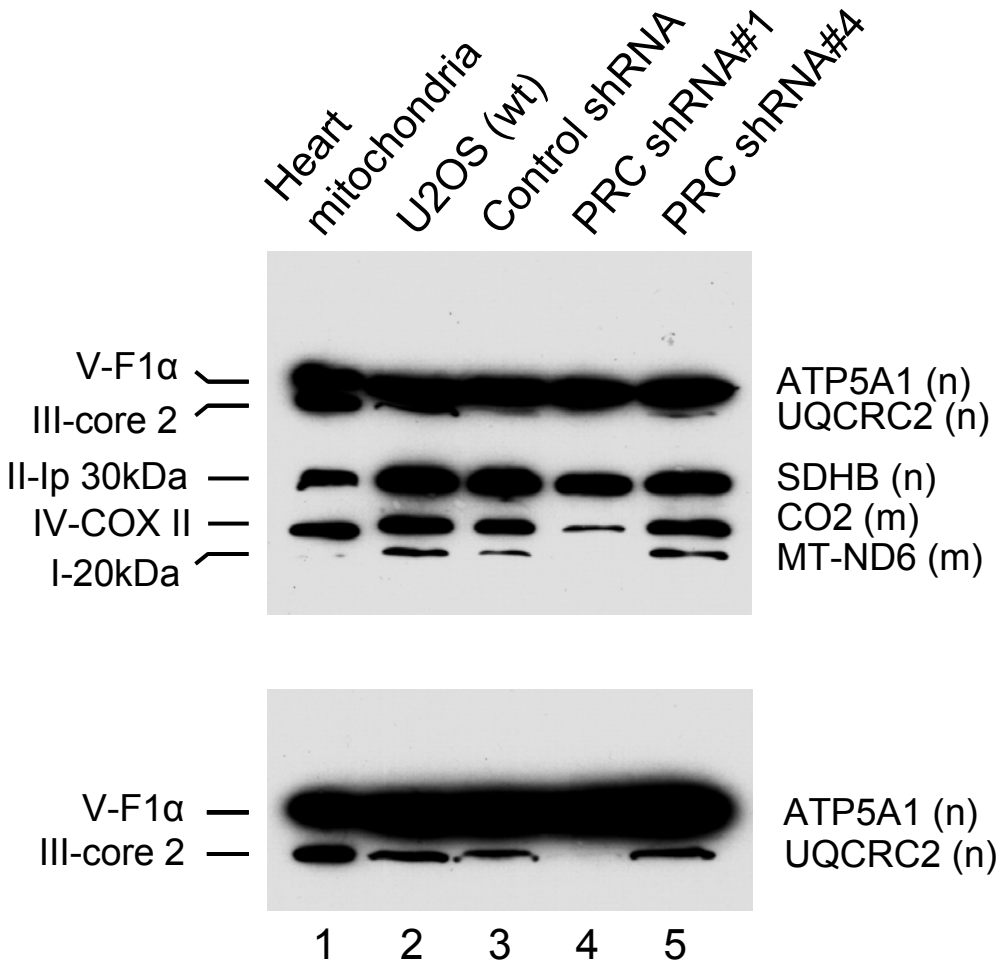
Heart mitochondria
U2OS (wt)
Control shRNA
PRC shRNA#1
PRC shRNA#4
V-F1α
III-core 2
II-Ip 30kDa
IV-COX II
I-20kDa
ATP5A1 (n)
UQCRC2 (n)
SDHB (n)
CO2 (m)
MT-ND6 (m)
V-F1α
III-core 2
ATP5A1 (n)
UQCRC2 (n)
1 2 3 4 5

The reduced expression of respiratory chain subunits in the PRC shRNA#1 transductants was accompanied by significantly decreased respiratory enzyme levels. As shown in **Figure 6.8A**, the levels of both NADH ubiquinone oxidoreductase (complex I) and cytochrome oxidase (complex IV) were reduced by approximately 60 percent in the PRC shRNA#1 transductant compared to the control. This result is consistent with the diminished levels of both ND6 (complex I) and COXII (complex IV) in the shRNA#1 transductant. In addition, the steady-state level of oligomycin sensitive ATP, which represents the mitochondrially produced ATP fraction, was reduced by approximately 50 percent in the PRC shRNA#1 transductant compared to control shRNA or PRC shRNA #4 transductants **(Figure 6.8B)** in keeping with the reduced respiratory enzyme levels **(Figure 6.8A)**. These results are consistent with the defect in respiratory growth and establish that loss of PRC is associated with a severe defect in the expression and function of the respiratory apparatus.

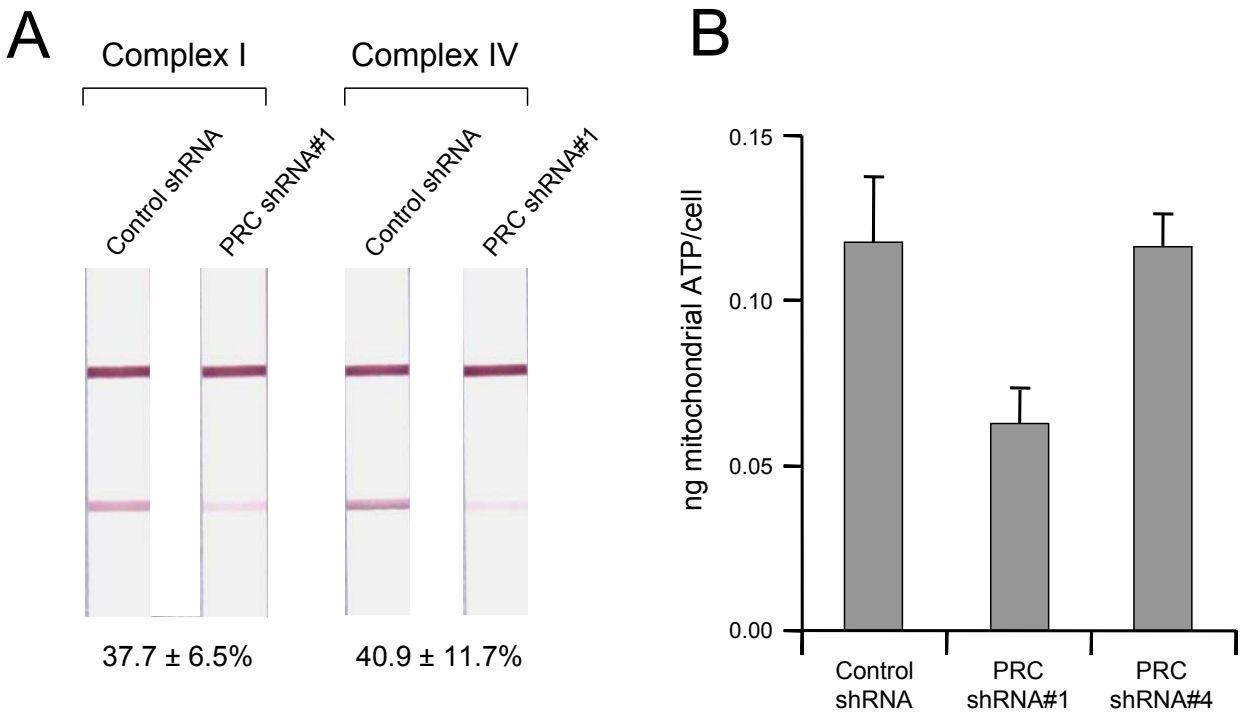

Figure 6.8. Respiratory enzyme and ATP levels in lentiviral transductants.

A. Levels of respiratory complexes I and IV in total cell extracts were quantitated by dipstick assay (MitoSciences). The top band represents the positive control signal; the bottom band represents the specific signal from the respective complexes. Membranes were scanned for densitometric analysis and the percent enzyme per unit protein in the PRC shRNA#1 transductant relative to the control shRNA is expressed as the average ± standard error of the mean for three separate determinations.

B. Steady-state ATP levels were quantitated in total cell extracts using a bioluminescent assay. Values for oligomycin sensitive ATP levels for control shRNA, PRC shRNA#1 and PRC shRNA#4 transductants are shown as the average ± standard error of the mean for three separate determinations.

The PGC-1 family coactivators are thought to function as positive regulators of respiratory gene expression and mitochondrial biogenesis (40). Thus, the diminished expression and function of the respiratory chain in the PRC shRNA#1 transductant may reflect a generalized down regulation of mitochondrial biogenesis in these cells. Mitochondrial number and morphology were examined by transmission electron microscopy. As shown in **Figure 6.9**, the cells are generally asymmetric with the majority of cytoplasm occupying one side of the cell. The cytoplasm of the control transductants contains a number of electron dense mitochondria that exhibit the classical double membrane structure with cristae visualized as invaginations of the inner membrane that extend into the matrix **(Figure 6.9, 6.10)**. In contrast, the shRNA#1 transductants contain an increased number of double membrane organelles that bear little resemblance to the control mitochondria **(Figure 6.9)**. In addition to being more abundant, these organelles exhibit much reduced electron density and instead of recognizable cristae, contain a granular internal structure. Electron micrographs of PRC shRNA#4 transductants show mitochondrial profiles that are intermediate between control and shRNA#1 cells with a modestly elevated mitochondrial content and a modestly reduced electron density relative to the control transductants, confirming that PRC is mediating the changes in mitochondrial number and morphology.

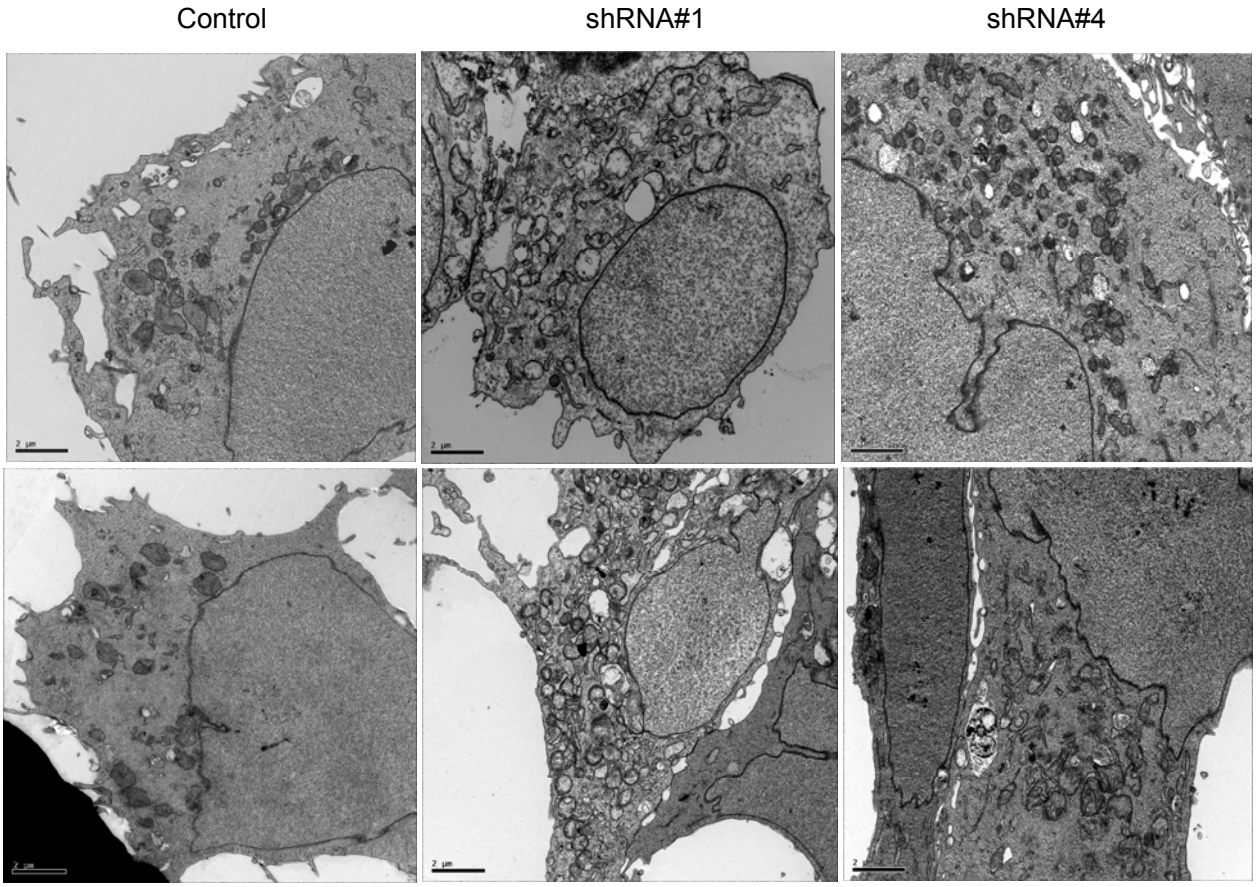

Figure 6.9. Evaluation of mitochondrial number and morphology by electron microscopy. U2OS cells stably infected with recombinant lentiviruses expressing a control shRNA, PRC shRNA#1 or PRC shRNA#4 were analyzed by transmission electron microscopy. Bars, 2 μm.

Closer examination of control and shRNA#1 mitochondria reveals striking structural differences **(Figure 6.10)**. Instead of well-formed cristae extending into the mitochondrial matrix as observed in the controls, the shRNA#1 mitochondria show blebbing of the inner mitochondrial membrane as though formation of proper cristae was truncated. In many cases the matrix space in completely devoid of any internal structure. In others, circular multi-membranous structures are found in the matrix spaces of a subset of shRNA#1 mitochondria. This may reflect an abnormality in organelle biogenesis in these cells.

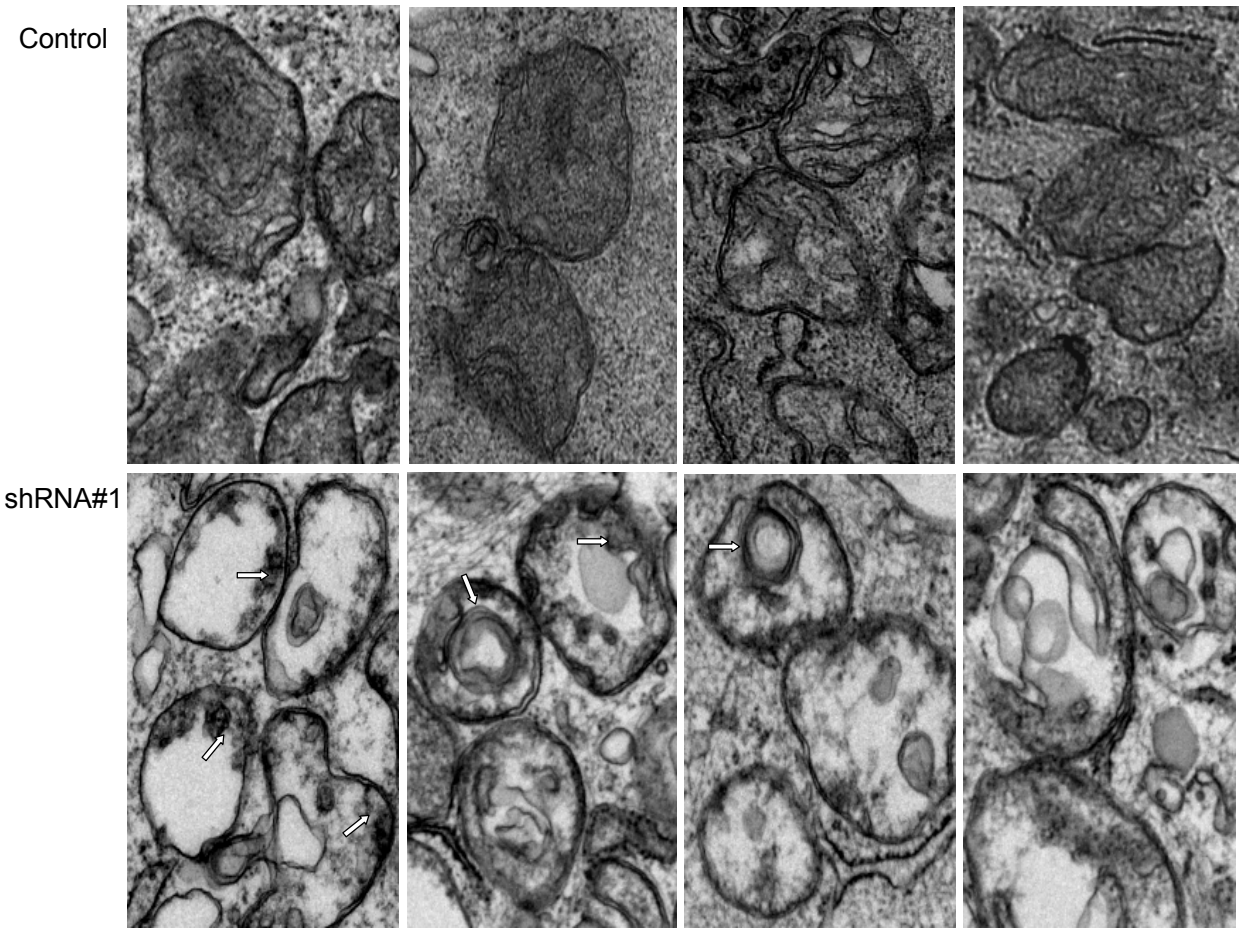

Figure 6.10. Mitochondrial ultrastructure in lentiviral transductants.

Panels show representative electron micrographs of mitochondria from lentiviral U2OS transductants. Upper panels are from the control shRNA transductant while lower panels are from the PRC shRNA#1 transductant. Arrows indicate the blebbing of the inner mitochondrial membrane and the circular multi-membranous structures seen in some mitochondria of the PRC shRNA#1 transductant.

The mitochondrial abundance was compared quantitatively by flow cytometric analysis using MitoTracker Green FM and by morphometric assessment of mitochondrial profiles. As shown in **Table 6.1**, the shRNA#1 transductants have twice the MitoTracker Green FM fluorescence on a per cell basis compared to the control. The MitoTracker Green FM fluorescence of the shRNA#4 transductant is intermediate between that of the control and shRNA#1. The mitochondrial accumulation of this fluorescent dye is independent of membrane potential and thus can be used to measure organelle content independent of function (168,169). The mitochondrial content as a percentage of the cytoplasm was also estimated morphometrically for 10 different cells per transductant **(Table 6.1)**. The results also show a two-fold greater abundance of mitochondrial content in the shRNA#1 transductants and a slight increase in the shRNA#4 transductants compared to the controls confirming the increase in mitochondrial abundance estimated by flow cytometry. Thus, the loss of PRC is associated with a proliferation of structurally abnormal mitochondria.

Table 6.1. Mitochondrial content in lentiviral transductants.

Lentiviral transductant	MitoTracker Green FM fluorescence[a] (mean ± SEM)	Mitochondrial content[b] (% cytoplasmic area ± SEM)
Control shRNA	647 ± 125 (1.0)	16 ± 1 (1.0)
PRC shRNA#1	1360 ± 84 (2.1)	34 ± 1 (2.1)
PRC shRNA#4	855 ± 58 (1.3)	19 ± 2 (1.3)

[a] Mean fluorescence intensity of MitoTracker Green FM as quantified by flow cytometry is the average of at least 3 separate determinations ± s.e.m.

[b] Mitochondrial content expressed as a percentage of cytoplasmic area ± s.e.m is derived from morphometrical analysis of 10 digital electron micrographs for each transductant such as those shown in **Figure 6.9**.

To investigate global changes in gene expression that result from suppressing PRC, we compared mRNA patterns of both PRC shRNA#1 and PRC shRNA#4 transductants to control shRNA cells by microarray analysis using an Illumina Whole-Genome Sentrix Human-6 v2 Expression BeadChip. This gene chip contains over 48000 probes derived from human genes and expressed sequence tags in the National Center for Biotechnology Information (NCBI) Reference Sequence (RefSeq), release 17, and UniGene, build 188, databases.

Large differences were found in the expression profiles from shRNA#1 and control shRNA cell lines. In total, 1517 gene transcripts were significantly changed, using a relatively high stringency screen with FDR adjusted p-value <0.05 and fold change >1.5. Of these genes, 828 transcripts showed statistically significant down regulation **(see Appendix Table A.1 for a partial list and Figure 6.11A)**, and 689 transcripts showed statistically significant up regulation **(see Appendix Table A.2 for a partial list and Figure 6.11B)** in PRC shRNA#1 cells compared to control shRNA cells. In contrast, the expression profiles from shRNA#4 and control shRNA cells showed 338 gene transcripts that were significantly changed, using the same high stringency screen. Of these gene transcripts, 179 were significantly reduced **(Figure 6.11A)**, and 159 were significantly increased **(Figure 6.11B)** in PRC shRNA#4 cells compared to control shRNA cells. The smaller number of genes that are changed between shRNA#4 and control shRNA cells compared to shRNA#1 and control shRNA cells is consistent with the partial phenotype we see in shRNA#4 cells, due to residual levels of PRC protein. Interestingly, 152 (or 45%) out of the 338 mRNAs that were altered in shRNA#4 cells were similar to mRNAs that were changed in shRNA#1 cells **(Figure 6.11A, 6.11B, and Table A.3)**. Most of these gene transcripts, but not all, were altered to a lesser degree in shRNA#4 than in shRNA#1 cells, indicative of a dose-dependent alteration by PRC. The pattern of induction or repression was

identical for the majority of the overlapping gene transcripts. The large number of overlapping transcripts altered by the introduction of two hairpin RNAs targeting different regions of PRC and their apparent dose-dependent degree of induction or repression further support the conclusion that these genes are PRC targets and that the observed defects are PRC-specific.

Figure 6.11. Schematic overview of changes in gene expression profiles caused by PRC silencing as assessed by microarray analysis.

A. Venn diagram representing the number of significantly down regulated genes present in PRC shRNA#1 cells and PRC shRNA#4 cells compared to control shRNA cells (left panel). Genes in common between shRNA#1 and shRNA#4 cells are shown in the middle of the diagram. A pie chart depicting major functional categories of the overlapping down regulated genes is shown in the right panel.

B. Venn diagram representing the number of significantly up regulated genes present in PRC shRNA#1 cells and PRC shRNA#4 cells compared to control shRNA cells (left panel). Genes in common between shRNA#1 and shRNA#4 cells are shown in the middle of the diagram. A pie chart depicting major functional categories of the overlapping up regulated genes is shown in the right panel.

A

Down regulated differentiated genes

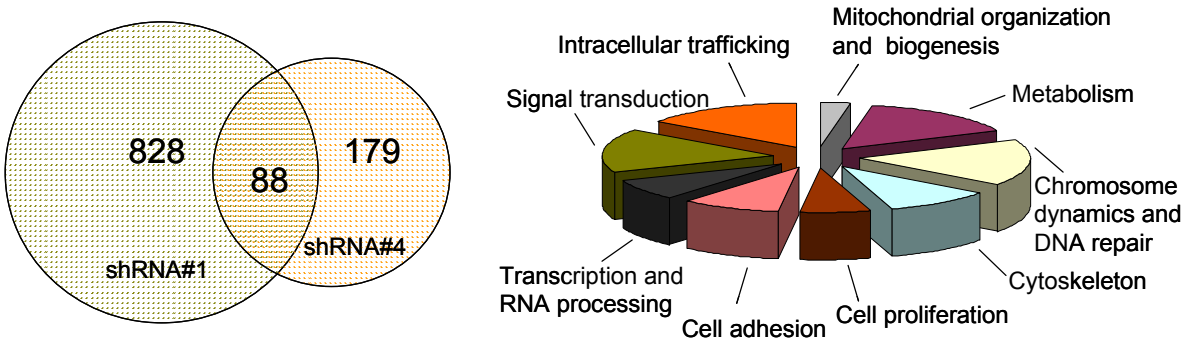

B

Up regulated differentiated genes

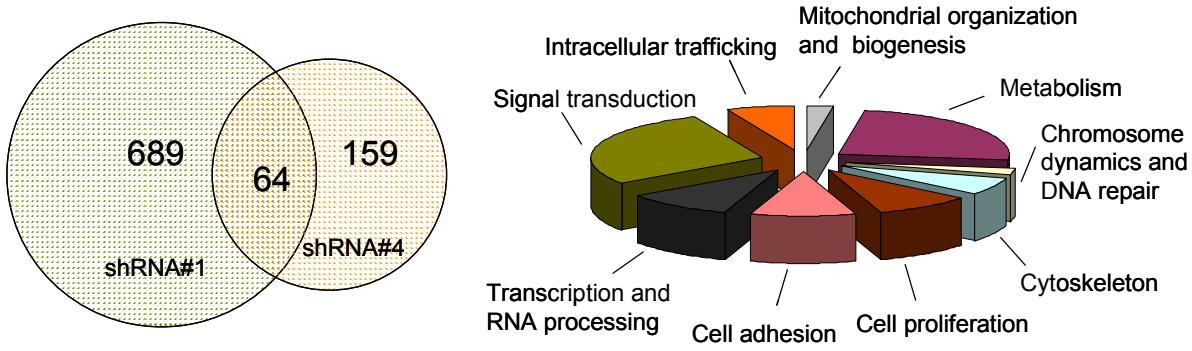

Notably, PRC expression was not identified as changed in shRNA#1 cells compared to control **(Table 6.2)**, despite a good hybridization signal of PRC mRNA to the array. On the other hand, PRC mRNA was down regulated 1.5-fold in PRC shRNA#4 cells compared to control. These changes in PRC expression do not correspond with the changes in PRC protein, which are quantitatively larger **(Figure 6.2)**. A BLAST search with the PRC probe sequence used on the array did not find any homologous genes, confirming the specificity of the hybridization signal. This further indicates that, in addition to their effects on mRNA degradation, both hairpins suppress PRC expression also on a translational level, with shRNA#1 the more potent one of the two.

We were interested in the possible altered expression of previously known PRC targets in the PRC shRNA#1 and #4 transductants, in particular the NRF target genes required for respiratory function shown in **Figure 6.6A**. Remarkably, these transcripts showed very small or no changes in response to PRC suppression by microarray analysis in either transductant **(Table 6.2)**. The changes in mRNA levels of these genes by real-time RT-PCR **(Figure 6.6A and Table 6.2)** were quantitatively larger than in the array. The low abundance of many of these factors combined with the limited sensitivity of microarray technology can explain this discrepancy. In particular, NRF-1 and PGC-1α were expressed at too low levels to be detected by microarray analysis in shRNA#1 cells, and PGC-1α and PGC-1β were not detected by microarray analysis in shRNA#4 cells. Transcript levels for CYCS, TFB1M and PPARGC1B were detectable but displayed very weak hybridization signals in shRNA#1 cells and therefore have to be interpreted with caution. It has to be noted that no mitochondrial genes were included on the gene chip.

Table 6.2. Effects of PRC silencing on the expression of mitochondrial transcriptional regulators and select respiratory chain genes.

Mean fold changes in gene expression in response to shRNA#1- and shRNA#4-mediated silencing of PRC relative to a negative control hairpin were assessed by Illumina microarray. The fold change in transcripts representing mitochondrial transcriptional regulators and select respiratory chain components is shown, with corresponding p-values and FDR adjusted p-values. A negative value indicates down regulation. An asterisk represents a low hybridization signal. *ND*, not determined.

Gene ID	Gene Symbol	Gene Description	PRC shRNA #1 fold change	PRC shRNA#1 p-value	PRC shRNA#1 FDR p-value	PRC shRNA #1 Real time PCR fold change	PRC shRNA #4 fold change	PRC shRNA#4 p-value	PRC shRNA#4 FDR p-value
23082	PPRC1	Peroxisome proliferator-activated receptor gamma, coactivator-related 1	-1.02	0.88991	0.93798	-1.85	-1.51	6.55E-06	0.0011993
10891	PPARGC1A	Peroxisome proliferator-activated receptor gamma, coactivator 1 alpha	ND	ND	ND	ND	ND	ND	ND
133522	PPARGC1B	Peroxisome proliferator-activated receptor gamma, coactivator 1 beta	1.07*	0.18438	0.33545	ND	ND	ND	ND
4899	NRF-1	Nuclear respiratory factor 1	ND	ND	ND	-2.70	-1.03	0.37402	0.6471
2551	GABPA	GA binding protein transcription factor, alpha subunit 60kDa	1.26	0.023944	0.077324	-1.11	1.04	0.51728	0.75437
2553	GABPB2	GA binding protein transcription factor, beta	-1.13	0.063145	0.15747	-1.72	-1.24	0.01484	0.095811
1385	CREB1	cAMP responsive element binding protein 1	1.07	0.24241	0.40563	-1.04	-1.13	0.017913	0.10785
7019	TFAM	Transcription factor A, mitochondrial	1.13	0.28599	0.45482	-1.28	-1.00	0.96178	0.98588
51106	TFB1M	Transcription factor B1, mitochondrial	1.08*	0.56834	0.71671	-1.20	1.00	0.98567	0.99486
64216	TFB2M	Transcription factor B2, mitochondrial	-1.40	0.013628	0.051344	-1.64	-1.08	0.26292	0.53999
54205	CYCS	Cytochrome c, somatic	1.05*	0.5636	0.713	-1.67	-1.05	0.21816	0.49072
1327	COX4I1	Cytochrome c oxidase, subunit IV isoform 1	-1.10	0.11549	0.24207	-1.43	-1.05	0.28854	0.56831
6390	SDHB	Succinate dehydrogenase complex, subunit B, iron sulfur (Ip)	-1.14	0.032035	0.095926	-1.59	-1.16	0.027985	0.14437

7385	UQCRC2	Ubiquinol-cytochrome c reductase core protein II	1.44	0.0009946	0.008181	-1.02	-1.01	0.83987	0.93567
498	ATP5A1	ATP synthase, H+ transporting, mitochondrial F1 complex, alpha subunit 1, cardiac muscle	-1.05	0.37668	0.54875	-1.14	-1.17	0.06678	0.24809

Because of the severe mitochondrial phenotype in PRC shRNA#1 cells, we decided to investigate the expression of mitochondrion-related genes that were significantly changed in PRC shRNA#1 cells by microarray analysis. We did observe alterations in many mitochondrion-related gene transcripts in PRC shRNA#1 cells compared to PRC shRNA#4 cells **(Figure 6.12A and Table 6.3)**. In particular, several respiratory subunit mRNAs (SDHA, ATP5J2, NDUFA7) were down regulated about 2-fold in PRC shRNA#1 cells. Several COX assembly factor mRNAs were also reduced, suggesting perhaps a defect in COX assembly. Furthermore, expression of the mitochondrial translocases TIMM23, TOMM7, TOMM20, TOMM22 and TOMM70A, and of the mitochondrial processing peptidase beta subunit, PMPCB, was changed, likely affecting import of proteins into mitochondria. In addition, expression of some mitochondrial ribosomal proteins, mitochondrial tRNA synthetases, and the translation elongation factor TSFM was altered in the PRC shRNA#1 cells, likely resulting in defects in mitochondrial translation. However, currently, these changes in gene expression in PRC shRNA#1 cells cannot explain the mitochondrial phenotype caused by complete PRC silencing. It is likely that not a single gene is responsible, but that instead small changes in expression of many genes contribute to the phenotype. Interestingly, a relatively small percentage (22%) of these genes were identified as changed in PRC shRNA#4 cells**(Figure 6.12A and Table 6.3)**, consistent with the much weaker respiratory phenotype in these cells, due to residual levels of PRC.

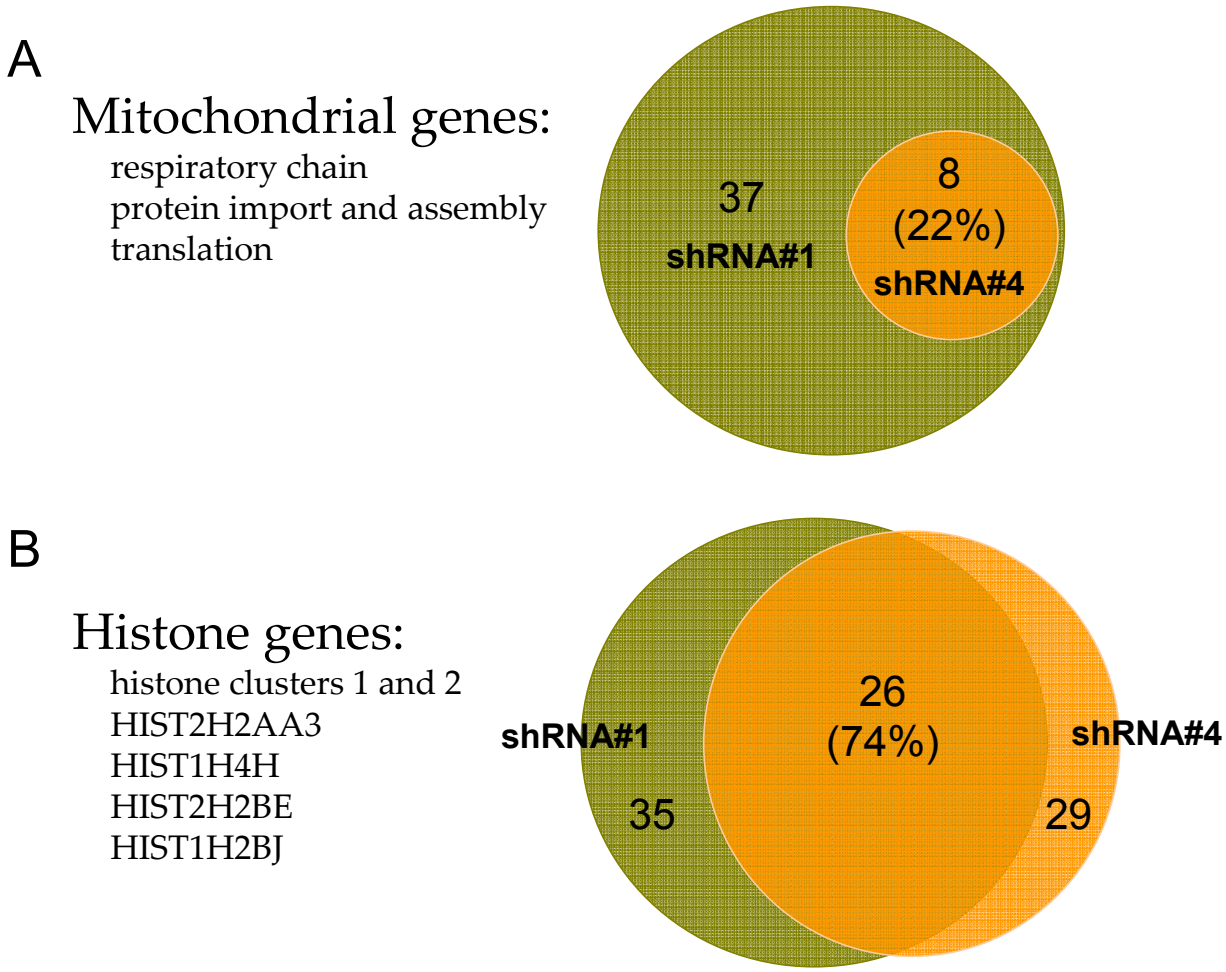

Figure 6.12. Venn diagrams of mitochondrial and histone genes affected by PRC silencing.

A. Venn diagram representing the number of significantly down regulated mitochondrial genes present in PRC shRNA#1 cells and PRC shRNA#4 cells compared to control shRNA cells.

B. Venn diagram representing the number of significantly down regulated histone genes present in PRC shRNA#1 cells and PRC shRNA#4 cells compared to control shRNA cells.

The number and percentage of genes in common between shRNA#1 and shRNA#4 cells are shown in each diagram.

Table 6.3. Effects of PRC silencing on the expression of mitochondrion-related genes.

Mean fold changes in gene expression in response to shRNA#1- and shRNA#4-mediated silencing of PRC relative to a negative control hairpin were assessed by Illumina microarray. Gene transcripts involved in mitochondrial respiratory chain, mitochondrial protein import and assembly, and mitochondrial translation that were significantly down regulated in PRC shRNA#1 or PRC shRNA#4 cells are shown, with corresponding p-values and FDR adjusted p-values. A negative value indicates down regulation.

Gene ID	Gene symbol	Gene description	PRC shRNA #1 fold change	PRC shRNA#1 p-value	PRC shRNA#1 FDR p-value	PRC shRNA #4 fold change	PRC shRNA#4 p-value	PRC shRNA#4 FDR p-value
Mitochondrial respiratory chain								
4726	NDUFS6	NADH dehydrogenase (ubiquinone) Fe-S protein 6	-1.29	0.002706	0.016335			
374291	NDUFS7	NADH dehydrogenase (ubiquinone) Fe-S protein 7	-1.38	0.003596	0.019868			
51103	NDUFAF1	NADH dehydrogenase (ubiquinone) 1 alpha subcomplex	-1.40	0.001847	0.012582			
4729	NDUFV2	NADH dehydrogenase (ubiquinone) flavoprotein 2	-1.51	0.00038	0.004465	-1.25	0.000811	0.016395
4696	NDUFA3	NADH dehydrogenase (ubiquinone) 1 alpha subcomplex	-1.64	0.000118	0.002096			
4701	NDUFA7	NADH dehydrogenase (ubiquinone) 1 alpha subcomplex, 7	-1.76	7.99E-06	0.000487			
6389	SDHA	succinate dehydrogenase complex, subunit A	-2.45	3.60E-05	0.001046	-1.31	0.000404	0.011107
517	ATP5G2	ATP synthase, H+ transporting, mitochondrial F0 C2	-1.43	0.000732	0.006772			
9551	ATP5J2	ATP synthase, H+ transporting, mitochondrial F0 F2	-2.01	4.40E-06	0.000383			
2110	ETFDH	electron-transferring-flavoprotein dehydrogenase	-1.48	0.00396	0.021286			
80777	CYB5B	cytochrome b5 type B (outer mitochondrial membrane)	-1.38	0.000225	0.003203			
Mitochondrial protein import and assembly								
1352	COX10	COX10 homolog, cytochrome c oxidase assembly protein	-1.35	0.002552	0.015709	-1.30	0.000185	0.00738
1355	COX15	COX15 homolog, cytochrome c oxidase assembly protein	-1.19	0.009606	0.039987			
10063	COX17	COX17 cytochrome c oxidase assembly homolog	-1.97	0.001293	0.0098	-1.59	0.000387	0.010877
90639	COX19	COX19 cytochrome c oxidase assembly homolog	-1.59	0.000136	0.002303			

Gene ID	Gene symbol	Gene description	PRC shRNA #1 fold change	PRC shRNA#1 p-value	PRC shRNA#1 FDR p-value	PRC shRNA #4 fold change	PRC shRNA#4 p-value	PRC shRNA#4 FDR p-value
55245	UQCC	ubiquinol-cytochrome c reductase complex chaperone	-1.57	0.002444	0.015184			
5188	PET112L	PET112-like (yeast)	-2.17	2.26E-06	0.000279			
6341	SCO1	SCO cytochrome oxidase deficient homolog 1 (yeast)	-1.67	3.18E-05	0.000977	-1.45	2.35E-05	0.002574
10431	TIMM23	translocase of inner mitochondrial membrane 23	-1.34	0.001215	0.009362	-1.21	0.001881	0.026692
54543	TOMM7	translocase of outer mitochondrial membrane 7	-1.25	0.010211	0.04176			
9804	TOMM20	translocase of outer mitochondrial membrane 20	-1.57	2.61E-05	0.000876			
56993	TOMM22	translocase of outer mitochondrial membrane 22	-1.84	0.000514	0.005437	-1.59	2.49E-05	0.002707
9868	TOMM70A	translocase of outer mitochondrial membrane 70	-1.48	0.000497	0.005328			
9512	PMPCB	peptidase (mitochondrial processing) beta	-2.16	1.72E-05	0.000711			
Mitochondrial translation								
55052	MRPL20	mitochondrial ribosomal protein L20	-1.50	0.000102	0.001944			
10573	MRPL28	mitochondrial ribosomal protein L28	-1.45	0.000287	0.003677			
9553	MRPL33	mitochondrial ribosomal protein L33	-1.94	4.57E-05	0.001236	-1.19	0.003628	0.039322
64979	MRPL36	mitochondrial ribosomal protein L36	-1.64	4.33E-05	0.001192			
64976	MRPL40	mitochondrial ribosomal protein L40	-1.45	0.000907	0.007705			
116540	MRPL53	mitochondrial ribosomal protein L53	-1.83	9.28E-06	0.00053			
128308	MRPL55	mitochondrial ribosomal protein L55	-1.79	4.95E-05	0.001296			
64951	MRPS24	mitochondrial ribosomal protein S24	-1.56	0.000769	0.006996			
65993	MRPS34	mitochondrial ribosomal protein S34	-1.30	0.008541	0.036955			
55157	DARS2	aspartyl-tRNA synthetase 2, mitochondrial	-2.02	5.48E-05	0.00139			
79587	CARS2	cysteinyl-tRNA synthetase 2, mitochondrial (putative)	-1.37	0.000183	0.002815			
55699	IARS2	isoleucyl-tRNA synthetase 2, mitochondrial	-1.66	7.29E-05	0.001612			

Gene ID	Gene symbol	Gene description	PRC shRNA #1 fold change	PRC shRNA#1 p-value	PRC shRNA#1 FDR p-value	PRC shRNA #4 fold change	PRC shRNA#4 p-value	PRC shRNA#4 FDR p-value
10102	TSFM	Ts translation elongation factor, mitochondrial	-1.72	8.22E-05	0.001732			

A large number of genes previously not reported to be regulated by PRC were identified in the microarray analysis. A major category of genes significantly decreased in both PRC shRNA#1 and #4 transductants included genes from histone clusters 1 and 2 (HIST2H2AA3, HIST1H4H, HIST1H4C, HIST1H2AC among many others) **(Figure 6.12 and Table 6.4)**. Notably, in both transductants these gene transcripts represented mRNAs that were most robustly down regulated. Here also, most of these gene transcripts, but not all, were altered to a lesser degree in shRNA#4 than in shRNA#1 cells, indicative of a dose-dependent alteration by PRC. In contrast to the mitochondrion-related transcipts, the number of overlapping histone gene products between shRNA#1 and shRNA#4 cells represents a large percentage (74%) **(Figure 6.12 and Table 6.4)**. Histone gene transcription is tightly coupled to cell cycle progression and DNA synthesis (170). The decrease in histone mRNAs seen in shRNA#1 and shRNA#4 cells is therefore consistent with the fact that both transductants display a reduced growth rate on glucose and blockage in G_1/S transition.

For a complete list of overlapping differentiated genes between PRC shRNA#1 and #4 cells, see **Appendix Table A3 and A4**. In addition to the above mentioned mitochondrial and histone genes, this list includes examples of genes with diverse roles in cell proliferation, signal transduction, cell-cell and cell-matrix junctions, cytoskeleton, cell metabolism, transcription and RNA processing, and intracellular trafficking, suggesting that PRC might serve a pleiotropic function **(Figure 6.11A and B; right panels)**.

Table 6.4. Effects of PRC silencing on the expression of histone genes.

Mean fold changes in gene expression in response to shRNA#1- and shRNA#4-mediated silencing of PRC relative to a negative control hairpin were assessed by Illumina microarray. Histone gene transcripts that were significantly down regulated in PRC shRNA#1 or PRC shRNA#4 cells are shown, with corresponding p-values and FDR adjusted p-values. A negative value indicates down regulation.

Gene ID	Gene Symbol	Gene Description	PRC shRNA #1 fold change	PRC shRNA#1 p-value	PRC shRNA#1 FDR p-value	PRC shRNA #4 fold change	PRC shRNA#4 p-value	PRC shRNA#4 FDR p-value
8337	HIST2H2AA3	Histone cluster 2, H2aa3	-45.58	5.02E-10	2.87E-06	-2.88	2.90E-07	0.00034694
8365	HIST1H4H	Histone cluster 1, H4h	-45.53	5.83E-11	8.79E-07	-3.92	9.96E-08	0.00017878
8364	HIST1H4C	histone cluster 1, H4c	-26.20	1.94E-07	5.52E-05			
8334	HIST1H2AC	Histone cluster 1, H2ac	-26.11	1.25E-09	3.46E-06	-3.21	2.96E-06	0.00088648
8349	HIST2H2BE	Histone cluster 2, H2be	-18.95	5.32E-08	2.36E-05	-3.15	3.24E-05	0.0029367
3006	HIST1H1C	histone cluster 1, H1c	-15.45	8.33E-09	1.07E-05	-1.87	2.28E-05	0.0025365
8970	HIST1H2BJ	Histone cluster 1, H2bj	-14.28	2.57E-09	5.53E-06	-3.35	1.90E-06	0.00083519
8370	HIST2H4A	histone cluster 2, H4a	-12.95	6.55E-07	0.00012335			
54145	H2BFS	H2B histone family, member S	-12.69	1.38E-09	3.46E-06			
8338	HIST2H2AC	Histone cluster 2, H2ac	-11.46	1.69E-08	1.21E-05	-2.37	4.32E-06	0.0010148
3017	HIST1H2BD	histone cluster 1, H2bd	-9.90	9.20E-09	1.07E-05	-1.65	0.00042943	0.011456
8344	HIST1H2BE	Histone cluster 1, H2be	-8.63	1.58E-07	4.87E-05	-2.17	3.62E-05	0.003034
8347	HIST1H2BC	Histone cluster 1, H2bc	-8.12	2.83E-07	6.65E-05	-2.25	7.70E-06	0.0013675
55766	H2AFJ	H2A histone family, member J	-7.67	1.29E-07	4.14E-05	-2.37	3.71E-06	0.00090135
8367	HIST1H4E	Histone cluster 1, H4e	-5.79	1.07E-08	1.12E-05	-2.38	8.76E-07	0.00054175
8351	HIST1H3D	histone cluster 1, H3d	-4.40	9.51E-07	0.00016214	-1.86	5.36E-07	0.00043713
8362	HIST1H4K	histone cluster 1, H4k	-3.01	6.70E-07	0.00012463	-1.21	0.00034285	0.010235
8357	HIST1H3H	histone cluster 1, H3h	-2.68	3.56E-06	0.00035062	-1.73	8.36E-05	0.0047475
8353	HIST1H3E	histone cluster 1, H3e	-2.26	3.44E-05	0.0010259	-1.36	4.25E-05	0.0033041
8969	HIST1H2AG	histone cluster 1, H2ag	-2.12	4.03E-05	0.0011338	-1.43	0.00038224	0.010783
317772	HIST2H2AB	histone cluster 2, H2ab	-2.01	6.60E-06	0.00045989	-1.43	3.47E-05	0.0030111
85236	HIST1H2BK	histone cluster 1, H2bk	-1.99	2.28E-05	0.00081395	-1.24	0.00021136	0.0078143
8350	HIST1H3A	histone cluster 1, H3a	-1.79	9.51E-06	0.00053246	-1.20	0.0036222	0.039322
3013	HIST1H2AD	histone cluster 1, H2ad	-1.77	6.62E-05	0.0015176	-1.48	0.00071241	0.015363
8335	HIST1H2AB	histone cluster 1, H2ab	-1.75	4.25E-06	0.00037642			
8343	HIST1H2BF	histone cluster 1, H2bf	-1.73	5.98E-05	0.001454	-1.18	0.0037099	0.039739
8968	HIST1H3F	histone cluster 1, H3f	-1.57	0.0003895	0.0045267	-1.31	9.19E-05	0.0049817
9555	H2AFY	H2A histone family, member Y	-1.41	0.0001946	0.0029216			
126961	HIST2H3C	histone cluster 2, H3c	-1.40	0.0006703	0.0064058	-1.26	0.0007424	0.01572
8366	HIST1H4B	histone cluster 1, H4b	-1.34	0.0003929	0.004563	-1.16	0.0043746	0.044095
8358	HIST1H3B	histone cluster 1, H3b	-1.33	0.0012431	0.0095236			

Gene ID	Gene Symbol	Gene Description	PRC shRNA #1 fold change	PRC shRNA#1 p-value	PRC shRNA#1 FDR p-value	PRC shRNA #4 fold change	PRC shRNA#4 p-value	PRC shRNA#4 FDR p-value
8345	HIST1H2BH	histone cluster 1, H2bh	-1.28	0.0008536	0.0074213			
8341	HIST1H2BN	histone cluster 1, H2bn	-1.26	0.0030143	0.017517			
8339	HIST1H2BG	histone cluster 1, H2bg	-1.23	0.0020863	0.013609	-1.15	0.0041838	0.042985
8360	HIST1H4D	histone cluster 1, H4d	-1.23	0.0029745	0.017413			
554313	HIST2H4B	histone cluster 2, H4b				-2.60	4.65E-06	0.0010422
3024	HIST1H1A	histone cluster 1, H1a				-1.34	0.001203	0.020517
3015	H2AFZ	H2A histone family, member Z				-1.22	0.00044302	0.011621

To validate the microarray results, we independently assessed the expression of a selection of genes that were changed quite dramatically in the shRNA#1 array by real time RT-PCR analysis **(Figure 6.13A and B)**. Four genes were tested that were changed in shRNA#1 cells compared to control shRNA cells (LUM, RAC2, HCFC1R1 and ANXA10) but not in shRNA#4 cells. We also validated selected overlapping genes between shRNA#1 and shRNA#4 cells that were significantly up **(Figure 6.13A)** or down regulated **(Figure 6.13B)** compared to control shRNA cells in the microarray. Significant induction or reduction was confirmed for all of the transcripts, although for some transcripts the degree of regulation was different than indicated by the microarray as shown in the accompanying inset **(Figure 6.13C)**.

Figure 6.13. Validation of the expression of selected genes by real-time RT-PCR analysis.

A. The expression of a selection of genes that were found to be significantly up regulated by microarray analysis was verified in PRC shRNA#1, PRC shRNA#4 and control shRNA cells by real-time RT-PCR.

B. The expression of a selection of genes that were found to be significantly down regulated by microarray analysis was verified in PRC shRNA#1, PRC shRNA#4 and control shRNA cells by real-time RT-PCR.

Relative steady-state mRNA levels were normalized to 18S rRNA as an internal control and expressed relative to the control shRNA level, which was assigned a value of 1. Values represent the averages ± standard deviation for three separate determinations.

C. Side-by-side comparison of the fold changes in gene expression by microarray or real time RT-PCR of the genes validated in *A*. and *B*.

A

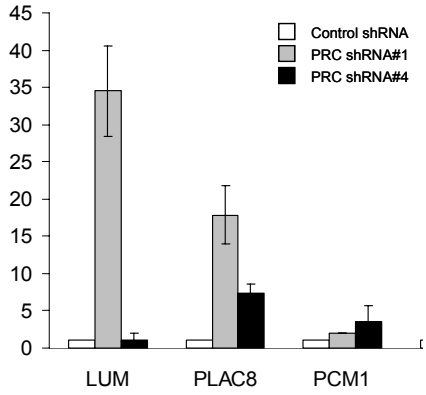

B

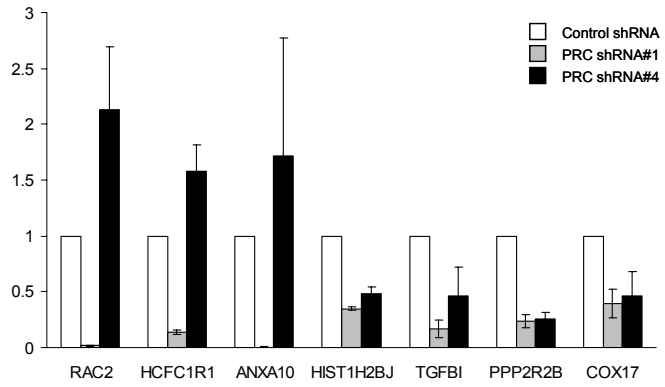

C

Gene Symbol	Gene description	PRC shRNA#1 Array Fold Change	PRC shRNA#1 PCR Fold Change	PRC shRNA#4 Array Fold Change	PRC shRNA#4 PCR Fold Change
LUM	Lumican	44.17	34.51	-1.13	1.11
PLAC8	Placenta-specific 8	17.78	17.89	5.74	6.07
PCM1	Pericentriolar material 1	2.67	1.99	2.49	6.01
PSD3	Pleckstrin and Sec7 domain containing 3	2.59	1.96	2.45	2.92
RAC2	Ras-related C3 botulinum toxin substrate 2	-13.08	-57.83	1.29	2.13
HCFC1R1	Host cell factor regulator	-7.57	-7.20	-1.09	1.58
ANXA10	Annexin A10	-152.65	-279.70	1.24	1.72
HIST1H2BJ	Histone cluster 1, H2bj	-14.28	-2.78	-3.35	-1.96
TGFBI	transforming growth factor, beta-induced, 68kDa	-6.25	-6.25	-3.09	-1.69
PPP2R2B	Protein phosphatase 2 (formerly 2A), regulatory subunit B, beta isoform	-3.06	-5.88	-2.06	-3.70
COX17	COX17 cytochrome c oxidase assembly homolog	-1.97	-2.27	-1.59	-2.17

DISCUSSION

Transcriptional expression of the respiratory chain in mammalian systems relies upon the interplay of nuclear transcription factors and the PGC-1 family of regulated coactivators (40,105,124). Ubiquitous transcription factors, exemplified by NRF-1, NRF-2(GABP) and ERRα, target many nuclear genes required for the direct expression of the respiratory complexes as well as many others that play indirect roles in assembly, protein import, heme biosynthesis and mtDNA maintenance. The PGC-1 coactivators are thought to impose integrative regulatory control on the pathway through their induction by environmental signals and their *trans*-activation of respiratory genes through the NRFs and other transcription factors. In this manner they function as positive regulators of respiratory chain expression and mitochondrial biogenesis. PRC is a growth-regulated member of the PGC-1 family (89,99). It has the characteristics of an immediate early gene in that it is rapidly induced in response to serum stimulation of quiescent fibroblasts in the absence of *de novo* protein synthesis and down regulated upon serum withdrawal or contact inhibition. PRC is indistinguishable from the other PGC-1 family members in its ability to *trans*-activate NRF target genes (46) and to interact with host cell factor (166), a major chromatin component required for progression through G_1 of the cell cycle (171). This, along with its immediate early expression, suggests that PRC may be involved in the expression of the respiratory apparatus in response to growth regulatory signals. This possibility is supported by the observation that a PRC subfragment containing the NRF-1/CREB binding site inhibits respiratory growth when expressed in *trans* (99). Here, we show that complete PRC knockdown in a PRC shRNA-expressing lentiviral transductant is associated with a severe respiratory deficiency marked by slow growth on galactose, defective respiratory subunit expression and reduced respiratory enzyme levels and ATP production. These changes coincide

with reductions in the expression of mRNAs of encoding nuclear transcription factors (NRF-1, NRF-2β), mitochondrial transcription factors (Tfam, TFB2M), as well as nucleus- and mitochondrion-encoded respiratory subunits. Moreover, mitochondria in the PRC deficient cells were more abundant than in the control cells and displayed severe structural abnormalities. In addition to the respiratory phenotype, PRC silencing also resulted in an inhibition of the G_1/S transition of the cell cycle. Microarray analysis of transcripts from control cells and two independent cell lines lacking PRC showed major differences in gene expression and a large number of overlapping transcripts, in particular histone mRNAs, between the two independent transductants lacking PRC.

RNA interference-based methodology is sometimes associated with non-specific silencing effects and activation of the interferon response. In this case, we find no evidence for non-specific silencing. Complete PRC silencing is observed in shRNA#1 transductants infected with Ad-NmycPRC, which massively over produces PRC in the control shRNA transductant. Interestingly, PRC expressed from Ad-NmycPRC is still observed in shRNA#4 cells, but is much reduced compared to control level. Thus, shRNA#1 can eliminate PRC expression whether it occurs from genomic DNA or from a potent extrachromosomal transcriptional unit, while shRNA#4 partially reduces PRC expression in both scenarios. This efficient knockdown is PRC specific because PGC-1α is abundantly expressed in the shRNA#1 and shRNA#4 transductants upon infection with Ad-PGC-1α. In addition, the generation of two different shRNAs, shRNA#1 and shRNA#4, targeting different regions of the PRC mRNA were used to confirm PRC specificity. Both the PRC shRNA#1 transductant, showing complete loss of PRC protein, and the shRNA#4 transductant, expressing reduced levels of PRC, display identical glucose growth deficiencies. This argues for a PRC-specific growth defect. This is further supported by the

inhibition of cell cycle progression from G_1 to S phase in both transductants. Even though the shRNA#4 transductant had only modestly reduced growth on galactose and no detectable loss of respiratory subunit expression or ATP production, it did have changes in mitochondrial content and morphology that were intermediate between the control and shRNA#1 transductants. Thus, although reduction of PRC to 15 percent of the control level can impair growth and affect mitochondrial profiles, it is sufficient to maintain respiratory function. The phenotypic overlap between the two transductant lines argues that the effects in each are mediated by PRC silencing. Furthermore, the large number of overlapping transcripts that were significantly changed by the introduction of two hairpin RNAs targeting different regions of PRC and their apparent dose-dependent degree of induction or repression as assessed by microarray analysis support the conclusion that specific silencing of PRC is responsible for the observed changes in gene expression. Finally, the respiratory phenotype does not result from activation of the interferon response. There is no global up regulation of interferon-stimulated genes (172,173), such as OAS1, OAS2, OAS3, STAT1 or IRF3 in U2OS cells stably expressing PRC shRNA#1 or shRNA#4 (as demonstrated by the microarray-not shown). Therefore, the observed changes in mitochondrial function and morphology, and in cell growth result from reduced PRC expression and not from non-specific silencing or activation of the interferon response.

In several instances the reductions in mRNA expression seen in the shRNA#1 cells differ from those of their respective proteins. Notably, PRC protein is undetectable in the shRNA#1 transductant whereas PRC mRNA is reduced by half in real-time RT-PCR analysis and unchanged in the microarray. This suggests that PRC shRNA#1 is inhibitory at both the transcriptional and post-transcriptional level, most probably through translational inhibition. Translational repression is most commonly observed with short interfering RNAs having

imperfect complementarity with their target sequences (174,175). However, a siRNA with perfect base complementarity to its target in the geminin gene also had a greater inhibitory effect on geminin protein expression relative to its mRNA, suggesting that gene silencing in this case occurs predominantly at the translational level (176). This is similar to what we see here with PRC shRNA#1, which has perfect sequence complementarity to a single target site in the PRC coding region. It is also noteworthy that PRC mRNA has a relatively rapid decay rate with a half-life of approximately two hours (99). Messenger RNAs that turn over rapidly may be more susceptible to shRNA-mediated translational repression (177).

The reductions in mitochondrial respiratory subunit expression are also much more dramatic at the protein level. In the case of UQCRC2 encoding core protein 2 of complex III, the dramatic down regulation of the protein occurs in the absence of any mRNA reduction. These discrepancies suggest that PRC may affect the expression of these genes through mechanisms not restricted to transcriptional inhibition. For example, PRC may control NRF target genes involved in mitochondrial translation or the import or assembly of respiratory subunits. In that respect, the microarray results show changes in the expression of genes involved in mitochondrial import and assembly and the mitochondrial translation machinery. It remains to be determined whether the respiratory defect results from relatively modest reductions in the expression of many genes or from a large reduction in a few genes or even a single gene.

The PGC-1 coactivators are thought to function as positive regulators of mitochondrial biogenesis. This conclusion comes largely from gain-of-function experiments where PGC-1α or β are ectopically expressed in cultured cells or transgenic mice. Under these conditions dramatic increases in respiratory gene expression, energy production, mitochondrial volume and cristae density have been observed (54,55,79). The respiratory chain deficiencies observed here upon

loss of PRC protein are consistent with a role for PRC as a positive regulator of respiratory chain expression. The severity of the defect contrasts with the relatively subtle changes in respiratory function observed in mice deficient in either PGC-1α (60,61) or PGC-1β (85,86). This is likely explained by the fact that U2OS cells have no detectable PGC-1α and thus are possibly more dependent on PRC to maintain basal respiratory function. Moreover, most of the available evidence points to PGC-1α and β as mediators of differentiation-induced mitochondrial content. For example, shRNA-mediated silencing of PGC-1β in a preadipocyte cell line derived from PGC-1α null mice led to a failure to establish and maintain differentiated levels of mitochondrial density in mature brown adipocytes (87). In the absence of both coactivators, mitochondrial content was maintained at the preadipocyte level. Loss of either coactivator alone had a relatively modest effect but together they provide complementary functions in maintaining the differentiated level. Mice with ablations of both PGC-1α and PGC-1β (88) exhibit normal early fetal formation of mitochondria, but show an arrest in perinatal mitochondrial biogenesis in the heart and brown adipose tissue and die shortly after birth as a result of heart failure. Possibly, PRC is responsible for the early maturation of mitochondria. In PGC-1β-deficient mice there is compensation for the loss of PGC-1β by PGC-1α (88). Here, we find no evidence of an increase in PGC-1α mRNA or protein levels in the cells where PRC is silenced, suggesting that PGC-1α cannot compensate for the loss of PRC in this system. Thus, synergies among members of the coactivator family may set the upper and lower limits for mitochondrial content in a given physiological context.

Gain-of-function experiments performed with PGC-1α and β suggest a tight coordination between expression of the respiratory chain and the biogenesis of the organelle. Over expression of either coactivator increases the expression of respiratory subunits concomitant with organelle

biogenesis (54,55,79). Thus, it is surprising that shRNA-mediated PRC knockdown results in an increase in mitochondrial content as measured by uptake of MitoTracker Green FM and by morphometric analysis of electron micrographs. This indicates that organelle biogenesis is not positively linked to the PRC-dependent expression of the respiratory chain in this system. It is notable that the elevation in mitochondrial density is associated with a severe morphological defect consisting of markedly disrupted cristae structure, blebbing of the inner mitochondrial membrane and reduced electron density within the matrix. This increase in structurally defective mitochondria may be a compensatory response to the respiratory chain deficiency mediated by the loss of PRC. One possibility, depicted in **Figure 6.14A**, is that organelle biogenesis increases in response to the respiratory defect mediated by the loss of PRC by a pathway that is PRC independent. In this scenario, anything that interferes with mitochondrial respiratory function might be expected to lead to increased organelle biogenesis. Although the expression of some respiratory chain genes is altered in response to various respiratory inhibitors, there is little evidence for a retrograde pathway mediating the up regulation of mitochondrial biogenesis in cultured cells (178,179). Alternatively, as shown in **Figure 6.14B**, PRC may regulate both the respiratory chain and an unidentified regulator(s) that modulates organelle biogenesis. Loss of PRC may lead to the down regulation of this putative factor and the consequent increase in mitochondrial content. In this case, both the respiratory chain and organelle biogenesis are under the control of PRC.

Figure 6.14. Alternative models depicting the association of respiratory chain expression with mitochondrial biogenesis.

A. Silencing of PRC results in the down regulation of respiratory chain expression and function. This leads to an increase in organelle content as a PRC-independent compensatory response to the loss of respiratory function. In this case, PRC regulates mitochondrial biogenesis indirectly through its effects on the respiratory apparatus.

B. Silencing of PRC results in the down regulation of both the respiratory chain and unidentified target(s) that control organelle content. Thus, the response to the loss of respiratory function occurs through a PRC-dependent pathway. In this case, PRC exerts direct control over respiratory chain expression and the factors that regulate organelle biogenesis.

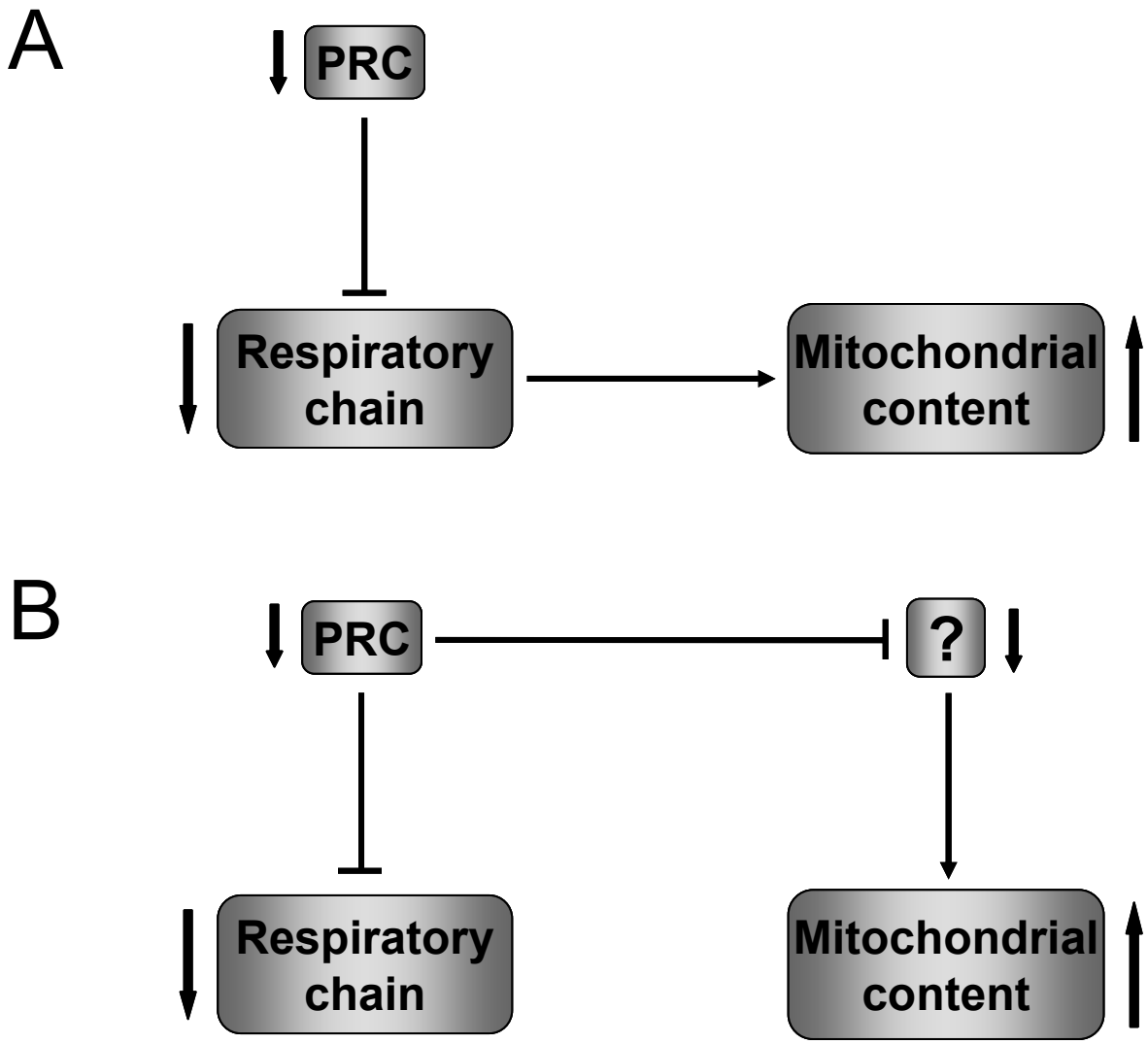
A
PRC
Respiratory chain
Mitochondrial content
B
PRC
?
Respiratory chain
Mitochondrial content

The absence of PGC-1α in these cells may also be a contributing factor. PGC-1α has recently been implicated in the ability of cells to recover from reduced ATP levels that were depleted because of treatment with a chemical uncoupler (180). Interestingly, increases in abnormal mitochondria are also observed in the muscle fibers of patients with certain mitochondrial myopathies leading to ragged red fibers as a diagnostic indicator. These are thought to arise as a compensatory response to respiratory chain deficiencies caused by mutation of mitochondrial DNA (181). In these patients extremely high levels of mutant mtDNA accumulate in the muscle fiber. An accumulation of abnormal mitochondria associated with reduced levels of mitochondrial transcripts, numerous ragged-red fibers with COX deficiency, reduced respiratory enzyme activities and decreased mitochondrial ATP synthesis rate is also seen in mice with skeletal muscle-specific disruption of Tfam expression (182). This is associated with progressively reduced levels of mtDNA in skeletal muscle of these mice. A similar increase in abnormal mitochondria with normal mtDNA copy number but increased mtDNA transcripts is seen in heart-specific mTERF3 knockout mice (28). These cases are in contrast to the current findings where mtDNA levels normalized to 18S rDNA remain the same in the PRC knockdown and the control, despite a reduction in mitochondrial transcript levels and respiratory subunits. It is possible that the mtDNA replication machinery cannot respond to the respiratory defect because of the absence of PRC or PGC-1α.

Interestingly, the microarray analysis of PRC shRNA#1 and PRC shRNA#4 versus control shRNA transcripts revealed dramatic down regulation of mRNAs of the histone gene clusters 1 and 2, encoding members of the histone families H1, H2A, H2B, H3 and H4, in shRNA#1 and shRNA#4 cells. The production of histones is closely linked to DNA synthesis. Control of histone protein biosynthesis occurs exclusively through control of histone gene

expression (reviewed in (170)). The number of histone transcripts increase when cells enter S phase, and at the end of S phase they are rapidly degraded (183). Repression of histone gene expression results in decreased DNA replication (184), and inhibition of DNA replication in turn causes degradation of histone mRNAs (185).

Perhaps this might explain the dramatic reductions in histone mRNA levels in PRC shRNA#1 and shRNA#4 cells. When entry into S phase is blocked by the lack of PRC, there is a decrease in DNA synthesis, which in turn might cause the histone transcript levels to drop. Or, conversely, the lack of PRC might negatively affect histone gene transcription, which then causes a decrease in DNA replication.

The mechanism by which PRC silencing disrupts cell cycle dynamics is not well understood. Perhaps it affects cell cycle regulators that control the progression from G_1 to S phase. Or it interferes directly with transcription of the histone genes. Notable genes positively associated with cell proliferation that were significantly decreased in the gene chip expression profiles of both transductants included transforming growth factor, beta-induced (TGFBI), protein phosphatase 2 (formerly 2A), regulatory subunit B, beta isoform (PPP2R2B), aurora kinase B (AURKB), McKusick-Kaufman syndrome (MKKS), calcium/calmodulin-dependent protein kinase I (CAMK1), fidgetin-like 1 (FIGNL1), and apolipoprotein B mRNA editing enzyme, catalytic polypeptide-like 3B (APOBEC3). We also detected increased expression of inhibitors of the cell cycle common between shRNA#1 and #4 in the microarray, in particular CCR4-NOT transcription complex, subunit 7 (CNOT7), v-abl Abelson murine leukemia viral oncogene homolog 1 (ABL1), TIMP metallopeptidase inhibitor 2 (TIMP2), signal-regulatory protein alpha (SIRPA), and family with sequence similarity 57, member A (FAM57A). Transcription of the numerous histone genes is coordinately regulated by various factors,

including NPAT, YY1 and HIRA (reviewed in (170)). It is not known how these factors collectively regulate histone gene expression during the cell cycle. Much of the histone mRNA regulation also occurs post-transcriptionally by the interaction of stem-loop binding proteins, SLBP, with the 3' end of histone mRNAs (170). It is possible that PRC acts as a coactivator for these transcription factors to stimulate expression of histone genes.

The microarray results provide us with a platform to study the mechanism of aberrant mitochondrial proliferation caused by PRC silencing and to unravel the mechanism by which PRC acts as a modulator of cell proliferation. In addition, it allows the identification of novel target genes responding to PRC deficiency. As stated above, many more transcripts were significantly altered in PRC shRNA#1 cells than in PRC shRNA#4 cells compared to control shRNA cells **(Figure 6.11A and B)**, consistent with the degree of PRC silencing in either transductant. We hypothesize that the common genes between shRNA#1 and #4 are the most direct targets of PRC, and therefore are more sensitive to even partial knockdown of PRC, whereas the others are more indirectly altered by PRC suppression. A closer look at the differentiated genes between control cells and cells lacking PRC suggests PRC functions as a pleiotropic protein. This complicates analyzing the significance of this differentiation. Major changes in gene expression may have little impact on the cell, whereas subtle changes in some genes can have huge consequences. In most cases the mRNA expression results from the microarray analysis follow the results obtained from real-time RT-PCR analysis, with the latter being more sensitive to detect low abundant transcripts. Further work is required to validate and interpret these changes in gene expression and to determine their biological impact.

In conclusion, these results show that PRC functions as an important regulator of respiratory chain expression and mitochondrial biogenesis in cells where PGC-1α is absent.

Therefore, PRC resembles the other PGC-1 family coactivators in controlling mitochondrial respiratory function through its induction by environmental signals and its *trans*-activation of respiratory genes through the NRFs and other transcription factors. In addition to their importance to mitochondrial function, these coactivators have a broad specificity and are involved in the regulation of many other cellular activities (40,123). Here, we show that PRC controls cell growth by mechanisms that are independent of its effects on mitochondrial function. It will be of interest to further understand the biological role of PRC and to examine the functional redundancy between the different members of the PGC-1 coactivator family.

MATERIALS AND METHODS

Cell culture.

U2OS cells and HEK-293 cells were obtained from ATCC and maintained in Dulbecco's modified Eagle's medium (DMEM; Invitrogen) with 10% fetal bovine serum (HyClone) and 1% penicillin-streptomycin (Invitrogen). 293FT cells (Invitrogen) were cultured in DMEM containing 10% fetal bovine serum (HyClone), 1% penicillin-streptomycin (Invitrogen) and 1mM MEM nonessential amino acids (Mediatech, Inc.) with 500μg/ml Geneticin (Invitrogen).

Generation of Lentiviral Transductants Expressing shRNA.

Double-stranded oligonucleotides targeting the human PRC gene (PRCsh#1S, CACCGCCATCAGGACATCACCATCACGAATGATGGTGATGTCCTGATGGC; PRCsh#1AS, AAAAGCCATCAGGACATCACCATCATTCGTGATGGTGATGTCCTGATGGC; PRC sh#2S, CACCGCGAAAGCCAAATCTCCTAAACGAATTTAGGAGATTTGGCTTTCGC;

PRC sh#2AS,
AAAAGCGAAAGCCAAATCTCCTAAATTCGTTTAGGAGATTTGGCTTTCGC; PRC sh#3S, CACCGCAAGCAAACTTATGGTTTCACGAATGAAACCATAAGTTTGCTTGC; PRCsh#3AS,
AAAAGCAAGCAAACTTATGGTTTCATTCGTGAAACCATAAGTTTGCTTGC; PRCsh#4S,
CACCGAGGCATTTGCAGCCATTGTTCAAGAGACAATGGCTGCAAATGCCTC; PRCsh#4AS,
AAAAGAGGCATTTGCAGCCATTGTCTCTTGAACAATGGCTGCAAATGCCTC) and a negative control sequence derived from the MISSION nontarget shRNA control vector (Sigma) (control shS,
CACCCAACAAGATGAAGAGCACCAACTCGAGTTGGTGCTCTTCATCTTGTTG; control shAS, AAAACAACAAGATGAAGAGCACCAACTCGAGTTGGTGCTCTTCATCTTGTTG) were ligated into the pENTR/U6 vector using the BLOCK-iT U6 RNAi Entry Vector kit (Invitrogen). The BLOCK-iT™ RNAi Designer from the Invitrogen website was used to design shRNA sequences targeting PRC. The control hairpin contains four base pair mismatches to any known human or mouse gene (164). The resulting entry vectors were designated pENTR/PRCshRNA#1, pENTR/PRCshRNA#4 and pENTR/control shRNA. The lentiviral expression vectors pLenti/PRCshRNA#1, pLenti/PRCshRNA#4, pLenti/control shRNA and pLenti-GW/U6-Lamin^{shRNA} were generated by transferring the U6-PRC, U6-control and U6-Lamin RNA-mediated interference cassettes into the pLenti6/BLOCK-iT DEST vector using the LR recombination reaction. Lentiviral particles of these constructs were generated in 293FT cells using the BLOCK-iT Lentiviral RNAi Expression system according to the manufacturer's

protocol (Invitrogen). U2OS cells were transduced with each lentiviral construct at a multiplicity of infection of 10, and individual clones stably expressing each shRNA were selected with blasticidin.

Adenoviral methods.

The recombinant adenoviral plasmids Ad-GFP and Ad-PGC-1α were a kind gift from Dr. D. P. Kelly (Burnham institute for Medical Research, Orlando) (55). The plasmid Ad-NmycPRC was constructed using the AdEasy® Basic Kit from ATCC. An N-terminal c-Myc tag was incorporated into PRC full-length cDNA by PCR using FL-Bam-PRC/pBSII (89) as a template, resulting in NmycPRC/pBSII. NmycPRC/pAdTrack-CMV was generated by cloning the *XhoI/NotI* fragment of NmycPRC/pBSII into *SalI/NotI* digested pAdTrack-CMV. NmycPRC/pAdTrack-CMV was then used in a recombination reaction with pAdEasy-1 to produce Ad-NmycPRC. The adenoviral plasmids were linearized and transfected into the packaging cell line HEK-293 with Lipofectamine (Invitrogen), and the resulting viral stock was amplified to high titer. U2OS cells were infected, and the infection efficiency (95-100%) was determined by GFP expression 24 h after infection. Cells were harvested for preparation of RNA or protein extracts 72h after infection.

Immunoblotting.

Whole cell lysates were prepared in NP-40 lysis buffer as described previously (89). Extracts were subjected to denaturing gel electrophoresis and the proteins transferred to nitrocellulose membranes (Schleicher & Schuell) with high molecular weight transfer buffer (50mM Tris, 380mM Glycine, 0.1% SDS, and 20% methanol) in the Mini Trans-Blot Cell tank

transfer system (Bio-Rad) for proteins 70kDa or larger, or by using a Trans-Blot SD semidry electrophoretic transfer cell (BioRad) with Towbin transfer buffer (141) for proteins under 70kDa. The following primary antibodies were used: rabbit anti-PRC (1047-1379) (99), rabbit anti-Lamin A/C (a kind gift from Dr. R.D. Goldman, Northwestern University, Chicago) (186), and rabbit anti-PGC-1α (a kind gift from Dr. D.P. Kelly, Burnham institute for Medical Research, Orlando) (55). The relative levels of the five human OXPHOS complexes were determined by using the MitoProfile Human Total OXPHOS Complexes detection kit (MitoSciences), containing antibodies against NADH dehydrogenase subunit 6 (MT-ND6) of complex I, succinate dehydrogenase iron-sulfur subunit (SDHB) of complex II, ubiquinol-cytochrome c reductase core protein II (UQCRC2) of complex III, cytochrome c oxidase subunit II (MT-CO2) of complex IV and subunit α of F1-ATPase (ATP5A1) of complex V. The premixed mouse monoclonal antibody cocktail was diluted to a working concentration of 7.2 μg/ml (MitoSciences). Human heart mitochondrial extract provided in the kit (0.5 μg/lane) was used as a positive control. All blots were visualized by SuperSignal West Pico chemiluminescent substrate (Pierce Biotechnology).

Flow cytometry.

For growth curves, 64000 U2OS cells were plated on day 0 in 6cm dishes in DMEM (Invitrogen) containing either 5mM glucose or 5mM galactose (Sigma). Media was changed daily and on days 3, 4 and 5 cells were trypsinized, centrifuged at 4000g for 2min and resuspended in fresh media. For absolute cell counting, 50μl of AccuCount Blank particles, 5.0-5.9 μm (Spherotech), were mixed with 450μl of the cell suspension and samples were counted on a CyAn flow cytometer (Beckman Coulter). On day 5, cells were labeled in fresh medium

containing 50 nM MitoTracker Green FM (Invitrogen) for 45min at 37°C immediately after trypsinization. After labeling, cells were centrifuged, resuspended in fresh media and AccuCount particles were added. The MitoTracker fluorescence of these cells was analyzed by flow cytometry using a CyAn flow cytometer (Beckman Coulter). Data was analyzed using Summit Software.

For DNA content analysis, exponentially grown control shRNA, PRC shRNA#1 and PRC shRNA#4 U2OS cells were trypsinized, washed in PBS and fixed in 70% ice-cold ethanol. Next, cells were washed with PBS and stained with propidium iodide (PI) staining solution containing RNase A (50 μg/ml PI, 0.1% Triton X-100, 0.2 mg/ml RNase A). Cell cycle analysis was done on a Beckman coulter Epics XL flow cytometer. Data was gated using pulse width and pulse area to exclude doublets, and the percent of cells present in each phase of the cell cycle was calculated using Modfit software (Verity Software House).

Real-time quantitative reverse transcription-PCR.

Total RNA was purified using TriZol reagent (Invitrogen). RNA samples were DNase treated with the TURBO DNA-*free* kit (Ambion) and reverse transcribed into cDNA using the TaqMan reverse transcription reagents (Applied Biosystems). Total genomic DNA was isolated using the GenElute Mammalian Genomic DNA miniprep kit (Sigma). Relative mRNA expression levels and relative mitochondrial DNA copy numbers were determined by Power SYBR Green (Applied Biosystems) quantitative real time PCR using the primer sets shown in **Table 6.5**. Messenger RNA quantities were normalized to 18S rRNA. The amount of mtDNA (as measured by amplification of the mtDNA-encoded COX1 gene and of a D-loop fragment) was normalized to 18S rDNA. Assays for both the gene of interest and the 18S control were

performed in triplicate using an ABI PRISM 7900HT Sequence Detection system. Relative gene expression levels and relative mtDNA copy numbers were determined by the comparative C_t method using SDS 2.1 software (Applied Biosystems).

Table 6.5. List of primers used for quantitative real-time PCR.

Gene name	Primer	Sequence (5'→3')
PRC	hPRC sybr S	AGTGGTTGGGGAAGTCGAAG
	hPRC sybr AS	CCTGCCGAGAGAGACTGAC
NRF-1	hNRF-1 sybr S	AACAAAATTGGGCCACGTTACA
	hNRF-1 sybr AS	TCTGGACCAGGCCATTAGCA
NRF-2α	hNRF-2a sybr S	AACAAGAACGCCTTGGGATAC
	hNRF-2a sybr AS	GTGAGGTCTATATCGGTCATGCT
NRF-2β	hNRF-2b sybr S	CCAACCAGTGGAATTGGTCAG
	hNRF-2b sybr AS	ACCGGGTAAAAGACTCCTTACTT
CREB	h CREB sybr S	CCAGCAGAGTGGAGATGCAG
	h CREB sybr AS	GTTACGGTGGGAGCAGATGAT
Tfam	hTFAM sybr S	CCGAGGTGGTTTTCATCTGTC
	hTFAM sybr AS	CAGGAAGTTCCCTCCAACGC
TFB1M	hTFB1M sybr S	CCTCCGTTGCCCACGATTC
	hTFB1M sybr AS	GCCCACTTCGTAAACATAAGCAT
TFB2M	hTFB2M sybr S	CGCCAAGGAAGGCGTCTAAG
	hTFB2M sybr AS	CTTTCGAGCGCAACCACTTTG
Cyt c	hcytc sybr S2	TGGGCCAAATCTCCATGGTCTCTT
	hcytc sybr AS2	TGCCTTTGTTCTTATTGGCGGCTG
COXIV	hCOX4 sybr S	TTTAGCCTAGTTGGCAAGCGA
	hCOX4 sybr AS	CCGATCCATATAAGCTGGGAGC
SDHB	hSDHB sybr S	CCACAGCTCCCCGTATCAAG
	hSDHB sybr AS	TCGGAAGGTCAAAGTAGAGTCAA
UQCRC2	UQCRC2 sybr 2S	TTCAGCAATTTAGGAACCACCC
	UQCRC2 sybr 2AS	GTCACACTTAATTTGCCACCAAC
ATP5A1	ATP synthase sybr 2S	TACATGGGCTGAGGAATGTTCA
	ATP synthase sybr 2AS	ACCAACTGGAACGTCCACAAT
COXII	hCOX2 sybr S	ACAGATGCAATTCCCGGACGTCTA
	hCOX2 sybr AS	GGCATGAAACTGTGGTTTGCTCCA
MT-ND6	hMT-ND6 sybr 2S	AGGATTGGTGCTGTGGGTGAAAGA
	hMT-ND6 sybr 2AS	ATAGGATCCTCCCGAATCAACCCT
Cyt b	hCYTB sybr S	AATTCTCCGATCCGTCCCTA
	hCYTB sybr AS	GGAGGATGGGGATTATTGCT
D-loop	hDloop-S	TTTCACGGAGGATGGTGGTCAA
	hDloop-AS	ACCAACAAACCTACCCACCCTT
COXI	hCOXI-S	AGGTTGAACAGTCTACCCTCCCTT
	hCOXI-AS	GGCGTTTGGTATTGGGTTATGGCA
18S rDNA	18SrDNA-S	ACCAGAGCGAAAGCATTTGCCA
	18SrDNA-AS	TCGGCATCGTTTATGGTCGGAA
LUM	hLUM-S	TTTCAATGTGTCATCCCTGGTTG
	hLUM-AS	CCAAACGCAAATGCTTGATCTT

Gene name	Primer	Sequence (5'→3')
RAC2	hRAC2-S	CAACGCCTTTCCCGGAGAG
	hRAC2-AS	TCCGTCTGTGGATAGGAGAGC
HCFC1R1	hHCFC1R1-S	GCAAGCAGTTTCTGTCTGAGG
	hHCFC1R1-AS	CAGTAGGGGTGGTCATTGTGC
ANXA10	hANXA10S6	GGAGCTGCTGGTTGCAATTGTTCT
	hANXA10AS6	CGTTTCCTTATGGTCAGCAGGTCT
HIST1H2BJ	HIST1H2BJ-S	CTGACACCGGCATTTCGTC
	HIST1H2BJ-AS	CGGCCTTAGTACCCTCGGA
TGFBI	TGFBI-S	CACTCTCAAACCTTTACGAGACC
	TGFBI-AS	CGTTGCTAGGGGCGAAGATG
PPP2R2B	PPP2R2B-S	CCACACGGGAGAATTACTAGCG
	PPP2R2B-AS	TGTATTCACCCCTACGATGAACC
COX17	COX17-S	TCTAATTGAGGCCCACAAGG
	COX17-AS	TCAGGAATTATTTATTCACACAGCA
PLAC8	PLAC8-S	GTCGTTGTGACCCAACCTGG
	PLAC8-AS	GGGAAACAAAATGTGCCACAG
PCM1	PCM1-S	TCCCTCTGCTTGTCTAGGCTT
	PCM1-AS	TGTCATCATGTCTGACGTTTGTT
PSD3	PSD3-S	TCTAGTGGCGTCACCAATGG
	PSD3-AS	CTAGCCGTGTTGTTTTCACCC

Dipstick immunoassay.

U2OS transductants expressing the control shRNA or PRCshRNA#1 were assayed for human complex I (NADH ubiquinone oxidoreductase) and complex IV (cytochrome c oxidase) using the respective MitoProfile Dipstick Assay kit (MitoSciences) according to the manufacturer's protocol. Briefly, cells were grown in DMEM containing 5mM glucose for 3 days, washed with cold PBS, and collected using a cell scraper. Total cell extract was prepared based on the manufacturer's protocol (MitoSciences). Levels of human complexes I and IV were determined using 5 μg and 2 μg of cell extract per dipstick, respectively. The signal intensity on each dipstick was measured using the *ImageJ* Image Processing and Analysis program (NIH).

ATP assay.

Cells were plated at a density of 200,000 cells per 6cm dish. Two days after plating, half the cells were treated with oligomycin at a final concentration of 20 μg/μl (Sigma) for 3 h at 37°C. Treated and untreated cells were trypsinized, counted, and diluted to 200,000 cells/ml. The cell suspension of 100μl was used to measure steady-state ATP levels using an Adenosine 5'-triphosphate (ATP) bioluminescent somatic cell assay kit (Sigma) according to the manufacturer's instructions in duplicate. An ATP calibration curve was prepared with the provided ATP standard stock. The amount of light emitted was measured with a Monolight 2010 luminometer (Analytical Luminescence Laboratory).

Transmission Electron microscopy.

U2OS cells were pelleted, embedded in 2% agar and fixed in 2.5% glutaraldehyde in 0.1M sodium cacodylate (pH 7.4) overnight at room temperature. Cells were rinsed in 0.1M

sodium cacodylate (pH 7.4), postfixed in 2% osmium in 0.1M sodium cacodylate (pH 7.4) for 1 h, rinsed in distilled water, and prestained with uranyl acetate for 30 min. Cells were then washed in distilled water and dehydrated in ascending grades of ethanol. After 3 changes of propylene oxide, cells were infiltrated in a mixture of propylene oxide and Epon/Araldite (1:1 ratio) for 1 h, embedded in Epon/Araldite resin and placed in a 60 degree oven overnight to polymerize. Thick sections (1 μm) were cut and stained with toluidine blue O for examination and selection of specific regions for further analysis. Thin sections (90 nm) were stained with uranyl acetate and lead citrate and examined in a JEOL JEM 1220 transmission electron microscope. Gatan DigitalMicrograph software was used for digital imaging. For morphometric analysis, a grid was placed over the digital image of 10 different cells per sample and the mitochondrial content as a percentage of the cytoplasm was estimated (187).

Microarray analysis using Illumina BeadChip.

Total RNA was isolated from PRC shRNA#1, PRC shRNA#4 and control cells using TriZol (Invitrogen) and DNase treated with the TURBO DNA-*free* kit (Ambion). RNA samples were further purified using the RNeasy MinElute Cleanup kit (Qiagen). Integrity of the RNA was evaluated using the Agilent 2100 BioAnalyzer. 500 ng of RNA was used to perform *in vitro* transcription in the presence of biotin UTP with the Illumina TotalPrep RNA amplification kit (Ambion). The amplified, labeled RNA (1.5 μg) was then hybridized in triplicate to an Illumina Whole-Genome Sentrix Human-6 v2 Expression BeadChip, and detected according to the Illumina user manual. Data normalization was performed using the statistical modeling language of R through the BioConductor lumi package. Quality control of the hybridization was performed using intensity box plots and sample clustering. To identify differentially expressed

genes, routines implemented in the limma package were applied to fit linear models to the normalized expression values. The variance used in the t-score calculation was corrected by an empirical Bayesian method for better estimation under small sample size (188). To control the effects of multiple testing, the false discovery rate (FDR) was limited to 5% (FDR adjusted p-value < 0.05) to identify probe sets that are statistically significant between control and PRC shRNA#1 or #4 samples.

Gene functional categories were assigned using the GO database (http://www.geneontology.org/) and NCBI's Entrez Gene database (http://www.ncbi.nlm.nih.gov/sites/entrez?db=gene).

ACKNOWLEDGMENTS

We thank Robert D. Goldman of Northwestern Medical School for the lamin A/C antibody and Daniel P. Kelly of the Burnham institute for Medical Research for the PGC-1α adenoviral plasmid and antibody. We are grateful to the Flow Cytometry Core Facility for help with the FACS analysis. Lennell Reynolds from the Cell Imaging Facility provided valuable help with the electron microscopy. We thank the Center for Genetic Medicine for processing the Illumina Beadchip and the BioInformatics Core for statistical analysis of the data generated from the microarray study.

This work was supported by United States Public Health Service grant GM32525-25.

CHAPTER 7:

ADENOVIRAL OVER EXPRESSION OF PRC

INTRODUCTION

Numerous *in vitro* and *in vivo* data establish a key role for the NRFs in mitochondrial biogenesis and function (reviewed in (189)). We have shown before that PRC is able to *trans*-activate through NRF-1 *in vitro*, and both *in vitro* and *in vivo* experiments support the specific interaction of PRC with NRF-1(89). This is consistent with a role for PRC in co-activating mitochondrial biogenesis. In addition, we have shown that NRF-2, a transcription factor associated with the expression of many respiratory genes, exists in a complex with PRC *in vivo* and its association with HCF-1 appears to be critical for *trans*-activation through NRF-2 (166). Furthermore, PGC-1α, a member from the same family of coactivators, has been shown to transcriptionally co-activate mitochondrial biogenesis, in part through NRF-1. The conservation of structurally similar domains, as shown for PGC-1α and PRC, is often indicative of related function. This lead us to hypothesize that PRC is involved in mitochondrial biogenesis. As described in **Chapter 6**, silencing of PRC in U2OS cells causes a severely reduced growth rate on galactose, reduced respiratory subunit expression and markedly lower complex I and IV enzyme levels and diminished mitochondrial ATP production, associated with proliferation of aberrant mitochondria. This provides *in vivo* evidence that PRC is essential for mitochondrial biogenesis. Surprisingly, PRC silencing causes an increase in mitochondrial content and not a decrease, as we initially expected. This shows that organelle biogenesis in this system is not positively linked to the PRC-dependent expression of the respiratory chain. The proliferation of aberrant mitochondria might result from compensation for the respiratory defect or from effects

on an unidentified regulator of organelle biogenesis mediated by the loss of PRC. To further dissect the role of PRC in the biogenesis of mitochondria *in vivo*, and to determine if PRC expression is sufficient to stimulate mitochondrial biogenesis, we want to do gain-of-function studies, in addition to the loss-of-function studies described in **Chapter 6**. It would be of interest to determine what the effects are of ectopic over expression of PRC on respiratory subunit expression, ATP production and mitochondrial content.

During the course of my dissertation research, we were able to transiently over express full-length PRC protein in 293FT cells from the mammalian expression vector FL-Bam-PRC/pSV-Sport, constructed previously by a post-doc (Dr. Ulf Andersson) in the lab, who also developed the initial PRC antibody, PRC(95-533). The generation of 2 additional PRC antibodies raised to different sub regions of PRC, PRC(400-467) and PRC(1047-1379), in collaboration with Raymond Al Pasko from the lab, was a great aid in identifying PRC protein. All three antibodies recognize the same 250kDa band in immunoblotting experiments, and we detected enhanced expression of this band upon transfecting 293FT cells with the expression vector FL-PRC/pSV-Sport compared to transfections with the empty vector, pSV-Sport **(see Figure 4.2)** (99). These results clearly confirm this 250kDa protein is PRC.

We investigated the effects of transient over production of PRC in 293FT cells on the expression of NRF target genes involved in mitochondrial biogenesis and/or function, but were unable to detect any significant changes by real-time RT-PCR analysis (not shown). This might be explained by the fact that PRC is highly regulated by serum and important for cell growth, and 293FT cells are a transformed cell line. Therefore, we decided to test the effects of ectopic over expression of PRC in a different cell line. Both mouse Balb/3T3 fibroblasts and human U2OS osteosarcoma cells are highly responsive to serum and show up regulation of PRC mRNA

and protein when serum-stimulated. Mouse C2C12 myoblast cells are not serum-responsive but have been shown to be an attractive system to study PGC-1α function (54), so we thought maybe they would be useful to evaluate PRC function as well. However, these cell lines are all limited in their utility by displaying rather low transfection efficiency. Gene delivery by viral vectors, particularly adenovirus, has proven a powerful means for introduction of genes into certain cell types. Therefore, we decided to switch to an adenoviral system. The AdEasy system **(Figure 7.1)** developed by He and Vogelstein (101,190) has the advantage that a recombinant adenoviral plasmid is generated with minimal enzymatic manipulations, using homologous recombination in bacteria rather than in eukaryotic cells. In addition, vectors used in this system contain a green fluorescent protein (GFP) gene incorporated into the adenoviral backbone, allowing direct observation of the efficiency of transfection and infection. Furthermore, this system has been successfully used to over express PGC-1α (55). We have previously received the adenoviral plasmids Ad-GFP and Ad-PGC-1α described in (55) from Dr. D.P. Kelly (Burnham institute for Medical Research, Orlando) and we have successfully produced high titer adenoviruses from these plasmids that were used to over express PGC-1α in C2C12 and HeLa cells **(Figure 3.10 and unpublished results)**. All plasmids and cells that are part of the AdEasy system were purchased from ATCC. As mentioned in the **Background (Chapter 2)**, one of the vectors, pAdEasy-1, we initially received from ATCC was missing an important piece of DNA. This chapter describes the work that was done with the correct vector obtained almost two years later.

Adenoviral gene transfer efficiency has been reported to correlate with cellular coxsackie and adenovirus receptor (CAR) expression (191). BALB/3T3 cells express very low levels of CAR (192). We decided to continue with C2C12 cells (193), which have relatively low levels of CAR but were used successfully to express PGC-1α from adenovirus, and U2OS (194) cells,

which have high levels of CAR and are serum-regulated. Initially, we decided to construct a number of epitope-tagged PRC constructs, i.e. N-terminal GAL4-tagged PRC and both N-terminal and C-terminal c-myc-tagged PRC to distinguish the adenovirally expressed protein from the endogenous protein. It is shown before ((89) and personal communication) that epitope-tagging helps increase the stability of PRC protein and does not interfere with PRC function. However, in the unlikely event that the tags pose any adverse effects on PRC expression and/or function, we also decided to produce an adenoviral vector containing untagged, wild-type PRC cDNA.

Here, we show that we can over express N-terminal c-myc-tagged and untagged PRC protein from an adenoviral vector in C2C12 and U2OS cells. Even though we were able to produce very high levels of protein beyond the physiological level of PRC, we observed no changes in NRF target gene expression or mtDNA copy number in the cells over producing PRC. Unexpectedly, PRC produced from the adenovirus was not able to *trans*-activate the NRF-1-dependent δ-ALAS promoter. This indicates that expression of PRC alone does not seem sufficient to induce mitochondrial biogenesis. Future experiments are needed to confirm this.

Figure 7.1. Outline of the AdEasy system for generating recombinant adenoviruses (adapted from He and Vogelstein, 1998).

The gene of interest is first cloned into a shuttle vector, e.g., pAdTrack-CMV. The resultant plasmid is linearized by digesting with restriction endonuclease *PmeI*, and subsequently cotransformed into E. coli BJ5183 cells with an adenoviral backbone plasmid, e.g., pAdEasy-1. Recombinants are selected for kanamycin resistance, and recombination confirmed by multiple restriction endonuclease analyses. Finally, the linearized recombinant plasmid is transfected into an adenovirus packaging cell line, e.g. 293 cells. Recombinant adenoviruses typically are generated within 7–10 days. The "left arm" and "right arm" represent the regions mediating homologous recombination between the shuttle vector and the adenoviral backbone vector. An, polyadenylation site; Bm, *BamHI*; RI, *EcoRI*; LITR, left-hand ITR and packaging signal; RITR, right-hand ITR; Sp, *SpeI*.

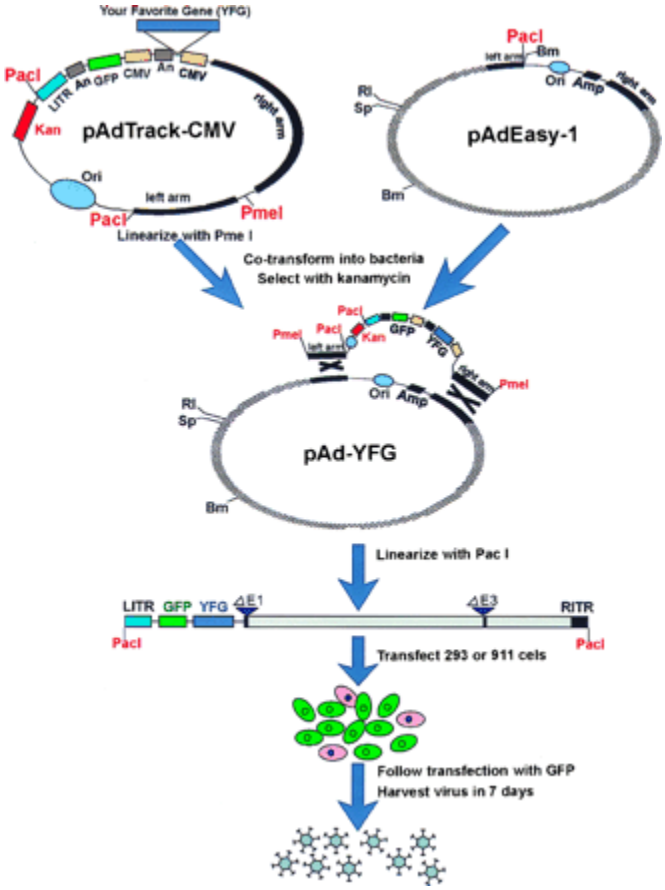
Your Favorite Gene (YFG)
PacI
LITR
Ad
GFP
CMV
An
CMV
Kan
pAdTrack-CMV
right arm
Ori
left arm
PacI
PmeI
Linearize with Pme I
PacI
Bm
left arm
Ori
Amp
right arm
RI
Sp
pAdEasy-1
Bm
Co-transform into bacteria
Select with kanamycin
PacI
PmeI
PacI
Kan
GFP
YFG
left arm
right arm
PmeI
Ori
Amp
RI
Sp
pAd-YFG
Bm
Linearize with Pac I
LITR
GFP
YFG
ΔE1
ΔE3
RITR
PacI
PacI
Transfect 293 or 911 cels
Follow transfection with GFP
Harvest virus in 7 days

RESULTS

Transient expression of PRC/pAdTrack-CMV constructs in 293FT cells.

Before generating the final recombinant adenoviral vectors by recombination of pAdTrack-CMV with the pAdEasy-1 plasmid, we wanted to check if we could express tagged and untagged PRC constructs inserted into the pAdTrack-CMV vector. 293FT cells were transiently transfected with Nmyc PRC/pAdTrack-CMV, Cmyc PRC/pAdTrack-CMV or untagged FL PRC/pAdTrack-CMV and whole cell extract was prepared from transfected and untransfected cells. The PRC antibody PRC(1047-1379) detects a 250kDa protein, similar in size to endogenous PRC protein, produced from all 3 vector constructs **(Figure 7.2A)**, identifying this protein as PRC. Endogenous PRC is detected by this antibody during longer exposure times but is not shown here for esthetical purposes only. However, when probing with an antibody against the c-myc tag, we could only detect N-terminally tagged PRC and not PRC protein with the c-myc tag at the C-terminus **(Figure 7.2B)**. This suggests translation of Cmyc tagged PRC is terminated prematurely and the c-myc epitope tag is not expressed. Therefore, we decided to continue with the adenoviral production of Nmyc PRC and untagged PRC.

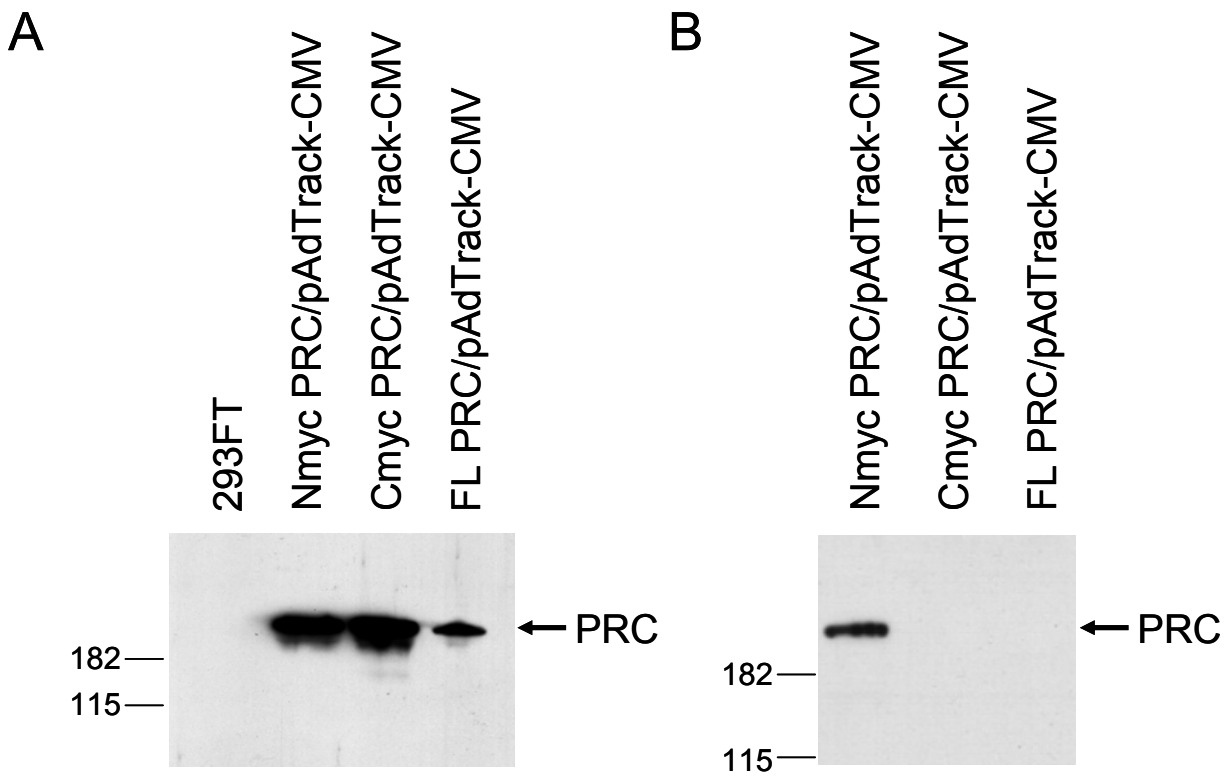

Figure 7.2. Transient over expression of Nmyc PRC, Cmyc PRC and untagged FL PRC from pAdTrack-CMV.

Total cell extracts were prepared from untransfected 293FT cells or from 293FT cells that were transiently transfected with Nmyc PRC/pAdTrack-CMV, Cmyc PRC/pAdTrack-CMV or untagged FL PRC/pAdTrack-CMV. PRC protein was detected by immunoblotting following denaturing gel electrophoresis using rabbit anti-PRC(1047-1379) serum (*A*) or mouse anti-c-myc antibody (*B*) to detect tagged proteins. Arrows indicate the position of PRC protein. Molecular mass standards in kilodaltons are indicated at the left.

Adenoviral expression of Nmyc PRC and FL PRC in C2C12 and U2OS cells.

High titer recombinant adenoviruses expressing N-terminally c-myc-tagged PRC, untagged FL PRC or the control Ad-GFP were used to infect C2C12 cells and U2OS cells. Although we were able to obtain infection efficiency in both cell types of near 100%, as evaluated by GFP expression, C2C12 cells seemed much less susceptible to adenoviral infection than U2OS cells and had to be infected at a much higher MOI to obtain the same efficiency. This is in accordance with the fact that C2C12 cells express much lower levels of the CAR receptor (193). Whole cell extracts were prepared 3 days after infection and were tested for expression of PRC. Abundant expression of Nmyc PRC and FL PRC protein, similar in size to endogenous PRC, was seen in both U2OS **(Figure 7.3A)** and C2C12 cells **(Figure 7.3B)**. With longer exposure times we are able to detect the much lower levels of endogenous PRC in cells infected with Ad-GFP. When probed for β-tubulin **(Figure 7.3A)** or Sp1 protein **(Figure 7.3B)**, equal loading was seen in all lanes. The β-tubulin antibody does not react with the mouse protein, therefore we used anti-Sp1 antibody as a loading control in C2C12 cells. Repeatedly, the levels of c-myc-tagged PRC protein were higher than the levels of untagged FL PRC protein, consistent with previous observations that the tag increases the stability of the protein.

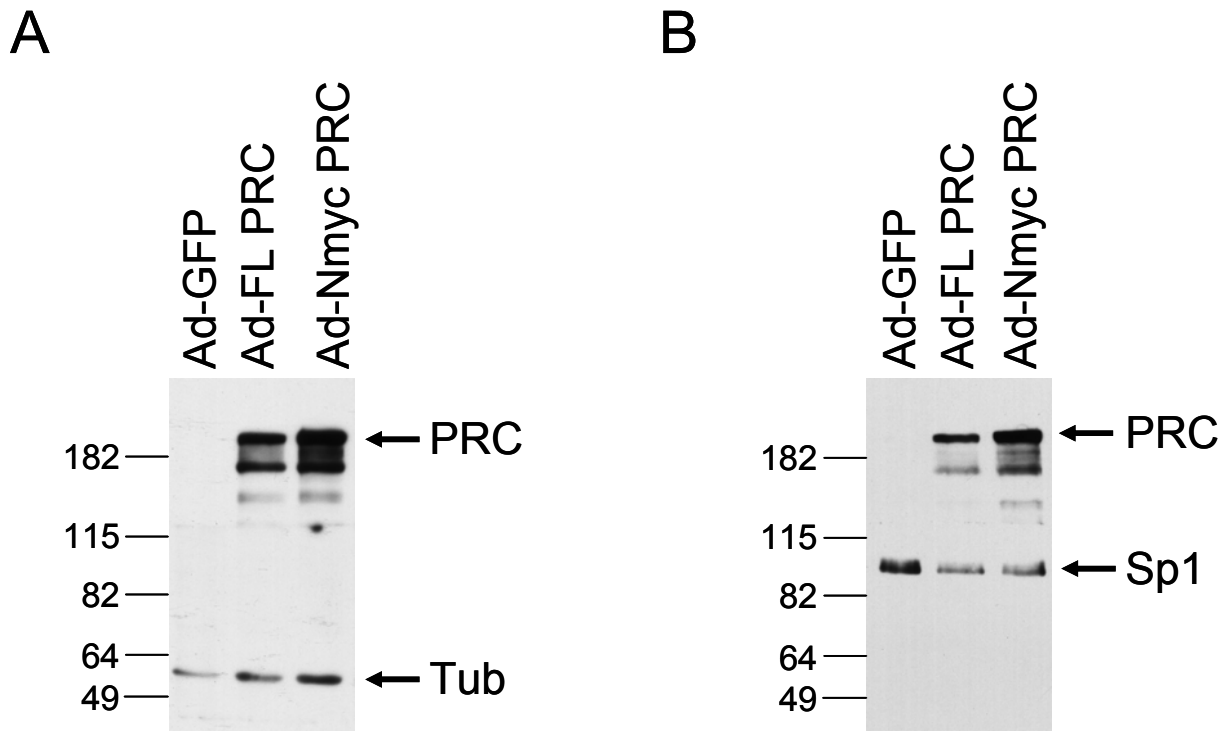

Figure 7.3. Adenoviral over expression of untagged FL PRC and Nmyc PRC in U2OS and C2C12 cells.

Whole cell extracts were prepared from U2OS cells (*A*) or C2C12 cells (*B*) infected with the recombinant adenoviruses Ad-GFP, Ad-FL PRC or Ad-Nmyc PRC. PRC, β-tubulin and Sp1 proteins were detected by immunoblotting following denaturing gel electrophoresis using rabbit anti-PRC(1047-1379) serum, mouse anti-β-tubulin and rabbit anti-Sp1 antibodies, respectively. Arrows indicate the positions of PRC, β-tubulin and Sp1. Molecular mass standards in kilodaltons are indicated at the left. Tub, β-tubulin.

Inability to detect downstream effects of PRC over expression.

PRC is a transcriptional coactivator that operates, at least in part, through the nuclear respiratory factors, NRF-1 and NRF-2, to activate the expression of NRF target genes. Therefore, we expected to see increased expression of mRNAs encoding NRF target genes involved in mitochondrial biogenesis and/or function in cells where PRC protein is over produced. When quiescent fibroblasts are induced to proliferate following serum-stimulation, a rapid induction of PRC and cytochrome c mRNAs is seen, accompanied by increases in nuclear (cyt c) and mitochondrial (COXII) encoded respiratory subunit mRNAs, along with mitochondrial transcription factors mRNAs (Tfam, TFB1M, TFB2M) and a slight increase in NRF-1 mRNA (46) **(Figure 3.9A)**. When PGC-1α is over expressed from an adenoviral vector in C2C12 myoblasts, we see induction of many of the same genes (46) **(Figure 3.10)**. We hypothesized a similar pattern of gene expression would be observed by exogenous over expression of PRC protein. To test this, we performed quantitative real-time RT-PCR analysis on RNA isolated from C2C12 cells infected with control Ad-GFP, Ad-FL PRC, Ad-Nmyc PRC and Ad-PGC-1α adenovirus **(Figure 7.4)**. No changes in mRNA expression of the genes assayed were observed in PRC over producing cells, despite the fact that PRC mRNA levels were induced several 1000-fold over endogenous levels in control Ad-GFP infected cells. Changes in incubation time or viral titer had no influence on NRF target gene expression. It has to be noted that PRC expressed from the adenovirus is human PRC. Since there is no background expression of endogenous human PRC mRNA present in C2C12 cells, we observe a massive induction of PRC mRNA in these cells upon adenoviral infection. In response to over production of (mouse) PGC-1α from adenoviral DNA, we detected induction of mRNAs for many of the genes tested, confirming the results from **Figure 3.10**. Perhaps the C2C12 cell line is not a good system to look at the effects

of PRC. Maybe there are some species differences and PRC of human origin is unable to induce the expression of mouse genes. Therefore, we next checked cytochrome c mRNA levels in the human U2OS osteosarcoma cell line infected with PRC adenovirus. Cytochrome c is an important mitochondrial marker and is one of the genes changed most robustly in serum-stimulated cells or in cells over expressing PGC-1α (46,108). We did not detect any changes in the expression of cyt c mRNA in U2OS cells infected with Ad-FL PRC or Ad-Nmyc PRC (data not shown), even though PRC mRNA was expressed at approximately 50-fold higher levels than in control Ad-GFP infected cells. A background of endogenous human PRC mRNA exists in U2OS cells and is detected by the primer pair used in the PCR reaction, explaining the lower level of induction in U2OS cells compared to C2C12 cells. Because of the lack of induction of cyt c mRNA, no other genes were tested in U2OS cells. These results indicate that species-species variation cannot explain the apparent unresponsiveness of both C2C12 and U2OS cell lines to PRC over expression. They rather suggest that PRC expression alone is not sufficient to induce expression of these genes.

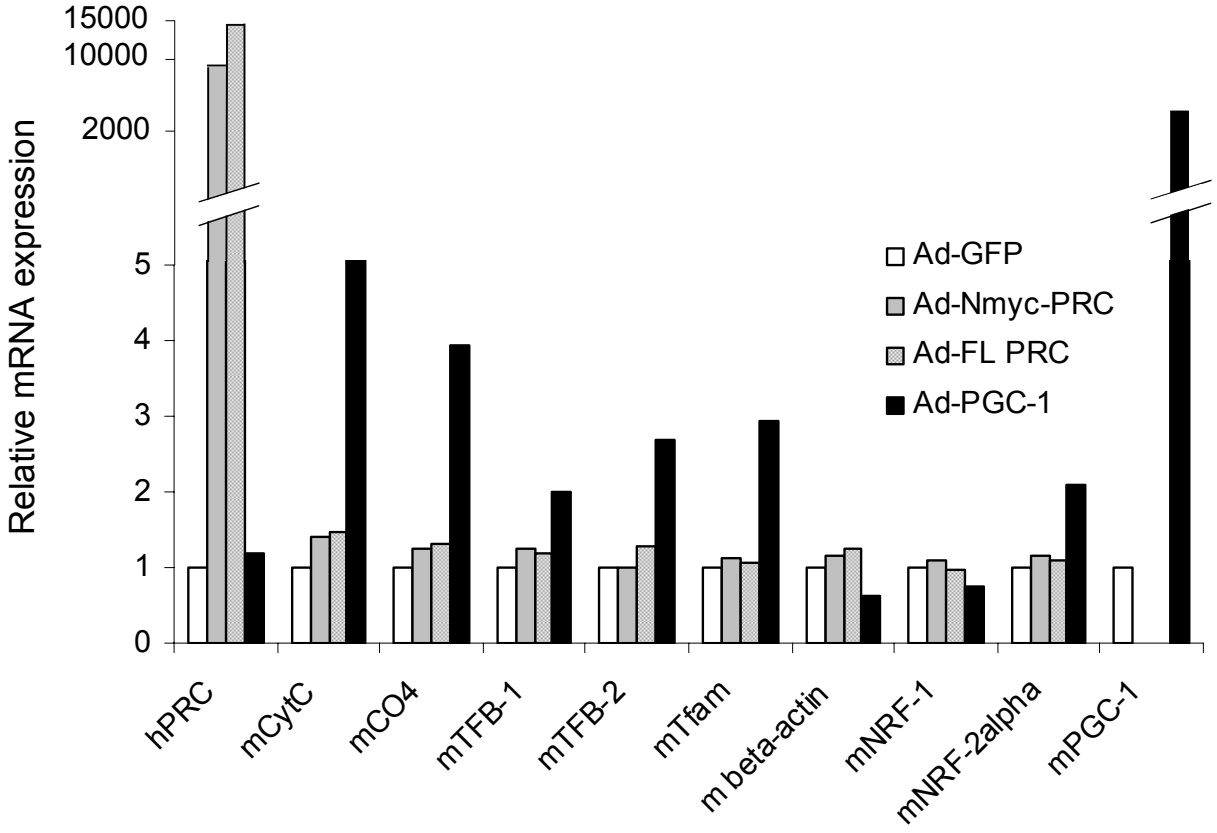

Figure 7.4. Quantitative real time RT-PCR analysis of C2C12 cells over expressing PRC. C2C12 cells were infected with control Ad-GFP (negative control), Ad-FL PRC, Ad-Nmyc PRC or Ad-PGC-1α (positive control) adenovirus and relative gene expression was monitored by real-time RT-PCR. Relative steady-state mRNA levels were normalized to 18S rRNA as an internal control and values expressed relative to Ad-GFP control, which was assigned a value of 1. For each case, values represent the average of two separate determinations.

The ectopic over expression of PGC-1α in cultured cells or transgenic mice induces mitochondrial biogenesis, as indicated by increases in mitochondrial DNA content and proliferation of organelles (54,55). To evaluate if increases in PRC were sufficient to induce mitochondrial biogenesis, we checked mitochondrial DNA copy number in C2C12 cells over expressing PRC by quantitative real-time PCR analysis using probes specific for the mitochondrial D-loop or the COXI transcriptional unit. We could not detect any significant change in mtDNA copy number normalized to 18S rDNA between PRC over expressing cells and control cells at 3 or 6 days post-infection (data not shown). Influence of incubation period or adenoviral titer on mtDNA copy number was negligible. This data indicates that PRC alone does not seem sufficient to increase mitochondrial DNA content in these cells.

Adenovirally expressed PRC is unable to *trans*-activate the δ-ALAS promoter.

It is possible that PRC protein expressed from the adenoviral DNA is inactive because of an oversight in the cloning process. This seems unlikely, since all constructs were subjected to careful sequence verification and exhaustive diagnostic restriction digests. In addition, the protein expressed from adenovirus is similar in size to endogenous protein, as assessed by immunoblotting. However, it is practically not feasible to sequence the complete adenoviral construct because of its large size (> 40kB), so the possibility of errors remains.

It was established previously that basal activity of the wild type δ-ALAS promoter is increased by PRC and PGC-1α expressed from FL PRC/pSV-SPORT (89) or PGC-1/pSV SPORT (our unpublished results and (66)). We were curious to see if PRC and PGC-1α expressed from adenoviral DNA also increased δ-ALAS promoter activity To test this, we transfected C2C12 cells that were infected with Ad-GFP (negative control), Ad-Nmyc PRC, Ad-FL PRC and Ad-PGC-1α (positive control) with a luciferase reporter plasmid driven by the wild type δ-ALAS promoter, δ-ALAS(-479)/pGL3 Basic and measured activity of this promoter **(Figure 7.5A)**. We saw a very minor, but reproducible *trans*-activation of the δ-ALAS promoter (1.35-fold over control) in the cells over expressing Nmyc PRC but no *trans*-activation of this promoter (1.1-fold over control) was seen in the cells over expressing FL PRC. PGC-1α protein expressed from an adenoviral vector was able to *trans*-activate the same promoter 11.5-fold, indicating that the ability to *trans*-activate is still maintained upon adenoviral expression. We considered the possibility that perhaps the cells were sensitive to the amount of PRC being produced. However, when we transfected the PRC-infected cells with the expression vector FL PRC/pSV-Sport, we were able once again to detect *trans*-activation of the δ-ALAS promoter,

indicating that the amount of PRC required to activate this promoter does not seem very critical **(Figure 7.5A)**.

We wanted to know if PRC expressed from the shuttle vector, pAdTrack-CMV, is able to *trans*-activate the δ-ALAS promoter. When the plasmids pAdTrack-CMV, FL PRC/pAdTrack-CMV, Nmyc PRC/pAdTrack-CMV or Cmyc PRC/pAdTrack-CMV were transiently co-transfected into C2C12 cells with the δ-ALAS promoter, all three PRC constructs were able to *trans*-activate the δ-ALAS promoter **(Figure 7.5B)**. In addition, we also tested the different PRC constructs cloned into the mammalian expression vector pSV-Sport for their ability to *trans*-activate this promoter. The pSV-Sport constructs were all more active than their corresponding pAdTrack-CMV constructs, and all tagged constructs were significantly better *trans*-activators than the untagged PRC construct in both C2C12 cells **(Figure 7.5B)** and Balb/3T3 cells (data not shown).

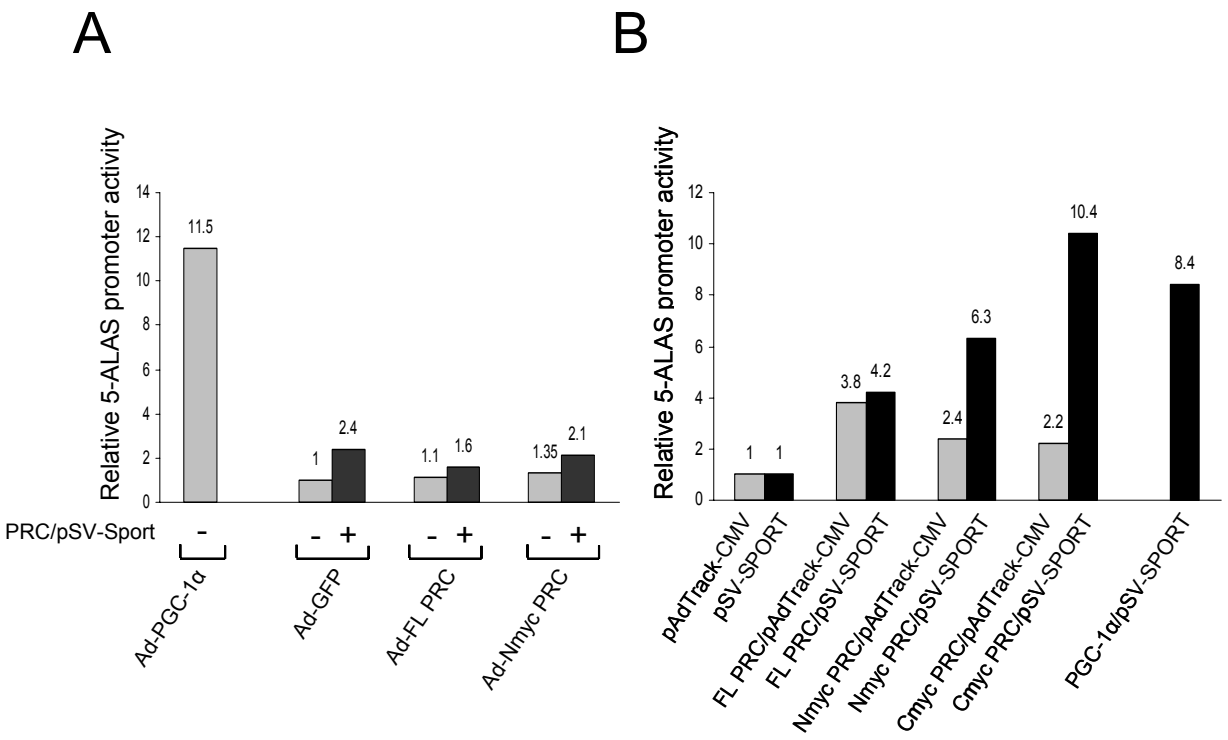

Figure 7.5. *Trans*-activation of the δ-ALAS promoter by adenovirally expressed PRC.

A. C2C12 cells infected with Ad-GFP, Ad-Nmyc PRC, Ad-FL PRC and Ad-PGC-1α were transfected with δ-ALAS(-479)/pGL3 Basic in the presence (*black*) or absence (*grey*) of PRC/pSV-Sport. Normalized luciferase activity obtained from the promoter fragment in Ad-GFP control cells was assigned a value of 1. Activity of the promoter fragment in other cells was expressed relative to this value.

B. The δ-ALAS promoter was assayed for *trans*-activation by indicated constructs in C2C12 cells. Values are the fold-activation measured relative to the pAdTrack-CMV (*grey bars*) or pSV-Sport negative control (*black bars*).

As shown in **Chapter 6**, amino terminally myc-tagged PRC expressed from the adenovirus Ad-Nmyc PRC is completely silenced by PRC shRNA#1 and partially silenced in PRCshRNA#4 transductants **(Figure 6.3)**, indicating that PRC mRNA expressed from adenovirus shows complete complementarity with both short hairpins.

This data indicates that the PRC constructs expressed from the shuttle vector, pAdTrack-CMV, are all correct and that the adenoviral PRC constructs are incorrect, based on their ability or inability to increase activity of the δ-ALAS promoter, respectively. Perhaps during the recombination of the pAdTrack-CMV constructs with pAdEasy-1 in bacteria some other rearrangements were introduced. But then again, viral production proceeds as normal and the protein produced from the adenoviral DNA is similar in size to endogenous protein. Furthermore, it seems unlikely that the same type of rearrangement occurred in both FL PRC and Nmyc PRC constructs. Currently, we have no explanation for the inability of adenovirally expressed PRC to *trans*-activate the δ-ALAS promoter.

DISCUSSION

We show here that we can over express untagged FL PRC and amino terminally myc-tagged PRC protein from an adenoviral vector in both C2C12 and U2OS cells. Elevated PRC levels do not affect mitochondrial DNA copy number or expression of NRF target genes under all the conditions tested. This is in contrast to ectopic over expression of the other two PGC-1 family members, PGC-1α and PGC-1β, in cultured cells or transgenic mice. There, an increase in mtDNA copy number and mitochondrial biogenesis, along with increased expression of respiratory subunits is observed (54,55,79). We have shown that expression of NRF target genes is closely linked to induction of mitochondrial biogenesis in cells over expressing PGC-1α,

during adipocyte differentiation and upon serum-stimulation of quiescent fibroblasts (46). The contrasting phenotype of PRC over expression versus PGC-1α and PGC-1β over expression is not likely the result from choice of cell line, since both mouse and human cell lines tested (C2C12 and U2OS) lacked a response to elevation of PRC. Furthermore, hairpin-mediated silencing of PRC caused an array of phenotypes in U2OS cells (100), demonstrating that PRC plays an important role in these cells. The inability of PRC to cause changes in NRF target gene expression or mtDNA copy number indicates that PRC alone is not sufficient to induce mitochondrial biogenesis. It should also be mentioned that no increases in NRF-1 or NRF-2 protein expression were seen (not shown). It would be of interest to determine more directly if there is an increase in mitochondrial proliferation in PRC-infected cells versus control cells by transmission electron microscopy or MitoTracker staining.

It is possible that PRC regulates mitochondrial biogenesis through different means than PGC-1α or PGC-1β. It might tightly control the number of mitochondria to ensure the cell does not produce too many. In this way, producing more PRC would not result in enhanced organelle proliferation, in contrast to PGC-1α or PGC-1β over expression. Repressing PRC, on the other hand, would have more severe consequences on the number of mitochondria. This is exactly what is demonstrated by the severe mitochondrial phenotype upon PRC silencing described in **Chapter 6**.

It is surprising that PRC produced from an adenoviral vector can only marginally *trans*-activate the wild type δ-ALAS promoter. First, we speculated that the high levels of PRC produced from the adenovirus might have an inhibitory effect on the promoter activity. Since this coactivator seems to be tightly regulated, the cell might be very sensitive to the level of PRC. However, the ability of the PRC/pSV-Sport plasmid to *trans*-activate the δ-ALAS promoter in

the presence of adenovirally produced PRC does not support this theory. This phenomenon rather suggests that PRC produced from the adenovirus is not active. The adenoviral PRC recombinant vector seems correct based on extensive restriction digests, sequence verification, and protein production. At present we have no explanation of why PRC expressed from adenovirus would be in an inactive form.

It is possible that a different set of unknown genes is under the control of PRC than the genes we analyzed by real-time RT-PCR, even though these are the ones induced when quiescent fibroblasts are stimulated to proliferate by serum. I propose to do a microarray on control cells expressing GFP and cells over expressing amino terminally myc-epitope tagged PRC. I think this will yield important information about gene expression profiles in cells producing large amounts of PRC. Even though PRC over production seems to exert no effect on mitochondrial biogenesis, it would still be of interest to determine if it affects cell growth or other important cellular functions. A microarray would provide a good starting point to search for any unknown genes that are regulated by PRC

MATERIALS AND METHODS

Plasmids.

All recombinant adenoviral plasmids were constructed using the AdEasy® Basic Kit from ATCC.

A C-terminal c-myc tag was incorporated into PRC full-length cDNA by PCR using FL-Bam-PRC/pBSII (89) as a template. The following primers were used: S, 5’-AAAAAAGGCCTCACCCTGCCGGAATGACATGAACA-3’; AS, 5’-AAAAAAGATATCTTACAGATCCTCTTCTGAGATGAGTTTTTGTTCCTGGGCCTGTTTC

AA-3'. The resulting plasmid was named Cmyc/pGem-T. The complete insert was sequence verified. The *XhoI/StuI* fragment from FL-Bam-PRC/pBSII and the *StuI/EcoRV* fragment from Cmyc/pGem-T were used in a 3-way ligation into *XhoI/EcoRV* digested pBluescriptII, resulting in CmycPRC/pBSII. CmycPRC/pAdTrack-CMV was generated by cloning the *XhoI/EcoRV* fragment of CmycPRC/pBSII into *XhoI/EcoRV* digested pAdTrack-CMV. CmycPRC/pAdTrack-CMV was then used in a recombination reaction with pAdEasy-1 in AdEasier-1 cells (BJ5186 cells containing pAdEasy-1 plasmid) to produce Ad-CmycPRC.

An N-terminal c-myc tag was incorporated into PRC full-length cDNA by PCR using FL-Bam-PRC/pBSII (89) as a template. The following primers were used: S, 5'-AAAAAATCGATATGGAACAAAAACTCATCTCAGAAGAGGATCTGGCGGCGCGCCGGGGA-3'; AS, 5'-AAAAAAGCTTGGGGGAAGAGGTCTCTAAGAAAGAGGGT-3', hereby generating Nmyc/pGem-T. The complete insert was sequence verified. The *ClaI/HindIII* fragment from Nmyc/pGem-T and the *HindIII/NotI* fragment from FL-Bam-PRC/pBSII were used in a 3-way ligation into *ClaI/NotI* digested pBluescriptII, resulting in NmycPRC/pBSII. NmycPRC/pAdTrack-CMV was generated by cloning the *XhoI/NotI* fragment of NmycPRC/pBSII into *SalI/NotI* digested pAdTrack-CMV. NmycPRC/pAdTrack-CMV was then used in a recombination reaction with pAdEasy-1 in AdEasier-1 cells to produce Ad-NmycPRC.

A *HindIII/DraI* fragment from FL-Bam-PRC/pBSII was cloned into pBluescriptII digested with *HindIII* and *EcoRV*, creating *HindIII/DraI* PRC/pBSII. An N-terminal GAL4 tag was introduced by cloning a *HindIII* GAL4-PRC fragment from FL KIAA/pSG424 into *HindIII/DraI* PRC/pBSII digested with *HindIII*, thereby creating GAL4PRC/pBSII. GAL4PRC/pAdTrack-CMV was generated by cloning a *ClaI(blunt)/NotI* fragment of GAL4PRC/pBSII into *SalI(blunt)/NotI* digested pAdTrack-CMV. GAL4PRC/pAdTrack-CMV

was then used in a recombination reaction with pAdEasy-1 in AdEasier-1 cells to produce Ad-GAL4PRC.

An adenoviral vector expressing untagged PRC cDNA was constructed by cloning a *XhoI/DraI* fragment from FL-Bam-PRC/pBSII into *XhoI/EcoRV* digested pAdTrack-CMV, resulting in FL PRC/pAdTrack-CMV. FL PRC/pAdTrack-CMV was then used in a recombination reaction with pAdEasy-1 in AdEasier-1 cells to produce Ad-FL PRC.

The recombinant adenoviral plasmids Ad-GFP and Ad-PGC-1α were a kind gift from Dr. D. P. Kelly (Burnham institute for Medical Research, Orlando) (55).

The plasmids δ-ALAS(-479)/pGL3 Basic, PRC/pSV-Sport and PGC-1α/pSV-Sport have been described previously (53,89). The pRL-TK control vector was obtained from Promega.

Adenoviral methods.

The adenoviral plasmids Ad-GFP, Ad-PGC-1α, Ad-FL PRC and Ad-Nmyc PRC were linearized with *PacI* and transfected into the packaging cell line HEK293 with Lipofectamine (Invitrogen). The resulting viral stock was amplified to high titer. U2OS or C2C12 cells were infected, and the infection efficiency (95-100%) was determined by GFP expression 24 h after infection. Cells were harvested for preparation of RNA or protein extracts 72 h after infection.

Cell lines and transfections.

C2C12 and U2OS cells were maintained in Dulbecco's modified Eagle's medium (DMEM; Invitrogen) containing 10% fetal bovine serum (HyClone) and 1% penicillin-streptomycin (Invitrogen). 293FT cells (Invitrogen) were cultured in the above medium supplemented with 1mM MEM nonessential amino acids (Mediatech, Inc.) and 500 μg/ml

Geneticin (Invitrogen). Transient transfections of 293FT cells were performed with Lipofectamine 2000 (Invitrogen) according to the manufacturer's instructions. Transient transfections of C2C12 cells were performed by calcium phosphate precipitation as described (89). Cells were plated at a density of 2,600 cells per cm^2 in six-well plates and transfected with 100 ng of δ-ALAS(-479)/pGL3 Basic (89) and 4 ng of pRL-TK control vector (Promega). For *trans*-activation, 2 μg each of full-length PRC (PRC/pSV-Sport) or PGC-1α (PGC-1α/pSV-Sport) were co-transfected. After 5-6 h, cells were washed twice with Dulbecco's phosphate-buffered saline (Invitrogen) and grown for additional 40 h in fresh media. Cell extracts were prepared, and luciferase assays were performed using the dual luciferase reporter assay system (Promega). Firefly luciferase activity from the δ-ALAS(-479)/pGL3 Basic reporter construct was normalized to *Renilla* luciferase luminescence from the pRL-TK control vector.

Immunoblotting.

Whole cell lysates were prepared in NP-40 lysis buffer as described previously (89). Extracts were subjected to denaturing gel electrophoresis and the proteins transferred to nitrocellulose membranes (Schleicher & Schuell) with high molecular weight transfer buffer (50mM Tris, 380mM Glycine, 0.1% SDS, and 20% methanol) in the Mini Trans-Blot Cell tank transfer system (Bio-Rad) for proteins 70kDa or larger, or by using a Trans-Blot SD semidry electrophoretic transfer cell (BioRad) with Towbin transfer buffer (141) for proteins under 70kDa. The following primary antibodies were used: PRC(1047-1379) (99), mouse monoclonal anti-c-myc (clone 9E10) (Roche Applied Science), mouse anti-β-tubulin (Sigma) and rabbit anti-Sp1 (Santa Cruz Biotechnology). All blots were visualized by SuperSignal West Pico chemiluminescent substrate (Pierce Biotechnology).

Real-time RT-PRC analysis.

Total RNA was purified using Trizol reagent (Invitrogen). RNA samples were DNase treated with the TURBO DNA-*free* kit (Ambion) and reverse transcribed into cDNA using the TaqMan reverse transcription reagents (Applied Biosystems). Total genomic DNA was isolated using the GenElute Mammalian Genomic DNA miniprep kit (Sigma). Relative mRNA expression levels and relative mitochondrial DNA copy numbers were determined by Power SYBR Green (Applied Biosystems) quantitative real time PCR using the primer sets shown in **Table 6.5**. Reactions were carried out using the following conditions: an initial step of 2 min at 50°C and 10 min at 95°C, followed by 45 cycles of 15 s at 95°C and 1 min at 60°C. Messenger RNA quantities were normalized to 18S rRNA. The amount of mtDNA (as measured by amplification of the mtDNA-encoded COX1 gene and of a D-loop fragment) was normalized to 18S rDNA. Assays for both the gene of interest and the 18S control were performed in triplicate using an ABI PRISM 7900HT Sequence Detection system. Relative gene expression levels and relative mtDNA copy numbers were determined by the comparative C_T method using SDS 2.1 software (Applied Biosystems).

CHAPTER 8:

FUTURE DIRECTIONS

PRC shRNA-mediated silencing.

To ultimately prove that the mitochondrial defects seen in PRC shRNA#1 cells are due to reduced levels of PRC, we want to rescue these cells by introducing a PRC vector construct that is refractory to hairpin#1. Therefore, we introduced 2 and 4 silent mutations in the region of PRC that is targeted by hairpin#1 using PCR mutagenesis. Currently, we are in the process of constructing both the mammalian expression vector pSV SPORT and the adenoviral vector pAd-Easy-1 containing these mutant forms of PRC. First, we want to transiently transfect shRNA-resistant PRC into control and PRC shRNA#1 U2OS cells to see if we can express the mutant protein and to see if it is resistant to degradation by hairpin#1. If this is the case, we will test for rescue, but low transfection efficiency of U2OS cells might be a problem. Therefore, we are also producing a high titer adenoviral stock of this construct. As mentioned before, U2OS cells are very sensitive to adenoviral infection, and we can obtain 100% infection efficiency (as observed by GFP expression). Real-time RT-PCR will be performed on RNA isolated from control and shRNA#1 cells infected with Ad-GFP and with adenovirus expressing mutant PRC. We will check if some transcripts that were reduced in PRC shRNA#1 cells are increased in PRC shRNA#1 cells expressing PRC refractory to degradation. In addition, we plan to perform immunoblotting and dipstick assays to check if respiratory subunit and enzyme levels are restored. Rescue of the mitochondrial phenotype by expression of shRNA-resistant PRC will prove directly that PRC is responsible. Inability of the mutant PRC transcripts to be expressed in shRNA#1 cells would indicate that hairpin#1 can degrade PRC transcripts even when there is

incomplete complementarity between the hairpin and PRC mRNA. Induction of mutant PRC mRNA but not of PRC protein would indicate that hairpin#1 functions more on a translational than on a transcriptional level. Unfortunately, a rescue experiment would not be possible in that case. However, it would also be useful to evaluate PRC silencing in the context of a different cell line. I have already infected BALB/3T3 fibroblasts, a serum-responsive mouse cell line, with lentivirus expressing PRC short hairpin RNA#1 and #4, lamin shRNA, and the negative control shRNA. Individual clonal isolates are stored in liquid nitrogen, ready to be tested. A similar phenotype upon knockdown of PRC in these cells from a different species will convince us that PRC is directly responsible and will support the biological significance of these effects.

We also need to further characterize the knockdown cells. What is the mechanism for mitochondrial proliferation in PRC shRNA#1 cells? What genes are responsible? How does PRC affect the level or function of those genes? How does PRC affect cell proliferation?

If the genes identified in the microarray are altered by PRC silencing, it is possible that they are direct targets for *trans*-activation by PRC, either through NRF-1 or other (unknown) transcription factors. Lack of PRC will thus cause a major reduction in mRNA expression levels of those genes. To test this hypothesis, we isolated putative promoter fragments of selected genes that were promising candidates for PRC *trans*-activation. Promoters of host cell factor-1 regulator 1 (HCFC1R1), annexin A10 (ANXA10), dynactin 6 (DNCT6), cell cycle-dependent kinase 6 (CDK6), transforming growth factor, beta induced (TGFBI), and several histone genes were chosen for cloning into the pGL3Basic luciferase reporter construct. The effects of PRC on promoter function were assayed by co-transfection of these constructs with the PRC-expressing vector FL PRC/pSV-Sport. Preliminary data (not shown) revealed PRC was able to *trans*-

activate the promoters of dynactin 6, host cell factor regulator 1, cell cycle-depent kinase 6 and ras-related C3 botulinum toxin substrate 2. The current data remains inconclusive about *trans*-activation of annexin A10 and of several histone gene promoters by PRC.

To examine the protein expression of some of the regulatory genes important for mitochondrial function, we performed a series of immunoblots **(Figure 8.1)**. Similar levels of regulatory factors are detected in cell extracts from the wild-type U2OS cells, control shRNA and PRC shRNA#4 transductants. This suggests that there are no major differences in the expression of these proteins in these cells. A notable exception is Sp1, which shows slightly diminished expression in PRC shRNA#4 cells. However, the PRC shRNA#1 transductant exhibits severely diminished or undetectable levels of NRF-1, CREB, P-CREB and Sp1, and modestly reduced levels of NRF-2α, NRF-2β, and Tfam. As previously shown in **Figure 6.2B**, PGC-1α protein is undetectable by immunoblotting in all cell lines tested. The reduced levels of major transcription factors in the PRC shRNA#1 cells is not a result of a general inhibition of translation in these cells since β-actin levels **(Figure 8.1)** and lamin A/C levels **(Figure 6.2A)** are similar to the levels in control shRNA cells. The reduced levels of these proteins correlate with reduced transcripts levels **(Figure 6.6A)** although the changes in protein expression are quantitatively larger. The reasons for the discrepancy between mRNA and protein for these transcription factors are unclear but may reflect gene-specific differences in transcription and post-transcriptional controls. PRC may control steady-state expression of transcription factors also through affecting some aspects of protein degradation or the mitochondrial or cytosolic translation machinery. There is evidence for decreased mRNAs of several genes functioning in mitochondrial import and assembly and mitochondrial translation in the microarray analysis of

PRC deficient cells. PRC might also act as “glue” holding transcription factor complexes together on DNA, and its absence might cause disintegration of the complex and target unbound proteins for degradation. It is also possible that PRC affects the expression of transcription factors involved in mitochondrial function by down regulating histone transcripts as demonstrated in the microarray. Perturbations in histone structure might target these factors for degradation. The dramatic down regulation of these transcription factors by PRC silencing is surprising but is probably at least partially responsible for the impaired respiratory growth of shRNA#1 cells.

Figure 8.1. PRC silencing dramatically reduces regulatory protein levels important for mitochondrial function.

Whole cell extracts were prepared from wild type U2OS cells (wt), and from stable lentiviral transductants expressing the control shRNA, lamin shRNA, PRC shRNA#1 or PRC shRNA#4, and subjected to immunoblotting following denaturing gel electrophoresis. NRF-1, NRF-2α, NRF-2 β, CREB, P-CREB, Sp1, Tfam, PGC-1α and β-actin proteins were detected using rabbit anti-NRF-1, rabbit anti-NRF-2α, rabbit anti-NRF-2β, rabbit anti-CREB, rabbit anti-phospho-CREB, rabbit anti-Tfam, rabbit anti-PGC-1α and mouse anti-β-actin antibodies, respectively. In a separate panel, an immunoblot is shown from cell extracts from Ad-GFP and Ad-PGC-1α infected U2OS cells to demonstrate the PGC-1α-specific band.

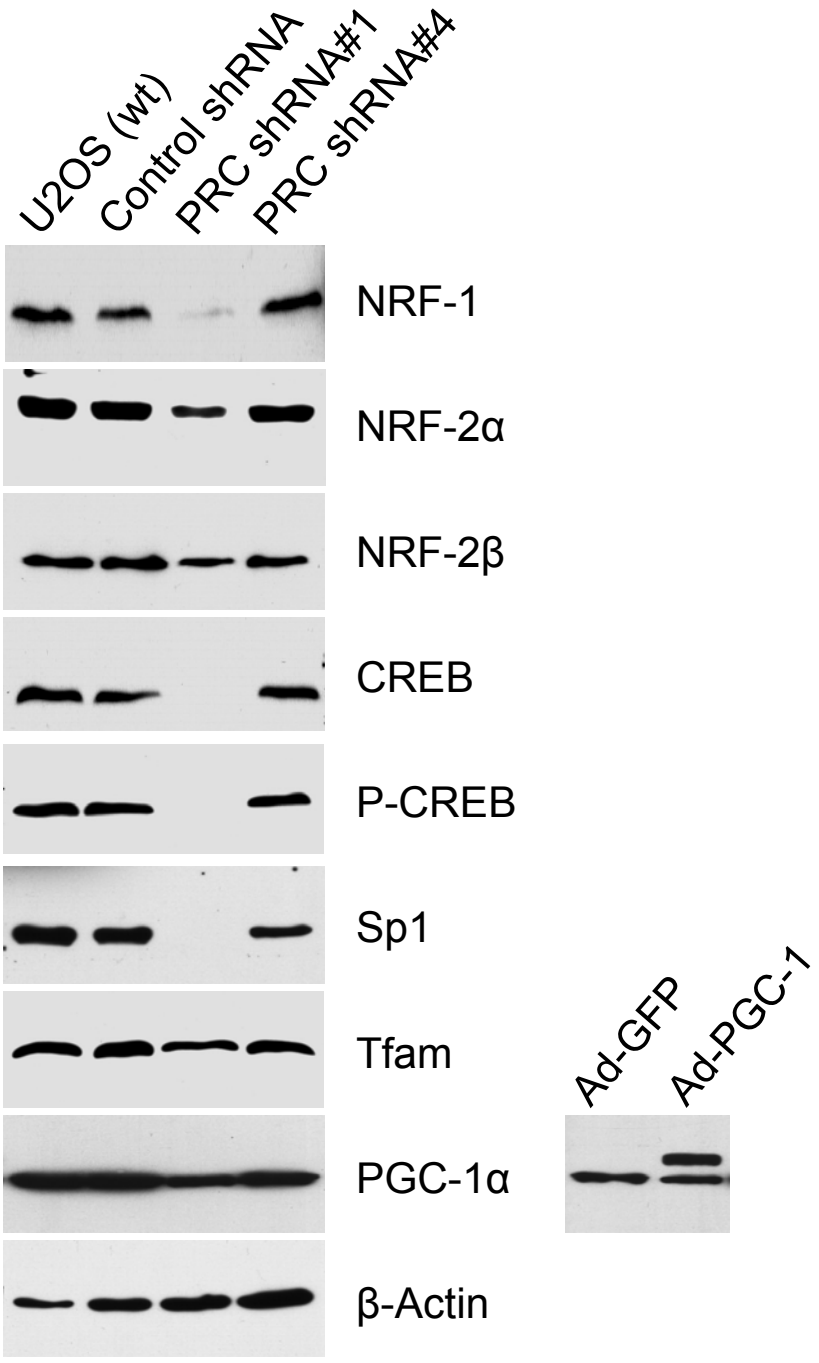
U2OS (wt)
Control shRNA
PRC shRNA#1
PRC shRNA#4
NRF-1
NRF-2α
NRF-2β
CREB
P-CREB
Sp1
Tfam
PGC-1α
β-Actin
Ad-GFP
Ad-PGC-1

It is also interesting to note that when we transiently transfected 293FT cells with control or PRC shRNA#1 entry vectors, we saw a number of increased transcripts in cells expressing pENTR/PRC shRNA#1 **(Figure 8.2)**, in striking contrast to the decreases of the same transcripts in the stably transduced PRC shRNA#1 U2OS cells. This leads us to speculate that there is some form of feedback mechanism in the cell that is trying to compensate for the loss of PRC by up regulating PRC target genes. This seems to be only a short term effect upon PRC deficiency. We think the stable transductants cannot overcome the long-term lack of PRC, causing down regulation of PRC targets instead. This putative feedback loop provides us with an interesting new angle for further studies.

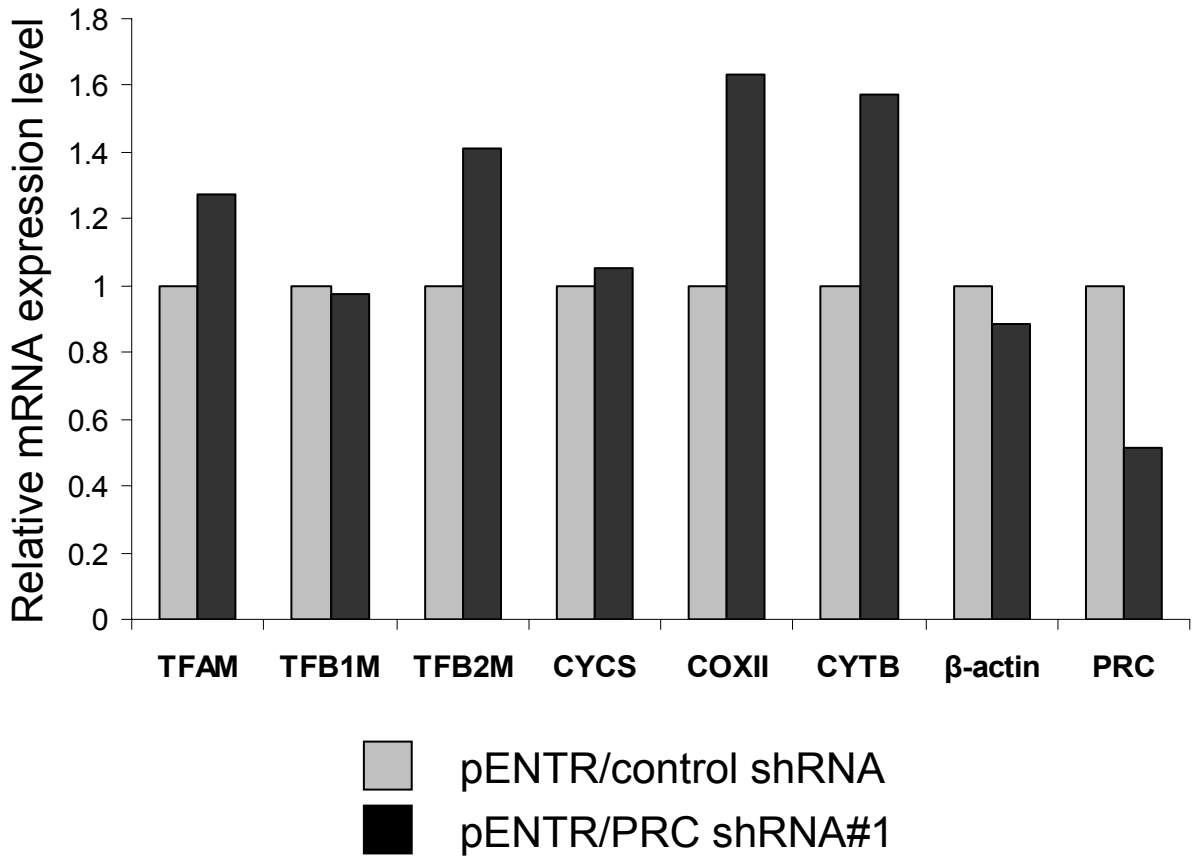

Figure 8.2. Real time RT-PCR analysis of 293FT cells exhibiting transient silencing of PRC. 293FT cells were transfected with pENTR/control shRNA and pENTR/PRC shRNA#1 constructs and relative gene expression was monitored by real-time RT-PCR. Relative steady-state mRNA levels were normalized to 18S rRNA as an internal control and values expressed relative to pENTR/control shRNA transfections, which were assigned a value of 1. The bars represent the average of two independent determinations.

The morphology of PRC shRNA#1 cells under a light microscope was different from control cells. Whereas control cells are more elongated, cells lacking PRC seemed more spread out and often had the appearance of a fried egg. We also observed the presence of very large cells in shRNA#1 transductants. We were interested to study these large cells in the absence of more normal looking cells. Therefore, we performed a re-selection of PRC shRNA#1 transductants in order to obtain clones containing only giant cells. We were unable to isolate such clones. Instead, all re-isolated shRNA#1 clones contained giant cells to a different degree, representing an estimated 2-15% of the cell population. **(Figure 8.3)**. Most of these large cells contained a single, but very large nucleus, although some of the cells were bi-nucleated. Isolates with more giant cells seemed to grow more slowly, but the presence of abnormal cells did not seem to change over time, suggesting they were either able to divide or arise from normal looking cells over time. Staining of these different clonal isolates for cytochrome oxidase activity revealed a mixture of COX positive and negative cells **(Figure 8.4)**, with varying ratios of stained to unstained cells. Remarkably, clone#6 was almost exclusively COX negative. Both COX positive and negative giant cells were observed, suggesting that the giant cell phenotype is not linked to the respiratory phenotype. Currently, four giant cell types have been described: Langhans giant cells, foreign body giant cells, osteoclast and HIV-1 induced $CD4^{+}$-T-cell derived syncytia. (195,196). However, these cells are all multinucleated, in contrast to PRC shRNA#1 giant cells, where we usually observe a single giant nucleus and occasionally two nuclei per cell. This rather suggests a defect in cell division. Analysis of DNA content of these cells by flow cytometry did not show any evidence for polyploidy **(Figure 6.5 and not shown)**. This is rather surprising, as we suspected these cells with enlarged nuclei would have increased DNA content. DNA content has long been considered to be strongly correlated with nuclear

volume and cell volume (197). However, recent reports in budding and fission yeast demonstrated that DNA content did not directly influence the size of the nucleus (198) (199). Instead, these studies found that in yeast nuclear size seems to be directly controlled by the amount of "surrounding" cytoplasm. Perhaps nuclear size and DNA content are not positively correlated in these enlarged cells, explaining why we are not detecting polyploidy.

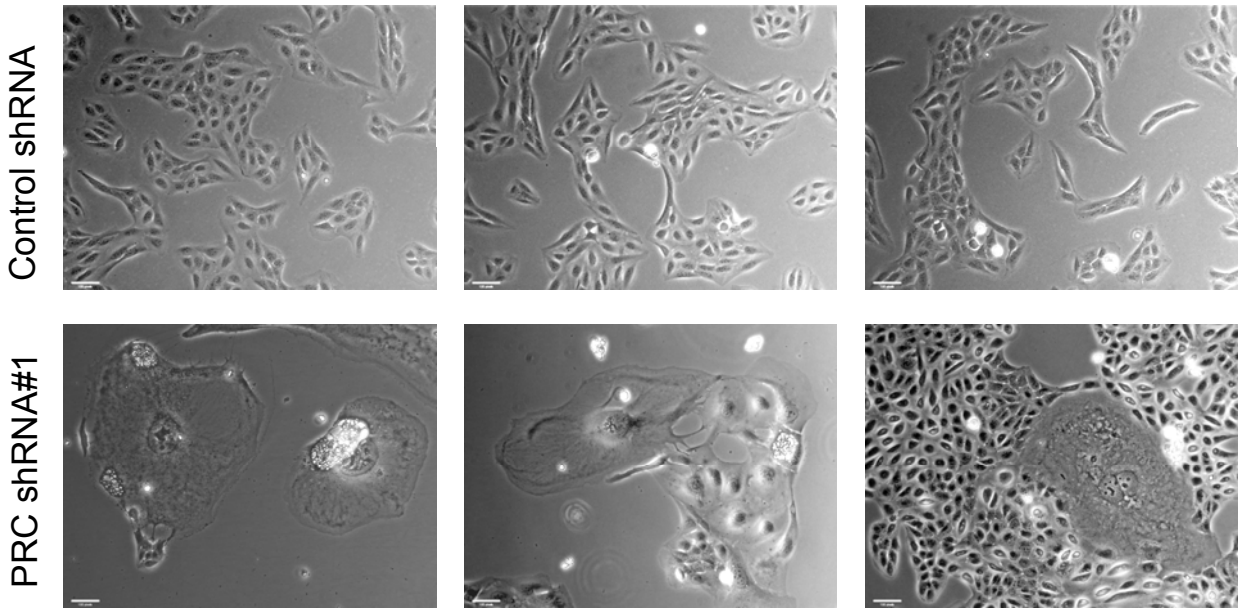

Figure 8.3. Morphology of PRC shRNA#1 transductants.

Phase-contrast images are shown for exponentially growing control shRNA cells (top) and PRC shRNA#1 cells (bottom) under a 10x objective.

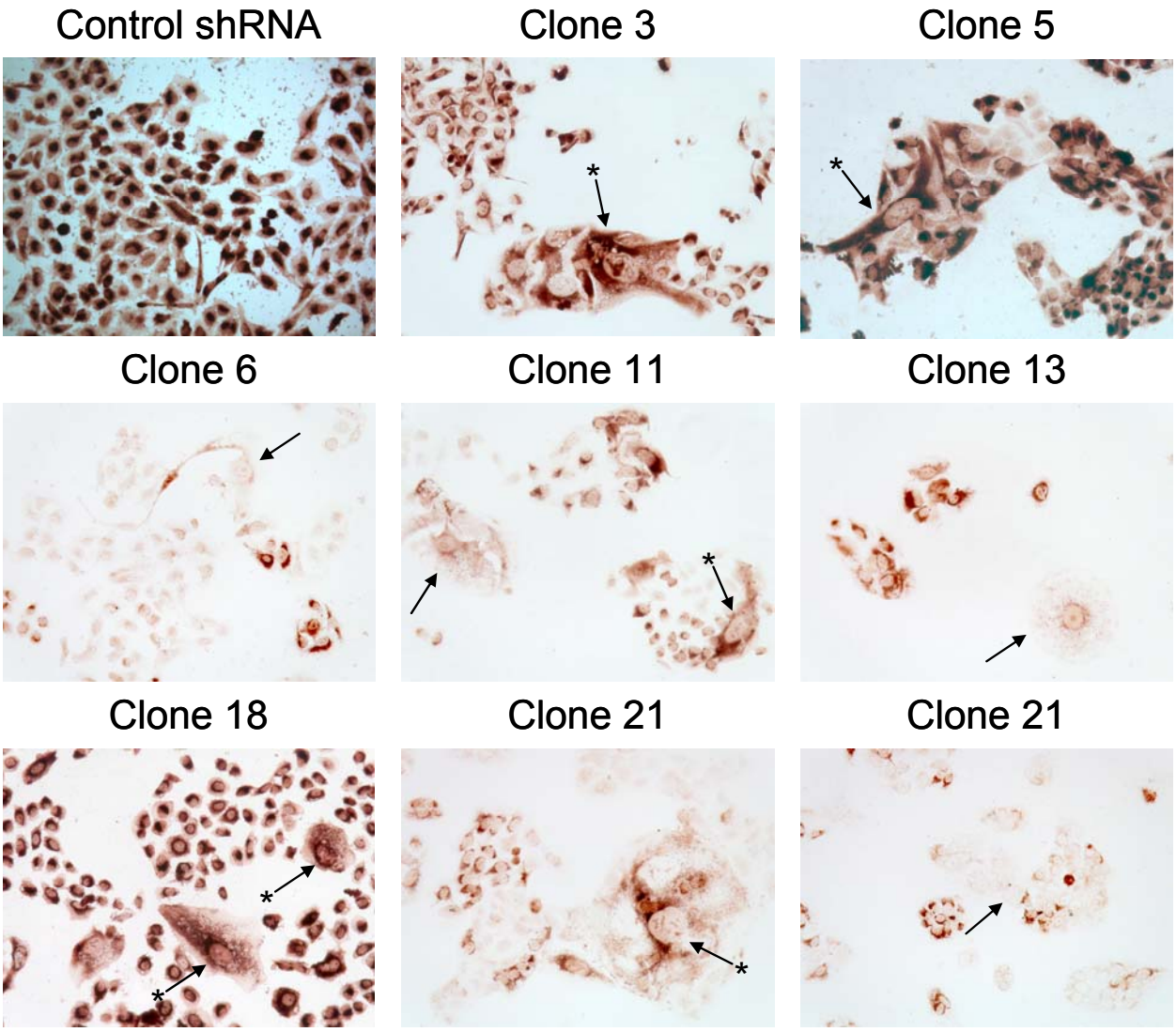

Figure 8.4. COX histochemistry of PRC shRNA#1 transductants.

Control shRNA cells and re-selected shRNA#1 clones 3, 5, 6, 11, 13, 18 and 21 were stained for cytochrome oxidase activity. Arrows point to enlarged cells. An asterisk indicates COX positive staining.

The altered morphology of PRC deficient U2OS cells in the phase-contrast images prompted us to look at the cytoskeletal and nuclear organization in these cells. To examine the distribution of F-actin and DNA, we used rhodamine-conjugated phalloidin (a kind gift from Dr. Jonathan Jones, Northwestern University) to label filamentous actin and DAPI (a kind gift from Dr. Sui Huang, Northwestern University) to label DNA. As shown in **Figure 8.5A**, control cells exhibited well-organized, mostly parallel actin filaments and uniform DAPI staining. In contrast, the majority of PRC shRNA#1 cells **(Figure 8.5B)** displayed an altered F-actin network, consisting of more disorganized and circular filaments. DAPI staining of the transductants lacking PRC also revealed several abnormalities. As in the phase-contrast images, we observed the presence of giant nuclei, some estimated to be eight times the size of normal looking nuclei. Frequently, disruptions in nuclear shape were detected. Some nuclei were highly lobulated and misshapen, with prominent nuclear herniations evident. This was not seen in control shRNA cells.

Figure 8.5. Localization of F-actin and DNA in control shRNA and PRC shRNA#1 transductants.

A. Exponentially grown control shRNA cells were labeled with rhodamine phalloidin and DAPI to visualize the F-actin network and DNA, respectively.

B. Exponentially grown PRC shRNA#1 cells were stained with rhodamine phalloidin and DAPI. Corresponding rhodamine-phalloidin (*red*, left panels), DAPI (*blue*, center panels) and merge images (right panels) are presented.

A

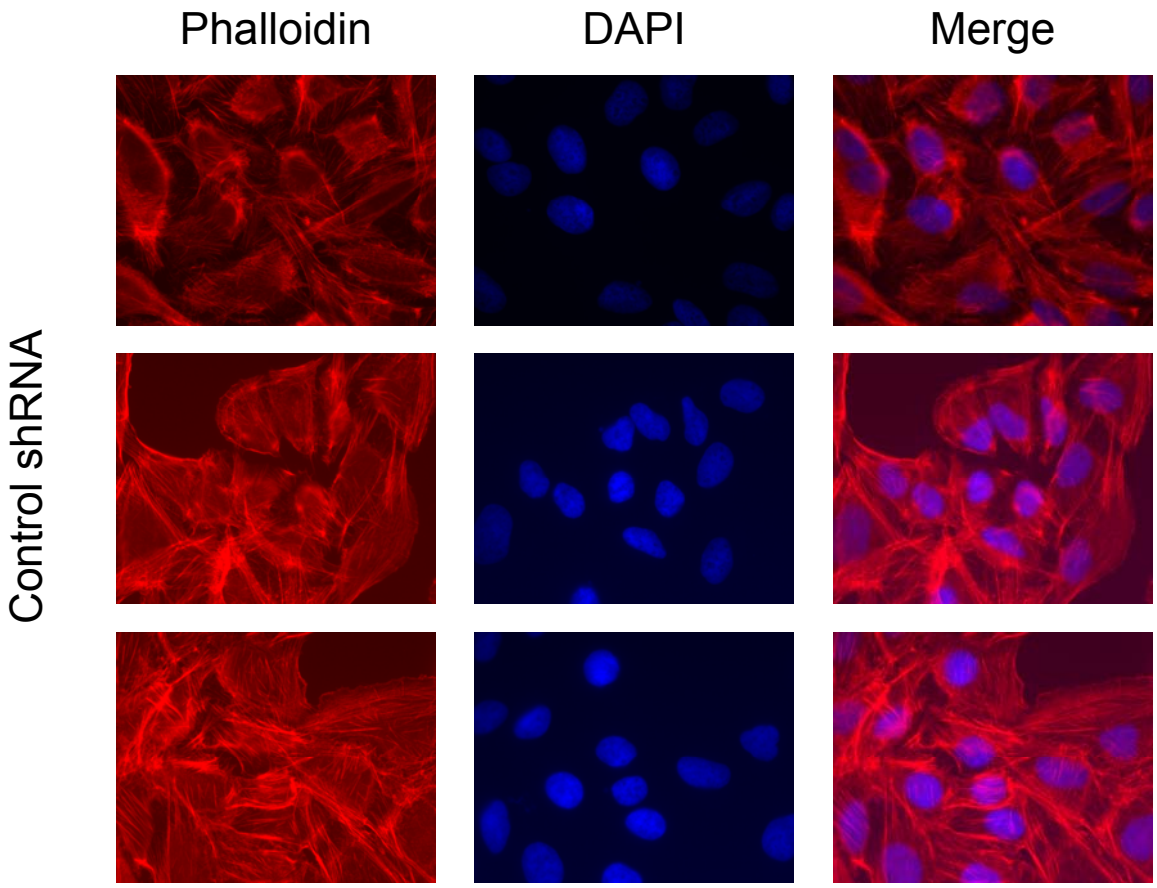

B

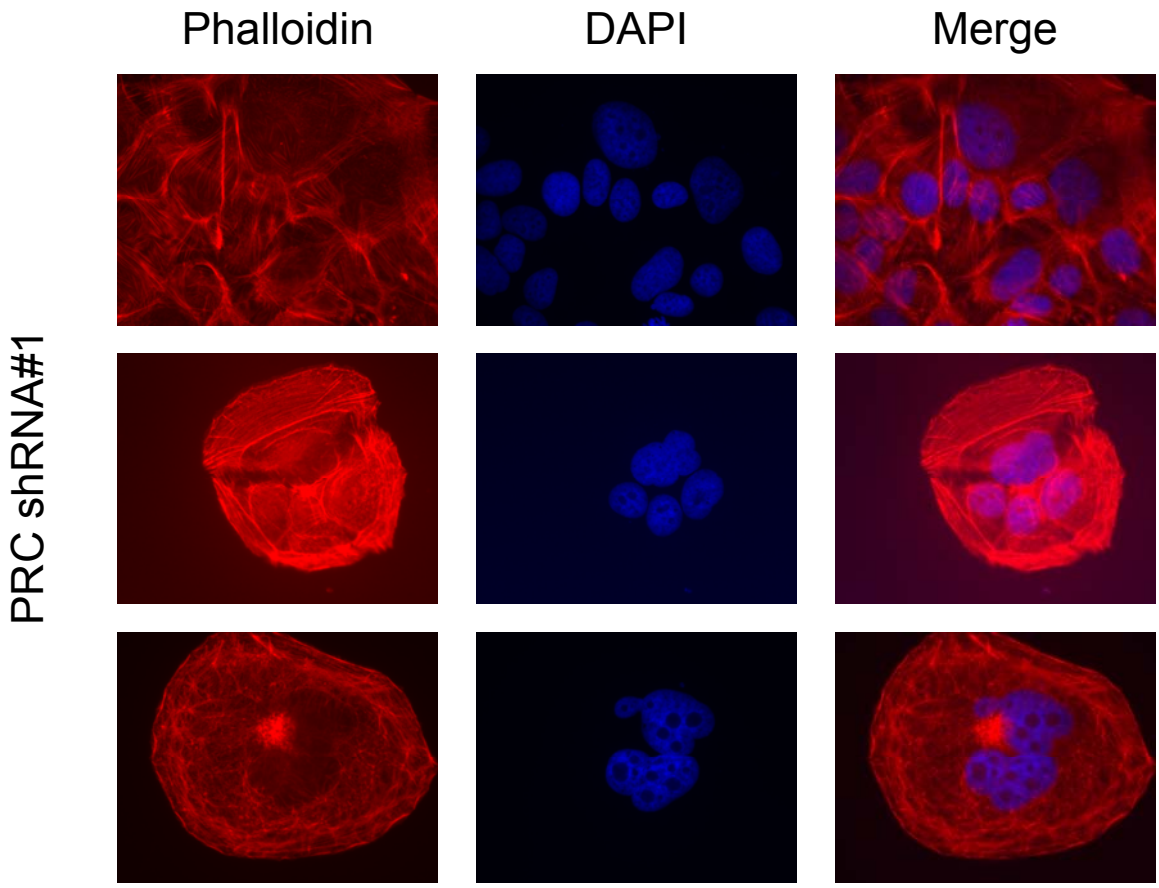

The reorganization of actin filaments in cells lacking PRC is not unexpected. Mitochondria are extremely dynamic and constantly fuse, divide, and move along cytoskeletal elements within the cell. Interaction of mitochondria with cytoskeletal elements appears to be critical for all mitochondrial processes (200). Thus, it is not so surprising that the morphology of both the cytoskeleton and mitochondria is altered by PRC silencing. The microarray study of PRC shRNA#1 and #4 compared to control cells identified many differentiated genes implicated in the regulation of the actin cytoskeleton, and is consistent with the phalloidin staining. In addition, the expression of other cytoskeletal components was also altered in cells lacking PRC as revealed by microarray analysis. It would be of interest to further characterize these and other cytoskeletal changes by labeling other components of the cytoskeleton in the PRC shRNA#1 transductants. Further studies are also needed to define the mechanism through which PRC causes alterations in cytoskeletal architecture.

Adenoviral over expression

Although there was no evidence for increased mitochondrial biogenesis upon PRC over expression by adenovirus as assessed by real-time RT-PCR analysis of NRF target genes or mtDNA copy number **(Figure 7.4 and data not shown)**, it is necessary to determine more directly if PRC alone is sufficient to induce mitochondrial proliferation. Therefore, we want to stain cells over expressing PRC and GFP-expressing control cells with MitoTracker CMXRos, a membrane potential-sensitive dye (201), and do flow cytometric analysis. An increase in MitoTracker fluorescence is indicative of proliferation of functional mitochondria. We cannot label adenovirus-infected cells with MitoTracker Green FM, a membrane potential-independent dye (201), since all our adenoviral constructs co-express GFP. GFP and MitoTracker Green FM

cannot be visualized together because both fluorophores emit green fluorescence upon excitation. It is possible that expression of PRC is not sufficient to drive mitochondrial proliferation, even though the two other members of the PGC-1 coactivator family, PGC-1α and PGC-1β, are.

If the gene transcripts altered by PRC silencing are true targets of PRC, we expect the expression level of at least a subset of these genes also to be altered by over expressing PRC. To test this, we will assay a few genes that were changed most robustly in the microarray study described in **Chapter 6** by real-time RT-PCR analysis of cells over expressing PRC.

To compare global gene expression patterns between cells over producing PRC and control cells, we will need to perform a microarray analysis of Ad-Nmyc PRC- and GFP-expressing cells. Due to the costly nature of this type of analysis, we will only attempt this if we are certain that we can over express functional PRC protein.

PRC promoter studies

As previously mentioned, we have determined by PRC mRNA half-life studies and nuclear run-on assay that the rapid induction of PRC in response to serum occurs mostly through increased transcriptional initiation, and not through regulated stabilization of PRC mRNA **(Chapter 5)**. In order to investigate how mitogens can regulate PRC expression, we wanted to test if PRC promoter activity is also up-regulated upon serum induction and which elements in the PRC promoter contribute to serum responsiveness. Before we can determine this, it is necessary to identify the transcription initiation site(s) of the PRC gene and to isolate the PRC promoter.

In order to identify the PRC promoter, we searched the NCBI database with the 5' end of the mouse PRC cDNA, and found a sequence upstream of that encompassing the putative mouse

PRC promoter. In a similar way we found the putative human PRC promoter. In general, it is reasonable to assume that the promoter should be included in a fragment about 1000 bp upstream of the putative transcription start site. This upstream PRC fragment was amplified by PCR and cloned into the luciferase reporter construct pGL3-Basic (Promega, USA). After sequence-verification, basal promoter activity of this PRC fragment was assayed by transient transfection of Balb/3T3 cells. Surprisingly, this promoter fragment was not active (not shown). It is possible that PRC has a rather weak basal promoter, and that its activity is dramatically increased by serum. Therefore, we also tested the serum inducibility of this promoter construct in Balb/3T3 cells. Under these circumstances, this upstream fragment of PRC also showed no promoter activity (not shown). Thus, we concluded that this sequence does not constitute the true PRC promoter.

The previous mRNAs for mouse and human PRC found in the NCBI database started ~10 bases upstream of the AUG. Upon re-examination of the database, we found more recently deposited longer mRNAs for human PRC **(Figure 8.6, upper blue arrow)** and mouse PRC **(Figure 8.6, lower blue arrow)**. Alignment of the human and mouse PRC 5' region showed a very high degree of homology that extended upstream to at least the start of the mouse mRNA, > 100 bp upstream of the AUG, suggesting that the mRNA sequences deposited in the database are probably not complete, and that the true 5' end of PRC mRNA is more upstream.

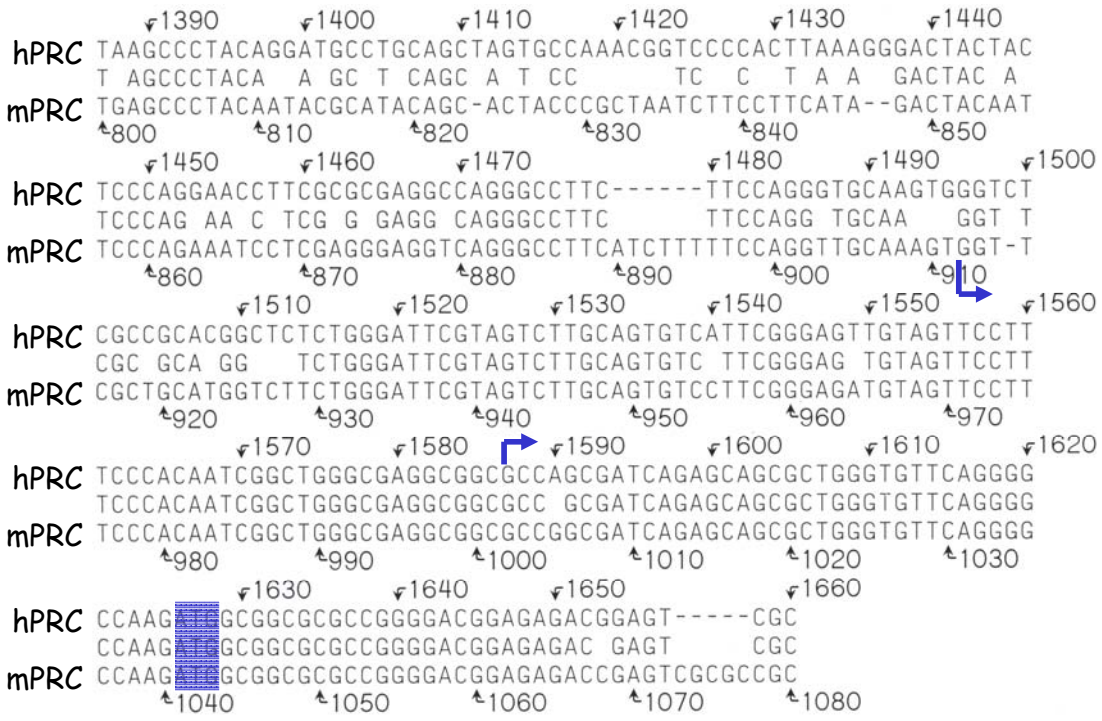

Figure 8.6. Alignment of the human and mouse PRC 5' region.

5' flanking mouse (*bottom*) and human (*top*) PRC sequences were aligned with the DNAseq program MegAlign. The middle line shows all overlapping positions. The AUG codon is marked in blue. The upper blue arrow indicates the start site of human PRC mRNA found in the NCBI database, the bottom blue arrow indicates the start site of mouse PRC mRNA in the NCBI database.

In order to find the true 5' start of PRC mRNA, we decided to do reverse transcription of total RNA isolated from mouse (liver and Balb/3T3) cells and human (HeLa) cells primed with oligod(T) as well as random hexamers, followed by PCR with an antisense primer from PRC exon 1 and sense primers progressively further removed from the known 5' end of the mouse and human mRNA. A schematic representation of the resulting PCR products is seen in **Figure 8.7A and B.** RNA that was reverse transcribed in the absence of reverse transciptase enzyme did not produce any PCR products, confirming these products are not derived from genomic DNA. Longer UTRs are often found in mRNAs encoding proteins that need to be tightly regulated, such as growth factors and transcriptional regulators, and are implicated in translational control (202). Since PRC is tightly regulated by serum, the presence of this relatively long UTR is thus not so surprising. It is also common for mRNAs encoding regulatory proteins to contain upstream open reading frames (202). Examining PRC mRNA revealed the presence of an ORF upstream of PRC exon 1.

Due to time constraints and involvement in other projects, the search for the true transcription start site of the PRC gene was discontinued. It would be interesting to pick up this project again to identify the start of mouse and human PRC mRNA. We can continue doing this with PCR analysis of reverse-transcribed total RNA with progressively upstream primers and further confirm the results by 5'RACE or primer extension. Upon finding the PRC transcription start site, the PRC promoter region can then be more accurately identified and be tested as described above. In future experiments we will continue to identify the elements in the PRC promoter contributing to the serum-responsiveness of PRC, and possible other elements that contribute to the regulation of PRC.

Figure 8.7. Identification of the 5' UTR of the mouse and human PRC gene.

A. Schematic representation of the mouse PRC gene upstream flanking region with sense and antisense PCR primers indicated at bottom and top. Weak and strong donor and acceptor splice sites are color-coded. A putative promoter region identified with the PromoterInspector algorithm from www.genomatix.de is framed by a dashed line. PCR products resulting from mouse fibroblast RNA that was reverse transcribed with oligod(T) or random hexamers are indicated by a solid black line.

B. Schematic representation of the human PRC gene upstream flanking region with sense and antisense PCR primers indicated at bottom and top. Weak and strong donor and acceptor splice sites are color-coded. PCR products resulting from HeLa RNA that was reverse transcribed with oligod(T) or random hexamers are indicated by a solid black line.

A

Mouse PRC gene upstream region

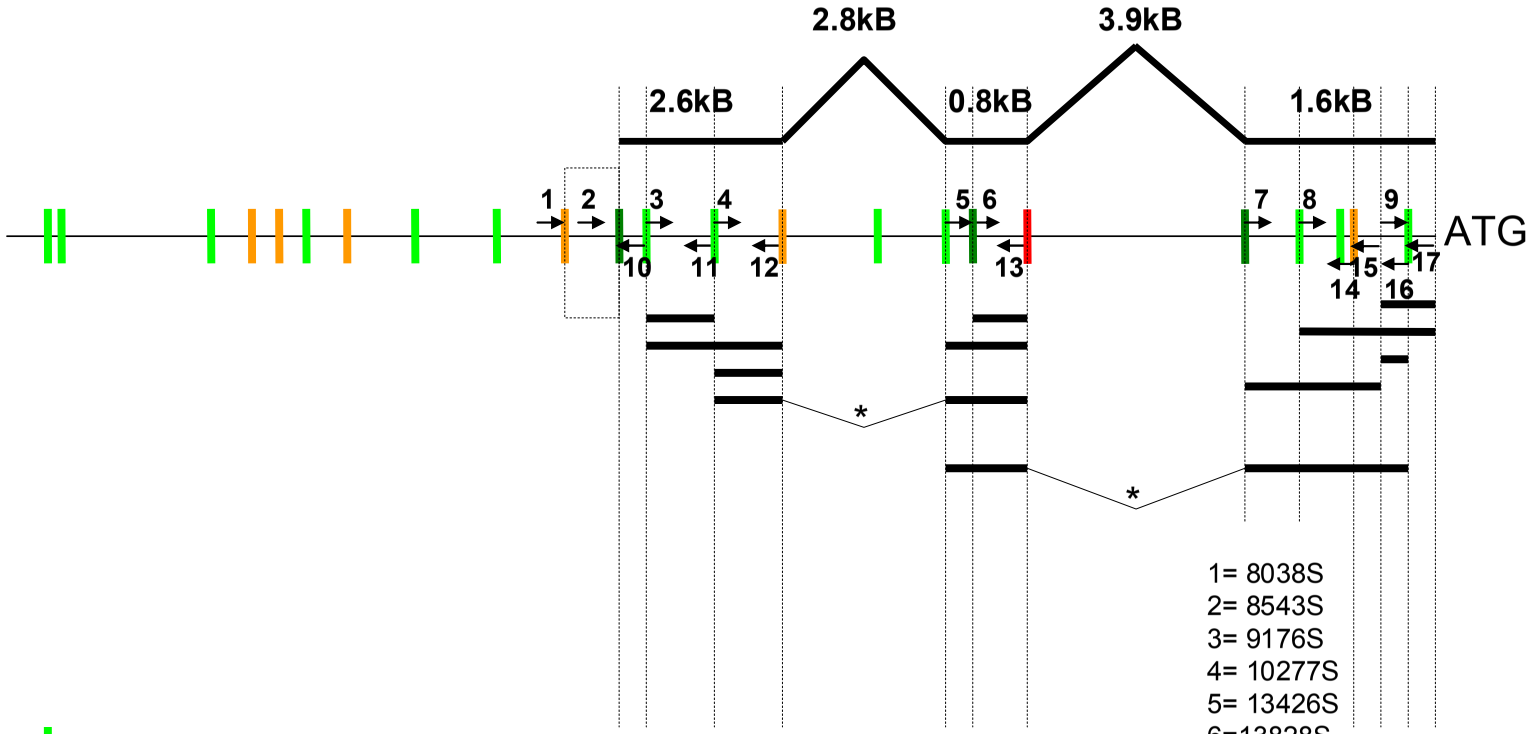

= weak acceptor

= strong acceptor

= weak donor

= strong donor

= predicted promoter (PromoterInspector on www.genomatix.de)

* after 2nd round of PCR

1= 8038S
2= 8543S
3= 9176S
4= 10277S
5= 13426S
6=13828S
7= 1938S
8= 2422S
9= 2972S
10= 9095AS
11= 9709AS
12= 10639AS
13= 14188AS
14= 18287AS
15= 18543AS
16= 205AS
17= PRCEX1nested AS

B

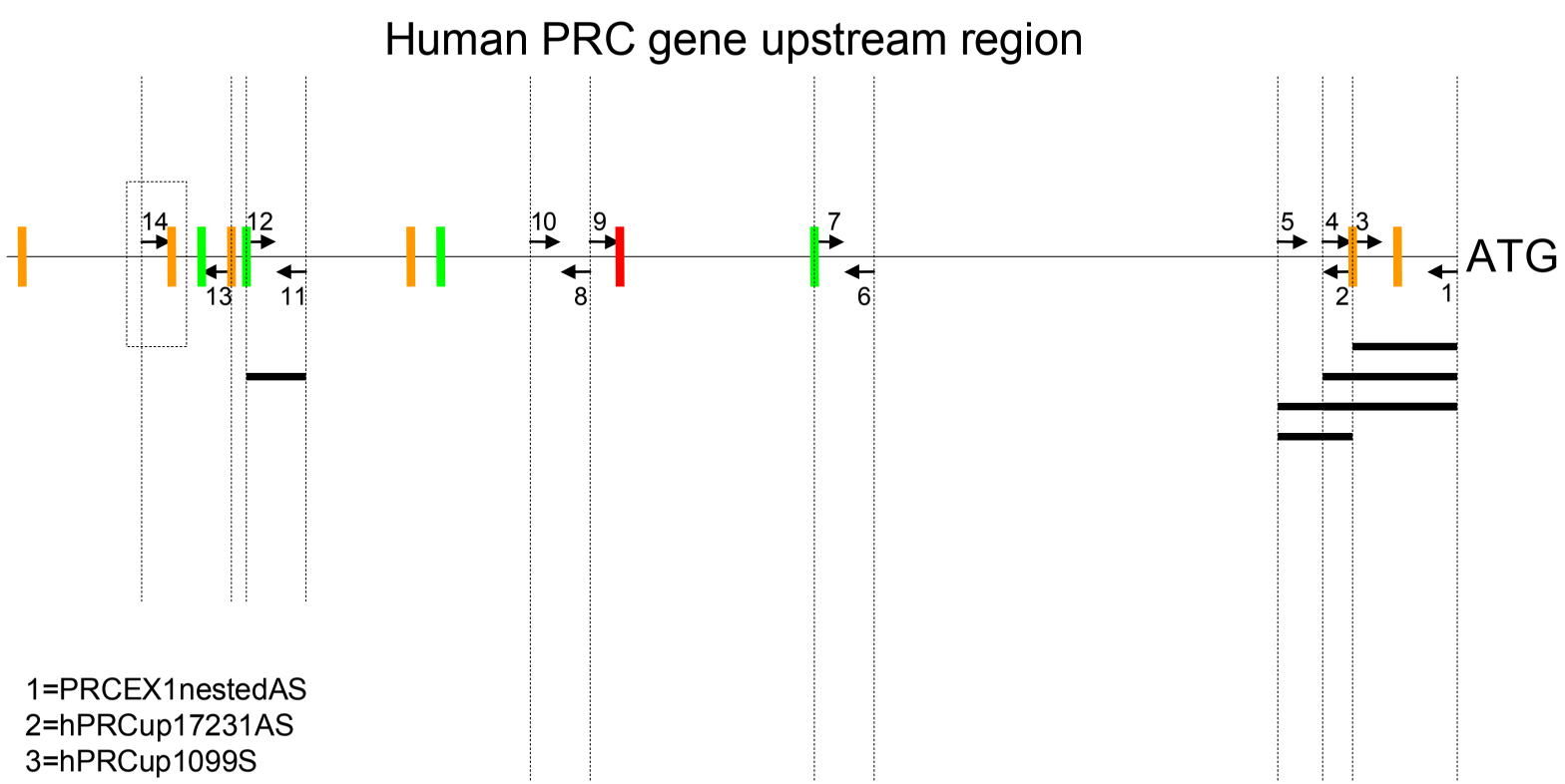

1=PRCEX1nestedAS
2=hPRCup17231AS
3=hPRCup1099S
4=hPRCup1017S
5=hPRCup877S
6=hPRCup14036AS
7=hPRCup13566S
8=hPRCup10382AS
9=hPRCup10428S
10=hPRCup10145S
11=hPRCup6969AS
12=hPRCup6697S
13=hPRCup6112AS
14=hPRCup5284S

= weak acceptor

= strong acceptor

= weak donor

= strong donor

MATERIALS AND METHODS

Plasmids.

Site-directed mutagenesis of PRC in the region targeted by shRNA#1 was performed by PCR utilizing FL PRC/pBSII (89) as template. Pairs of internal overlapping oligonucleotides with the desired mutations along with flanking PRC primers (hPRC 3601S: 5'-GACAGCTTGGCTGTAGGAAAC-3', PRCStuI asen: 5'-GGCAGGGTGAGGCCTCAGGGGACAGCA-3') were used to generate mutations (117). After verifying all site-directed mutations by sequencing, the PRC fragments containing the mutations were re-inserted as *AgeI-StuI* fragments into FL PRC/pBSII. Sense (S) and antisense (AS) mutagenesis primers with mutated nucleotides underlined are as follows:

Sh1mut2 (S) GTCAAGCGCCATCAAGATATCACCATCA

Sh1mut2 (AS) TGATGGTGATATCTTGATGGCGCTTGAC

Sh1mut4 (S) GTCAAGCGCCACCAAGATATCACAATCA

Sh1mut4 (AS) TGATTGTGATATCTTGGTGGCGCTTGAC

The *XhoI*/*NotI* fragments of the resulting plasmids FL PRCsh1mut2/pBSII and FL PRCsh1mut4/pBSII, containing the full length PRC cDNA with the mutations, were then cloned into pSV SPORT and pAdTrack-CMV digested with *SalI/NotI*, resulting in FL PRCsh1mut2/pSV SPORT and FL PRCsh1mut4/pSV SPORT, and FL PRCsh1mut2/pAdTrack-CMV and FL PRCsh1mut4/pAdTrack-CMV, respectively.

Immunoblotting.

Immunoblotting was performed as described previously **(Chapter 6, "Materials and Methods")** (100).The following primary antibodies were used: rabbit anti-PRC (1047-1379)

(99), rabbit anti-Lamin A/C (a kind gift from Dr. R.D. Goldman, Northwestern University, Chicago) (186), rabbit anti-PGC-1α (a kind gift from Dr. D.P. Kelly, Burnham institute for Medical Research, Orlando) (55), rabbit anti-NRF-1 (113), rabbit anti-NRF-2α, rabbit anti-NRF-2β, rabbit anti-CREB (Santa Cruz Biotechnology), rabbit anti-phospho-CREB (Upstate Biotechnology), rabbit anti-Tfam, and mouse anti-β-actin antibodies (Sigma).

Light and Fluorescent Microscopy.

Exponentially growing cells were visualized under phase-contrast with a 10x objective, for a total magnification of 100x, with a Leica DMIRE2 inverted microscope (Leica Microsystems) using Openlab software (Improvision). For labeling, exponentially growing cells were cultured on glass coverslips. They were fixed with 3.7% formaldehyde followed by permeabilization with 0.2% Triton X-100. Cells were stained with rhodamine phalloidin (Invitrogen) at a 1:100 dilution for 1 h at 37°C, washed with PBS and subsequently stained with 4',6-diamidino-2-phenylindole (DAPI; Sigma) at a 1:5000 dilution (1mg/ml) for 1 min at RT. Coverslips were mounted with VectaMount AQ (Vector Laboratories) and examined with a Nikon Eclipse E800 epifluorescent microscope equipped with a SenSys cooled CCD camera (Photometrics). Images were captured using MetaView image acquisition software (Universal Imaging).

COX staining.

COX histochemistry was performed exactly as described in **Chapter 5 "Materials and Methods"** (166). The coverslips were examined with an upright Leica microscope (Leica Microsystems) under a 20x objective.

Real time RT PCR analysis.

This was done exactly as described in **Chapter 6 "Materials and Methods"** (100).

ACKNOWLEDGMENTS

We are grateful to Dr. Jonathan Jones (Northwestern University) for sharing rhodamine-conjugated phalloidin and Dr. Sui Huang (Northwestern University) for sharing DAPI and her fluorescent microscope.

SUMMARY AND CONCLUSION

Most of the genes important for mitochondrial function are not encoded by the mitochondrial genome due to its size limitations, but instead are encoded by the nuclear genome. Examples include subunits of the respiratory chain, mitochondrial transcription and replication factors, and import and assembly factors. The synthesis of all these proteins has to be under tight control to ensure proper execution of mitochondrial function. The current three members of the PGC-1 family of transcriptional coactivators, PGC-1α, PGC-1β, and PRC, have been targeted for their involvement in mitochondrial biogenesis. The well-studied member PGC-1α is known to be a master regulator of energy metabolism. It has been shown to interact with a variety of transcription factors that regulate different aspects of cell metabolism and can thereby integrate multiple transcriptional pathways controlling mitochondrial biogenesis in response to environmental stimuli. Of particular interest is its interaction with key transcription factors stimulating mitochondrial genes such as NRF-1, NRF-2 and ERRα. Notably, PGC-1α is induced only by distinct environmental stimuli such as cold exposure, fasting and exercise, suggesting the existence of additional factors controlling mitochondrial function under different circumstances demanding increased energy production. Furthermore, even though gain-of-function studies in cultured myoblasts and myocytes and in transgenic mice demonstrate that PGC-1α and PGC-1β are powerful inducers of mitochondrial proliferation and activate respiratory subunit genes, loss-of-function studies of PGC-1α or PGC-1β in mice display much milder effects. Animals lacking these coactivators are viable and have very weak mitochondrial phenotypes, exacerbated by stress, indicating that although PGC-1α and PGC-1β are important for energy metabolism, they are not required for mitochondrial biogenesis or maintenance. This also indicates that other

factors are able to compensate for the loss of either PGC-1α or PGC-1β. Recently, a double knockout mouse was created lacking both PGC-1α and PGC-1β. Not surprisingly, defects in these animals are much more severe. They die shortly after birth as a result of heart failure, and exhibit an arrest in perinatal mitochondrial biogenesis in the heart and brown adipose tissue. This indicates PGC-1α and PGC-1β share important functions but also serve complementary roles.

Our lab discovered PGC-1-related coactivator (PRC) based on sequence similarities with PGC-1α. Interestingly, PRC mRNA is dramatically induced when quiescent fibroblasts are stimulated to proliferate by serum, conditions where PGC-1α is not expressed. PRC is also more constitutively expressed than PGC-1α and is up regulated in proliferating cells and down regulated in confluent cells. PRC is indistinguishable from PGC-1α in its *in vitro* and *in vivo* interaction with NRF-1 and co-activation of NRF target genes. Because of its structural and functional similarities to PGC-1α but its different pattern of induction, **we hypothesized that PRC is an important transcriptional regulator that links mitochondrial function to cellular proliferation**.

This thesis research provides several lines of evidence supporting this hypothesis. First, we established that PRC can co-activate promoters of the mitochondrial transcription factors TFB1M and TFB2M through NRF1 and NRF-2 sites, and we demonstrated a high correlation between PRC induction and induction of genes important for mitochondrial biogenesis during serum stimulation. We also classified PRC as an immediate early gene by showing that its induction by serum does not require *de novo* protein synthesis and occurs mainly at the transcriptional level. Serum induction also results in increased occupancy of the cytc promoter *in vivo*, enforcing a regulatory role for PRC in transcriptional expression during the transition from G_0 to G_1. We demonstrated that PRC likely functions through NRF-2 *in vivo* by existing in a

complex with NRF-2 and the coactivator HCF-1, a key regulator of cell proliferation. A dominant-negative fragment of PRC inhibited respiratory growth on galactose, supporting an *in vivo* function for PRC in regulating respiratory growth. Finally, we showed that stably silencing PRC expression with two different short hairpin RNAs that were lentivirally introduced into U2OS cells resulted in cell cycle defects and a severe reduction in respiratory function in the context of proliferation of structurally abnormal mitochondria. More pleiotropic effects of PRC were also indicated by global gene profiling of PRC deficient cells. **Hereby, we established that PRC is an important regulator of cell proliferation, respiratory gene expression and mitochondrial function in cells where PGC-1α is absent**.

This thesis project fills an important void in the field of mitochondrial biology by showing that PRC can regulate mitochondrial function linked to cell proliferation. Together, these results contribute to our understanding of the biological role of PGC-1 family member PRC, and expand our knowledge of how this family of coactivators can regulate mitochondrial function. Insight into normal mitochondrial function is the key to understanding mitochondrial dysfunction associated with many human disease states, such as diabetes, obesity, and insulin resistance among others, and may ultimately lead to therapeutic interventions for these diseases.

REFERENCES

1. Fernandez-Moreno, M. A., Bornstein, B., Petit, N., and Garesse, R. (2000) *Mol. Gen. Metab.* **71,** 481-495.

2. Falkenberg, M., Larsson, N. G., and Gustafsson, C. M. (2007) *Annu. Rev. Biochem.* **76,** 679-699.

3. Clayton, D. A. (1991) *Annu. Rev. Cell Biol.* **7,** 453-478.

4. Shadel, G. S. and Clayton, D. A. (1997) *Annu. Rev. Biochem.* **66,** 409-435.

5. Garesse, R. and Vallejo, C. G. (2001) *Gene* **263,** 1-16.

6. Tyynismaa, H., Sembongi, H., Bokori-Brown, M., Granycome, C., Ashley, N., Poulton, J., Jalanko, A., Spelbrink, J. N., Holt, I. J., and Suomalainen, A. (2004) *Hum. Mol. Genet.* **13,** 3219-3227.

7. Holt, I. J., Lorimer, H. E., and Jacobs, H. T. (2000) *Cell* **100,** 515-524.

8. Yang, M. Y., Bowmaker, M., Reyes, A., Vergani, L., Angeli, P., Gringeri, E., Jacobs, H. T., and Holt, I. J. (2002) *Cell* **111,** 495-505.

9. Yasukawa, T., Yang, M. Y., Jacobs, H. T., and Holt, I. J. (2005) *Mol. Cell* **18,** 651-662.

10. Brown, T. A., Cecconi, C., Tkachuk, A. N., Bustamante, C., and Clayton, D. A. (2005) *Genes Dev.* **19,** 2466-2476.

11. Fish, J., Raule, N., and Attardi, G. (2004) *Science* **306,** 2098-2101.

12. Masters, B. S., Stohl, L. L., and Clayton, D. A. (1987) *Cell* **51,** 89-99.

13. Tiranti, V., Savoia, A., Forti, F., D'Apolito, M. F., Centra, M., Racchi, M., and Zeviani, M. (1997) *Hum. Mol. Genet.* **6,** 615-625.

14. Diffley, J. F. and Stillman, B. (1991) *Proc. Natl. Acad. Sci. USA* **88,** 7864-7868.

15. Larsson, N. G., Wang, J. M., Wilhelmsson, H., Oldfors, A., Rustin, P., Lewandoski, M., Barsh, G. S., and Clayton, D. A. (1998) *Nature Genetics* **18,** 231-236.

16. Falkenberg, M., Gaspari, M., Rantanen, A., Trifunovic, A., Larsson, N.-G., and Gustafsson, C. M. (2002) *Nat. Genet.* **31,** 289-294.

17. McCulloch, V., Seidel-Rogol, B. L., and Shadel, G. S. (2002) *Mol. Cell. Biol.* **22,** 1116-1125.

18. McCulloch, V. and Shadel, G. S. (2003) *Mol. Cell. Biol.* **23,** 5816-5824.

19. Seidel-Rogol, B. L., McCulloch, V., and Shadel, G. S. (2003) *Nat. Genet.* **33,** 23-24.

20. Cotney, J. and Shadel, G. S. (2006) *J. Mol. Evol.* **63,** 707-717.

21. Wang, Z., Cotney, J., and Shadel, G. S. (2007) *J. Biol. Chem.* **282,** 12610-12618.

22. Christianson, T. W. and Clayton, D. A. (1986) *Proc. Natl. Acad. Sci. USA* **83,** 6277-6281.

23. Christianson, T. W. and Clayton, D. A. (1988) *Mol. Cell. Biol.* **8,** 4502-4509.

24. Kruse, B., Narasimhan, N., and Attardi, G. (1989) *Cell* **58,** 391-397.

25. Fernandez-Silva, P., Martinez-Azorin, F., Micol, V., and Attardi, G. (1997) *EMBO J.* **16,** 1066-1079.

26. Asin-Cayuela, J., Schwend, T., Farge, G., and Gustafsson, C. M. (2005) *J. Biol. Chem.* **280,** 25499-25505.

27. Linder, T., Park, C. B., sin-Cayuela, J., Pellegrini, M., Larsson, N. G., Falkenberg, M., Samuelsson, T., and Gustafsson, C. M. (2005) *Curr. Genet.* **48,** 265-269.

28. Park, C. B., sin-Cayuela, J., Camara, Y., Shi, Y., Pellegrini, M., Gaspari, M., Wibom, R., Hultenby, K., Erdjument-Bromage, H., Tempst, P., Falkenberg, M., Gustafsson, C. M., and Larsson, N. G. (2007) *Cell* **130,** 273-285.

29. Hyvarinen, A. K., Pohjoismaki, J. L., Reyes, A., Wanrooij, S., Yasukawa, T., Karhunen, P. J., Spelbrink, J. N., Holt, I. J., and Jacobs, H. T. (2007) *Nucleic Acids Res.* **35,** 6458-6474.

30. Rossmanith, W., Tullo, A., Potuschak, T., Karwan, R., and Sbisà, E. (1995) *J. Biol. Chem.* **270,** 12885-12891.

31. Tomecki, R., Dmochowska, A., Gewartowski, K., Dziembowski, A., and Stepien, P. P. (2004) *Nucleic Acids Res.* **32,** 6001-6014.

32. Nagaike, T., Suzuki, T., Katoh, T., and Ueda, T. (2005) *J. Biol. Chem.* **280,** 19721-19727.

33. Slomovic, S. and Schuster, G. (2008) *RNA.* **14,** 310-323.

34. Spremulli, L. L., Coursey, A., Navratil, T., and Hunter, S. E. (2004) *Prog. Nucleic Acid Res. Mol. Biol.* **77,** 211-261.

35. Schultz, R. A., Swoap, S. J., McDaniel, L. D., Zhang, B. Q., Koon, E. C., Garry, D. J., Li, K., and Williams, R. S. (1998) *J. Biol. Chem.* **273,** 3447-3451.

36. Ekstrand, M. I., Falkenberg, M., Rantanen, A., Park, C. B., Gaspari, M., Hultenby, K., Rustin, P., Gustafsson, C. M., and Larsson, N.-G. (2004) *Hum. Mol. Genet.* **13,** 935-944.

37. Scarpulla, R. C. (2002) *Gene* **286,** 81-89.

38. Escrivá, H., Rodríguez-Peña, A., and Vallejo, C. G. (1999) *Biochimie* **81,** 965-971.

39. Cotney, J., Wang, Z., and Shadel, G. S. (2007) *Nucleic Acids Res.* **35,** 4042-4054.

40. Scarpulla, R. C. (2008) *Physiol Rev.* **88,** 611-638.

41. Evans, M. J. and Scarpulla, R. C. (1990) *Genes Dev.* **4,** 1023-1034.

42. Virbasius, J. V. and Scarpulla, R. C. (1991) *Mol. Cell. Biol.* **11,** 5631-5638.

43. Scarpulla, R. C. (2002) *Biochem. Biophys. Acta* **1576,** 1-14.

44. Virbasius, J. V. and Scarpulla, R. C. (1994) *Proc. Natl. Acad. Sci. USA* **91,** 1309-1313.

45. Braidotti, G., Borthwick, I. A., and May, B. K. (1993) *J. Biol. Chem.* **268,** 1109-1117.

46. Gleyzer, N., Vercauteren, K., and Scarpulla, R. C. (2005) *Mol. Cell. Biol.* **25,** 1354-1366.

47. Huo, L. and Scarpulla, R. C. (2001) *Mol. Cell Biol.* **21,** 644-654.

48. Ristevski, S., O'Leary, D. A., Thornell, A. P., Owen, M. J., Kola, I., and Hertzog, P. J. (2004) *Mol. Cell. Biol.* **24,** 5844-5849.

49. Dhar, S. S., Ongwijitwat, S., and Wong-Riley, M. T. (2008) *J. Biol. Chem.* **283,** 3120-3129.

50. Ongwijitwat, S., Liang, H. L., Graboyes, E. M., and Wong-Riley, M. T. (2006) *Gene* **374,** 39-49.

51. Cam, H., Balciunaite, E., Blias, A., Spektor, A., Scarpulla, R. C., Young, R., Kluger, Y., and Dynlacht, B. D. (2004) *Mol. Cell* **16,** 399-411.

52. Spiegelman, B. M. and Heinrich, R. (2004) *Cell* **119,** 157-167.

53. Puigserver, P., Wu, Z., Park, C. W., Graves, R., Wright, M., and Spiegelman, B. M. (1998) *Cell* **92,** 829-839.

54. Wu, Z., Puigserver, P., Andersson, U., Zhang, C., Adelmant, G., Mootha, V., Troy, A., Cinti, S., Lowell, B., Scarpulla, R. C., and Spiegelman, B. M. (1999) *Cell* **98,** 115-124.

55. Lehman, J. J., Barger, P. M., Kovacs, A., Saffitz, J. E., Medeiros, D. M., and Kelly, D. P. (2000) *J. Clin. Invest.* **106,** 847-856.

56. Russell, L. K., Mansfield, C. M., Lehman, J. J., Kovacs, A., Courtois, M., Saffitz, J. E., Medeiros, D. M., Valencik, M. L., McDonald, J. A., and Kelly, D. P. (2004) *Circ. Res.* **94,** 525-533.

57. Lin, J., Wu, H., Tarr, P. T., Zhang, C. Y., Wu, Z. D., Boss, O., Michael, L. F., Puigserver, P., Isotani, E., Olson, E. N., Lowell, B. B., Bassel-Duby, R., and Spiegelman, B. M. (2002) *Nature* **418,** 797-801.

58. Schreiber, S. N., Knutti, D., Brogli, K., Uhlmann, T., and Kralli, A. (2003) *J. Biol. Chem.* **278,** 9013-9018.

59. Schreiber, S. N., Emter, R., Hock, M. B., Knutti, D., Cardenas, J., Podvinec, M., Oakeley, E. J., and Kralli, A. (2004) *Proc. Natl. Acad. Sci. USA* **101,** 6472-6477.

60. Lin, J., Wu, P., Tarr, P. T., Lindenberg, K. S., St-Pierre, J., Zhang, C., Mootha, V. K., Jäger, S., Vianna, C. R., Reznick, R. M., Cui, L., Manieri, M., Donovan, M. X., Wu, Z., Cooper, M. P., Fan, M. L., Rohas, L. M., Zavacki, A. M., Cinti, S., Shulman, G. I., Lowell, B. B., Krainc, D., and Spiegelman, B. M. (2004) *Cell* **119,** 121-135.

61. Leone, T. C., Lehman, J. J., Finck, B. N., Schaeffer, P. J., Wende, A. R., Boudina, S., Courtois, M., Wozniak, D. F., Sambandam, N., Bernal-Mizrachi, C., Chen, Z., Holloszy, J. O., Medeiros, D. M., Schmidt, R. E., Saffitz, J. E., Abel, E. D., Semenkovich, C. F., and Kelly, D. P. (2005) *PLoS. Biol.* **3,** 0672-0687.

62. Puigserver, P., Adelmant, C., Wu, Z. D., Fan, M., Xu, J. M., O'Malley, B., and Spiegelman, B. M. (1999) *Science* **286,** 1368-1371.

63. Wallberg, A. E., Yamamura, S., Malik, S., Spiegelman, B. M., and Roeder, R. G. (2003) *Mol. Cell* **12,** 1137-1149.

64. Monsalve, M., Wu, Z., Adelmant, G., Puigserver, P., Fan, M., and Spiegelman, B. M. (2000) *Mol. Cell* **6,** 307-316.

65. Vega, R. B., Huss, J. M., and Kelly, D. P. (2000) *Mol. Cell. Biol.* **20,** 1868-1876.

66. Handschin, C., Lin, J., Rhee, J., Peyer, A. K., Chin, S., Wu, P. H., Meyer, U. A., and Spiegelman, B. M. (2005) *Cell* **122,** 505-515.

67. Michael, L. F., Wu, Z. D., Cheatham, R. B., Puigserver, P., Adelmant, G., Lehman, J. J., Kelly, D. P., and Spiegelman, B. M. (2001) *Proc. Natl. Acad. Sci. USA* **98,** 3820-3825.

68. Handschin, C., Chin, S., Li, P., Liu, F., Maratos-Flier, E., Lebrasseur, N. K., Yan, Z., and Spiegelman, B. M. (2007) *J. Biol. Chem.*

69. Yoon, J. C., Puigserver, P., Chen, G. X., Donovan, J., Wu, Z. D., Rhee, J., Adelmant, G., Stafford, J., Kahn, C. R., Granner, D. K., Newgard, C. B., and Spiegelman, B. M. (2001) *Nature* **413,** 131-138.

70. Rhee, J., Ge, H., Yang, W., Fan, M., Handschin, C., Cooper, M., Lin, J., Li, C., and Spiegelman, B. M. (2006) *J. Biol. Chem.* **281,** 14683-14690.

71. Herzig, S., Long, F. X., Jhala, U. S., Hedrick, S., Quinn, R., Bauer, A., Rudolph, D., Schutz, G., Yoon, C., Puigserver, P., Spiegelman, B., and Montminy, M. (2001) *Nature* **413,** 179-183.

72. Handschin, C., Rhee, J., Lin, J. D., Tarr, P. T., and Spiegelman, B. M. (2003) *Proc. Natl. Acad. Sci. USA* **100,** 7111-7116.

73. Cao, W. H., Daniel, K. W., Robidoux, J., Puigserver, P., Medvedev, A. V., Bai, X., Floering, L. M., Spiegelman, B. M., and Collins, S. (2004) *Mol. Cell. Biol.* **24,** 3057-3067.

74. Nisoli, E., Clementi, E., Paolucci, C., Cozzi, V., Tonello, C., Sciorati, C., Bracale, R., Valerio, A., Francolini, M., Moncada, S., and Carruba, M. O. (2003) *Science* **299,** 896-899.

75. Lin, J., Puigserver, P., Donovan, J., Tarr, P., and Spiegelman, B. M. (2002) *J. Biol. Chem.* **277,** 1645-1648.

76. Kressler, D., Schreiber, S. N., Knutti, D., and Kralli, A. (2002) *J. Biol. Chem.* **277,** 13918-13925.

77. Meirhaeghe, A., Crowley, V., Lenaghan, C., Lelliott, C., Green, K., Stewart, A., Hart, K., Schinner, S., Sethi, J. K., Yeo, G., Brand, M. D., Cortright, R. N., O'Rahilly, S., Montague, C., and Vidal-Puig, A. J. (2003) *Biochem. J.* **373,** 155-165.

78. Lin, J. D., Tarr, P. T., Yang, R. J., Rhee, J., Puigserver, P., Newgard, C. B., and Spiegelman, B. M. (2003) *J. Biol. Chem.* **278,** 30843-30848.

79. St Pierre, J., Lin, J., Krauss, S., Tarr, P. T., Yang, R. J., Newgard, C. B., and Spiegelman, B. M. (2003) *J. Biol. Chem.* **278,** 26597-26603.

80. Lin, J., Yang, R., Tarr, P. T., Wu, P. H., Handschin, C., Li, S., Yang, W., Pei, L., Uldry, M., Tontonoz, P., Newgard, C. B., and Spiegelman, B. M. (2005) *Cell* **120,** 261-273.

81. Wolfrum, C. and Stoffel, M. (2006) *Cell Metab* **3,** 99-110.

82. Kamei, Y., Ohizumi, H., Fujitani, Y., Nemoto, T., Tanaka, T., Takahashi, N., Kawada, T., Miyoshi, M., Ezaki, O., and Kakizuka, A. (2003) *Proc. Natl. Acad. Sci. USA* **100,** 12378-12383.

83. Arany, Z., Lebrasseur, N., Morris, C., Smith, E., Yang, W., Ma, Y., Chin, S., and Spiegelman, B. M. (2007) *Cell Metab* **5,** 35-46.

84. Vianna, C. R., Huntgeburth, M., Coppari, R., Choi, C. S., Lin, J., Krauss, S., Barbatelli, G., Tzameli, I., Kim, Y. B., Cinti, S., Shulman, G. I., Spiegelman, B. M., and Lowell, B. B. (2006) *Cell Metab* **4,** 453-464.

85. Lelliott, C. J., Medina-Gomez, G., Petrovic, N., Kis, A., Feldmann, H. M., Bjursell, M., Parker, N., Curtis, K., Campbell, M., Hu, P., Zhang, D., Litwin, S. E., Zaha, V. G.,

Fountain, K. T., Boudina, S., Jimenez-Linan, M., Blount, M., Lopez, M., Meirhaeghe, A., Bohlooly, Y., Storlien, L., Stromstedt, M., Snaith, M., Oresic, M., Abel, E. D., Cannon, B., and Vidal-Puig, A. (2006) *PLoS. Biol.* **4,** 2042-2056.

86. Sonoda, J., Mehl, I. R., Chong, L. W., Nofsinger, R. R., and Evans, R. M. (2007) *Proc. Natl. Acad. Sci. U. S. A* **104,** 5223-5228.

87. Uldry, M., Yang, W., St-Pierre, J., Lin, J., Seale, P., and Spiegelman, B. M. (2006) *Cell Metab* **3,** 333-341.

88. Lai, L., Leone, T. C., Zechner, C., Schaeffer, P. J., Kelly, S. M., Flanagan, D. P., Medeiros, D. M., Kovacs, A., and Kelly, D. P. (2008) *Genes Dev.* **22,** 1948-1961.

89. Andersson, U. and Scarpulla, R. C. (2001) *Mol. Cell. Biol.* **21,** 3738-3749.

90. Wallace, D. C. (2005) *Annu. Rev. Genet.* **39,** 359-407.

91. Zeviani, M. (2001) *Semin. Cell Dev. Biol.* **12,** 407-416.

92. Puigserver, P. and Spiegelman, B. M. (2003) *Endocrine Reviews* **24,** 78-90.

93. Schon, E. A. and Manfredi, G. (2003) *Journal of Clinical Investigation* **111,** 303-312.

94. Handschin, C., Kobayashi, Y. M., Chin, S., Seale, P., Campbell, K. P., and Spiegelman, B. M. (2007) *Genes Dev.* **21,** 770-783.

95. Savagner, F., Mirebeau, D., Jacques, C., Guyetant, S., Morgan, C., Franc, B., Reynier, P., and Malthièry, Y. (2003) *Biochem. Biophys. Res. Commun.* **310,** 779-784.

96. Pei, Y. and Tuschl, T. (2006) *Nat. Methods* **3,** 670-676.

97. Harborth, J., Elbashir, S. M., Vandenburgh, K., Manninga, H., Scaringe, S. A., Weber, K., and Tuschl, T. (2003) *Antisense Nucleic Acid Drug Dev.* **13,** 83-105.

98. Devroe, E. and Silver, P. A. (2002) *BMC. Biotechnol.* **2,** 15.

99. Vercauteren, K., Pasko, R. A., Gleyzer, N., Marino, V. M., and Scarpulla, R. C. (2006) *Mol. Cell Biol.* **26,** 7409-7419.

100. Vercauteren, K., Gleyzer, N., and Scarpulla, R. C. (2008) Short hairpin RNA-mediated silencing of PGC-1-related coactivator (PRC) results in a severe respiratory chain deficiency associated with the proliferation of aberrant mitochondria.

101. He, T.-C., Zhou, S., da Costa, L. T., Yu, J., Kinzler, K. W., and Vogelstein, B. (1998) *Proc. Natl. Acad. Sci. USA* **95,** 2509-2514.

102. Clayton, D. A. (2003) *IUBMB Life* **55,** 213-217.

103. Poyton, R. O. and McEwen, J. E. (1996) *Annu. Rev. Biochem.* **65,** 563-607.

104. Bogenhagen, D. F. (1996) *J. Biol. Chem.* **271,** 12036-12041.

105. Kelly, D. P. and Scarpulla, R. C. (2004) *Genes Dev.* **18,** 357-368.

106. Rantanen, A., Gaspari, M., Falkenberg, M., Gustafsson, C. M., and Larsson, N.-G. (2003) *Mammalian Genome* **14,** 1-6.

107. Gugneja, S., Virbasius, J. V., and Scarpulla, R. C. (1995) *Mol. Cell. Biol.* **15,** 102-111.

108. Herzig, R. P., Scacco, S., and Scarpulla, R. C. (2000) *J. Biol. Chem.* **275,** 13134-13141.

109. Wilson-Fritch, L., Burkart, A., Bell, G., Mendelson, K., Leszyk, J., Nicoloro, S., Czech, M., and Corvera, S. (2003) *Mol. Cell. Biol.* **23,** 1085-1094.

110. Antoshechkin, I. and Bogenhagen, D. F. (1995) *Mol. Cell. Biol.* **15,** 7032-7042.

111. Dairaghi, D. J., Shadel, G. S., and Clayton, D. A. (1995) *J. Mol. Biol.* **249,** 11-28.

112. Choi, Y. S., Lee, H. K., and Pak, Y. K. (2002) *Biochim. Biophys. Acta Gene Struct. Expression* **1574,** 200-204.

113. Virbasius, C. A., Virbasius, J. V., and Scarpulla, R. C. (1993) *Genes Dev.* **7,** 2431-2445.

114. Li, R., Hodny, Z., Luciakova, K., Barath, P., and Nelson, B. D. (1996) *J. Biol. Chem.* **271,** 18925-18930.

115. Zaid, A., Li, R., Luciakova, K., Barath, P., Nery, S., and Nelson, B. D. (1999) *J. Bioenerg. Biomembr.* **31,** 129-135.

116. Gugneja, S. and Scarpulla, R. C. (1997) *J. Biol. Chem.* **272,** 18732-18739.

117. Higuchi, R. (1990) Recombinant PCR. In Innis, M. A., Gelfand, D. H., Sninsky, J. J., and White, T. J., editors. *PCR Protocols. A guide to methods and applications.*, Academic Press, San Diego, CA

118. Andrews, N. C. and Faller, D. V. (1991) *Nucleic Acids Res.* **19,** 2499.

119. Takahashi, Y., Rayman, J. B., and Dynlacht, B. D. (2000) *Genes Dev.* **14,** 804-816.

120. Herzig, R. P., Andersson, U., and Scarpulla, R. C. (2000) *J. Cell Sci.* **113,** 4263-4273.

121. Gaspari, M., Larsson, N. G., and Gustafsson, C. M. (2004) *Biochim. Biophys. Acta Bio-Energetics* **1659,** 148-152.

122. Scarpulla, R. C. (2006) *J. Cell Biochem.* **97,** 673-683.

123. Lin, J., Handschin, C., and Spiegelman, B. M. (2005) *Cell Metab.* **1,** 361-370.

124. Puigserver, P. (2005) *Int. J. Obesity* **29,** 55-59.

125. Scarpulla, R. C. (1999) Nuclear transcription factors in cytochrome *c* and cytochrome oxidase expression. In Papa, S., Guerrieri, F., and Tager, J. M., editors. *Frontiers of cellular bioenergetics: Molecular biology, biochemistry, and physiopathology*, Plenum Publishing Company, London

126. Evans, M. J. and Scarpulla, R. C. (1989) *J. Biol. Chem.* **264,** 14361-14368.

127. Gopalakrishnan, L. and Scarpulla, R. C. (1994) *J. Biol. Chem.* **269,** 105-113.

128. Nathans, D., Lau, L. F., Christy, B., Hartzell, S., Nakabeppu, Y., and Ryder, K. (1988) *Cold Spring Harbor Symp. Quant. Biol.* **53,** 893-900.

129. Winkles, J. A. (1998) *Prog. Nucleic Acid Res. Mol. Biol.* **58,** 41-78.

130. Cen, B., Selvaraj, A., and Prywes, R. (2004) *J. Cell. Biochem.* **93,** 74-82.

131. Shaywitz, A. J. and Greenberg, M. E. (1999) *Annu. Rev. Biochem.* **68,** 821-861.

132. De, C. D., Fimia, G. M., and Sassone-Corsi, P. (1999) *Trends Biochem. Sci.* **24,** 281-285.

133. Robinson, B. H. (1996) *Methods Enzymol.* **264,** 454-464.

134. Gonzalez, G. A., Menzel, P., Leonard, J., Fischer, W. H., and Montminy, M. R. (1991) *Mol. Cell. Biol.* **11,** 1306-1312.

135. Montminy, M. (1997) *Annu. Rev. Biochem.* **66,** 807-822.

136. Johannessen, M., Delghandi, M. P., and Moens, U. (2004) *Cell Signal.* **16,** 1211-1227.

137. Radhakrishnan, I., Pérez-Alvarado, G. C., Parker, D., Dyson, H. J., Montminy, M. R., and Wright, P. E. (1997) *Cell* **91,** 741-752.

138. Kouzarides, T. (1999) *Curr. Opin. Genet. Dev.* **9,** 40-48.

139. Virbasius, J. V., Virbasius, C. A., and Scarpulla, R. C. (1993) *Genes Dev.* **7,** 380-392.

140. Wilson, A. C., Freiman, R. N., Goto, H., Nishimoto, T., and Herr, W. (1997) *Mol. Bio. Cell.* **17,** 6139-6146.

141. Towbin, H., Staehelin, T., and Gordon, J. (1979) *Proc. Natl. Acad. Sci. USA* **76,** 4350-4354.

142. Livak, K. J. and Schmittgen, T. D. (2001) *Methods* **25,** 402-408.

143. Hatefi, Y. (1985) *Annu. Rev. Biochem.* **54,** 1015-1069.

144. Cannon, B. and Nedergaard, J. (2004) *Physiol Rev.* **84,** 277-359.

145. Scarpulla, R. C. (2004) Molecular biology of the OXPHOS system. In Smeitink, J. A. M., Sengers, R. C. A., and Trij, J. M. F., editors. *Oxidative Phosphorylation in Health and Disease*, Landes Bioscience, New York

146. Bonawitz, N. D., Clayton, D. A., and Shadel, G. S. (2006) *Mol. Cell* **24,** 813-825.

147. Yang, Z. F., Mott, S., and Rosmarin, A. G. (2007) *Nat. Cell Biol.* **9,** 339-346.

148. Finck, B. N. and Kelly, D. P. (2006) *J. Clin. Invest* **116,** 615-622.

149. Wysocka, J. and Herr, W. (2003) *Trends Biochem. Sci.* **28,** 294-304.

150. Wilson, A. C., LaMarco, K., Peterson, M. G., and Herr, W. (1993) *Cell* **74,** 115-125.

151. Vogel, J. L. and Kristie, T. M. (2000) *Proc. Natl. Acad. Sci. U. S. A* **97,** 9425-9430.

152. Goto, H., Motomura, S., Wilson, A. C., Freiman, R. N., Nakabeppu, Y., Fukushima, M., Herr, W., and Nishimoto, T. (1997) *Genes Dev.* **11,** 726-737.

153. Julien, E. and Herr, W. (2003) *EMBO J.* **22,** 2360-2369.

154. Vogel, J. L. and Kristie, T. M. (2000) *EMBO J.* **19,** 683-690.

155. Mootha, V. K., Handschin, C., Arlow, D., Xie, X. H., St Pierre, J., Sihag, S., Yang, W. L., Altshuler, D., Puigserver, P., Patterson, N., Willy, P. J., Schulman, I. G., Heyman, R. A., Lander, E. S., and Spiegelman, B. M. (2004) *Proc. Natl. Acad. Sci. USA* **101,** 6570-6575.

156. Gugneja, S., Virbasius, C. A., and Scarpulla, R. C. (1996) *Mol. Cell. Biol.* **16,** 5708-5716.

157. Handschin, C. and Spiegelman, B. M. (2006) *Endocr. Rev.* **27,** 728-735.

158. Puigserver, P., Rhee, J., Lin, J., Wu, Z., Yoon, J. C., Zhang, C. Y., Krauss, S., Mootha, V. K., Lowell, B. B., and Spiegelman, B. M. (2001) *Mol. Cell* **8,** 971-982.

159. Matsushima, Y., Garesse, R., and Kaguni, L. S. (2004) *J. Biol. Chem.* **279,** 26900-26905.

160. Matsushima, Y., Adan, C., Garesse, R., and Kaguni, L. S. (2005) *J. Biol. Chem.* **280,** 16815-16820.

161. LaMarco, K. L. and McKnight, S. L. (1989) *Genes Dev.* **3,** 1372-1383.

162. Kristie, T. M. and Sharp, P. A. (1990) *Genes Dev.* **4,** 2383-2396.

163. Salviati, L., Hernandez-Rosa, E., Walker, W. F., Sacconi, S., DiMauro, S., Schon, E. A., and Davidson, M. M. (2002) *Biochem. J.* **363,** 321-327.

164. Moffat, J., Grueneberg, D. A., Yang, X., Kim, S. Y., Kloepfer, A. M., Hinkle, G., Piqani, B., Eisenhaure, T. M., Luo, B., Grenier, J. K., Carpenter, A. E., Foo, S. Y., Stewart, S. A., Stockwell, B. R., Hacohen, N., Hahn, W. C., Lander, E. S., Sabatini, D. M., and Root, D. E. (2006) *Cell* **124,** 1283-1298.

165. Balaban, R. S. (1990) *Am. J. Physiol. Cell Physiol.* **258,** C377-C389.

166. Vercauteren, K., Gleyzer, N., and Scarpulla, R. C. (2008) *J. Biol. Chem.* **283,** 12102-12111.

167. Adan, C., Matsushima, Y., Hernandez-Sierra, R., Marco-Ferreres, R., Fernandez-Moreno, M. A., Gonzalez-Vioque, E., Calleja, M., Aragon, J. J., Kaguni, L. S., and Garesse, R. (2008) *J. Biol. Chem.* **283,** 12333-12342.

168. Septinus, M., Berthold, T., Naujok, A., and Zimmermann, H. W. (1985) *Histochemistry* **82,** 51-66.

169. Metivier, D., Dallaporta, B., Zamzami, N., Larochette, N., Susin, S. A., Marzo, I., and Kroemer, G. (1998) *Immunol. Lett.* **61,** 157-163.

170. Marzluff, W. F. and Duronio, R. J. (2002) *Curr. Opin. Cell Biol.* **14,** 692-699.

171. Wysocka, J., Reilly, P. T., and Herr, W. (2001) *Mol. Cell Biol.* **21,** 3820-3829.

172. Bridge, A. J., Pebernard, S., Ducraux, A., Nicoulaz, A. L., and Iggo, R. (2003) *Nat. Genet.* **34,** 263-264.

173. Sledz, C. A. and Williams, B. R. (2004) *Biochem. Soc. Trans.* **32,** 952-956.

174. Zeng, Y., Yi, R., and Cullen, B. R. (2003) *Proc. Natl. Acad. Sci. U. S. A* **100,** 9779-9784.

175. Doench, J. G., Petersen, C. P., and Sharp, P. A. (2008) *Genes Dev.* **17,** 438-442.

176. Saxena, S., Jonsson, Z. O., and Dutta, A. (2003) *J. Biol. Chem.* **278,** 44312-44319.

177. Valencia-Sanchez, M. A., Liu, J., Hannon, G. J., and Parker, R. (2006) *Genes Dev.* **20,** 515-524.

178. Butow, R. A. and Avadhani, N. G. (2004) *Mol. Cell* **14,** 1-15.

179. Biswas, G., Guha, M., and Avadhani, N. G. (2005) *Gene* **354,** 132-139.

180. Rohas, L. M., St-Pierre, J., Uldry, M., Jager, S., Handschin, C., and Spiegelman, B. M. (2007) *Proc. Natl. Acad. Sci. U. S. A* **104,** 7933-7938.

181. Wallace, D. C. (1992) *Annu. Rev. Biochem.* **61,** 1175-1212.

182. Wredenberg, A., Wibom, R., Wilhelmsson, H., Graff, C., Wiener, H. H., Burden, S. J., Oldfors, A., Westerblad, H., and Larsson, N. G. (2002) *Proc. Natl. Acad. Sci. USA* **99,** 15066-15071.

183. Harris, M. E., Bohni, R., Schneiderman, M. H., Ramamurthy, L., Schumperli, D., and Marzluff, W. F. (1991) *Mol. Cell Biol.* **11,** 2416-2424.

184. Nelson, D. M., Ye, X., Hall, C., Santos, H., Ma, T., Kao, G. D., Yen, T. J., Harper, J. W., and Adams, P. D. (2002) *Mol. Cell Biol.* **22,** 7459-7472.

185. Sittman, D. B., Graves, R. A., and Marzluff, W. F. (1983) *Proc. Natl. Acad. Sci. U. S. A* **80,** 1849-1853.

186. Moir, R. D., Montag-Lowy, M., and Goldman, R. D. (1994) *J. Cell Biol.* **125,** 1201-1212.

187. Weibel, E. R. (1969) *Int. Rev. Cytol.* **26,** 235-302.

188. Smyth, G. K. (2004) *Stat. Appl. Genet. Mol. Biol.* **3,** Article3.

189. Scarpulla, R. C. (1997) *J. Bioenerg. Biomembr.* **29,** 109-119.

190. Luo, J., Deng, Z. L., Luo, X., Tang, N., Song, W. X., Chen, J., Sharff, K. A., Luu, H. H., Haydon, R. C., Kinzler, K. W., Vogelstein, B., and He, T. C. (2007) *Nat. Protoc.* **2,** 1236-1247.

191. Bergelson, J. M., Cunningham, J. A., Droguett, G., Kurt-Jones, E. A., Krithivas, A., Hong, J. S., Horwitz, M. S., Crowell, R. L., and Finberg, R. W. (1997) *Science* **275,** 1320-1323.

192. Kossila, M., Jauhiainen, S., Laukkanen, M. O., Lehtolainen, P., Jaaskelainen, M., Turunen, P., Loimas, S., Wahlfors, J., and Yla-Herttuala, S. (2002) *Mol. Ther.* **5,** 87-93.

193. Nalbantoglu, J., Pari, G., Karpati, G., and Holland, P. C. (1999) *Hum. Gene Ther.* **10,** 1009-1019.

194. Kawashima, H., Ogose, A., Yoshizawa, T., Kuwano, R., Hotta, Y., Hotta, T., Hatano, H., Kawashima, H., and Endo, N. (2003) *Cancer Sci.* **94,** 70-75.

195. Anderson, J. M. (2000) *Curr. Opin. Hematol.* **7,** 40-47.

196. Chambers, T. J. (1978) *J. Pathol.* **126,** 125-148.

197. Cavalier-Smith, T. (2005) *Ann. Bot. (Lond)* **95,** 147-175.

198. Neumann, F. R. and Nurse, P. (2007) *J. Cell Biol.* **179,** 593-600.

199. Jorgensen, P., Edgington, N. P., Schneider, B. L., Rupes, I., Tyers, M., and Futcher, B. (2007) *Mol. Biol. Cell* **18,** 3523-3532.

200. Boldogh, I. R. and Pon, L. A. (2007) *Trends Cell Biol.* **17,** 502-510.

201. Pendergrass, W., Wolf, N., and Poot, M. (2004) *Cytometry A* **61,** 162-169.

202. Meijer, H. A. and Thomas, A. A. (2002) *Biochem. J.* **367,** 1-11.

APPENDIX

Table A.1. Transcripts showing reduced level of expression as a result of PRC silencing in PRC shRNA#1 cells.

Mean fold changes in gene expression in response to shRNA#1-mediated silencing of PRC compared to cells expressing a negative control hairpin were assessed by Illumina microarray. The 25 gene transcripts that showed the greatest fold reduction upon PRC silencing are shown. A negative value indicates down regulation.

Gene symbol	Gene description	PRC shRNA#1 fold change	FDR adjusted p-value
ANXA10	Annexin A10	-152.65	1.39E-05
HIST2H2AA3	Histone cluster 2, H2aa3	-45.579	2.87E-06
HIST1H4H	Histone cluster 1, H4h	-45.532	8.79E-07
LOC643031		-36.447	1.16E-05
HIST1H4C	Histone cluster 1, H4c	-26.195	5.52E-05
HIST1H2AC	Histone cluster 1, H2ac	-26.108	3.46E-06
HIST2H2BE	Histone cluster 2, H2be	-18.945	2.36E-05
HIST1H1C	Histone cluster 1, H1c	-15.446	1.07E-05
HIST1H2BJ	Histone cluster 1, H2bj	-14.279	5.53E-06
VAMP8	Vesicle-associated membrane protein 8 (endobrevin)	-13.497	1.07E-05
RAC2	Ras-related C3 botulinum toxin substrate 2 (rho family small GTP binding protein Rac2)	-13.076	0.00031767
HIST2H4A	Histone cluster 2, H4a	-12.954	0.00012335
H2BSF	H2B histone family, member S	-12.691	3.46E-06
HIST2H2AC	Histone cluster 2, H2ac	-11.46	1.21E-05
HIST1H2BD	Histone cluster 1, H2bd	-9.8967	1.07E-05
SRGN	serglycin	-8.644	6.28E-05
HIST1H2BE	Histone cluster 1, H2be	-8.6294	4.87E-05
HIST1H2BC	Histone cluster 1, H2bc	-8.1176	6.65E-05
KISS1	KiSS-1 metastasis-	-8.0276	0.00146531

Gene symbol	Gene description	PRC shRNA#1 fold change	FDR adjusted p-value
	suppressor		
C7orf10	Chromosome 7 open reading frame 10	-7.8183	0.00035327
H2AFJ	H2A histone family, member J	-7.6732	4.14E-05
HCFC1R1	Host cell factor C1 regulator 1 (XPO1 dependent)	-7.568	5.92E-05
PDGFC	Platelet derived growth factor C	-7.0938	0.00016214
SCARA3	Scavenger receptor class A, member 3	-6.93	2.04E-05
SERPINE1	Serpin peptidase inhibitor, clade E	-6.8754	0.00054621

Table A.2. Transcripts induced by PRC silencing in PRC shRNA#1 cells.

Mean fold changes in gene expression in response to shRNA#1-mediated silencing of PRC compared to cells expressing a negative control hairpin were assessed by Illumina microarray. The 25 gene transcripts that showed the greatest fold induction following PRC silencing are shown. A positive number indicates up regulation.

Gene symbol	Gene description	PRC shRNA#1 fold change	FDR adjusted p-value
LUM	Lumican	44.171	7.79E-06
PLAC8	Placenta-specific 8	17.776	0.00114893
SPANXA1	Sperm protein associated with the nucleus, X-linked, family member A1	9.1079	1.21E-05
SPANXC	SPANX family, member C	9.0892	3.92E-05
GAGE5	G antigen 5	8.0383	0.00042304
AKRIC3	Aldo-keto reductase family 1, member C3 (3-alpha hydroxysteroid dehydrogenase, type II)	7.6676	0.00324248
GAGE4	G antigen 4	7.563	0.0004632
CCDC62	Coiled-coil domain containing 62	7.3778	0.00028654
LOC645037		7.2919	0.00058589
GAGE2	G antigen 2	7.2152	0.00056517
GAGE8	G antigen 8	7.1788	0.00051707
GAGE7B	G antigen 7B	7.1198	0.00064953
GAGE6	G antigen 6	6.9747	0.00027898
SERPINB7	Serin peptidase inhibitor, clade B (ovalbumin), member7	6.3022	3.46E-06
SPANXB1	SPANX family, member B1	6.3008	6.34E-05
SPANXB2	SPANX family, member B2	6.0352	1.39E-05
NLRP2	NLR family, pyrin domain containing 2	5.2257	4.12E-05
GPC5	Glypican 5	5.171	1.21E-05
ZNF545	Zinc finger protein 545	4.7991	6.30E-06
ASS1	Argininosuccinate synthetase 1	4.6925	7.54E-05
F2RL2	Coagulation factor II	4.5869	0.001387

Gene symbol	Gene description	PRC shRNA#1 fold change	FDR adjusted p-value
	(thrombin) receptor-like 2		
CHD5	Chromodomain helicase DNA binding protein 5	4.0016	0.000409
C6orf15	Chromosome 6 open reading frame 15	3.9148	6.65E-05
DDR2	Discoidin domain receptor family, member 2	3.9074	0.000245
FAM27E3	Family with sequence similarity 27, member E3	3.8677	0.000409

Table A.3. Overlapping down regulated transcripts in PRC shRNA#1 and #4 cells compared to control shRNA cells.

Mean fold changes in gene expression in response to shRNA#1- or shRNA#4-mediated silencing of PRC compared to cells expressing a negative control hairpin were assessed by Illumina microarray. The complete list of common gene transcripts significantly down regulated upon PRC silencing by both hairpins#1 and #4 are shown with corresponding p-values and FDR adjusted p-values. A negative value indicates down regulation.

Gene ID	Gene Symbol	Gene Description	PRC shRNA #1 fold change	PRC shRNA#1 p-value	PRC shRNA#1 FDR p-value	PRC shRNA #4 fold change	PRC shRNA#4 p-value	PRC shRNA#4 FDR p-value
8337	HIST2H2AA3	Histone cluster 2, H2aa3	-45.58	5.02E-10	2.87E-06	-2.88	2.90E-07	0.00034694
8365	HIST1H4H	Histone cluster 1, H4h	-45.53	5.83E-11	8.79E-07	-3.92	9.96E-08	0.00017878
8334	HIST1H2AC	Histone cluster 1, H2ac	-26.11	1.25E-09	3.46E-06	-3.21	2.96E-06	0.00088648
8349	HIST2H2BE	Histone cluster 2, H2be	-18.95	5.32E-08	2.36E-05	-3.15	3.24E-05	0.0029367
3006	HIST1H1C	histone cluster 1, H1c	-15.45	8.33E-09	1.07E-05	-1.87	2.28E-05	0.0025365
8970	HIST1H2BJ	Histone cluster 1, H2bj	-14.28	2.57E-09	5.53E-06	-3.35	1.90E-06	0.00083519
8338	HIST2H2AC	Histone cluster 2, H2ac	-11.46	1.69E-08	1.21E-05	-2.37	4.32E-06	0.0010148
3017	HIST1H2BD	histone cluster 1, H2bd	-9.90	9.20E-09	1.07E-05	-1.65	0.00042943	0.011456
8344	HIST1H2BE	Histone cluster 1, H2be	-8.63	1.58E-07	4.87E-05	-2.17	3.62E-05	0.003034
8347	HIST1H2BC	Histone cluster 1, H2bc	-8.12	2.83E-07	6.65E-05	-2.25	7.70E-06	0.0013675
55766	H2AFJ	H2A histone family, member J	-7.67	1.29E-07	4.14E-05	-2.37	3.71E-06	0.00090135
5118	PCOLCE	procollagen C-endopeptidase enhancer	-6.35	1.03E-06	0.00016842	-1.71	0.0028893	0.034153
7045	TGFBI	transforming growth factor, beta-induced, 68kDa	-6.25	2.73E-06	0.00030716	-3.09	5.82E-05	0.0039175
8367	HIST1H4E	Histone cluster 1, H4e	-5.79	1.07E-08	1.12E-05	-2.38	8.76E-07	0.00054175
2791	GNG11	guanine nucleotide binding protein (G protein), gamma 11	-5.01	3.51E-06	0.00034794	1.53	2.73E-06	0.00088648

Gene ID	Gene Symbol	Gene Description	PRC shRNA #1 fold change	PRC shRNA#1 p-value	PRC shRNA#1 FDR p-value	PRC shRNA #4 fold change	PRC shRNA#4 p-value	PRC shRNA#4 FDR p-value
5653	KLK6	kallikrein-related peptidase 6	-4.73	1.14E-05	0.00057582	2.42	0.00035557	0.010449
1140	CHRNB1	cholinergic receptor, nicotinic, beta 1 (muscle)	-4.70	2.06E-07	5.74E-05	-1.67	3.95E-05	0.0032208
8351	HIST1H3D	histone cluster 1, H3d	-4.40	9.51E-07	0.00016214	-1.86	5.36E-07	0.00043713
9945	GFPT2	Glutamine-fructose-6-phosphate transaminase 2	-4.19	1.88E-06	0.000247	-2.15	1.33E-05	0.001903
11055	ZPBP	Zona pellucida binding protein	-4.14	1.11E-08	1.12E-05	-2.18	7.38E-08	0.000157
4248	MGAT3	Mannosyl (beta-1,4-)-glycoprotein beta-1,4-N-acetylglucosaminyltransferase	-3.34	5.66E-05	0.001423	-2.05	6.05E-06	0.000157
9984	THOC1	THO complex 1	-3.18	5.48E-08	2.36E-05	-1.57	0.00038459	0.010833
8764	TNFRSF14	tumor necrosis factor receptor superfamily, member 14 (herpesvirus entry mediator)	-3.11	0.000263	0.0034624	-1.76	0.0024847	0.031317
5521	PPP2R2B	Protein phosphatase 2 (formerly 2A), regulatory subunit B, beta isoform	-3.06	0.006515	0.03023	-2.06	3.37E-06	0.000886
79822	ARHGAP28	Rho GTPase activating protein 28	-3.06	0.001865	0.012621	-1.51	0.00045754	0.011863
968	CD68	CD68 molecule	-2.84	0.000548	0.0056545	-1.52	0.0011032	0.019636
2192	FBLN1	fibulin 1	-2.75	0.000122	0.0021412	-1.80	0.00043003	0.011456
58191	CXCL16	chemokine (C-X-C motif) ligand 16	-2.72	1.70E-06	0.00023731	-1.59	4.98E-06	0.001048
8357	HIST1H3H	histone cluster 1, H3h	-2.68	3.56E-06	0.00035062	-1.73	8.36E-05	0.0047475
6578	SLCO2A1	Solute carrier organic anion transporter family, member 2A1	-2.65	0.001805	0.012373	-2.83	9.32E-09	8.36E-05
5243	ABCB1	ATP-binding cassette, sub-family B (MDR/TAP), member 1	-2.58	8.93E-06	0.00051717	-1.71	8.78E-06	0.0014845
11211	FZD10	frizzled homolog 10 (Drosophila)	-2.56	2.86E-05	0.00091848	-1.51	6.31E-06	0.0011798
120	ADD3	adducin 3 (gamma)	-2.55	1.81E-05	0.00073383	-1.78	9.23E-05	0.0049859
7781	SLC30A3	solute carrier family 30 (zinc transporter), member 3	-2.39	1.57E-05	0.00067481	-1.52	0.00012757	0.005985

Gene ID	Gene Symbol	Gene Description	PRC shRNA #1 fold change	PRC shRNA#1 p-value	PRC shRNA#1 FDR p-value	PRC shRNA #4 fold change	PRC shRNA#4 p-value	PRC shRNA#4 FDR p-value
5266	PI3	peptidase inhibitor 3, skin-derived (SKALP)	-2.38	0.002446	0.01519	-1.66	0.00011839	0.0057256
26277	TINF2	TERF1 (TRF1)-interacting nuclear factor 2	-2.32	0.002257	0.014388	-1.50	0.00061295	0.013956
23416	KCNH3	potassium voltage-gated channel, subfamily H (eag-related), member 3	-2.26	1.98E-05	0.00076511	1.52	0.00014094	0.0063376
3394	IRF8	interferon regulatory factor 8	-2.21	3.50E-06	0.00034794	-1.81	8.85E-06	0.0014845
401472	FLJ45248	FLJ45248 protein	-2.20	0.007921	0.034905	-1.91	0.00010982	0.0054886
3490	IGFBP7	insulin-like growth factor binding protein 7	-2.17	0.00071	0.0066268	2.42	0.00083266	0.0166
284217	LAMA1	laminin, alpha 1	-2.17	0.000216	0.0031087	-1.56	9.08E-05	0.0049801
3689	ITGB2	integrin, beta 2 (complement component 3 receptor 3 and 4 subunit)	-2.15	3.50E-06	0.00034794	-1.58	7.64E-06	0.0013675
4747	NEFL	neurofilament, light polypeptide 68kDa	-2.14	7.11E-05	0.0015815	-2.06	0.0004067	0.011153
84767	SPRYD5	SPRY domain containing 5	-2.13	1.09E-05	0.00056517	-1.61	4.71E-05	0.00348
8774	NAPG	N-ethylmaleimide-sensitive factor attachment protein, gamma	-2.12	5.80E-06	0.00042304	-1.82	0.00022387	0.008082
2948	GSTM4	glutathione S-transferase M4	-2.07	8.41E-05	0.0017393	1.66	0.00072217	0.015499
84978	FRMD5	FERM domain containing 5	-2.06	2.20E-05	0.00080364	1.64	7.60E-05	0.0045071
23492	CBX7	chromobox homolog 7	-2.05	0.00199	0.013171	-1.71	6.80E-07	0.0004688
27147	DENND2A	DENN/MADD domain containing 2A	-2.04	0.003241	0.01847	2.64	1.61E-05	0.002092
9212	AURKB	aurora kinase B	-2.04	0.000542	0.0056123	-1.93	5.26E-06	0.001048
1075	CTSC	cathepsin C	-2.04	0.00012	0.0021184	1.70	0.00033527	0.010176
29887	SNX10	sorting nexin 10	-2.03	0.000212	0.0030729	-1.71	6.65E-07	0.0004688
649970	LOC649970	similar to creatine kinase, mitochondrial 1B precursor	-2.03	1.20E-06	0.00018811	-1.73	2.82E-06	0.00088648

Gene ID	Gene Symbol	Gene Description	PRC shRNA #1 fold change	PRC shRNA#1 p-value	PRC shRNA#1 FDR p-value	PRC shRNA #4 fold change	PRC shRNA#4 p-value	PRC shRNA#4 FDR p-value
197021	LCTL	lactase-like	-2.02	8.24E-06	0.00049421	1.51	0.00027031	0.0089316
10063	COX17	COX17 cytochrome c oxidase assembly homolog	-1.97	0.001293	0.0097997	-1.59	0.00038737	0.010877
9929	JOSD1	Josephin domain containing 1	-1.94	1.62E-05	0.0006892	-1.86	2.17E-06	0.00088606
306	ANXA3	annexin A3	-1.91	3.85E-05	0.0010927	1.52	2.03E-06	0.00084771
84953	MICALCL	MICAL C-terminal like	-1.90	0.000823	0.0072764	-1.63	3.20E-05	0.0029367
1854	DUT	dUTP pyrophosphatase	-1.89	0.000248	0.0033569	-1.91	4.88E-07	0.00043713
22995	CEP152	centrosomal protein 152kDa	-1.88	0.000656	0.0063268	-1.61	0.0040407	0.041967
8685	MARCO	macrophage receptor with collagenous structure	-1.87	0.001346	0.010057	-1.65	0.00060156	0.013801
376267	RAB15	RAB15, member RAS onocogene family	-1.87	2.91E-05	0.00092373	-1.60	0.0031964	0.036274
54471	SMCR7L	Smith-Magenis syndrome chromosome region, candidate 7-like	-1.87	2.81E-05	0.0009147	-1.53	0.00029858	0.0094069
56993	TOMM22	translocase of outer mitochondrial membrane 22	-1.84	0.000514	0.0054366	-1.59	2.49E-05	0.0027074
8195	MKKS	McKusick-Kaufman syndrome	-1.84	7.18E-06	0.00046829	-1.97	2.35E-07	0.00030114
23236	PLCB1	phospholipase C, beta 1 (phosphoinositide-specific)	-1.83	4.65E-05	0.001244	-1.58	0.000194	0.0075178
6000	RGS7	regulator of G-protein signaling 7	-1.82	8.30E-05	0.0017386	1.69	0.0025685	0.031826
11019	LIAS	lipoic acid synthetase	-1.80	6.40E-05	0.0014986	-1.65	6.82E-05	0.0042803
26258	PLDN	pallidin homolog (mouse)	-1.77	0.000227	0.0032099	-1.64	0.0002654	0.0088344
256586	LYSMD2	LysM, putative peptidoglycan-binding, domain containing 2	-1.77	0.001249	0.0095619	-1.89	2.77E-05	0.0028099
8536	CAMK1	calcium/calmodulin-dependent protein kinase I	-1.75	0.003316	0.018803	-1.54	0.00016245	0.0069399
132299	OCIAD2	OCIA domain containing 2	-1.74	0.007557	0.033733	1.90	1.35E-05	0.0019044
1809	DPYSL3	Dihydropyrimidinase-like 3	-1.74	0.002833	0.016876	-3.60	1.23E-07	0.0002
51087	YBX2	Y box binding protein 2	-1.72	0.004633	0.023799	-2.18	3.39E-08	0.000101
22837	COBLL1	COBL-like 1	-1.72	0.000652	0.0063076	-1.54	0.0023145	0.030136

Gene ID	Gene Symbol	Gene Description	PRC shRNA #1 fold change	PRC shRNA#1 p-value	PRC shRNA#1 FDR p-value	PRC shRNA #4 fold change	PRC shRNA#4 p-value	PRC shRNA#4 FDR p-value
93273	LEMD1	LEM domain containing 1	-1.71	0.009645	0.040041	-1.50	7.18E-05	0.004368
5216	PFN1	profilin 1	-1.70	6.39E-05	0.0014981	-1.63	0.00014261	0.0063648
708	C1QBP	complement component 1, q subcomponent binding protein	-1.69	0.003603	0.019883	-1.71	0.00010344	0.005318
460	ASTN1	astrotactin 1	-1.69	2.81E-05	0.00091458	-1.52	1.23E-05	0.0018248
2944	GSTM1	glutathione S-transferase M1	-1.66	0.000345	0.004179	1.80	0.0010402	0.018872
10463	SLC30A9	solute carrier family 30 (zinc transporter), member 9	-1.66	2.52E-05	0.00086037	-1.51	8.63E-05	0.004824
4927	NUP88	nucleoporin 88kDa	-1.65	7.85E-05	0.001685	-1.70	1.87E-06	0.00083519
79083	MLPH	melanophilin	-1.64	0.001597	0.011354	-1.84	4.03E-06	0.00096314
10762	NUP50	nucleoporin 50kDa	-1.63	0.002487	0.01539	-1.90	0.00032306	0.0099081
11249	NXPH2	neurexophilin 2	-1.62	0.000499	0.0053392	-1.77	1.59E-05	0.0020771
63979	FIGNL1	fidgetin-like 1	-1.62	0.000882	0.0075771	-1.67	3.41E-05	0.0029835
9582	APOBEC3B	Apolipoprotein B mRNA editing enzyme, catalytic polypeptide-like 3B	-1.61	0.005494	0.026795	-2.63	2.20E-07	0.000301
7139	TNNT2	troponin T type 2 (cardiac)	-1.61	0.003538	0.019721	1.73	0.0011152	0.019752
23466	CBX6	chromobox homolog 6	-1.58	0.000539	0.0055977	-1.73	2.91E-06	0.00088648
174	AFP	alpha-fetoprotein	-1.55	0.001153	0.0090188	-1.79	2.29E-05	0.0025365
9022	CLIC3	chloride intracellular channel 3	-1.54	0.003621	0.019942	1.74	0.00049223	0.012369
84888	SPPL2A	signal peptide peptidase-like 2A	-1.50	0.000275	0.0035782	-1.62	1.53E-05	0.0020497

Table A.4. Overlapping up regulated transcripts in PRC shRNA#1 and #4 cells compared to control shRNA cells.

Mean fold changes in gene expression in response to shRNA#1- or shRNA#4-mediated silencing of PRC compared to cells expressingd a negative control hairpin were assessed by Illumina microarray. The complete list of common gene transcripts significantly up regulated upon PRC silencing by both hairpins#1 and #4 are shown with corresponding p-values and FDR adjusted p-values. A positive value indicates up regulation.

Gene ID	Gene Symbol	Gene Description	PRC shRNA #1 fold change	PRC shRNA#1 p-value	PRC shRNA#1 FDR p-value	PRC shRNA #4 fold change	PRC shRNA#4 p-value	PRC shRNA#4 FDR p-value
51316	PLAC8	Placenta-specific 8	17.78	4.11E-05	0.00114893	5.74	1.65E-07	0.000247
284406	ZNF545	Zinc finger protein 545	4.80	3.42E-09	6.30E-06	2.74	7.85E-08	0.000157
2151	F2RL2	Coagulation factor II (thrombin) receptor-like 2	4.59	5.45E-05	0.001387	2.08	6.60E-05	0.004186
1404	HAPLN1	hyaluronan and proteoglycan link protein 1	3.38	0.0038422	0.020838	1.75	7.62E-05	0.0045071
56952	PRTFDC1	phosphoribosyl transferase domain containing 1	3.05	3.95E-06	0.00036096	-1.73	1.91E-06	0.00083519
8076	MFAP5	microfibrillar associated protein 5	2.95	2.48E-06	0.00028654	-1.57	4.61E-05	0.0034643
9639	ARHGEF10	Rho guanine nucleotide exchange factor (GEF) 10	2.90	5.32E-08	2.36E-05	1.86	2.63E-06	0.00088648
29	ABR	active BCR-related gene	2.68	1.43E-05	0.00065221	1.83	5.44E-06	0.0010719
5108	PCM1	Pericentriolar material 1	2.67	4.00E-07	8.62E-05	2.49	9.28E-05	0.004992
2222	FDFT1	Farnesyl-diphosphate farnesyltransferase 1	2.61	0.00020188	0.002981	2.64	3.15E-06	0.000886
871	SERPINH1	serpin peptidase inhibitor, clade H (heat shock protein 47), member 1, (collagen binding protein 1)	2.60	2.20E-07	5.92E-05	1.84	1.45E-06	0.00076757

Gene ID	Gene Symbol	Gene Description	PRC shRNA #1 fold change	PRC shRNA#1 p-value	PRC shRNA#1 FDR p-value	PRC shRNA #4 fold change	PRC shRNA#4 p-value	PRC shRNA#4 FDR p-value
23362	PSD3	Pleckstrin and Sec7 domain containing 3	2.59	5.06E-06	0.000409	2.45	0.00021619	0.007916
2280	FKBP1A	FK506 binding protein 1A, 12kDa	2.50	7.68E-06	0.00048403	1.77	2.84E-05	0.0028197
29883	CNOT7	CCR4-NOT transcription complex, subunit 7	2.35	1.50E-06	0.000226	2.49	1.03E-05	0.0016519
29928	TIMM22	translocase of inner mitochondrial membrane 22 homolog (yeast)	2.34	8.19E-07	0.00014745	1.55	1.70E-05	0.0021414
55326	AGPAT5	1-acylglycerol-3-phosphate O-acyltransferase 5 (lysophosphatidic acid acyltransferase, epsilon)	2.34	0.00014589	0.0024029	1.70	2.77E-05	0.0028099
2022	ENG	endoglin (Osler-Rendu-Weber syndrome 1)	2.31	0.004835	0.024487	1.59	1.38E-06	0.00075611
252969	NEIL2	Nei-like 2 (E. Coli)	2.30	2.26E-05	0.000811	2.05	3.66E-05	0.003054
5033	P4HA1	procollagen-proline, 2-oxoglutarate 4-dioxygenase (proline 4-hydroxylase), alpha polypeptide I	2.29	7.93E-05	0.0016963	1.53	0.0029141	0.034307
51031	GLOD4	glyoxalase domain containing 4	2.29	8.59E-07	0.0001503	1.70	1.72E-06	0.00083519
55174	INTS10	Integrator complex subunit 10	2.22	4.76E-06	0.000409	2.22	7.05E-07	0.000469
7531	YWHAE	tyrosine 3-monooxygenase/tryptophan 5-monooxygenase activation protein, epsilon polypeptide	2.20	7.97E-06	0.00048699	1.63	6.18E-06	0.0011671
50628	GEMIN4	gem (nuclear organelle) associated protein 4	2.17	0.00012163	0.0021348	1.62	2.38E-06	0.00088648
84660	CCDC62	coiled-coil domain containing 62	2.16	9.59E-05	0.0018933	1.59	5.15E-05	0.0036407
26012	NELF	nasal embryonic LHRH factor	2.12	1.75E-05	0.00071928	1.61	0.00034057	0.010218
285761	DCBLD1	discoidin, CUB and LCCL domain containing 1	2.10	1.50E-05	0.00067005	1.76	1.29E-05	0.0018619
6836	SURF4	surfeit 4	2.09	8.80E-05	0.001789	1.54	0.00056603	0.013433
83700	JAM3	junctional adhesion molecule 3	2.07	0.00077839	0.0070346	-1.99	1.06E-05	0.0016709

Gene ID	Gene Symbol	Gene Description	PRC shRNA #1 fold change	PRC shRNA#1 p-value	PRC shRNA#1 FDR p-value	PRC shRNA #4 fold change	PRC shRNA#4 p-value	PRC shRNA#4 FDR p-value
1398	CRK	v-crk sarcoma virus CT10 oncogene homolog (avian)	2.06	3.26E-06	0.00033443	1.82	4.74E-06	0.0010456
221061	C10orf38	chromosome 10 open reading frame 38	2.05	1.24E-05	0.00059655	1.88	0.00027166	0.0089434
7991	TUSC3	Tumor suppressor candidate 3	2.02	7.42E-06	0.000474	2.66	3.84E-07	0.000393
2889	RAPGEF1	Rap guanine nucleotide exchange factor (GEF) 1	2.01	2.18E-05	0.00080283	1.60	3.61E-06	0.00089856
5157	PDGFRL	Platelet-derived growth factor receptor-like	1.97	0.00067013	0.006406	2.48	2.73E-05	0.002802
55684	C9orf86	chromosome 9 open reading frame 86	1.89	5.34E-06	0.00040937	1.57	9.45E-05	0.0050032
50863	HNT	Neurotrimin	1.89	0.0092079	0.038925	3.12	1.90E-05	0.002287
92285	ZNF585B	zinc finger protein 585B	1.89	3.12E-05	0.0009747	1.63	2.89E-06	0.00088648
25	ABL1	v-abl Abelson murine leukemia viral oncogene homolog 1	1.89	0.0034387	0.019276	1.72	7.49E-05	0.0044691
10439	OLFM1	olfactomedin 1	1.86	1.93E-05	0.0007512	-2.56	1.66E-06	0.00083519
11253	MAN1B1	mannosidase, alpha, class 1B, member 1	1.78	0.00059998	0.0060086	1.63	0.00037644	0.010704
875	CBS	cystathionine-beta-synthase	1.77	0.00049158	0.0052989	-1.57	2.17E-05	0.0024655
65992	C20orf116	chromosome 20 open reading frame 116	1.75	1.14E-05	0.00057582	1.66	2.35E-05	0.0025742
64975	MRPL41	mitochondrial ribosomal protein L41	1.74	0.00027948	0.0036133	1.73	2.27E-05	0.0025365
55178	RNMTL1	RNA methyltransferase like 1	1.73	0.0012101	0.0093468	1.50	0.0011771	0.020382
116225	ZMYND19	zinc finger, MYND-type containing 19	1.73	0.00060802	0.0060494	1.50	0.00028576	0.0091885
6453	ITSN1	intersectin 1 (SH3 domain protein)	1.72	0.0019714	0.013092	1.74	0.00052322	0.012766
7077	TIMP2	TIMP metallopeptidase inhibitor 2	1.70	0.0010919	0.0086829	1.64	8.04E-05	0.0046506
9772	KIAA0195	KIAA0195	1.70	0.0069464	0.031715	1.55	2.54E-05	0.0027206
3799	KIF5B	kinesin family member 5B	1.68	8.32E-05	0.0017386	-1.51	0.0023254	0.030138

Gene ID	Gene Symbol	Gene Description	PRC shRNA #1 fold change	PRC shRNA#1 p-value	PRC shRNA#1 FDR p-value	PRC shRNA #4 fold change	PRC shRNA#4 p-value	PRC shRNA#4 FDR p-value
140885	SIRPA	signal-regulatory protein alpha	1.65	4.86E-05	0.0012829	1.81	0.0003745	0.010691
51206	GP6	glycoprotein VI (platelet)	1.63	0.0095859	0.039929	1.78	0.00039409	0.010962
6238	RRBP1	ribosome binding protein 1 homolog 180kDa (dog)	1.62	0.0006823	0.0064674	-2.38	6.68E-06	0.0012113
205	AK3L1	adenylate kinase 3-like 1	1.62	0.00033355	0.004068	-1.77	5.94E-05	0.0039794
1508	CTSB	cathepsin B	1.61	0.00084377	0.0074018	2.08	5.80E-06	0.0011183
79850	FAM57A	family with sequence similarity 57, member A	1.59	0.00031234	0.0039106	1.73	6.84E-07	0.0004688
56675	NRIP3	nuclear receptor interacting protein 3	1.59	0.0018625	0.012621	-1.57	8.45E-05	0.0047699
29085	PHPT1	phosphohistidine phosphatase 1	1.56	0.0012005	0.0092918	1.57	0.0011743	0.020377
5217	PFN2	profilin 2	1.56	3.63E-05	0.001049	-1.57	0.0024937	0.031376
4072	TACSTD1	Tumor-associated calcium signal transducer 1	1.55	0.00060467	0.006034	2.49	5.35E-08	0.000137
389860	PAGE2B	P antigen family, member 2B	1.50	0.00024534	0.0033411	-1.91	9.62E-06	0.0015693
5986	RFNG	RFNG O-fucosylpeptide 3-beta-N-acetylglucosaminyltransferase	1.50	0.0037949	0.020642	1.59	4.51E-06	0.0010277